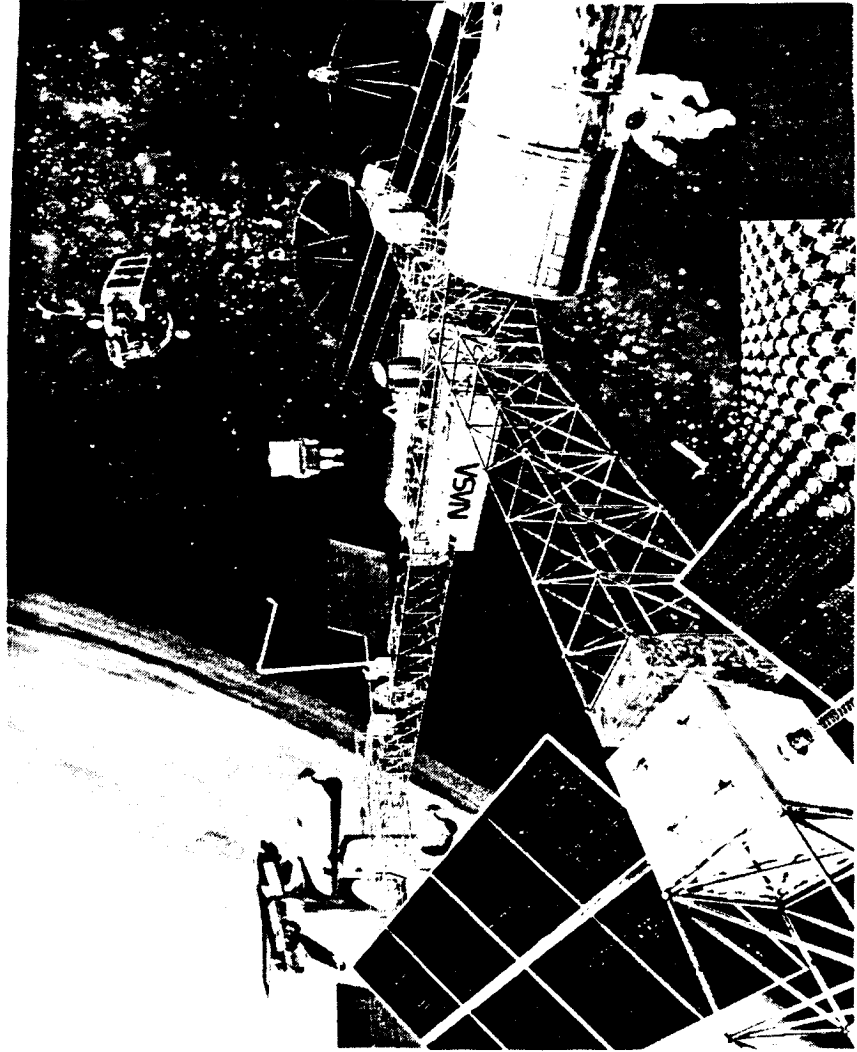


Design, Fabrication, and Delivery of a Miniature Cassegrainian Concentrator Solar Array System



**Engineering and Test
Division**
TRW Space & Technology Group
One Space Park
Redondo Beach, CA 90278



Final Technical Report
October 1987
Contract Number NAS8-36159
Document Number 45050-6001-UT-00 1

Prepared by
Mark A. Krueger

Work Performed for:
Marshall Space Flight Center
National Aeronautics and
Space Administration
Huntsville, Alabama 35812

TABLE OF CONTENTS

	PAGE
1. INTRODUCTION	1
2. MCC HISTORY AT TRW	8
3. DESIGN DEVELOPMENT	13
3.1 OBJECTIVES AND PROGRESS	13
3.2 TASK STATEMENTS	14
3.3 OPTIC INVESTIGATION AND TEST	15
3.3.1 NAS8-35635 Investigation	15
3.3.1.1 Physical Measurements	15
3.3.1.2 Measurement of Optical Losses	20
3.3.1.3 System Effects	21
3.3.1.4 Summary	24
3.3.1.5 Electrical Measurements	24
3.3.2 Analyses	24
3.3.2.1 Specular Reflectance Analysis	24
3.3.2.2 Tolerance Analysis	24
3.3.2.3 Optical Design	28
3.3.2.4 Support Analysis	33
3.3.2.5 New Design Optics	39
3.3.2.6 Part Physical Measurements	39
3.3.2.7 Optical Measurements	46
3.3.2.8 Concentration Ratio Check-Energy Throughput	46
3.3.2.9 Element Performance	46
3.3.2.10 Coatings	46
3.3.2.11 Electrical/Optical Test Results of the Improved MCC	57
3.3.2.12 Multi-Element String Measurements	61
3.3.2.13 Correction Methods for MCC Element and String Test Data	68
3.4 CELL STACK DESIGN AND INVESTIGATION	75
3.4.1 Solder Investigation	78
3.4.2 Alternate Bonding Methods	78
3.4.2.1 Adhesive Bonding-Top Contacts	78
3.4.2.2 Gold Germanium Eutectic	78
3.4.2.3 Welding	79
3.4.2.4 Stack Subassembly	82

TABLE OF CONTENTS (CONTINUED)

	PAGE
3.4.3 Electrically connected Versus Isolated Cell Stack-Heat Sink	82
3.4.3.1 Heat Sink Bond	85
3.4.4 Coverglass	85
3.4.5 Cover Adhesive	85
3.4.6 Conic Mirror	85
3.4.7 Cell and MCC Element Electrical Interconnections	88
3.4.8 Summary	93
3.5 STRUCTURAL DESIGN OF THE MCC	97
3.5.1 MCC Primary Mirror	97
3.5.2 MCC Secondary Mirror	97
3.5.3 Secondary Mounting	97
3.5.4 Mirror Manufacturing Methods	101
3.5.5 MCC Element Bonding Methods	101
3.5.6 Complete MCC Element Assembly	101
3.6 MCC SUPPORT STRUCTURE	108
3.6.1 Frame Design	108
3.6.2 Insert Design	115
4. ANALYSIS	125
4.1 THERMAL CONSIDERATIONS	125
4.1.1 Thermal Performance for Cell Output	125
4.1.2 Secondary Mirror Temperatures	125
4.2 WEIGHT	127
4.3 PERFORMANCE ANALYSIS	130
4.3.1 Overall electrical Achievement	130
4.3.2 Electrical Output Corrected for Known Defects	130
4.4 ADVANCED DESIGNS	133
4.4.1 Material Thickness Change	133
4.4.2 Material Type Change	133
4.4.3 Coatings	133
4.4.4 Advanced Cells	133
4.4.5 Combined	134
4.4.6 Manufacturing	134
4.4.7 Offpoint Performance	134

TABLE OF CONTENTS (CONTINUED)

	PAGE
5. CONCLUSIONS	135
6. RECOMMENDED FOLLOW-ON WORK	136
APPENDICES	138
A TEST AND INSPECTION DATA	
B ELECTRICAL MANUFACTURING	
C MECHANICAL MANUFACTURING	

FIGURE INDEX

	PAGE
Figure 1-1 Miniature Cassegrainian Concentrator Concept	2
Figure 1-2 Front of Large Deliverable Panel	3
Figure 1-3 Back Of Large Panel Showing Flat Cable Harness	3
Figure 1-4 Front of Small Panel	4
Figure 1-5 Back of Small Panel Showing Flat Cable Harness	5
Figure 1-6 15 x 56 Array in Operation	6
Figure 1-7 Close-up of the Assembly Just After Completion in the Manufacturing Facility	7
Figure 2-1 Contract NAS8-34131 Technical Results Summary	9
Figure 2-2 Contract NAS8-35635 Technical Results Summary	10
Figure 2-3 MCC Element Evolution	11
Figure 2-4 Tri-Hex Grid (THG) Panel Evolution	12
Figure 3-1 Front Side View of Predecessor NAS8-35635 MCC Element in Tri-Hex Grid	15A
Figure 3-2 Surface Accuracy Error Measurements for #15 Primary and Secondary	16
Figure 3-3 Surface Accuracy Error Measurements for #12 Primary and Secondary	17
Figure 3-4 Element #12 Tolerance Errors	18
Figure 3-5 Element #15 Tolerance Errors	18
Figure 3-6 Rounded Areas of the Primary were Found not to Contribute to Collection Efficiency as Designed	19
Figure 3-7 NAS8-35635 Mirrors were Relatively Diffuse	22
Figure 3-8 Distortion can Cause Significant Loss of Output	23
Figure 3-9 Test Result-70 vs 77% Optical Transmission Investigation	25
Figure 3-10 Test Results-Off Axis Performance Investigation	26
Figure 3-11 Effect of Mirror Finish on Performance	27
Figure 3-12 Through 3-17 Effect of Selected Tolerances on MCC Performance New vs Old Design	29

FIGURE INDEX **(CONTINUED)**

	PAGE
Figure 3-18 Multiple Misalignment Test Case vs Two Measured Assemblies	30
Figure 3-19 MCC Element Off-Pointing Performance with Concentration Ratio as a Parameter	31
Figure 3-20 MCC Element Off-Pointing Performance of CODE V Optimized Designs	32
Figure 3-22 New Design Showing Ray Trace for Entrance of Rays with Zero Pointing Error	34
Figure 3-23 New Design Showing Ray Trace for Entrance from Three Degrees from the Left	35
Figure 3-24 New Design Showing Ray Trace for Entrance from Three Degrees from the Right	35
Figure 3-25 Energy on Cell vs Tracking Error Collimated Source	36
Figure 3-26 Rays Reaching Cell vs Variations of Secondary Offpoint Collection Angles	37
Figure 3-27 New vs Hyperbolic Output	38
Figure 3-28a The New Primary MCC 000 Rev E.	40
Figure 3-28b Coatings on the Front and Back Provide Precise Optical and Thermal Properties MCC 000 Sheet 2	41
Figure 3-29a The New Secondary MCC 010B	42
Figure 3-29b Equation for the Secondary Mirror Surface	43
Figure 3-30 The New Cone Provides Tooling Reference Points	44
Figure 3-31 Tolerance Allowance for Nominal Offpoint Performance	45
Figure 3-32 The Specularity of the Uncoated Mirror is a Factor of Ten Improved Over the Previous Design	47
Figure 3-33 Specularity of the New Mirror Remains Five Times Better Than the Previous Design After Coating	48
Figure 3-34 MCC Off-Point Curves for LIPS III Hardware	49
Figure 3-35 Coating Sequence for Optic Surfaces (Primary Sub-assembly Without Spider Shown)	51

FIGURE INDEX (CONTINUED)

	PAGE
Figure 3-36 Front of New Element Shown While Operating, Spider and Secondary Back are Painted with S13GLO	52
Figure 3-37 Back of MCC Element Showing Mounting Position, Solder Bonds for Electrical Interconnection, and Complete S13GLO Coating	53
Figure 3-38 Method for Finding Specular Reflectance of Cone	55
Figure 3-39 Conic Mirror to Cell Output Ratio as a Function of Cone Reflectance	56
Figure 3-40 Total Fraction of Light to Reach Cell Which is First Redirected by the Conic Mirror (Zero and Typical Tolerance Allowances Shown)	58
Figure 3-41 Both Deliverable Panels were Tested Using a Solar Tracker, Adapted from a Celestron Telescope Mount	59
Figure 3-42 The Operation of the Seven Accepted Secondary Proof Items Shows Higher Than Desired Variation, But Still Within Reason in the Projected Operating Maximum Angle of 1.1 Degrees	60
Figure 3-43 Reasonable Shaped I-V Curves Result from Operation of a Six Element String Near Normal Offpoint	62
Figure 3-44 Some Mismatch Phenomena Are Visible in the String I-V Performance	63
Figure 3-45 Large Mismatch Losses are Easily Visible in a Number of Severely Offpointed Strings	64
Figure 3-46 Reverse Bias Test of Element Within String in Natural Sunlight (No Corrections)	65
Figure 3-47 Five Six-Element By One-Element Strings of a Group Designated "A" Show Some Variation from Ideal Output After Correction for the Conic Mirror	66
Figure 3-48 Strings of Group "B" Show Less Variation than Group "A"	67
Figure 3-49 Offpoint Performance of Two Sub-Arrays (5 Parallel x 6 Series) Compared to Perfect Optic Performance (Corrected for Cone Deficiency R = 70%)	69

FIGURE INDEX **(CONTINUED)**

	PAGE
Figure 3-50 Temperature vs Resistance Reading for Mounted Thermistor 1M001-XXX	70
Figure 3-51 Illustration of Mismatch Caused by Cell Efficiency Combined with Mirror Offpoint	72
Figure 3-52 Small Panel Mismatch Tally and Calculation	74
Figure 3-53 Test Result-Assembly Loss (11%) Investigation	76
Figure 3-54 Solder Test Investigation Data	77
Figure 3-55 Cell Performance Test (100 Sun Flasher Intens., Room Temperature) Before & After Weld/Solder Of Front Cell Contact	80
Figure 3-56 Weld Schedules Developed for All Vendors	81
Figure 3-57 Cell Performance Before and After Vapor Phase Soldering of Cell Rear Contact to be BeO Substrate	83
Figure 3-58 Cell Heat Spreader Trade	84
Figure 3-59 SK-MCC-063 Insulator, Heat Sink	86
Figure 3-60 Cell Cover (Plain) MCC 050	87
Figure 3-61 Cell Stack Mechanical Attachments Investigated	89
Figure 3-62 Adhesive Trade for Cone to Cover Bond	90
Figure 3-63 Cell Top Interconnect	91
Figure 3-64 Interconnect to Heat Sink	92
Figure 3-65 Interconnect to Heat Sink Weld Test Results	93
Figure 3-66 Cell Stack Electrical Interconnection Design	95
Figure 3-67 Cell Stack Materials Trade	96
Figure 3-68 Assembly with Secondary Mirror Shown	98
Figure 3-69 Mechanical Design Options	99
Figure 3-70 Picture of Spider to Primary Mounting Position Showing Mounting Boss	100
Figure 3-71 Mirror Material and Manufacturing Trade	102
Figure 3-72 Optic Mechanical Attachments Investigated	103

FIGURE INDEX APPENDICES

	PAGE
APPENDIX A:	
Figure A1	Materials Used on Test Plate for Acoustic Exposure and Thermal Cycling A2
Figure A2	Thermal Cycling Results A2
Figure A3	Acoustic Spectrum A5
Figure A4	Half String Outputs for 15" x 21" Panel Corrected for Insolation and Temperature A6
Figure A5	Combined Strings Corrected for Insolation and Temperature A9
Figure A6	Combined and Individual Half String Data Normalized for Output at ISC and Corrected for Conic Mirror Reflectance of 0.70 A10
Figure A7	Data for 15 x 56 Panel Corrected for Temperature and Insolation A12
Figure A8	Data from 15 x 56 Panel Corrected for Conic Mirror Reflectance of 0.70 A15
Figure A9	Secondary Proof Mirrors Effect on Offpoint A21
Figure A10	Secondary Proof Normalization and Conversion A22
Figure A11	Coating and Part Defects in Small 15" x 21" Panel A24
Figure A12	Inspection Results of 15" x 56" Panel A25
Figure A13	Electrical Test notes showing locations of shorted and open cells A26
APPENDIX B:	
Figure B1	BeO welding tool (left) and conic mirror course alignment tool B4
Figure B2	Conic mirror to coverglass bonding tool. B6
Figure B3	Cell and BeO insulator to primary vapor phase solder tool, and secondary to spide vapor phase solder tool B9
Figure B4	MCC Vapor Phase Yields B11
Figure B5	MCC Panels - Kitting Plan B16

**FIGURE INDEX
(CONTINUED)**

	PAGE
Figure 3-73 Complete Miniature Cassegrainian Concentrator Assembly	104
Figure 3-74 Assembly of MCC Element into Panel Showing Detail of Snap Insert	105
Figure 3-75 Third Generation MCC Hardware from the NAS8-36159 Contract	106
Figure 3-76 Existing MCC Assembly Process Flow Diagram	107
Figure 3-77a Large Tri Hex Grid	109
Figure 3-77b Small Tri Hex Grid	110
Figure 3-77c Detail Assembly of MCC Elements into Tri Hex Grid	111
Figure 3-78 Hex vs Tri-Hex Trade	112
Figure 3-79 THG Fabrication Process Trades	113
Figure 3-80 Compaction Methods	114
Figure 3-81 THG Mechanical Attachments Investigated	116
Figure 3-82 Fixed Insert	117
Figure 3-83 Sliding Insert	118
Figure 3-84 The sliding-to-fixed insert bond	119
Figure 3-85 THG Insert Design Requirements	121
Figure 3-86 Insert Materials	122
Figure 3-87 Plastic Options for Baseline Insert Design	123
Figure 3-88 Push Strength (LBS) for Adhesives for Sliding Insert	124
Figure 4-1 The latest temperature prediction for LEO	126
Figure 4-2 MCC Panel Weight Analysis	128
Figure 4-3 Weight of Piece Parts and Weight Summary	129
Figure 4-4 MCC Element Capability	131
Figure 6-1 Recommended Follow-On Development Plan	137

FIGURE INDEX
APPENDICES
(Continued)

	PAGE
Figure B6 Harness Fabrication Instructions for 15 x 21 and 15 x 56 Panels	B17
Figure B7 Schematic (66 Optic Panel)	B19
APPENDIX C:	
Figure C1 Trapped Rubber Molding Concept	C2
Figure C2 Strip Samples and Tooling	C3
Figure C4 Cross Strip Sample in Test Fixture	C4
Figure C5 Mini Panel with Tooling	C6
Figure C6 Insert tooling for Tri Hex Grid	C7
Figure C7 Rubber Insert Mold	C8
Figure C8 The Screw Pin Concept allowed easy disassembly	C9
Figure C9 Baseline Insert Assembly Design	C11
Figure C10 THG Process Manufacturing Development	C12
Figure C11 Tooling for the small THG panel	C14
Figure C12 Tri-Hex Grid Specifications	C15
Figure C13 15" x 21" Panels with 15" x 56" Layup Tool	C16
Figure C14 Drawing TOW Through Die	C18
Figure C15 Layup Process	C19
Figure C16 Rubber Inserts Installed in Panel	C20
Figure C17 Straightening Setup	C21
Figure C18 15" x 56" Flatness Results	C21

ACKNOWLEDGEMENTS

The following personnel contributed to this project in the capacities shown:

IRA ALLARD	MANUFACTURING ENGINEERING
PETER BARRETT	DYNAMIC ANALYSIS
SAUL BASHIN	PRODUCT DESIGN
FRED DENINGER	MANUFACTURING ENGINEERING
MANNY GARZA	ELECTRICAL TESTING
LARRY GILMAN	MECHANICAL DESIGN
JERRY JACOBY	OPTICAL DESIGN
MARK KRUER	PROJECT MANAGER
JOEL MARKS	ELECTRICAL TESTING
GEORGE MESCH	MANUFACTURING
MARK MYERS	MANUFACTURING
DEBBIE TILLER	SUBCONTRACTS

Special thanks to Mr. Mark Myers and Mr. Fred Deninger of the manufacturing division for long hours of painstaking effort beyond the call of duty.

1. INTRODUCTION

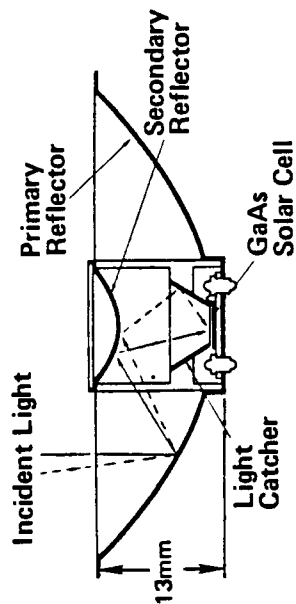
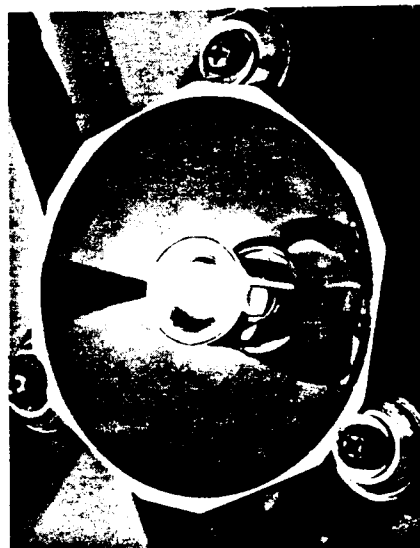
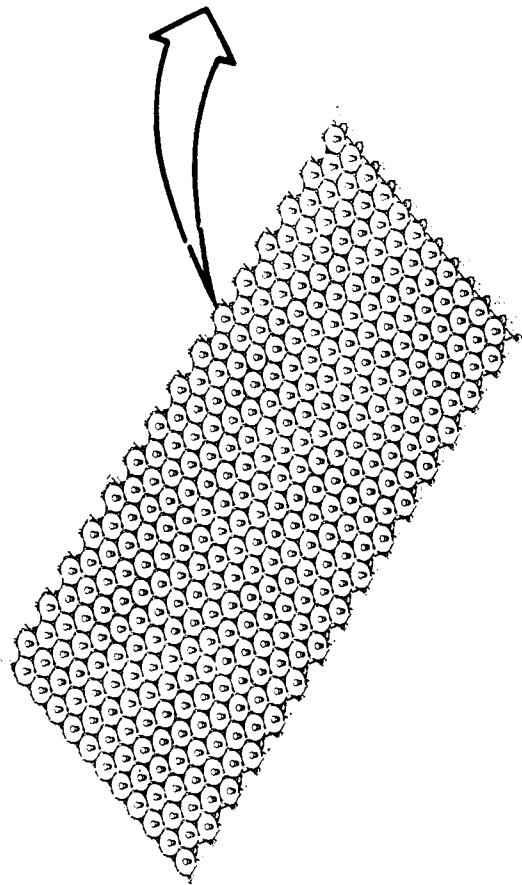
This miniature cassegrainian concentrator (MCC) development project is third in a series of NASA sponsored programs conceived to advance photovoltaic concentrator designs for spaceborne arrays. Achieved during this project were broadened solar acceptance angle, increased optical efficiency, and increased manufacturability of both the optical elements and the support structure. The MCC was raised to NASA development level 5 (Component of engineering model tested in relevant environment) through thermal cycle and qualification acoustic testing. A pilot line quantity (270) of MCC elements were produced, three of which were submitted for flight on the LIPPS III experimental satellite.

Previously set goals of $>28\text{W/kg}$ at the panel levels and $>160\text{W/m}^2$ are projected to have been achieved by the present hardware and new capability projections of as much as 87W/kg using ultra lightweight optics and advanced 27.5% silicon concentrator cells seem feasible, all at a cost of less than \$500/W.

Shown in figure 1-1 is the basic operational characteristics of a cassegrainian type concentrator. The chief advantages are small storage volume, passive thermal cooling and the capability to fine tune the optical input through multiple mirror surface shape reflectance control.

Figures 1-2 and 1-3 show the back and front of the large fully operational 35 x 142 cm panel built during this contract. Figures 1-4 and 1-5 show the back and front of the small fully operational 35 x 53 cm panel built during this contract. Figure 1-6 shows a close up of the panel in operation. Figure 1-7 is a close up at the completion of assembly in the manufacturing area.

Miniature Cassegrainian Concentrator Concept



Required cell area reduced by 99%

Permits cost-effective use of high-efficiency solar cells

Provides potential for significant reduction in array cost and area

Figure 1-1

ORIGINAL PAGE 13
OF POOR QUALITY

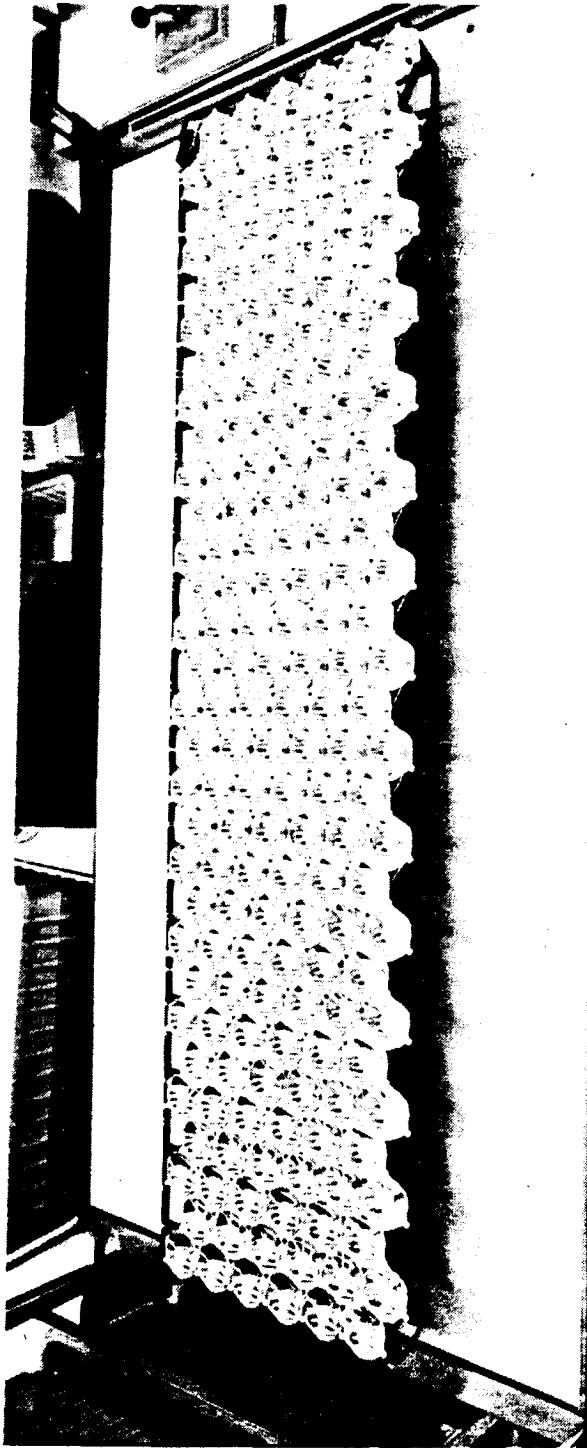


Figure 1-2. Front of Large Deliverable Panel.

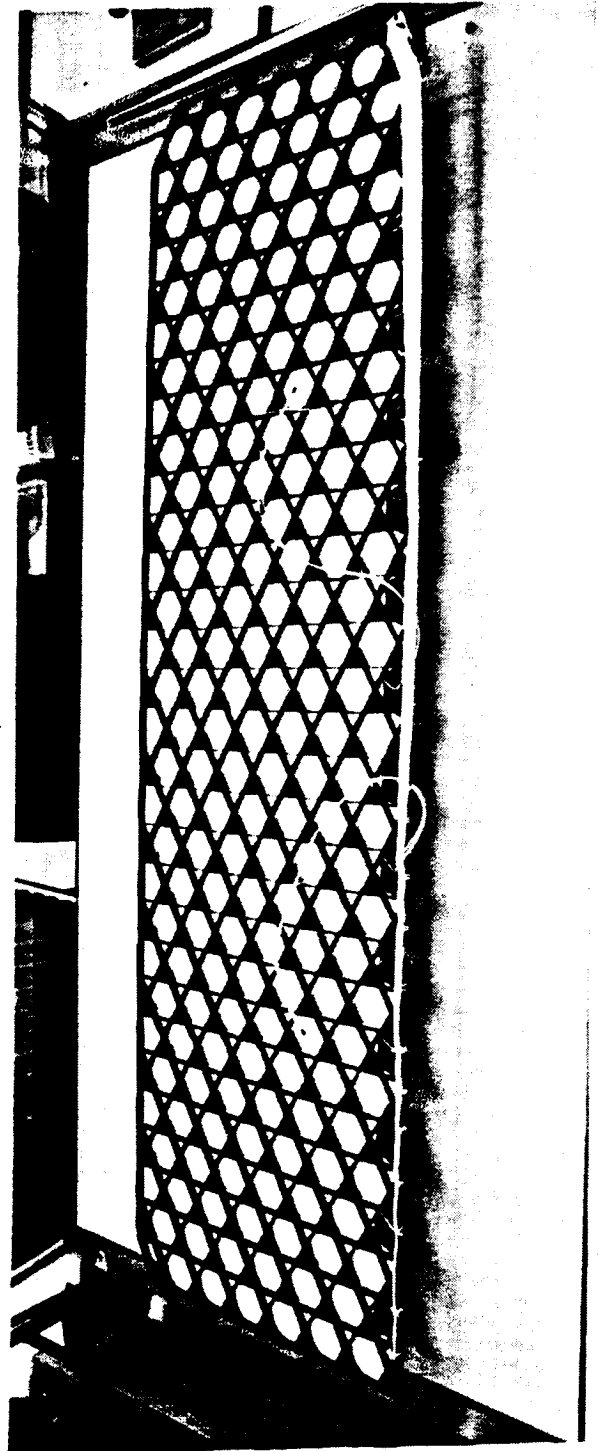


Figure 1-3. Back of Large Pa Showing Flat Cable Harness.

ORIGINAL PAGE IS
OF POOR QUALITY.

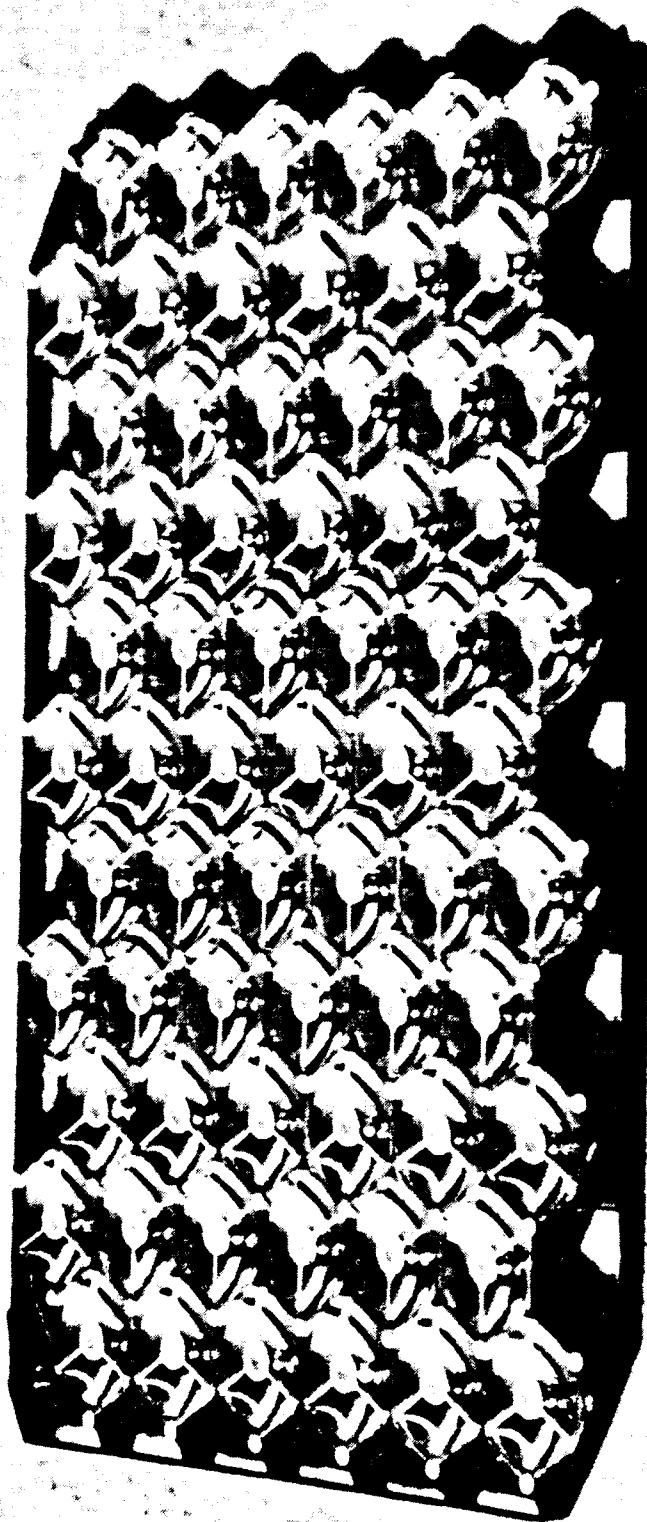


Figure 1-4. Front of Small Panel.

ORIGINAL PAGE IS
OF POOR QUALITY



Figure 1-5. Back of Small Panel Showing Flat Cable Harness.

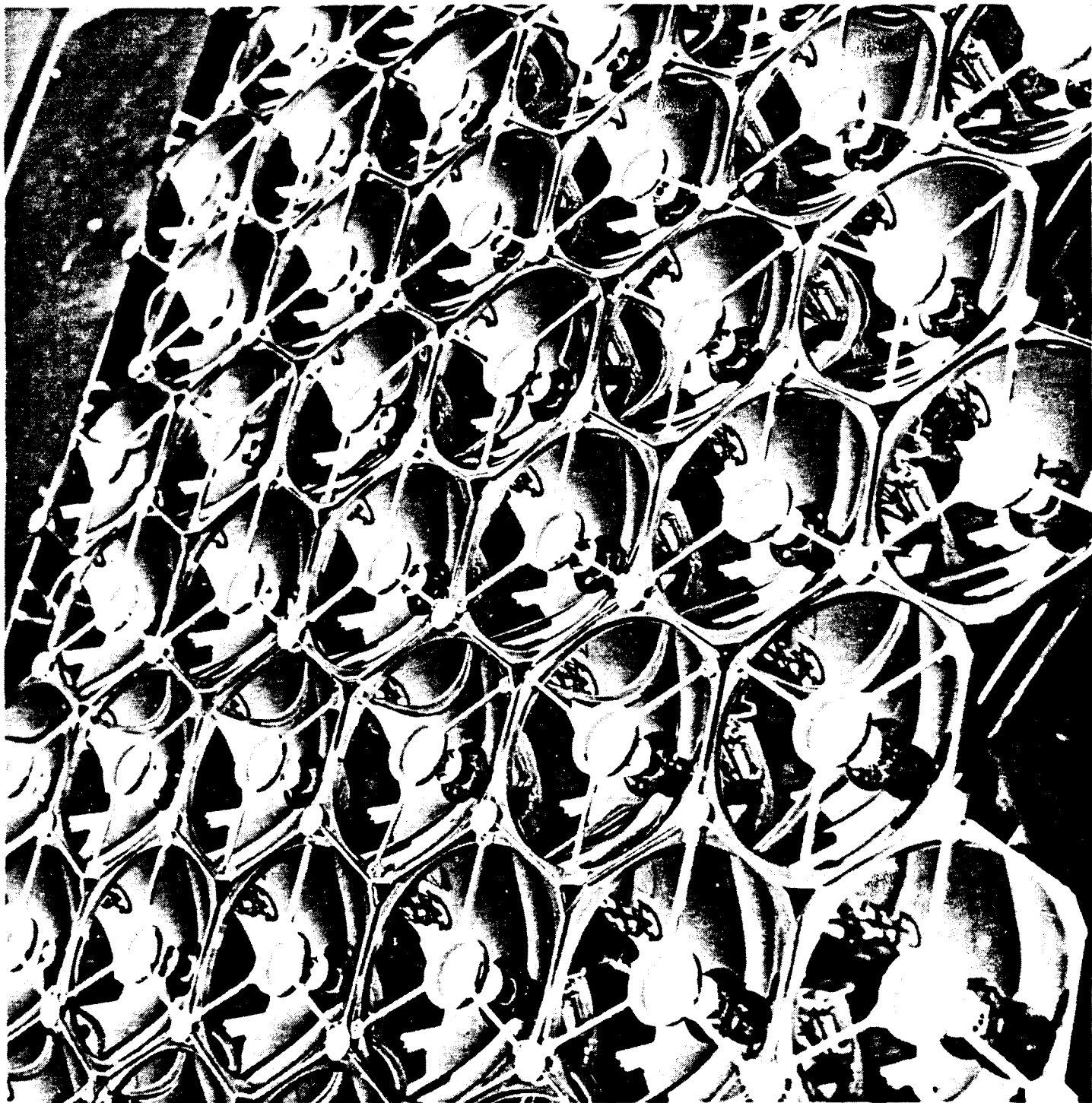


Figure 1-6. 15 x 56 Array in Operation.

ORIGINAL PAGE IS
OF POOR QUALITY

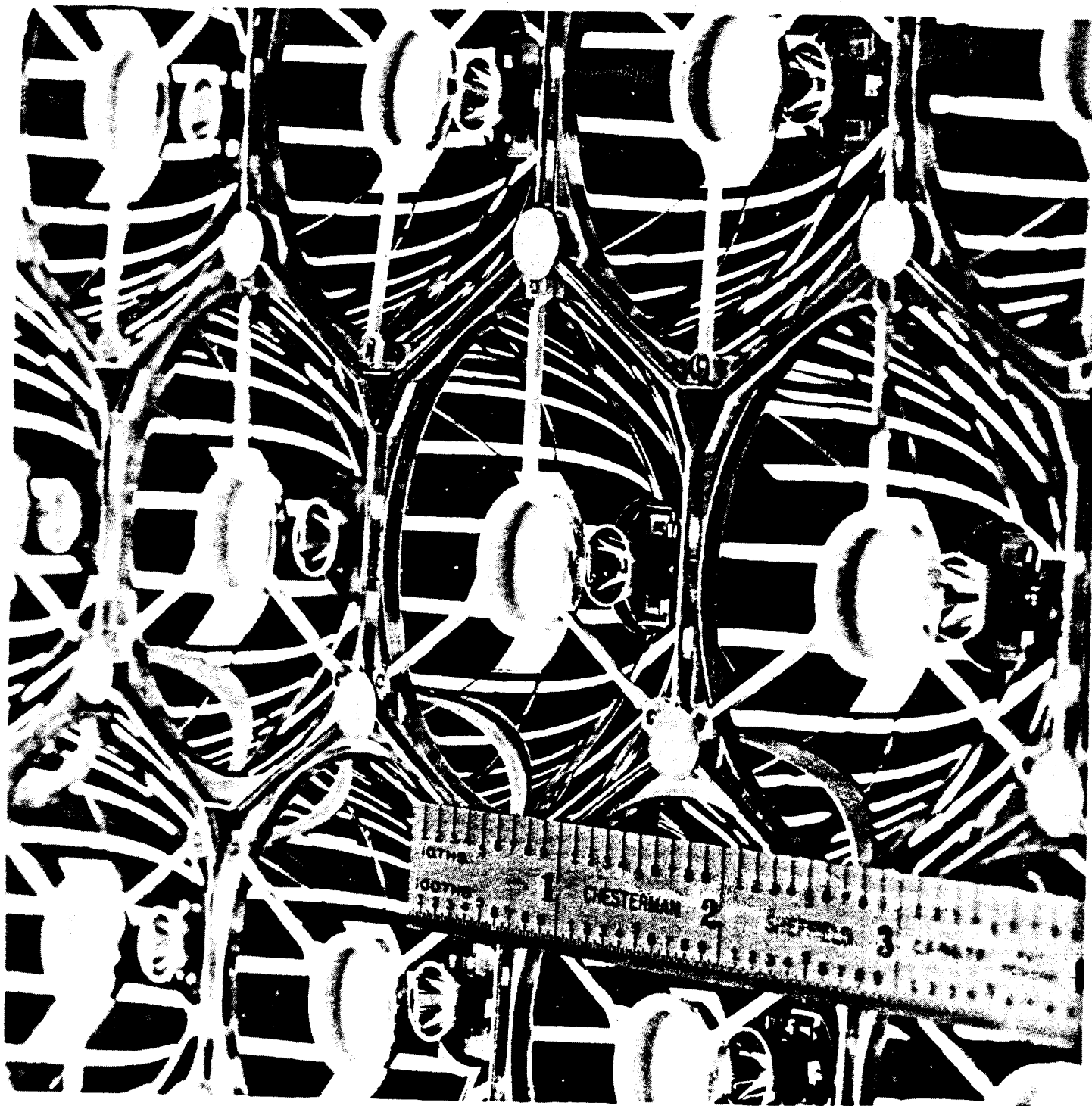


Figure 1-7. Close-up of the Assembly Just After Completion
in the Manufacturing Facility.

ORIGINAL PAGE IS
OF POOR QUALITY.

2. MCC HISTORY AT TRW

Figure 2-1 shows the early development of the MCC design under contract NAS8-34131. Goals of 160 W/m^2 and 28 W/kg were established as reasonable for the MCC design assuming current technology capabilities. Feasibility was demonstrated through construction and test of a nine element module.

Figure 2-2 presents the results of the immediate predecessor contract for MCC development, NAS8-35635. Significant improvements were made in the pursuit of the goals established in NAS8-34131.

The evolution into third generation hardware of the element (Figure 2-3) and the support structure (Figure 2-4) were set as goals for the present NAS8-36159 contract. All goals have been met by analysis of test articles.

Contract NAS8-34131 Technical Results Summary



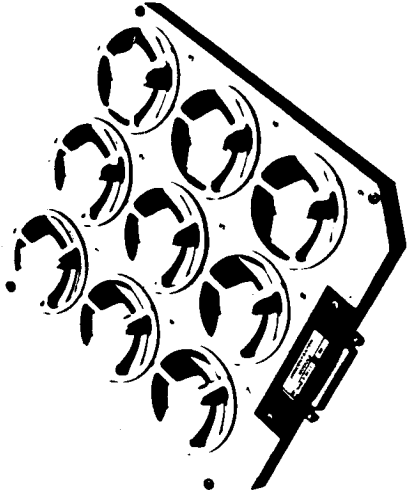
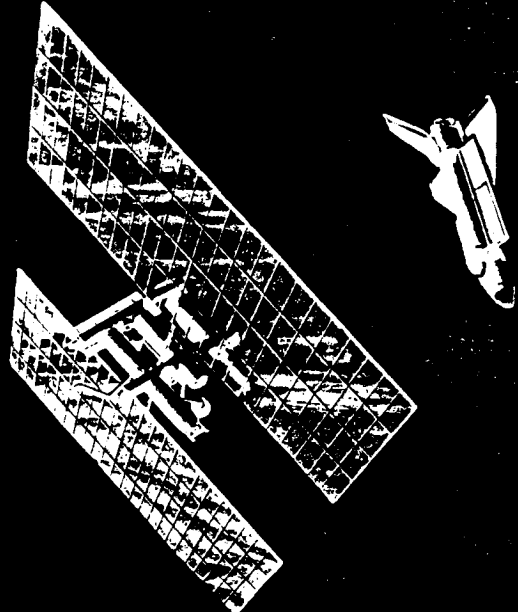
<p>NINE-ELEMENT CASSEGRAINIAN CONCENTRATOR DEMONSTRATION MODULE</p>		<ul style="list-style-type: none"> • TEST RESULTS SUPPORT TECHNICAL FEASIBILITY • 85°C CELL TEMPERATURE IN LOW EARTH ORBIT CONFIRMED BY THERMAL VACUUM TEST • CELL STACK ASSEMBLED USING CONVENTIONAL JOINING PROCESSES • OPTICAL ELEMENTS ALIGNED USING MECHANICAL INTERFERENCE FIT
<p>100 KW BOL CASSEGRAINIAN CONCENTRATOR SOLAR ARRAY SYSTEM STUDY</p>		<ul style="list-style-type: none"> • TWO WING DESIGN BASELINED BUT CONFIGURATIONS ARE NOT CONSTRAINED • FOLD-OUT RIGID PANELS WITH FOLDING BEAM SUPPORT (USED ON SKYLAB) • MODULAR CONCEPT (12.5 KW PER SUBWING MODULE) • ACCURATE ELEMENT POINTING (MAXIMUM RSS OF 1.1°) • 160 W/m² (CURRENT TECHNOLOGY) • 28 W/kg (CURRENT TECHNOLOGY) • POTENTIAL OF 60 W/kg WITH TECHNOLOGY DEVELOPMENT • ERECTABLE (EVA) ARRAY OPTIONAL

Figure 2-1

Contract NAS8-35635 Technical Results Summary



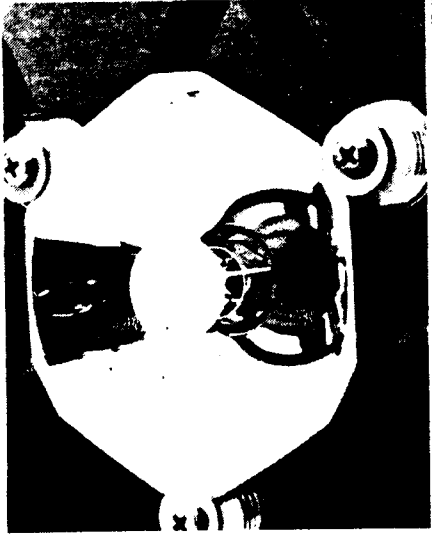
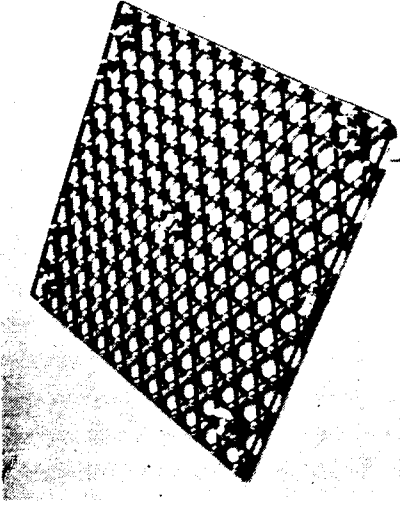
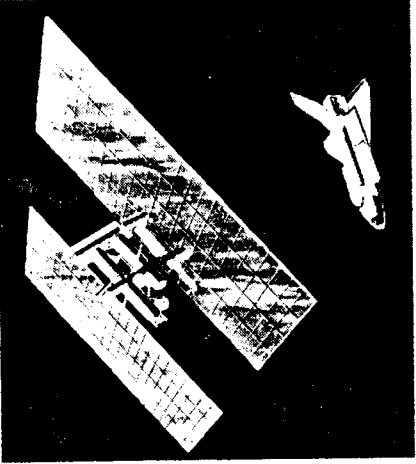
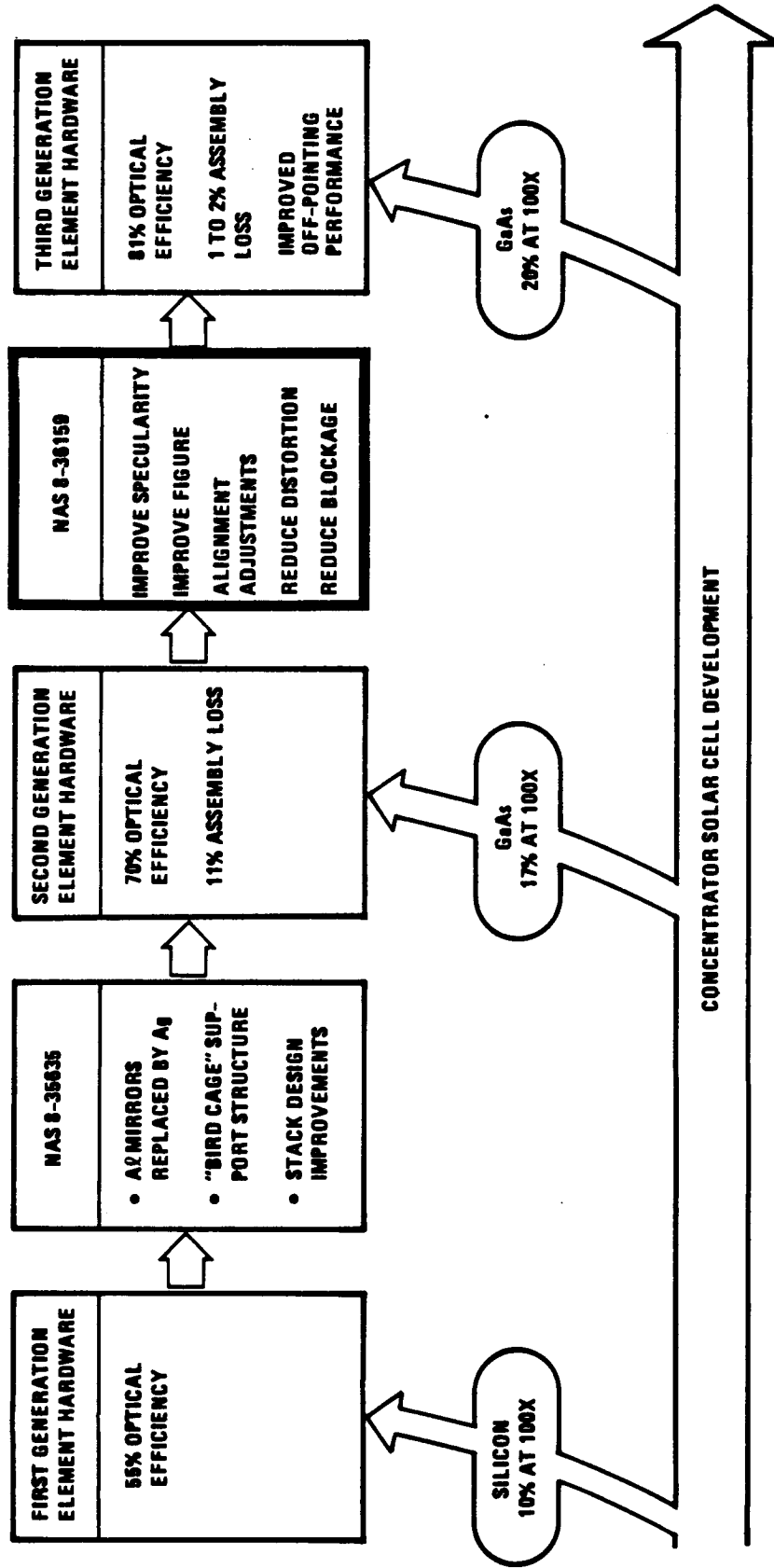
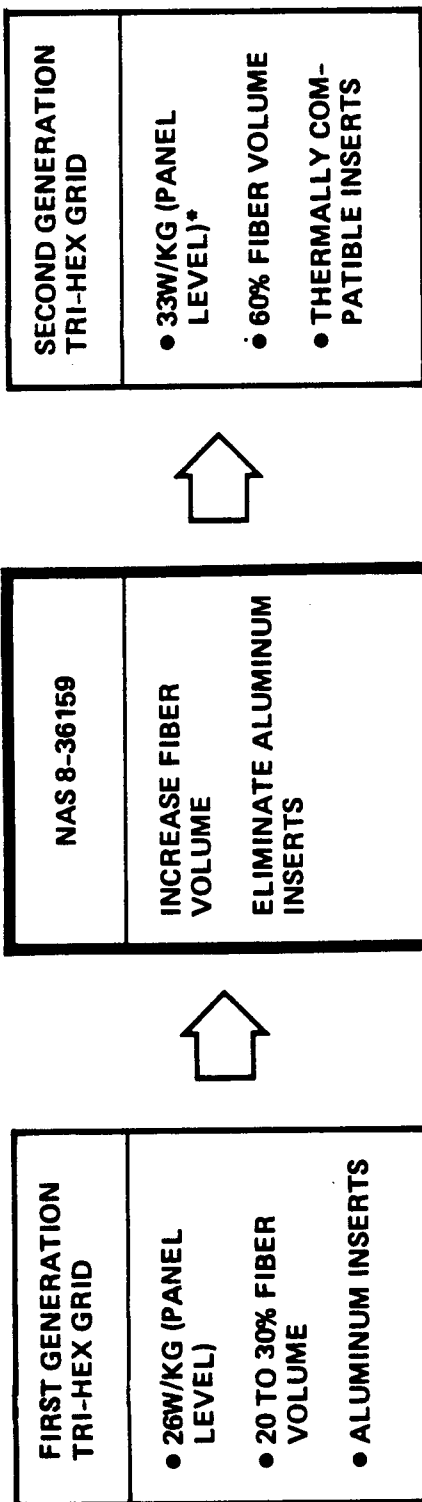
MCC Element	MCC Module	100-kW Array Predictions
 <ul style="list-style-type: none"> • Optical efficiency improved from 55 to 70 percent • AMO 100X cell efficiencies of 17 to 18 percent at 28°C 	 <ul style="list-style-type: none"> • Graphite epoxy tri-hex grid fabricated by Fiber Science • Load deflection tests verified predicted stiffness 	 <ul style="list-style-type: none"> • 160 W/m² BOL • 28 W/kg BOL

Figure 2-2

MCC Element Evolution



Tri-Hex Grid (THG) Panel Evolution



*CORRESPONDS TO 28W/KG
AT THE ARRAY SYSTEM
LEVEL

3. DESIGN DEVELOPMENT

3.1 OBJECTIVES AND PROGRESS

The objectives of this contract were to :

- a. Improve the miniature Cassegrainian concentrator (MCC) optic design in terms of total energy throughput and offpointability
- b. Design a cell stack compatible with the MCC and capable of low earth orbit operation for five years
- c. Manufacture the complete optic and cell stack and measure the improvements
- d. Further develop the support structure of the MCC panel
- e. Manufacture the improved support structure and enough MCC elements to fully populate two testable panels.

All objectives have been met.

3.2 TASK STATEMENTS

The task statements listed here were followed in performance of this contract. NASA directed modifications to the tasks following the basic statements.

- o Element Optical Design
 - Improve normal and off-pointing performance
 - Select materials and process based upon performance and cost
- o Cell Stack Development
 - Isolated/nonisolated element designs
 - Analysis/development test for 30,000 LEO cycle goal
- o Panel Development
 - Select substrate type (hexagonal/trihex grid)
 - Incorporate redesigned element
 - Finalize element attachment design
 - Test development hardware (elements, substrated, attachments)
 - Design panel wiring for 30,000 LEO cycles, manufacturability, low cost
 - Fabricate 15" x 56" panel (10 active elements)
 - Perform development tests in support of LEO goal
- o Pre-prototype Panel
 - Panel level design update
 - Fabricate 15" x 21" panel (100% active elements)
 - Deliver for long-term thermal cycling
- o NASA Modifications
 - Deliver the three elements developed in tasks 1 and 2 to NRL to support launch of test articles
 - Paint the primary and secondary emitting surfaces with S13GLO white thermal control coating

3.3 OPTIC INVESTIGATION AND TEST

Two efforts were initiated to improve the optic design of the MCC elements as compared to the design produced and tested under contract NAS8-35635 pictured in Figure 3-1.

The first effort was directed at finding reasons why performance of the design was not significantly in accordance with predictions. The second effort was directed to finding how to improve the offpoint performance of the design by changes in the mirror surface and interrelated geometries.

3.3.1 NAS8-35635 Investigation

3.3.1.1 Physical Measurements

The size and geometry of the primary mirrors was measured using a Cordex 3000 by sampling points along the surface in an absolute coordinate system. Results shown in Figures 3-2 and 3-3 indicate $\pm .0025$ inch error in the figure X coordinates compared to the theoretical design values. This is equivalent to a 6' arc error. The cup bottom on which the birdcage assembly rests was flat to within $\pm .0005$ inch. The cup center was offset from the primary surface figure center by 2 mils.

The center of the front surface of the solar cell was offset from the cup center by 3.8 mils. The height of the front surface of the solar cell from the cup interior surface was 1 mil lower than the designed placement.

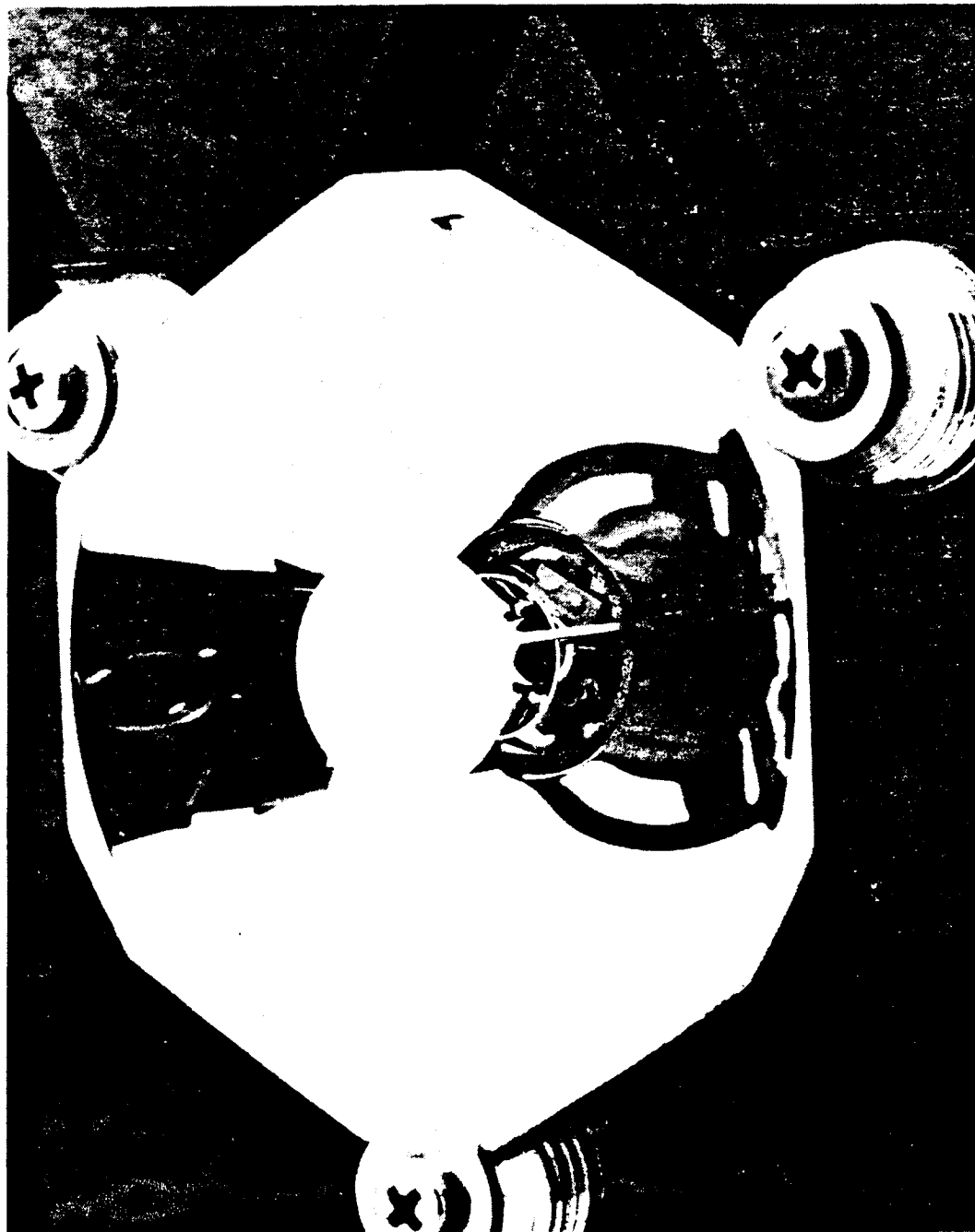
The placement of the secondary in the birdcage brought the tip of the secondary 12.5 mils above the nominal Z direction design point. The secondary was found to be tilted by $.12^\circ$ compared to the XY reference plane of the primary cup. A Numerex Surface Profilometer measured the surface of the secondary by dragging a scribe across in various radial directions. The surface geometry was within a 6' arc error.

When combined with the birdcage offsets, the secondary absolute position in the XY plane was found to be 10 mils offset from the primary mirror cup center.

FIGURE 3-1. FRONT SIDE VIEW OF PREDECESSOR NAS8-35635 MCC ELEMENT IN
TRI-HEX GRID



ORIGINAL PAGE IS
OF POOR QUALITY



SURFACE ACCURACY ERROR MEASUREMENTS
FOR #15 PRIMARY AND SECONDARY



Engineering & Test Division
TRW Space & Technology Group

	0	60	120	180	240	300	THEORY	\bar{X}	σ	Δ	TILT
PARABOLA	0						0				
.22	.0779	.0765	.0755	.0755	.0751	.0763	.0770	.0761	.0010	(.0009)	.27°
.294	.0810	.0807	.0802	.0796	.0795	.0806	.0802	.0803	.0006	.0001	.14°
.305	.1301	.1292	.1290	.1288	.1289	.1299	.1293	.1293	.0005	0	.09°
.438	.1763	.1775	.1765	.1745	.1765	.1776	.1746	.1765	.0011	.0019	.17°
.532	.2355	.2356	.2344	.2334	.2345	.2359	.2331	.2349	.0009	.0018	.11°
.633	.3105	.3099	.3080	.3075	.3082	.3100	.3076	.3090	.0013	.0014	.11°
.742	.3915	.3907	.3889	.3884	.3896	.3911	.3880	.3900	.0013	.0020	.10°
.844	.4741	.4734	.4727	.4708	.4725	.4743	.4712	.4730	.0013	.0018	.10°
.938	.5343	.5397	.5359	.5356	.5344	.5422	.5370	.5370	.0032	0	.22°
1.012	.5348	.5346	.5349	.5346	.5346	.5349	.5370	.5347	.0002	.0023	
1.025	.5855	.5852	.5853	.5850	.5851	.5855	.5370				
+ FIXT	.4392						.4328			.0064	
HYPERBOLA	0						.4656	.4715	.0012	.0059	.63°
.132	.4723		.4701	.5086	.4720	.5110	.5032	.5095	.0013	.0063	.43°
.200	.5107	.5085	.5080	.5418	.5099	.5434	.5369	.5430	.0007	.0061	.22°
.250	.5437	.5437	.5427		.5426						

FIGURE 3-2

SURFACE ACCURACY ERROR MEASUREMENTS FOR #12
PRIMARY AND SECONDARY



Engineering & Test Division
TRW Space & Technology Group

	0	60	120	180	240	300	THEORY	\bar{X}	σ	Δ	TILT°
PARABOLA 0	.0001	.0002	.0001	.0000	.0001	.0002	0				
.22	.0001	.0001	.0000	.0001	.0001	.0000	0				
.294	.0777	.0759	.0750	.0755	.0765	.0770	.0770	.0763	.0010	(.0007)	.26°
.305	.0810	.0801	.0797	.0802	.0804	.0800	.0802	.0802	.0004	0	.12°
.438	.1300	.1286	.1283	.1280	.1285	.1289	.1293	.1287	.0007	(.0006)	.11°
.532	.1762	.1765	.1759	.1742	.1764	.1773	.1746	.1761	.0010	.0015	.08°
.633	.2356	.2346	.2342	.2332	.2344	.2354	.2331	.2346	.0009	.0015	.06°
.742	.3110	.3087	.3078	.3079	.3082	.3093	.3076	.3088	.0012	.0012	.12°
.844	.3919	.3892	.3883	.3890	.3889	.3910	.3880	.3897	.0014	.0017	.12°
.938	.4755	.4721	.4712	.4722	.4710	.4732	.4712	.4725	.0017	.0013	.14°
1.012	.5342	.5352	.5418	.5424	.5335	.5359	.5370	.5372	.0039	.0002	---
1.025	.5348	.5347	.5350	.5349	.5349	.5348	.5370	.5349	.0001	(.0021)	.006
HYPERBOLA 0	.4453						.4328	.4453		.0125	
.132	.4776	.4773	.4768	---	.4767	---	.4656	.4771	.0004	.0115	.13°
.200	.5160	.5156	.5142	.5149	.5149	.5163	.5032	.5153	.0008	.0121	.30°
.250	.5482		.5479		.5489		.5369	.5483	.0005	.0114	.11°
FIXTURE LIP	.0507	.0506	.0504	.0504	.0505	.0506					

FIGURE 3-3

.12°	SECONDARY TILT
.6°	BIRDCAGE TILT
1.8°	CONE TILT
.0118	SECONDARY XY DISPLACEMENT
.005	CONE XY DISPLACEMENT
.0125	SECONDARY + Z DISPLACEMENT
.024	CONE + Z DISPLACEMENT
6'	PRIMARY ARC ERROR
6'	SECONDARY ARC ERROR
31.1°	CONE ARC ERROR (.4)
.0038	BIRDCAGE XY DISPLACEMENT (CELL DISPLACED)

FIGURE 3-4: ELEMENT #12 TOLERANCE ERRORS

.006	SECONDARY XY DISPLACE
.006	SECONDARY \bar{X} DISPLACE UP
.010	CONE DISPLACE Z UP
.005	CONE DISPLACE XY
.12	SECONDARY TILT
0.8	CONE TILT
0	BIRDCAGE DISPLACE X AXIS
.6	BIRDCAGE TILT
6	MINUTE PRIMARY ARC ERROR
2	MINUTE SECONDARY ARC ERROR
31.1°	CONE ARC ERROR

FIGURE 3-5: ELEMENT #15 TOLERANCE ERRORS

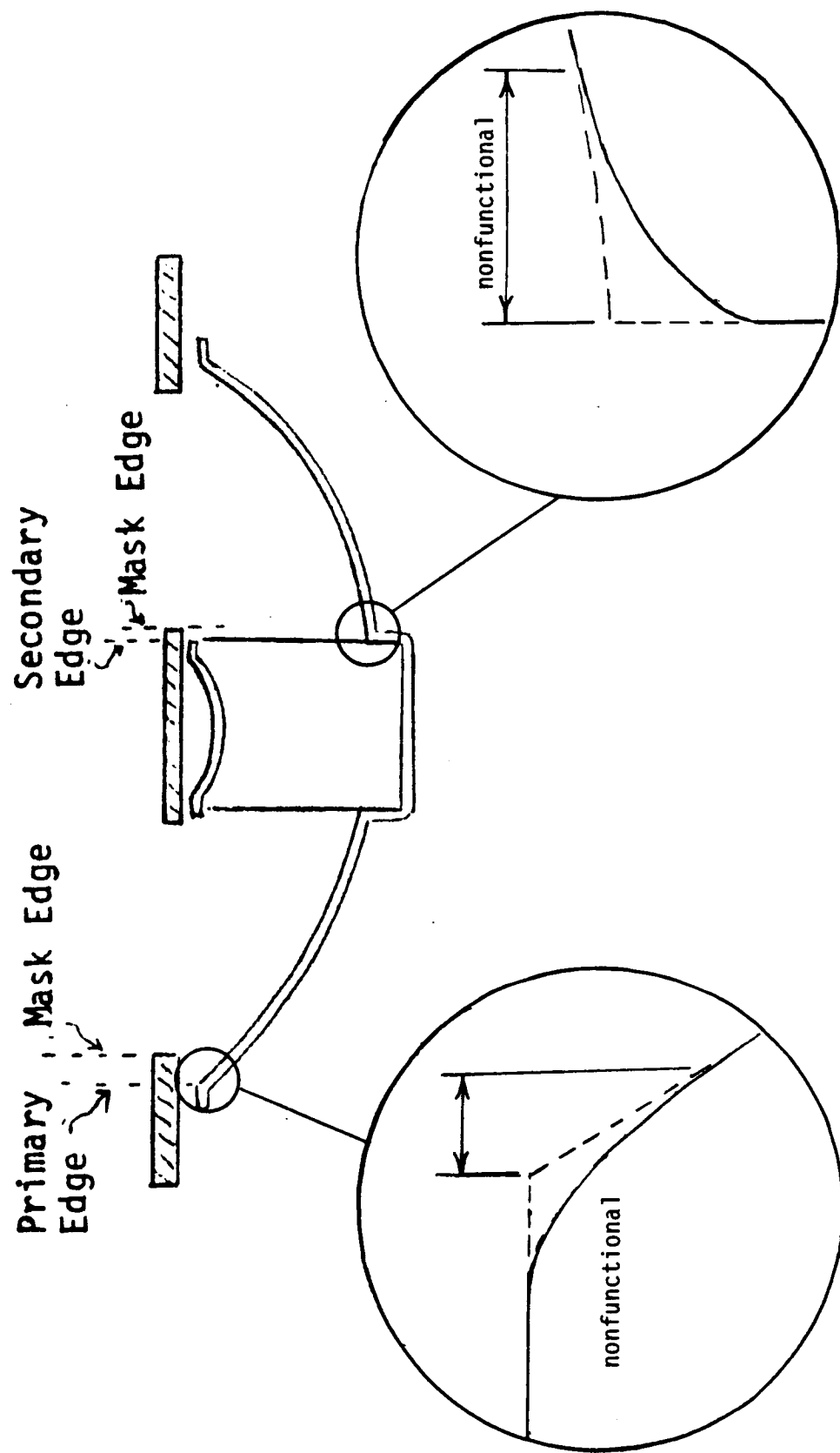


FIGURE 3-6. ROUNDED AREAS OF THE PRIMARY WERE FOUND NOT TO CONTRIBUTE TO COLLECTION EFFICIENCY AS DESIGNED.

The cone lower edge was 10 to 20 mils above the cell. This compares to a design goal of zero Z displacement. The cone XY plane offset was measured at 5 mils from the cup center. The cone angle designed to be 31.5° , was measured to be 31.1° . The cone as mounted in the birdcage was tilted from the XY plane by 1.3° .

The average measurements above are summarized from Figures 3-4 and 3-5.

3.3.1.2 Measurement of Optical Losses

Primary Mirror. It was noted that there was some rounding of the optic edges at the inside and outside of the primary (Figure 3-6). To see if this contributed to energy collection losses, a number of masks were created to successively shadow more and more portions of the mirror in those positions using the theory that shadowing of unused portions would produce no change in output. The optic was set in a solar tracker specially designed for this application and current output was monitored. Successive masking of the outer edge was performed until a noticeable drop in current was seen. The size of the mask inner diameter was compared to the optic design and was noted to be approximately 19 mils less in radius than the primary mirror outer edge. This represented a 4% loss in collection efficiency from expected.

More masks were placed on the secondary mirror with successively greater diameters until again a noticeable drop in output was noted. This radius represented the unusable portion of the primary mirror near the inner cup edge. The distance, .298 mils or 33 mils greater than the inner cup radius design, represented approximately 2% loss in collection efficiency.

The primary mirror was physically distorted by screwing the edges down in the holding fixture with excessive force to see the effective change in output. A 2.1% loss in output was noted at the extreme range of distortion, estimated at 10 to 20 mils of "squeeze."

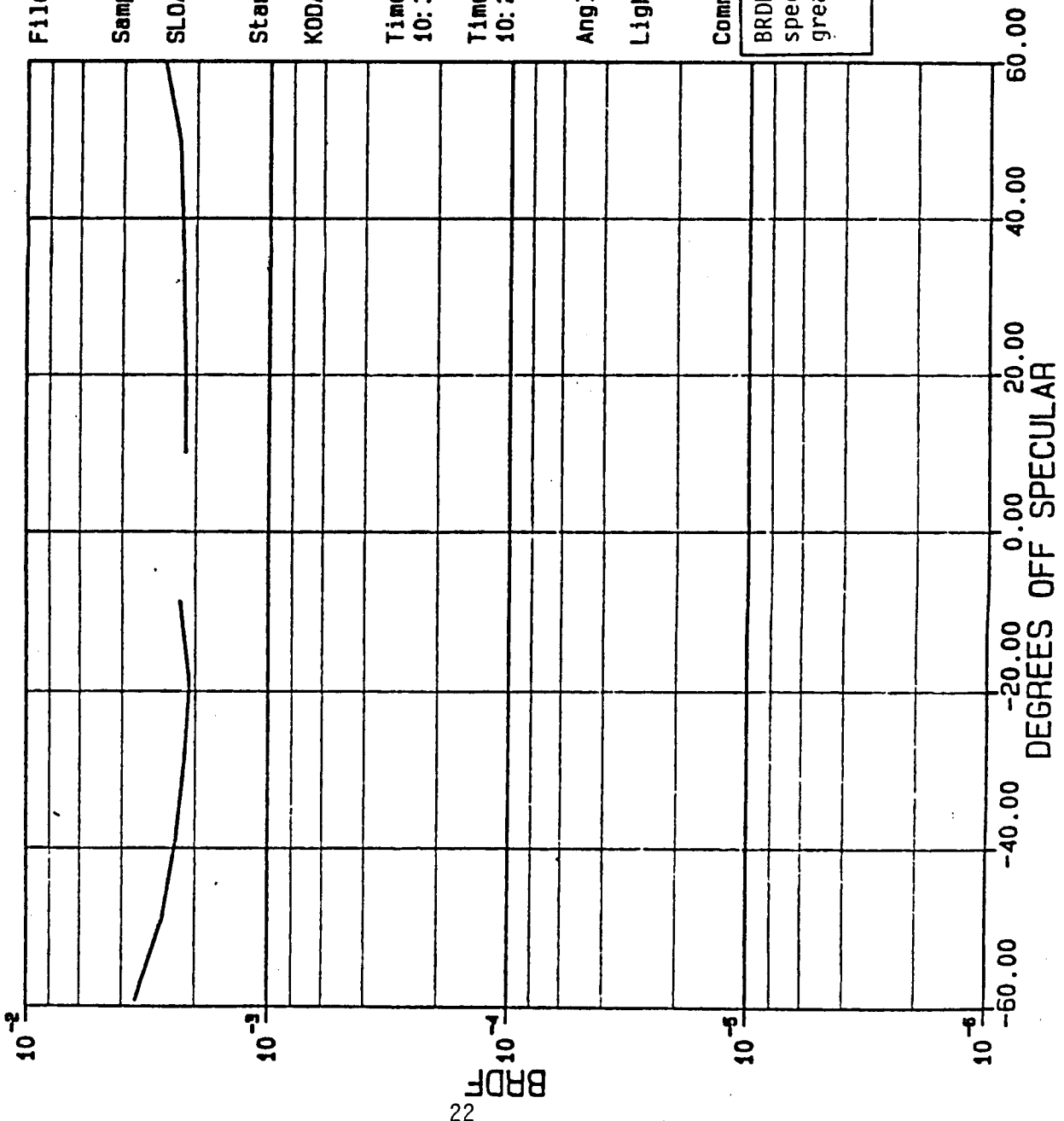
Conic Mirror. The gap between the cone and the cell represented an "escape" route for the collected light. To check this the optic was mounted in a fixture such that the cone could be varied from 0 to 80 mils from the surface of the cell. The measured loss was 0.3%/mil of gap for 0 pointing error and with a 15 mil gap, a 14% loss was experienced at 2° offpoint.

3.3.1.3 System Effects

Mirror Reflectance. The reflectance of each mirror has a direct effect on energy throughput. In all positions, the primary and secondary mirrors will redirect the light with some resulting reflectance loss composed of absorbed light and diffusely reflected light not reaching the cell. The amount of light reflected by the cone is a function of offpoint. The AMO reflectance of silver is generally quoted at 95% energy throughput. Since the GaAs cell only responds to light with wavelength between 0.4 and 0.9 micrometer,, the reflectance of the mirrors in this range is of interest and must be used for energy throughput calculations as measured by a GaAs device. To this end, spectral reflectance measurements of primary and secondary mirror samples were made. Based upon these measurements, the effective reflectance in the band 0.4 to 0.9 micrometer, was calculated for solar outputs of AMO, AM1, and AM2. The AMO reflectance averaged 0.965 for the secondary and 0.985 for the primary, and was not significantly different when calculated for AM1 and AM2 standard suns.

Specular Reflectance. Mirror samples were submitted for overall scatter measurements. A measurement is shown in Figure 3-7. The measurement corresponds to roughly 11% loss of usable light in the MCC optical system.

Misalignment Effects. The intention of this test was to get a feel for the sensitivity of the optics to possible assembly misalignments. A MCC element was mounted in the solar tracker and the birdcage containing the cone and secondary were misaligned from the most stable position. Slight movements (5 to 10 mils) of the birdcage resulted in output changes of up to 10% (see Figure 3-8).



File name = SST03727 BY SSTVI

Sample title:

SLOAR CELL MIRROR 2

Standard title:

KODAK WHITE STANDARD

Time of sample run:

10:30 AM WED., 30 APR., 1986

Time of standard run:

10:24 AM WED., 30 APR., 1986

Angle of incidence = 0.0

Light source = White light

Comments:

BRDF is indication of energy at off specular positions. Higher BRDF means greater off axis scatter.

FIGURE 3-7. NAS8-35635 MIRRORS WERE RELATIVELY DIFFUSE.

Distortion Can Cause Significant Loss of Output



ELEMENT 15

- = EXISTING DISTORTION, WITH CONE
- · - = EXTRA DISTORTION, CONE
- - - = EXISTING DISTORTION, NO CONE
- - - = EXTRA DISTORTION, NO CONE
- - - = UPPER-PREDICTED, WITH CONE
- - - = LOWER-PREDICTED, W/O CONE

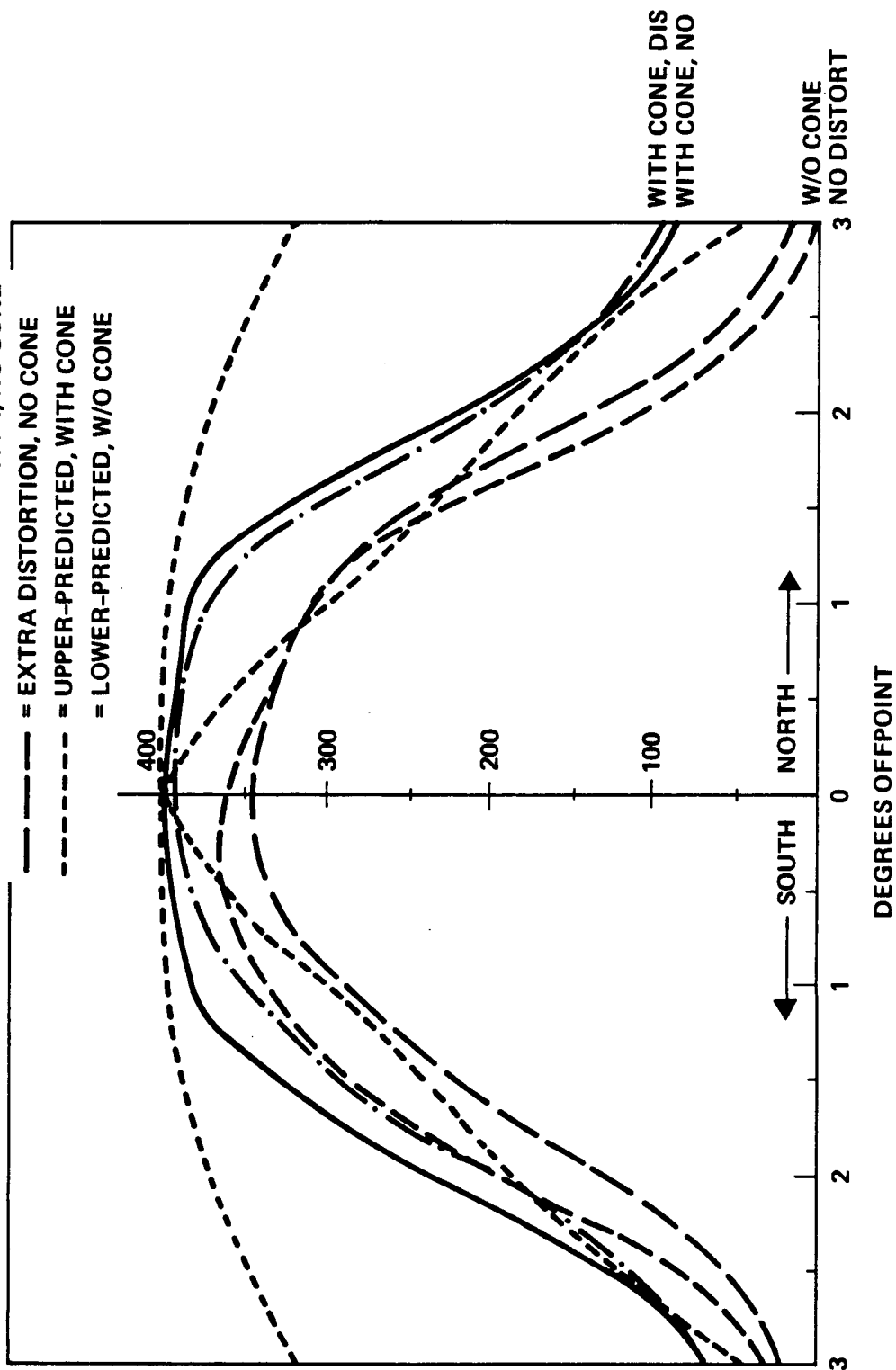


Figure 3-8

3.3.1.4 Summary

A summary of the optical testing of the NAS8-35635 design is shown in Figure 3-9 for on point measurements and Figure 3-10 for offpoint measurements.

The many potential loss mechanisms that were apparent could easily account for the nine percent onpoint loss (7%/77%). Offpoint losses for the design could be even worse especially due to the misalignments inherent in any manufacturing process.

3.3.1.5 Electrical Measurements

Electrical output measurements of the optics studied above were reported in NAS8-35635 as 9 to 11% loss in output during onpoint with the expected concentration ratio of 127 not met by the test measurements of ~114. These measurements were reconfirmed. Offpoint testing was also performed as in Figure 3-8 to reconfirm the data.

3.3.2 Analyses

Two analyses were performed to support the investigation and testing of the NAS8-35635 MCC.

3.3.2.1 Specular Reflectance Analysis

A computer model of the MCC element was generated and energy loss due to scatter from the mirror surface was calculated as a function of overall mirror reflectance and RMS surface roughness. The results, shown graphically in Figure 3-11, indicate that surface roughness must be tightly controlled to minimize scatter losses. The NAS8-35635 polished to a "commercial" finish had a finish between 200 angstrom to 1000 angstrom roughness. At 200 angstrom and .98 mirror reflectance, the loss of energy attributable to scatter alone was 0.19 $-[1-(.98)^2] = .15$ i.e., 15%.

3.3.2.2 Tolerance Analysis

The mirror assembly was analyzed for output using the IPAGOS optical analysis program as modified for the MCC system to determine collection efficiency as a function of offpoint. The standard curve for perfectly aligned optics is the one shown for technology development goals. However, since mirrors are

TEST RESULT - 70 vs. 77% OPTICAL TRANSMISSION INVESTIGATION



Engineering & Test Division
TRW Space & Technology Group

POTENTIAL LOSS MECHANISM	METHOD OF INVESTIGATION		% LOSS EFFECT
A. GAP BETWEEN CONE AND CELL	TEST	Change gap from 0 to 80 mils distance from cell and measure output. (Note gap 40 mils, should be 0)	0.3%/mil
	ANALYSIS	Tolerance analysis of sub assemblies and piece parts for effect on output.	0% all distances
B. LIGHT NOT FOCUSED COMPLETELY ON CELL (DISTORTION OR FIGURE IRREGULARITIES)	TEST	Test element with and without cone in place. Note any stray light not hitting cell.	.2% to .7%
C. MISALIGNMENT OF ASSEMBLY PARTS	TEST	Purposely misalign mirrors to see effect on output	—
	ANALYSIS	Tolerance analysis as above	up to 10% for small dev.
D. DISTORTION OF MIRRORS (INDUCED BEYOND ALREADY DISTORTED UNRECTIFIED MIRROR.)	TEST	Distort mirrors while testing.	.9 to 2.1%
	ANALYSIS	Note types of distortions and effect on output. Tolerance analysis as above	
E. MIRRORS OUT OF SPECIFICATION REQUIREMENTS	TEST	Shadow various portions of mirror surface to find effect on output. Compare to theoretical effect on output.	6%
	ANALYSIS	Tolerance analysis as above.	
F. SPECTRAL SHIFT OF AMI SUNLIGHT THROUGH OPTICAL ELEMENTS	TEST	Measure spectral reflectance of mirrors.	N/A
	ANALYSIS	Calculate mirror reflectance based on cell response wavelengths 0.38 to 0.93 μ m and AMO and AMI solar spectrum.	-5.6%
G. NON SPECULAR REFLECTANCE	TEST	Use modified integrating sphere for direct vs. diffuse reflectance from mirror parts. BRDF measurement equipment.	—
	ANALYSIS	Calculate effect of progressively diffuse surface based on surface roughness and spectral reflectance	up to 40% 10 % most likely
H. TEST EQUIPMENT	TEST	Check wiring.	0
		Check sun tracking capability. Acquire GaAs standard for incorporation into test setup.	+ 1.5%
I. PROGRAM ERROR	ANALYSIS		1%

FIGURE 3-9

TEST RESULTS - OFF AXIS PERFORMANCE INVESTIGATION

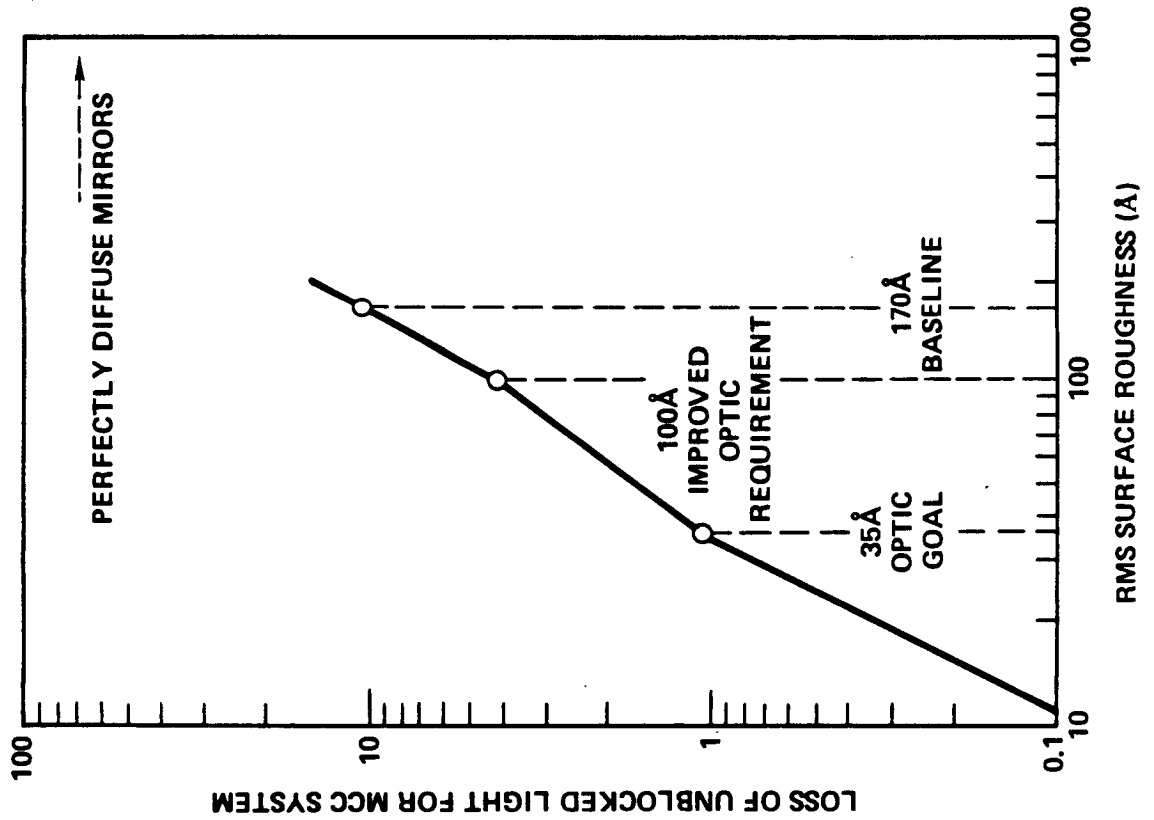


Engineering & Test Division
TRW Space & Technology Group

POTENTIAL LOSS MECHANISM	METHOD OF INVESTIGATION		% LOSS EFFECT
A. GAP BETWEEN CONE AND CELL	TEST	Change gap from 0 to 80 mils distance from cell and measure output. (Note gap \approx 15 mils, should be 0).	1° - 2% 2° - 14% 3° - 38%
	ANALYSIS	Tolerance analysis of sub assemblies and piece parts for effect on output.	1° - 7.6%/10 mils 2° - 13.1%/10 mils 3° - 42%/10 mils
B. LIGHT NOT FOCUSED COMPLETELY ON CELL (DISTORTION OR FIGURE IRREGULARITIES)	TEST	Test element with and without cone in place. Note any stray light not hitting cell.	1° - 9% 2° - 1% 3° - .4%
	ANALYSIS		
C. MISALIGNMENT OF ASSEMBLY PARTS	TEST	Purposely misalign mirrors to see effect on output.	—
	ANALYSIS	Tolerance analysis as above.	F.3-12 - 3-17
D. DISTORTION OF MIRRORS (INDUCED BEYOND ALREADY DISTORTED UNRES-TRICTED MIRROR).	TEST	Distort mirrors while testing.	1° - 5% 3° - 12% 2° - 11%
	ANALYSIS	Tolerance analysis as above.	F.3-12 - 3-17
E. MIRRORS OUT OF SPECIFICATION REQUIREMENTS	TEST	Shadow various portions of mirror surface to find effect on output. Compare to theoretical effect on output.	Same as on axis
	ANALYSIS	Tolerance analysis as above	F.3-12 - 3-17
F. PROGRAM ERROR	ANALYSIS	Change method of ray trace inputs to see if variation causes change in offpoint prediction	1° - 7% 2° - 10% 3° ~ 0%

FIGURE 3-10

Effect of Mirror Finish On Performance



- AVERAGE MEASURED ROUGHNESS FOR NAS8-35635 WAS 170 Å
- OUTPUT REDUCTION EXPECTED: 10.3%
— RELATIVE TO 78% NORMALIZATION: 7%
- BASED ON GAAS RESPONSE REGION
0.4 TO 0.9 μm , AMO
- BASED ON MCC BASELINE CONCENTRATING OPTIC

not ideal surfaces due to inherent piece part manufacturing tolerance allowances, and mirror assemblies further suffer from tolerance allowances, it was decided to investigate the sensitivity of the optic design to these tolerances.

Each mirror component was considered separately and then as a typical composite based on measurements of the optics as assembled from section 3.3.1.1.

Each component was analyzed for the effect on energy collection as a function of translations along three orthogonal axes, rotations about three orthogonal axes and surface allowances as called out in the mirror manufacturing specifications such as the 10 arc minute allowance variation in the figure of the primary mirror or the $31^{\circ} \pm .5^{\circ}$ cone angle allowance.

The results are illustrated in Figures 3-12 to 3-17, for individual components. In some cases, the design is very sensitive to tolerances which are fairly tight in the design. When a combination of factors is considered, the resulting offpoint is illustrated in Figure 3-18. Included in the figure are the test results from two measured optics. The test performance is actually better than that predicted since the prediction assumed all worst case directions for output loss.

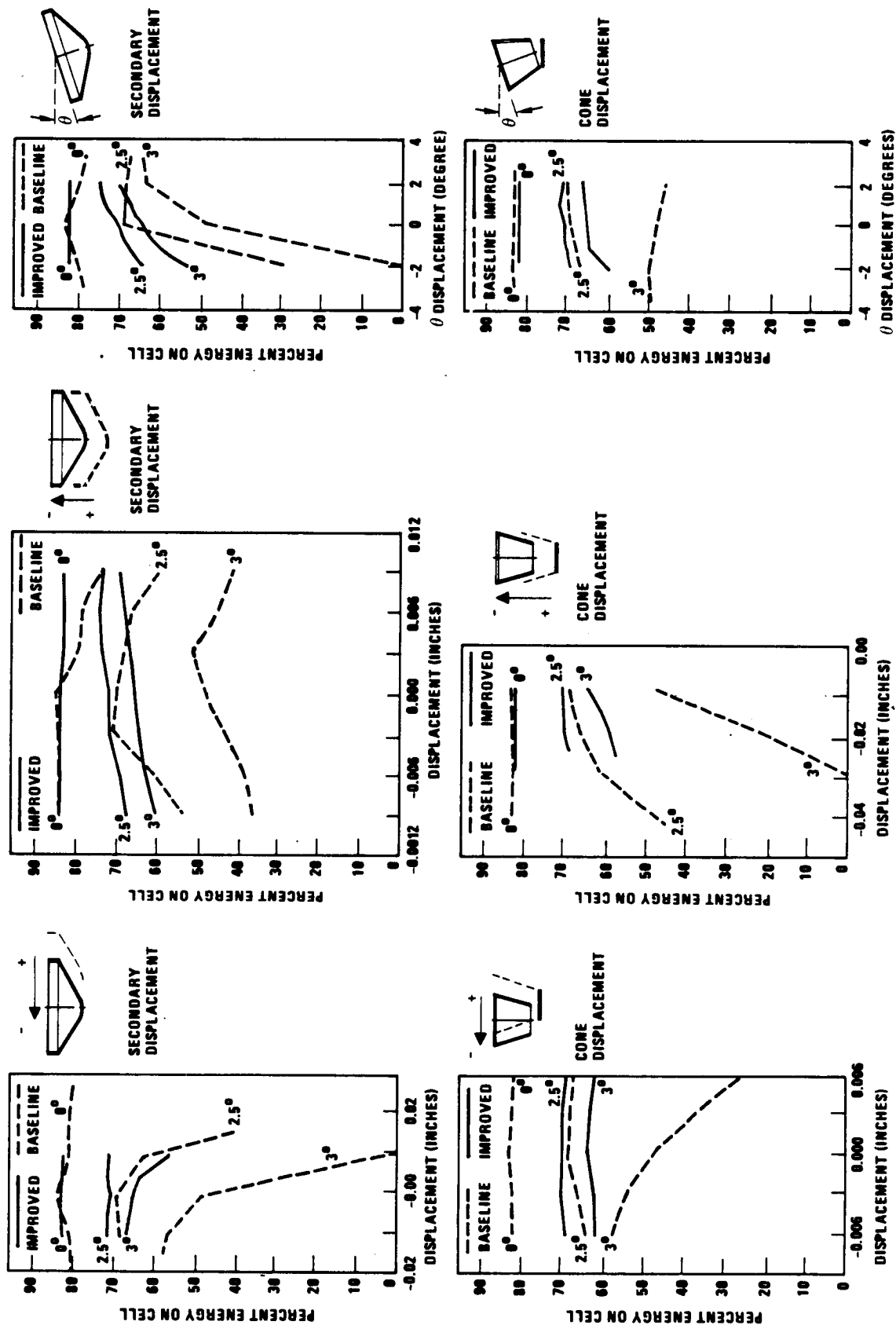
3.3.2.3 Optical Design

The design of the conventional Cassegrain system was varied to determine what improvements in offpointability could be achieved without significantly decreasing onpointed output. Results from an IR&D project showed that changing the geometric concentration ratio from the baseline 163 to lower values improved offpointability at increasing loss of optical transmission (Figure 3-19).

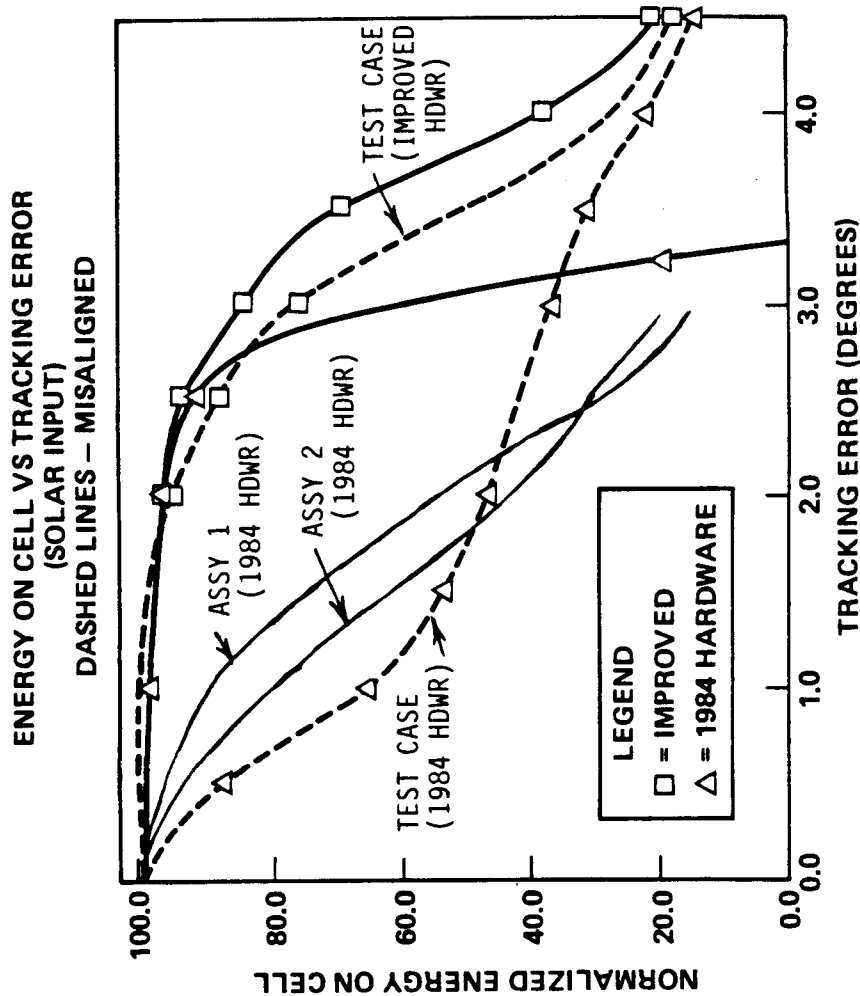
If the thickness of the system was allowed to vary, improvements in offpointability could also be achieved (Figure 3-20) but with significant decrease in volumetric packing for launch.

Some slight improvements could be made by varying the conic mirror surface, but none would address the inherent problem of tolerance allowance losses (missing of the mirror entirely).

FIGURES 3-12 to 3-17. EFFECT OF SELECTED TOLERANCES ON MCC PERFORMANCE
NEW VS. OLD DESIGN.



Multiple Misalignment Test Case



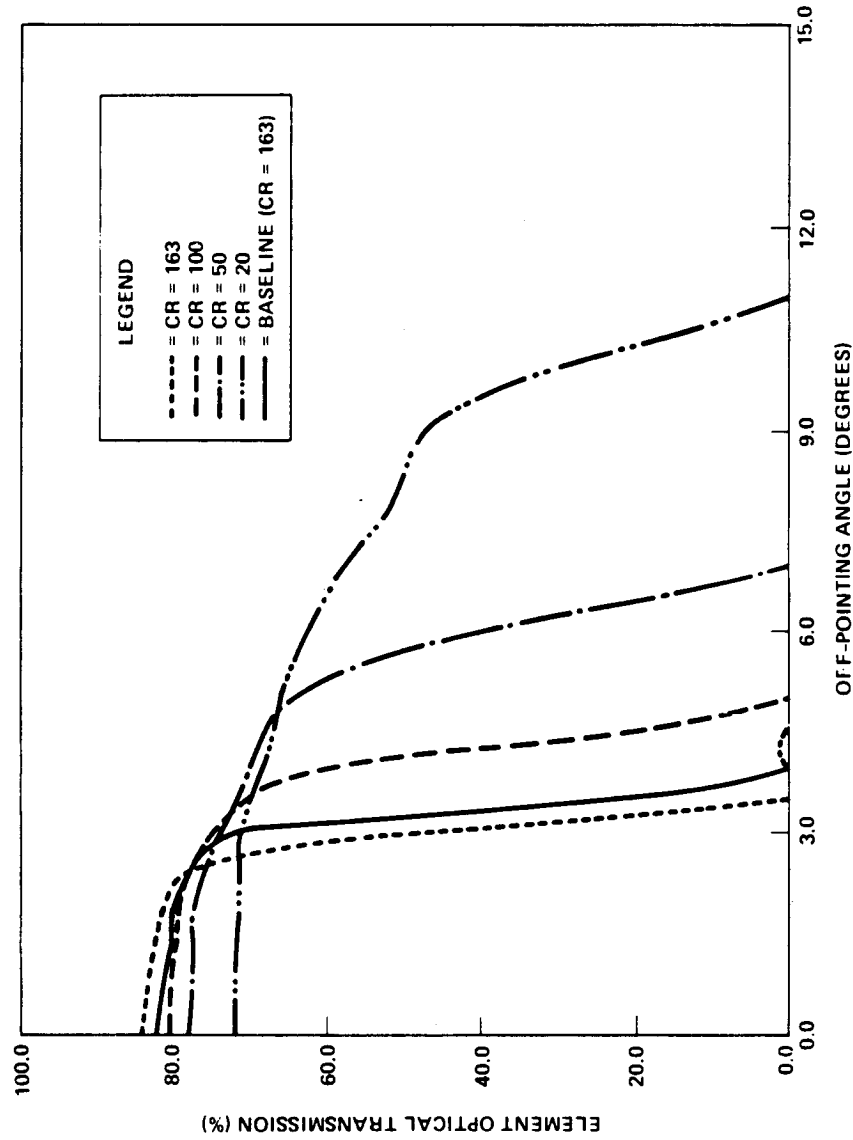
SAMPLE MISALIGNMENT	TEST CASE	ASSY 1	ASSY 2
PRIMARY FIGURE	0.1°	0.1°	0.1°
SECONDARY HORIZONTAL DISPLACEMENT	0.002"	0.0118"	0.006"
SECONDARY VERTICAL DISPLACEMENT	0.0015"	0.0125"	0.006"
SECONDARY OPTIC AXIS TILT	0.15°	0.12°	0.12°
CONE HORIZONTAL DISPLACEMENT	0.002"	0.005"	0.005"
CONE VERTICAL DISPLACEMENT	0.0095"	0.024"	0.010"
CONE OPTIC AXIS TILT	0.25°	1.8°	0.8°

- MAXIMUM IN-LINE TOLERANCE EFFECT
- BASELINE SENSITIVE TO MULTIPLE TOLERANCES
- IMPROVED DESIGN SIGNIFICANTLY LESS SENSITIVE

FIGURE 3-18

Optical Design Investigation Performance versus Concentration Ratio

Engineering and Test
Division
TRW Space &
Technology Group



- Reduced concentration ratio:
- Improves off pointing
 - Degrades on pointing
 - Significantly increases cost (GaAs solar cell size)

FIGURE 3-19 MCC ELEMENT OFF-POINTING PERFORMANCE WITH CONCENTRATION RATIO AS A PARAMETER

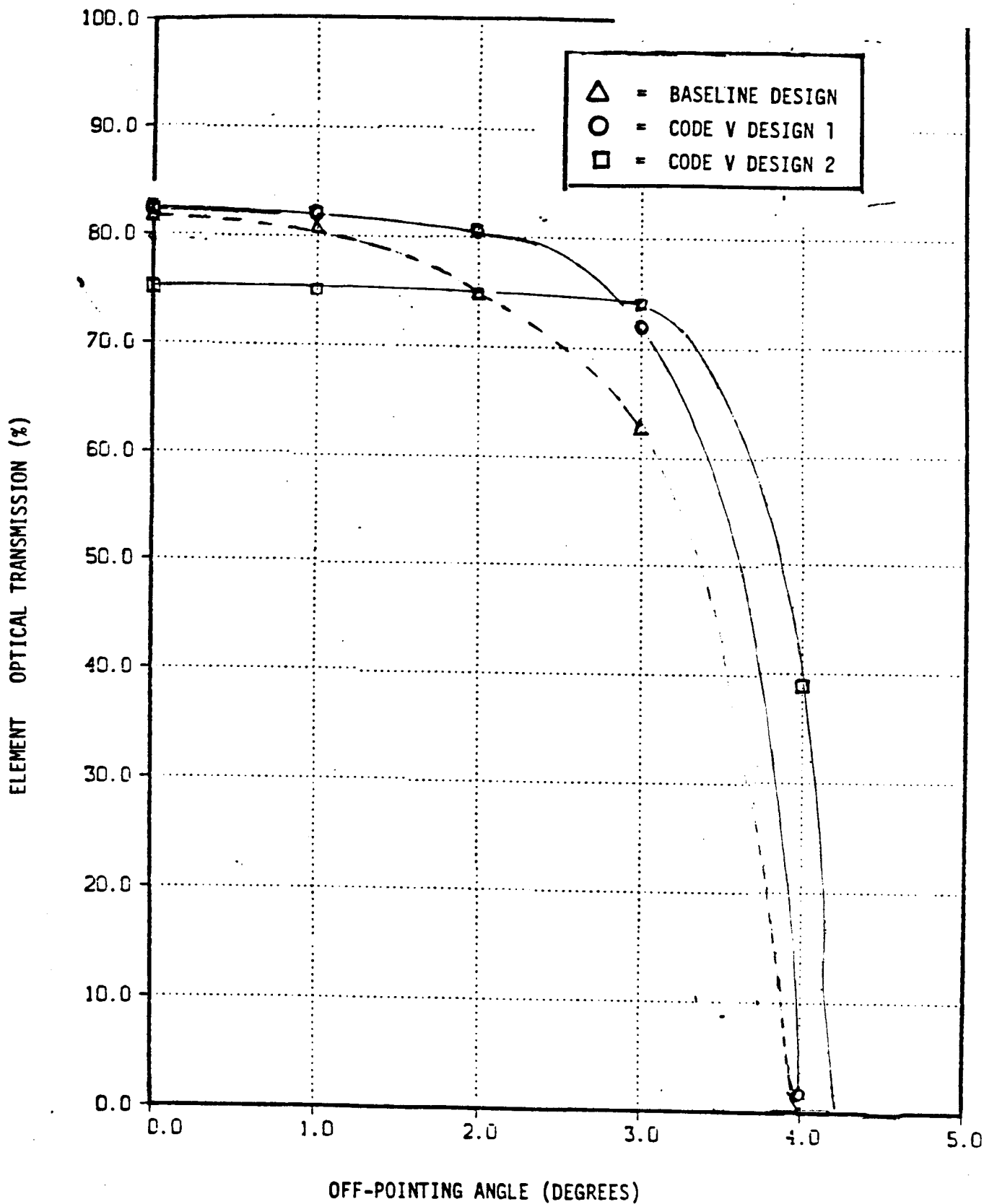


FIGURE 3-20: MCC Element Off-Pointing Performance of CODE V Optimized Designs

It was decided to dispense with conventional optical design techniques to achieve offpoint enhancement. Instead, a technique was conceptualized to use portions of the secondary mirror to redirect light from the primary during offpoint conditions toward the cell (Figure 3-21) as well as modify the surface figure of the portions used during onpointing to also direct any remaining offpointed light to the cone and thence to the cell. It was decided to optimize the design for three degrees of offpoint. The NAS8-35635 secondary mirror blockage diameter of 0.564 inches was retained to allow comparison with the NAS8-35635 design even though the actual mirror surface was only 0.50 inches in diameter. After a number of two dimensional iterations of the optic stack surface figures, the resulting operation of the stack in two dimensions seemed satisfactory as shown in Figures 3-22 through 3-24. Except for a very few rays, all rays entering the optic reach the cell.

3.3.2.4 Support Analysis

A three dimensional computer model was constructed for IPAGOS analyses. Calculation of the offpoint performance showed tremendous improvement over the baseline design (Figure 3-25).

The model was analyzed for tolerance effects as was the baseline and again tremendous improvement was seen. Figures 3-12 through 3-17 show the improved capabilities compared to the baseline design. The multiple parameter tolerance buildup was input to the model and again the improvement was great (Figure 3-18).

The secondary mirror was further optimized for output by consideration of changing the angles of the mirror portion devoted to redirecting the offpointed rays. Figure 3-26 shows the effect of varying the inner and outer zones from the baseline.

The design was checked against an optimal hyperbolic secondary which used the full 0.564 diameter of the secondary mirror blockage size for light collection. Cone angle was varied to check for possible synergistic design effects. Figure 3-27 displays the results of this comparison. The new secondary is clearly superior in the quantity of light collected.

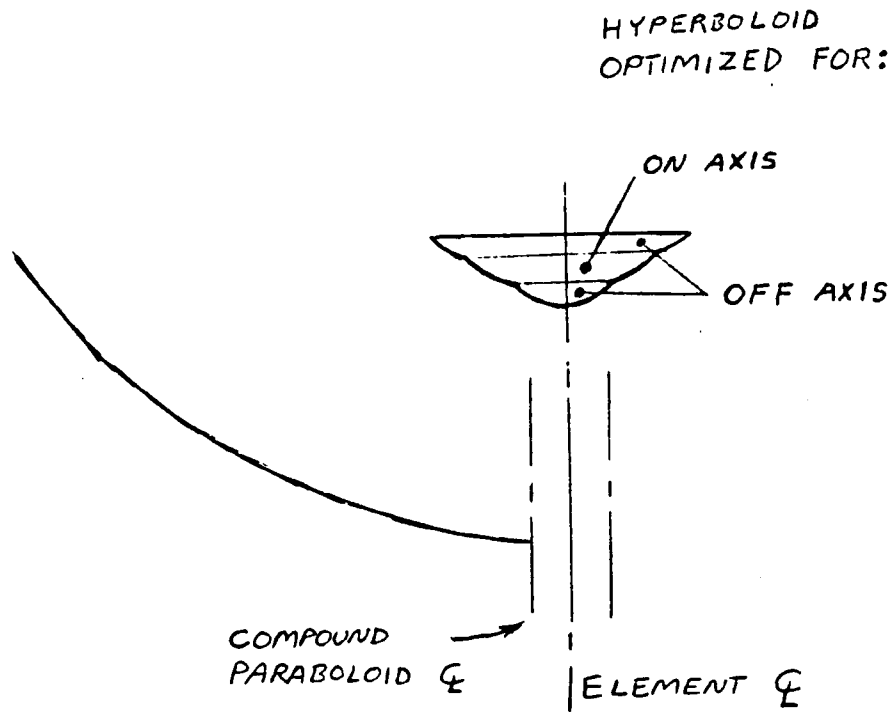


FIGURE 3-21: CONCEPT USED TO REDESIGN THE COMPLETE MCC OPTICAL STACK.

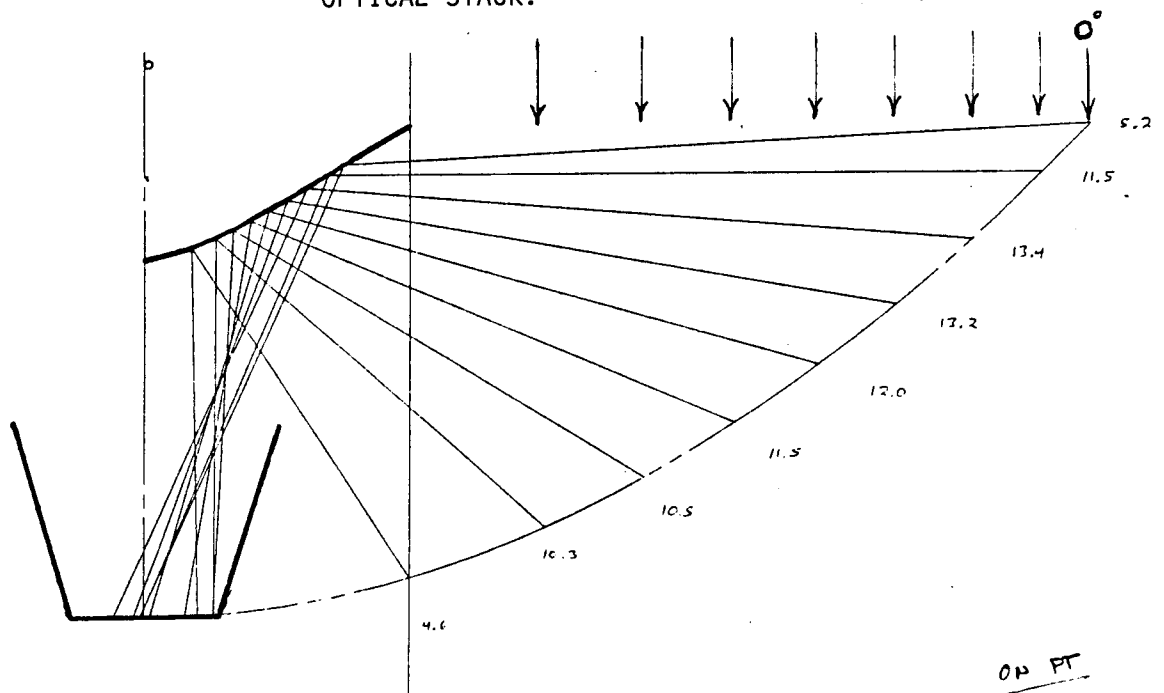


FIGURE 3-22: NEW DESIGN SHOWING RAY TRACE FOR ENTRANCE OF RAYS WITH ZERO POINTING ERROR.

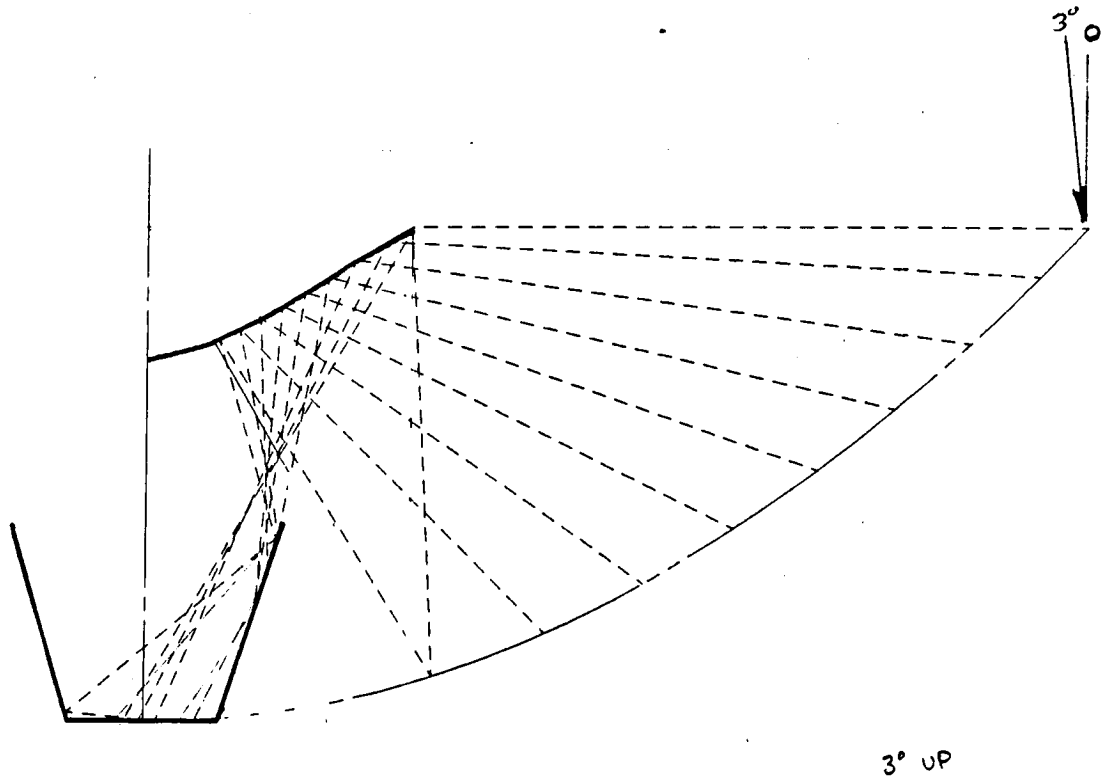


FIGURE 3-23: NEW DESIGN SHOWING RAY TRACE FOR ENTRANCE FROM THREE DEGREES FROM THE LEFT.

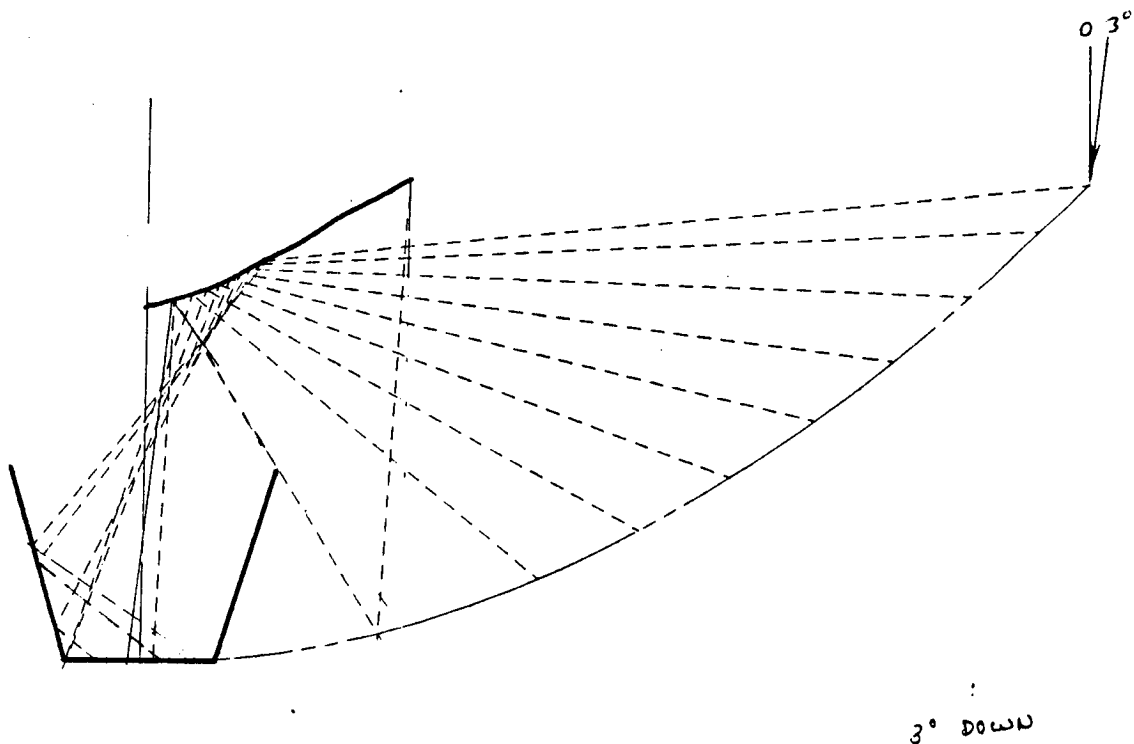
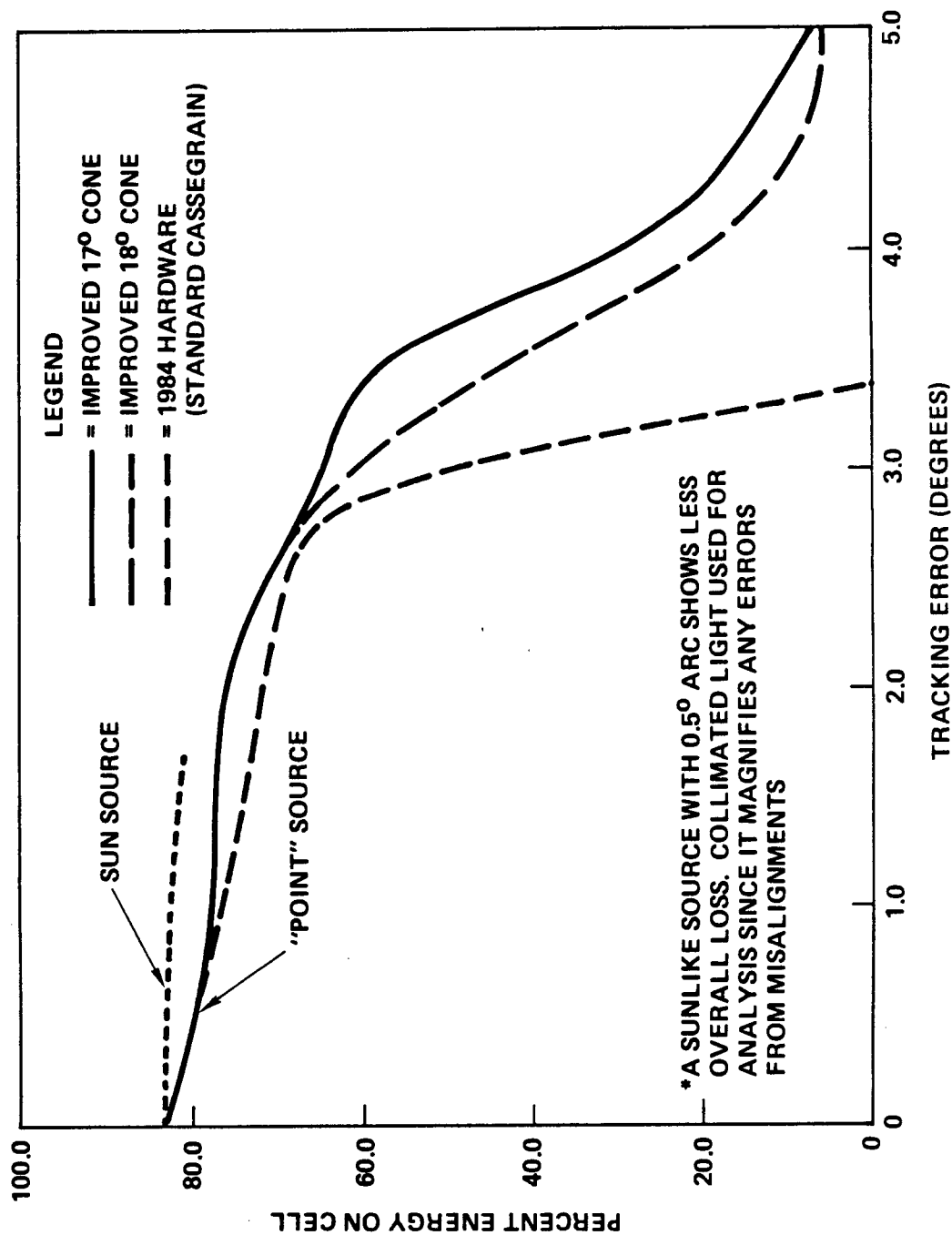


FIGURE 3-24: NEW DESIGN SHOWING RAY TRACE FOR ENTRANCE FROM THREE DEGREES FROM THE RIGHT.

Energy on Cell vs Tracking Error Collimated Source*



Rays Reaching Cell versus Variations of Secondary Offpoint Collection Angles. The New Design is Fairly Insensitive to Figure Errors



OFFPOINT ANGLE	BASELINE (15°) (30°)	VARY ANGLE 1				VARY ANGLE 2*	
		10° (30°)	20° (30°)	25° (30°)	30° (30°)	(15°) 27°	(15°) 33°
0	4524	4524	4524	4524	4524	4524	4524
2	4286	4286	4286	4286	4286	4286	4286
2.5	4039	4039	4039	4031	4035	4035	4047
3	3698	3698	3698	3686	3680	3680	3718
3.5	3222	3183	3218	3202	3190	3190	3139
4	1686	1600	1680	1662	1647	1647	1260
4.5		806	908	898			
NAME	SEC140	SEC640	SEC540	SEC440	SEC141	SEC142	

*NORMALIZED TO SAME OBSCURATION AS BASELINE

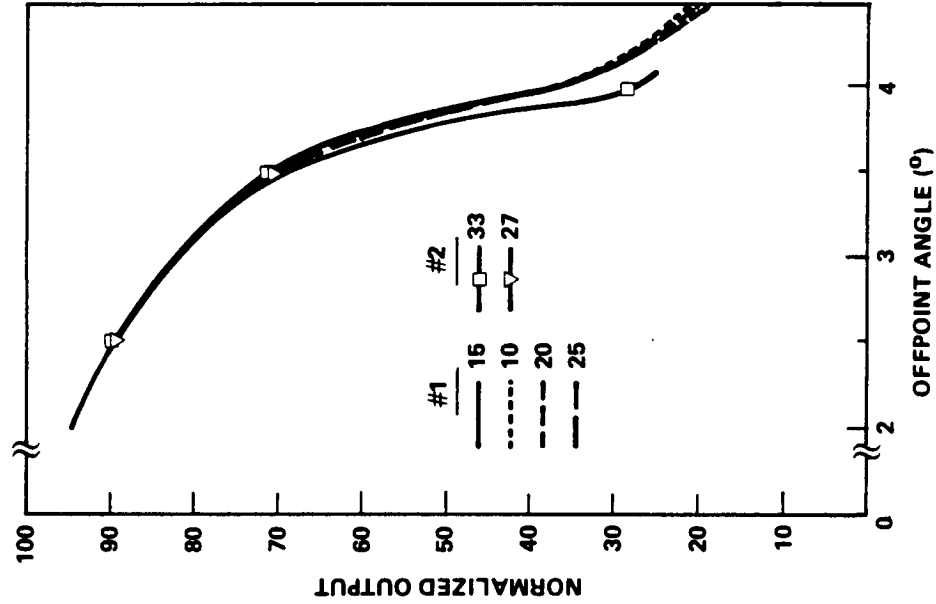
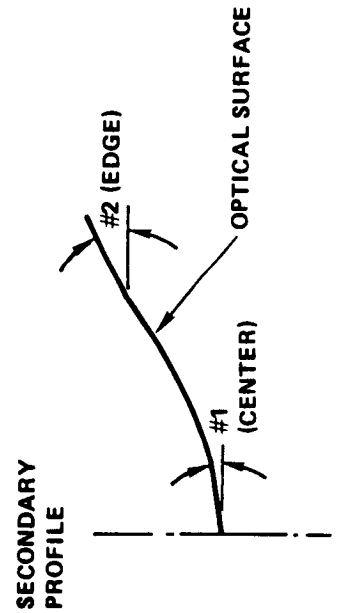


Figure 3-26

New vs Hyperbolic Output

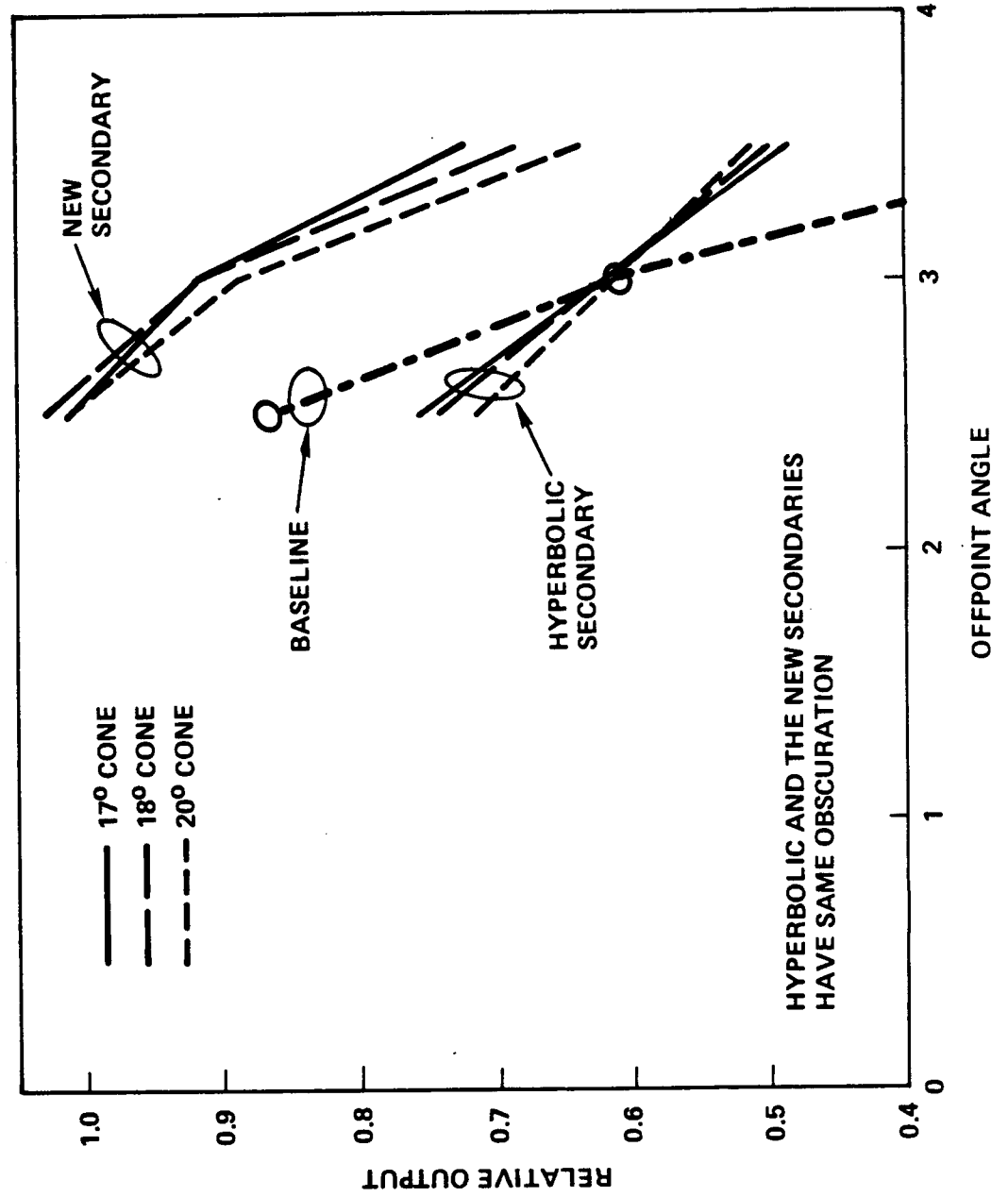


Figure 3-27

The cone angle for the new system was optimized at 17° . A 17° versus 18° cone angle comparison is shown in Figure 3-25.

3.3.2.5 New Design Optics

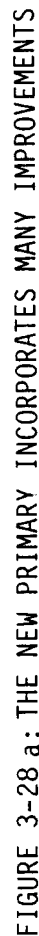
The new primary is shown in Figure 3-28. The new secondary is shown in Figure 3-29 and the new cone in Figure 3-30.

3.3.2.6 Part Physical Measurements

New optics were ordered to the design derived in the above analyses. The first articles were measured for surface figure and part tolerances. Since the parts were designed with keying for assembly measurements to these keys were added together for the various components to create tolerance build up potential offsets.

As for the NAS8-35635 design, the positioning of the cell surface and XY placement within the cup, the XYZ positioning of the secondary mirror considering the tolerances measured, and the XYZ positioning of the cone considering the tolerances measured were determined. All part dimensions except for the secondary figure were found to be within the tolerance allowances generated for the part manufacturing specifications (Figure 3-31) from the tolerance analyses. Actual values are given in Appendix A.

A Jones & Lambson EPIC 30 comparator was used to check for figure accuracy of the cone, secondary and primary against an accurate mylar of the drawings in the appropriate magnification range. A casting of the primary was made from the first article which was then checked on the comparator at 10 x magnification. The cone and the secondary were directly checked at 20 x. The primary and cone were within the required figure tolerance. The secondaries (ten in all) deviated from the required figure by varying amounts. Due to schedule constraints, it was decided to use seven of them which were believed to be close enough but not within tolerance, with the intention of checking the effect of the variations by electrical measurements of a single standard primary subassembly which included everything except the secondary and secondary mounting.



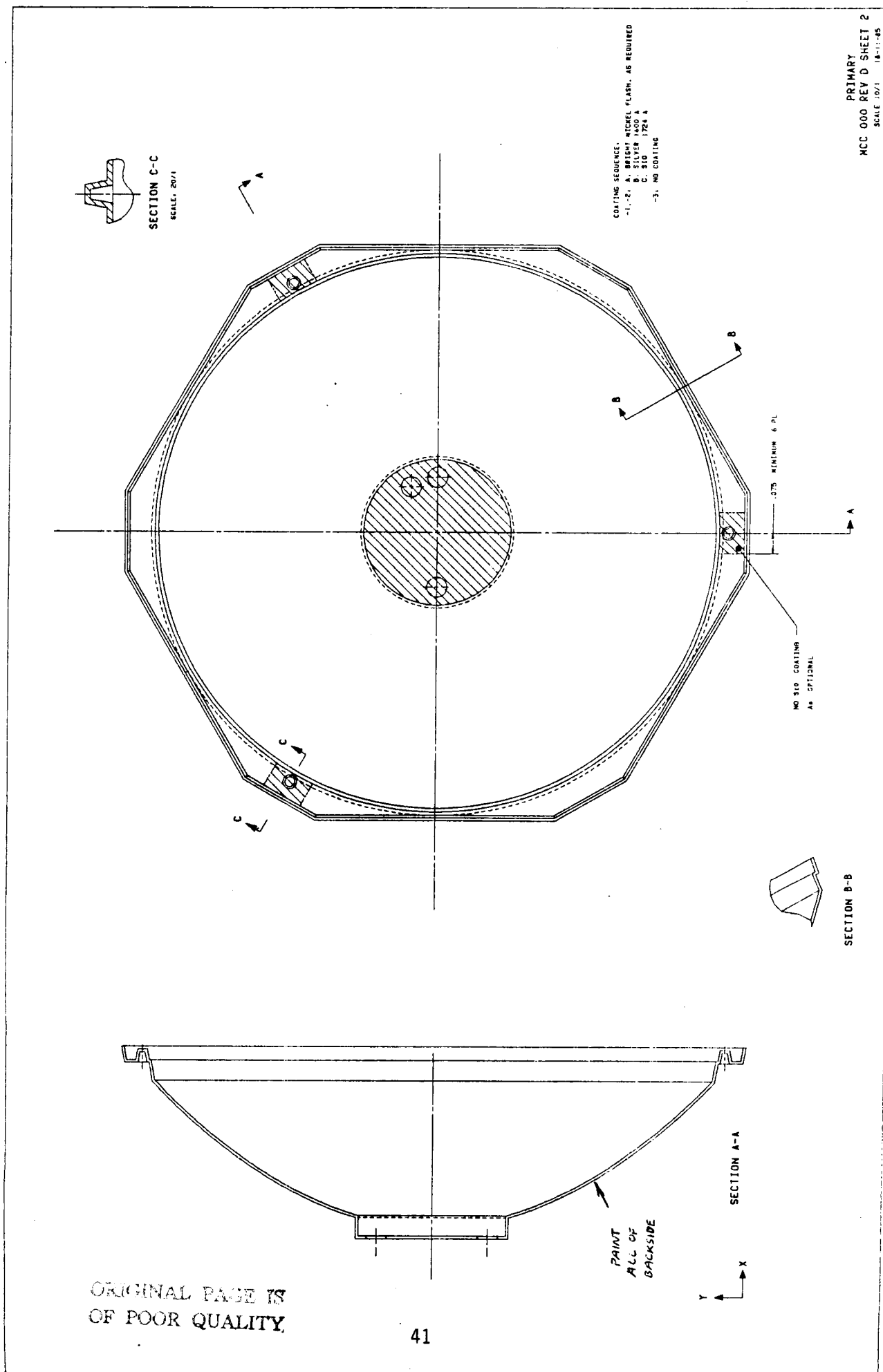


FIGURE 3-28b: COATINGS ON THE FRONT AND BACK PROVIDE PRECISE OPTICAL AND THERMAL PROPERTIES.



ACTUAL SIZE

- 1) MATL: -1 ELECTROFORMED NICKEL, 10 MILS
-2 ELECTROFORMED NICKEL, 60 MILS

COATING SEQUENCE:

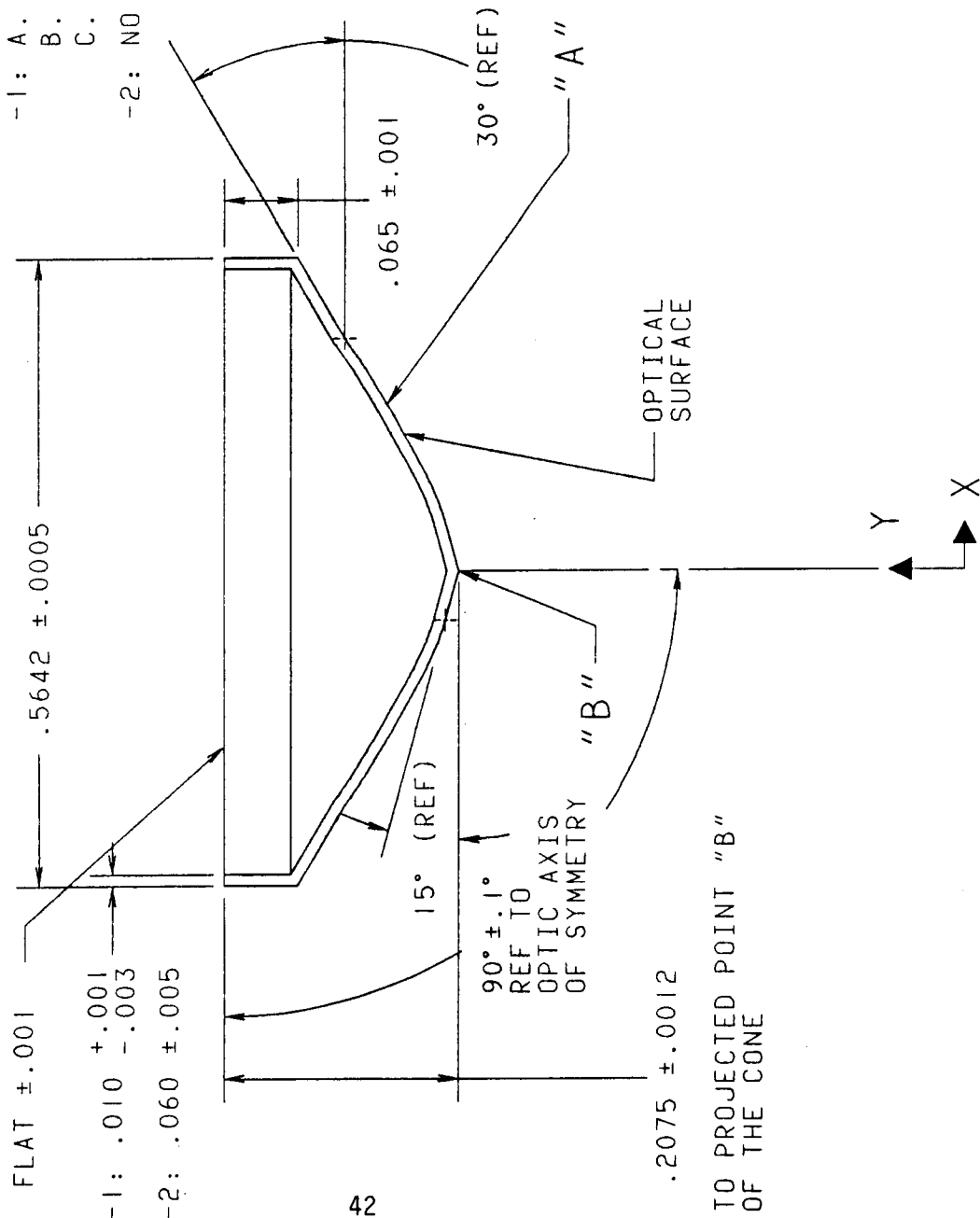
- 1: A. BRIGHT NICKEL FLASH, AS REQUIRED
B. SILVER 1600 A
C. SiO₂ 1724 A

-2: NO COATING

- 2) CONFIGURATION
SYMMETRY AXIS: Y AXIS

- 3) SURFACE "A" TO BE
PROVIDED AS A SERIES
OF X-Y COORDINATES FROM
(0,0) REFERENCE POINT "B".
FOR EQUATION SEE SHEET 2.

- 4) MIRROR NEAR POINT "B"
MAY BE ROUNDED AS MUCH AS
.010 RAD.



ORIGINAL PAGE IS
OF POOR QUALITY

SECONDARY
MCC 010B

SCALE 10/1 09-24-85

FIGURE 3-29a: THE NEW SECONDARY IS A PRECISION OPTIC COMPONENT.

Secondary Reflector - Sheet 2 of MCC-010B

This reflector is a surface of revolution whose profile is defined in the x, y plane by the following table of points. The origin of the x, y coordinate system is defined in Sheet 1 of MCC-010B

<u>X</u>	<u>Y</u>	<u>X</u>	<u>Y</u>	<u>X</u>	<u>Y</u>
0	0	.099620	.035240	.159421	.068776
.044298	.011870	.101384	.036190	.161206	.069854
.044366	.011889	.103148	.037144	.162991	.070931
.046296	.012430	.104908	.038101	.164775	.072008
.048220	.012990	.106668	.039060	.166561	.073084
.050139	.013569	.108427	.040021	.168347	.074158
.052051	.014167	.110185	.040983	.170135	.075229
.053956	.014785	.111943	.041945	.171924	.076298
.055858	.015423	.113701	.042908	.173716	.077364
.057752	.016078	.115459	.043870	.175508	.078427
.059638	.016752	.117216	.044831	.177300	.079491
.061519	.017443	.118975	.045794	.179092	.080557
.063394	.018152	.120732	.046756	.180882	.081626
.065262	.018878	.122490	.047720	.182668	.082701
.067124	.019620	.124247	.048684	.184450	.083782
.068979	.020379	.126004	.049650	.186227	.084872
.070827	.021153	.127759	.050616	.187998	.085972
.072669	.021943	.129514	.051584	.189761	.087084
.074505	.022749	.131268	.052554	.191515	.088210
.076334	.023569	.133021	.053526	.193259	.089351
.078156	.024403	.134772	.054500	.194993	.090508
.079972	.025250	.136522	.055477	.196715	.091681
.081782	.026110	.138270	.056456	.198431	.092865
.083586	.026982	.140017	.057438	.200141	.094056
.085385	.027865	.141763	.058423	.201851	.095248
.087179	.028758	.143506	.059411	.203564	.096436
.088968	.029661	.145248	.060402	.205279	.097621
.090752	.030573	.146987	.061398	.206995	.098804
.092533	.031493	.148724	.062397	.208712	.099986
.094309	.032420	.150484	.063415	.210429	.101168
.096083	.033355	.152275	.064482	.210445	.101178
.097854	.034295	.154063	.065552	.282101	.142548
		.155851	.066625		
		.157636	.067700		

FIGURE 3-29b: EQUATION FOR THE SECONDARY MIRROR SURFACE

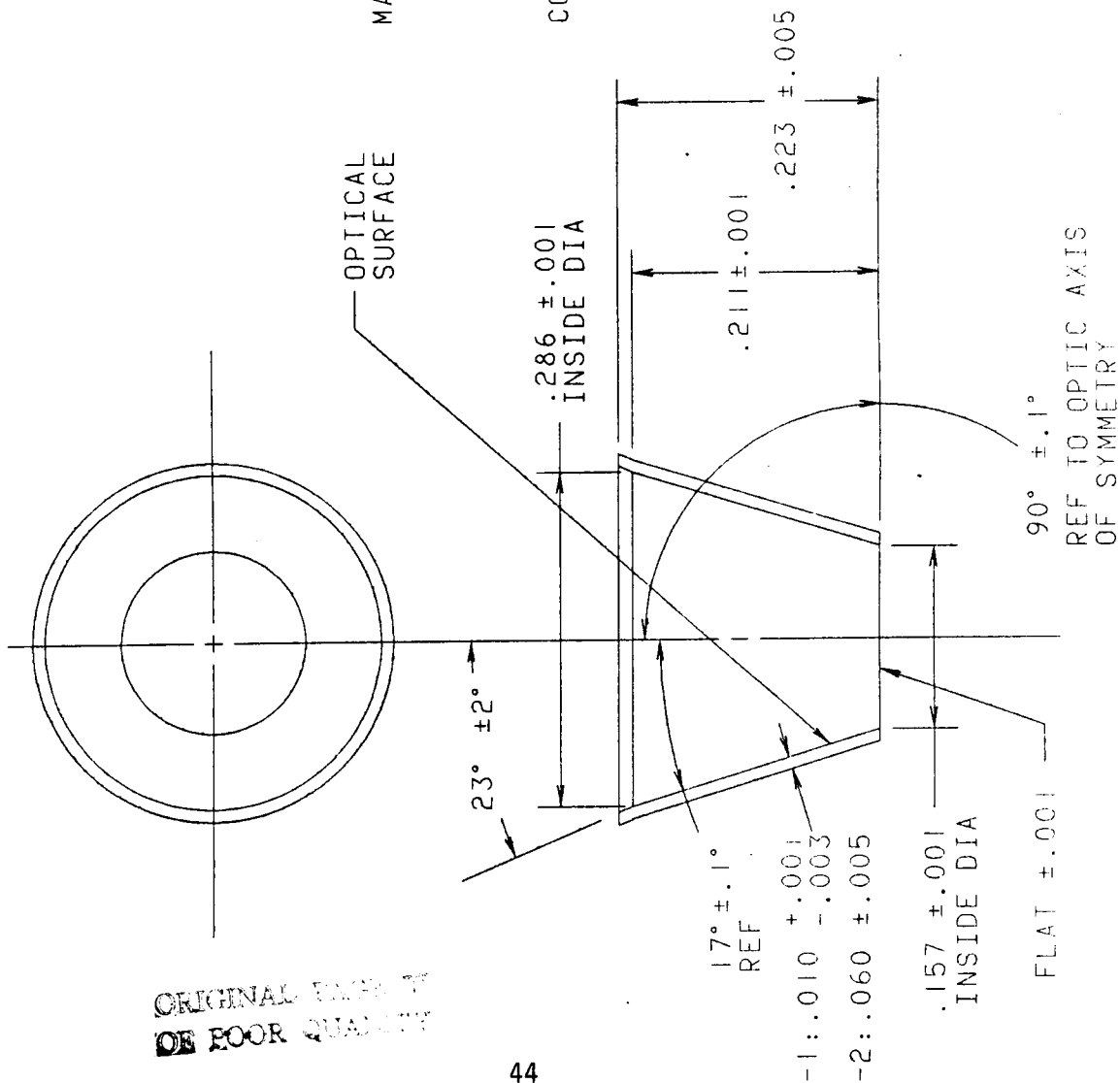


FIGURE 3-30: THE NEW CONE PROVIDES TOOLING REFERENCE POINTS.

ASSEMBLED ITEM	2.5°	3°
Y, X AXIS DISPLACEMENT OF SECONDARY	0.002	.0005
Z AXIS DISPLACEMENT OF SECONDARY	.0025	.0005
TILT OF SECONDARY	.05°.0005 spid Δ .0025 para Δ	.02°
Y, X AXIS DISPLACEMENT OF CONE	.002	.0003
Z AXIS DISPLACEMENT OF CONE RELATIVE TO CELL SURFACE	.0035	.0003
TILT OF CONE	.7° (2 mils Δ)	.6°
SLOPE DEVIATION OF PRIMARY	1'	.5'
SLOPE DEVIATION OF SECONDARY	> 10'	3.5'
SLOPE DEVIATION OF CONE	> 1°	.05°

ASSUME 1% LOSS AT ANGLE ALLOWED PER ITEM
FOR TOTAL 8/5% LOSS AT ANGLE. DOUBLE
ALLOWED LOSS GIVE DOUBLE TOLERANCE
ALLOWANCE.

Figure 3-31. Tolerance Allowance

3.3.2.7 Optical Measurements

The specular reflectance of a primary mirror sample was measured to be a factor of ten improved over the NAS8-35635 hardware before coating and a factor of five improved after coating (Figures 3-32 and 3-33). As required, all mirror edges were sharp and no unusual surface variations were observed. Testing for poor output portions of the mirror due to surface or figure variations was therefore not required.

The gap between the cone and the cell was set at 8 ± 1 mils by the cover and adhesive (see cell stack design).

3.3.2.8 Concentration Ratio Check - Energy Throughput

Two optics were measured for energy throughput by measuring current of the cell with and without the secondary in place. A mask with a hole the size of the cell active area was placed over the cone to measure 1 sun output without the secondary in place, then the mask was removed, the secondary was replaced, and the total MCC element output at concentration was measured.

The measured concentration ratio was 114 and 117 versus an expected concentration ratio of 134.7. When corrected (section 3.3.2.13) for known deficiencies in the conic mirror (see Coatings), the CR became 134.4.

3.3.2.9 Element Performance

The offpoint performance of three MCC elements was measured (Figure 3-34). As expected, the performance was significantly improved over the NAS8-35635 hardware, though slightly lower than predictions. The lower offpoint output was subsequently explained to be due to conic mirror coating deficiency (see Coatings). At this time, the decision was made to continue with the design into Phase 4, complete population of the deliverable panels with MCC elements of the new design.

3.3.2.10 Coatings

It was not the intent of the design program to address coating applications. Only data and design concepts which were applicable to this design and available from scientific or engineering literature were incorporated into the design. A brief summarization follows.

File name = SST03732 BY SSTVI

Sample title:

SOLAR CELL MIRROR 4

Standard title:

KODAK WHITE STANDARD

Time of sample run:

11:29 AM WED., 30 APR., 1986

Time of standard run:

10:21 AM WED., 30 APR., 1986

Angle of incidence = 0.0

Light source = White light

Comments:

The BRDF for this new mirror is almost an order of magnitude lower than the mirror in Figure 3-32. The energy lost to scatter is less.

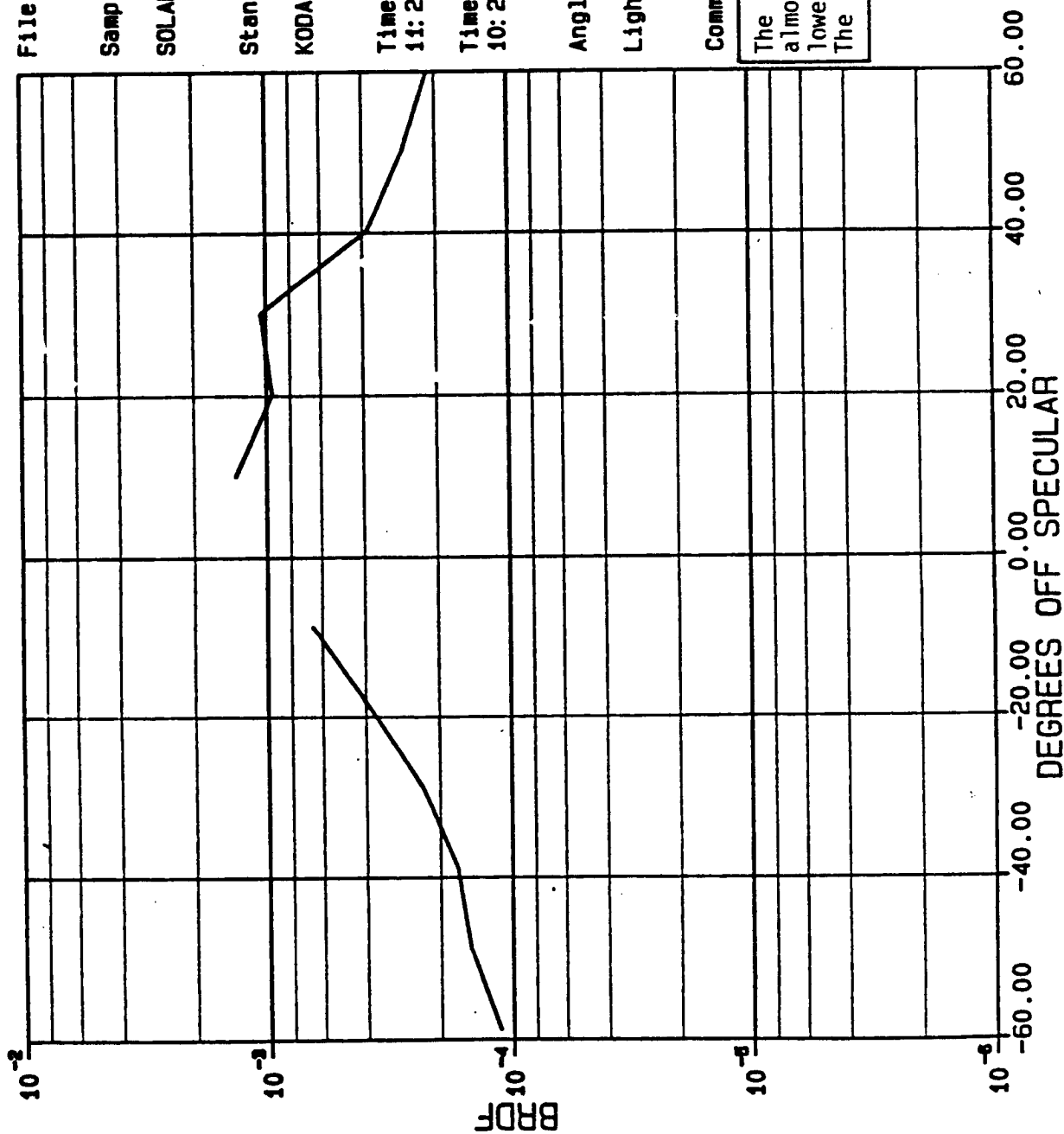


FIGURE 3-32: THE SPECULARITY OF THE UNCOATED MIRROR IS A FACTOR OF TEN IMPROVED OVER THE PREVIOUS DESIGN.

File - SST04555 / VI

Sample title:

SOLAR CELL MIRROR, MCC [2]

Standard title:

KODAK WHITE STANDARD

Time of sample run:

5:15 PM WED., 16 JULY, 1986

Time of standard run:

3:50 PM WED., 16 JULY, 1986

Angle of incidence = 0.0

Light source = White light

Comments:

KRUER

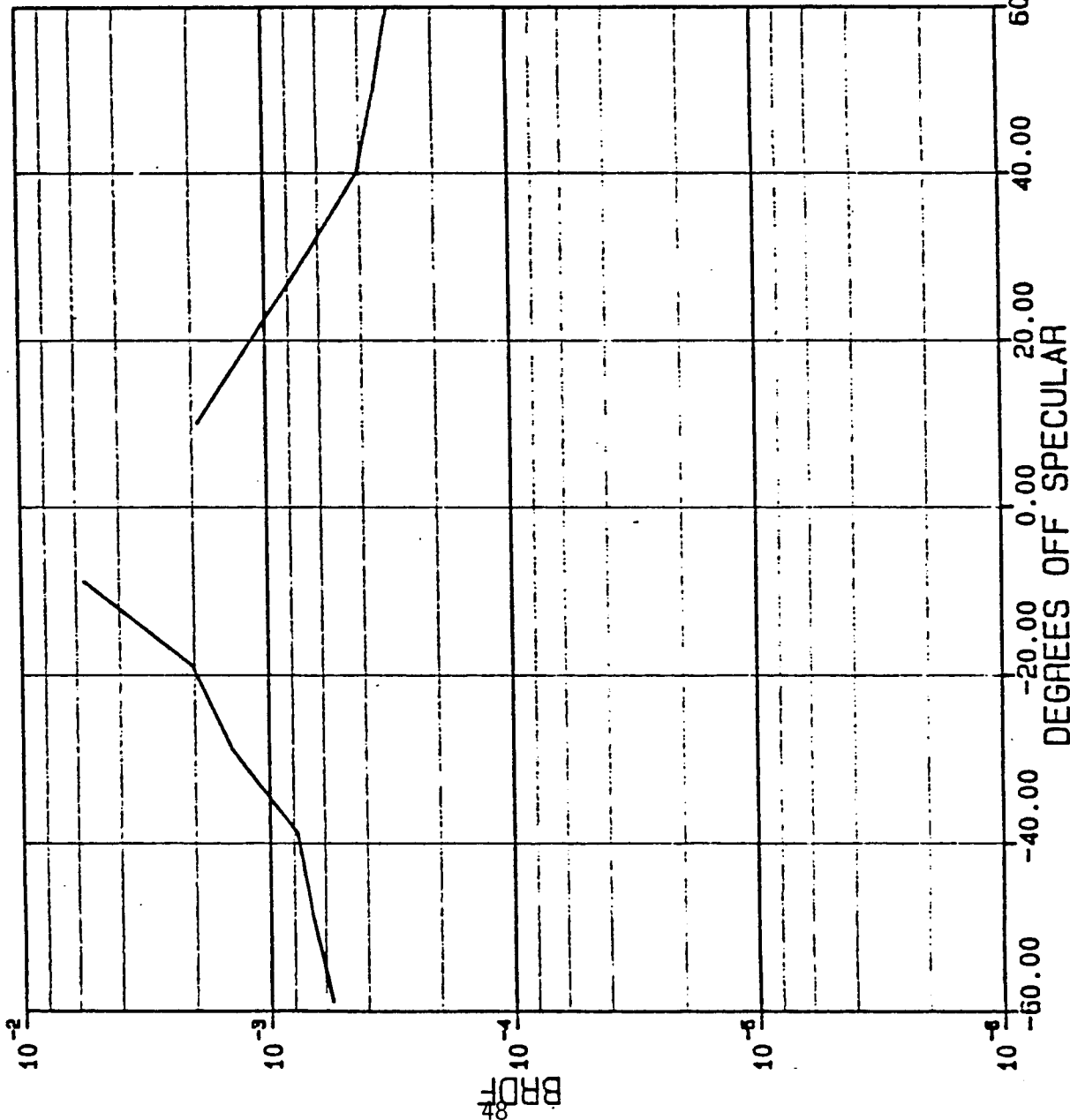


FIGURE 3-33: SPECULARITY OF THE NEW MIRROR REMAINS FIVE TIMES BETTER THAN THE PREVIOUS DESIGN AFTER COATING.

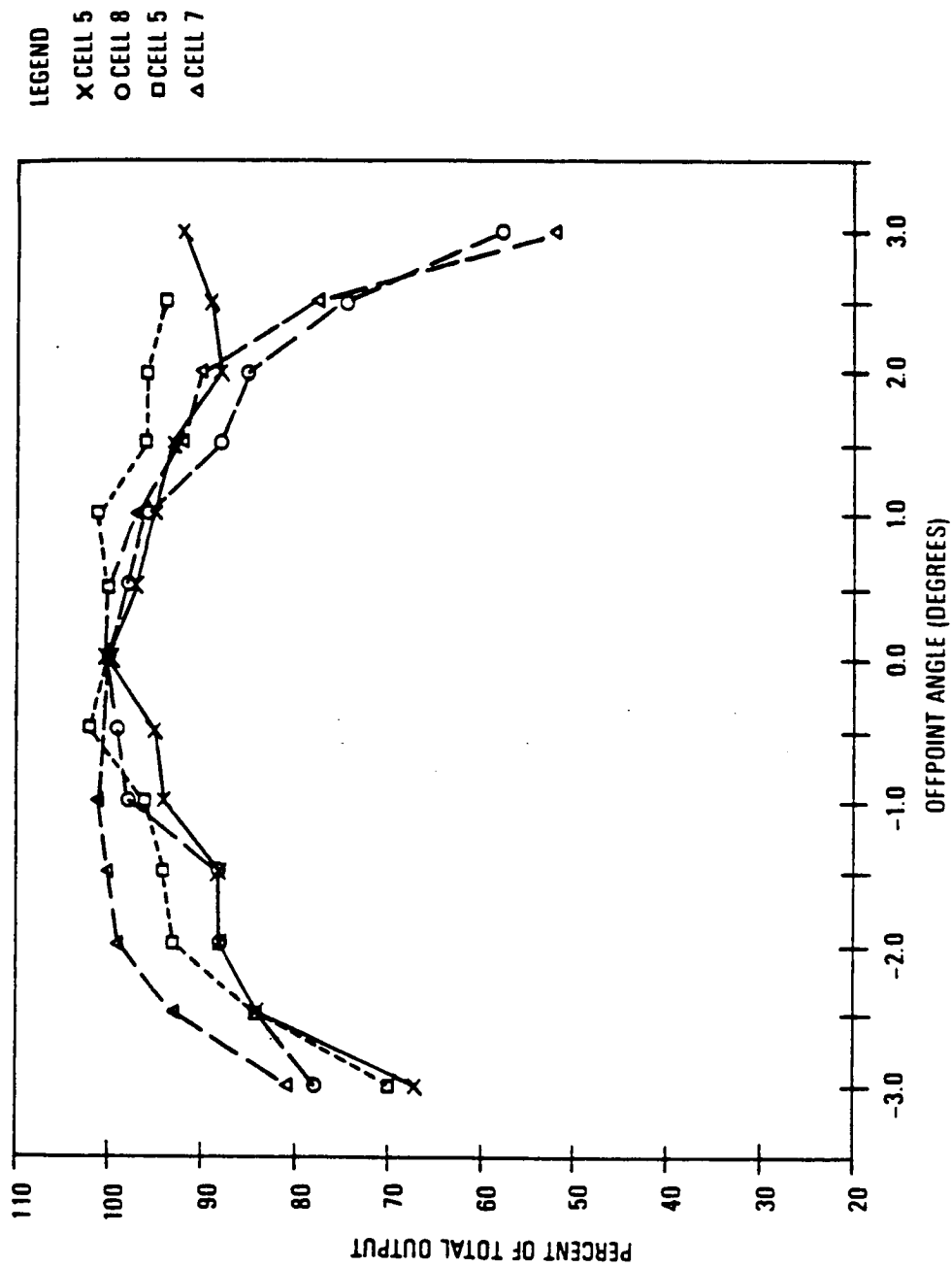


Figure 3-34: MCC Off-point Curves for LIPS III Hardware

Optical Coatings. The coatings required for this design were identical to those for contract NAS8-35635 hardware. Silicon oxide of 1700 Å was vacuum deposited over 1600 Å of silver which was vacuum deposited on the reflective nickel surface of the mirrors (Figure 3-35). The SiO coating is projected to be able to protect the optic from atomic oxygen effects based on extensive analyses performed by many companies and NASA centers nation wide. Other coatings such as indium tin oxide are also acceptable and can be incorporated as they are defined and tested.

Protective Coatings. Only the solar cell interconnect with silver metallization is subject to environmental attack in this design. A thin coating of silicone adhesive could be used for protection. It was not included in the present design.

Thermal Control Coatings. An added task to the design was the incorporation of S13GLO paint for thermal control of the MCC element. This silicone based white paint was used to coat the back (sun facing) surface of the secondary mirror, the sun facing surface of the spider mount for the secondary mirror (Figure 3-36) and the back surface of the primary optic (Figure 3-37).

Standard procedures using solvent wipe of the nickel and aluminum surfaces prior to a spray paint coating with the S13GLO were found to be sufficient for good adhesion of the paint to the painted surfaces. To test for adhesion, a MIL SPEC procedure was followed which consisted of scribing the painted surface of a sample, applying tape, and pulling the tape from the sample. No failure occurred. The sample was thermal shock cycled 100 times from -192° to +60°C. The tape test was performed again and no adhesion failures were observed.

Other Considerations

- o Primary and Secondary Mirror Coating Quality. The adhesion of the optical coatings was of varying quality. The mirror vendor used two vendors as coating subcontractors but did not maintain traceability. Subsequent assembly of the primary and secondary mirrors incorporated the use of a protective and cleaning polymer which was spread on the surface, let dry, and removed with tape. When the polymer coating was pulled off, the surface coating of some

COATING SEQUENCE:

- 1: A. BRIGHT NICKEL FLASH, AS REQUIRED
B. SILVER 1600 A
C. SIO 1724 A

ORIGINAL PAGE IS
OF POOR QUALITY

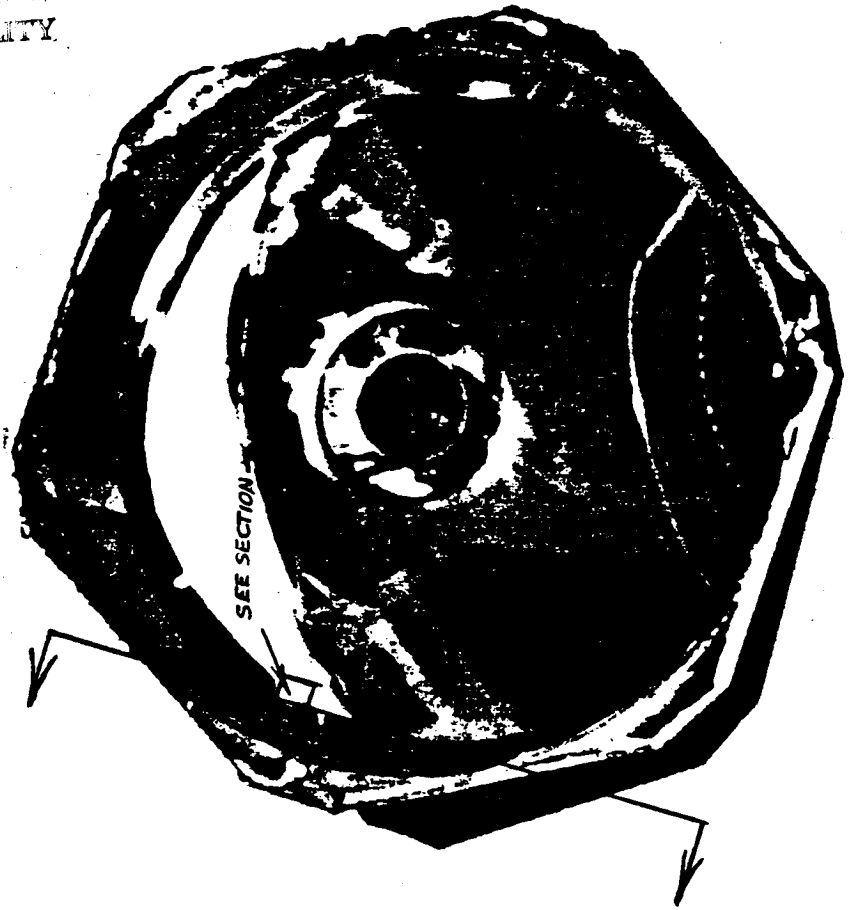
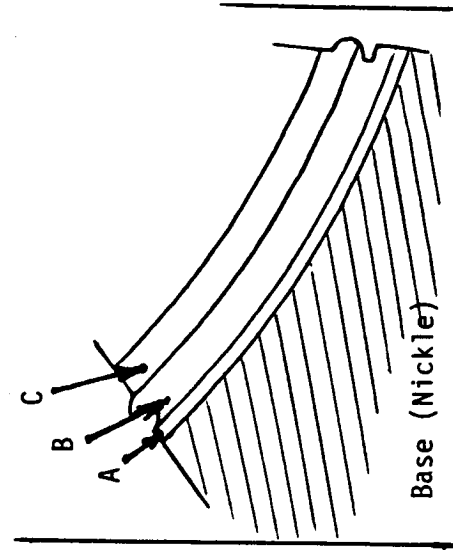


FIGURE 3-35. COATING SEQUENCE FOR OPTIC SURFACES (Primary sub-assembly without spider shown)



Figure 3-36. Front of New Element Shown While Operating,
Spider and Secondary Back are Painted with S13GL0.

REPRODUCED PAGE IS
OF POOR QUALITY

ORIGINAL PAGE IS
OF POOR QUALITY

ORIGINAL PAGE IS
OF POOR QUALITY

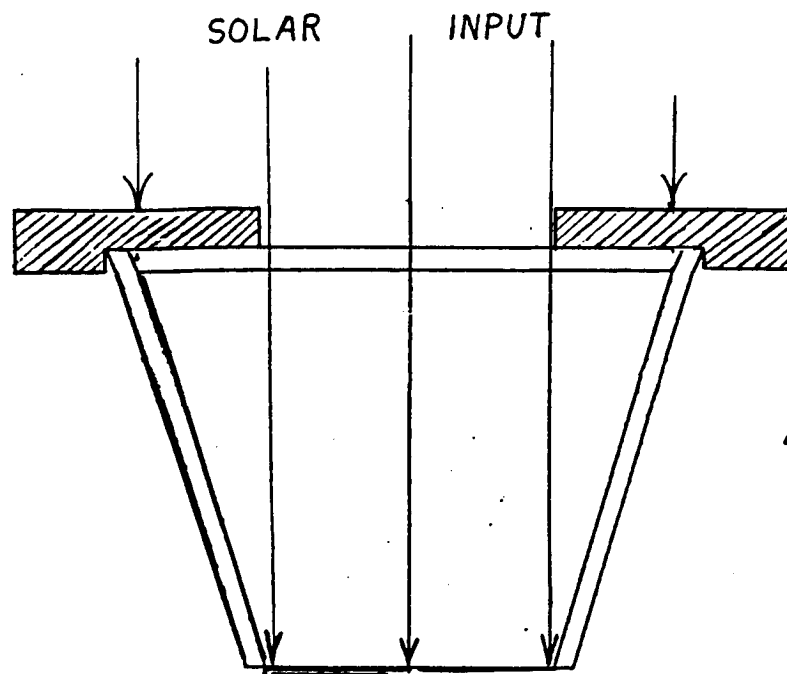


Figure 3-37. Back of MCC Element Showing Mounting Position, Solder Bonds for Electrical Interconnection, and Complete S13GL0 Coating.

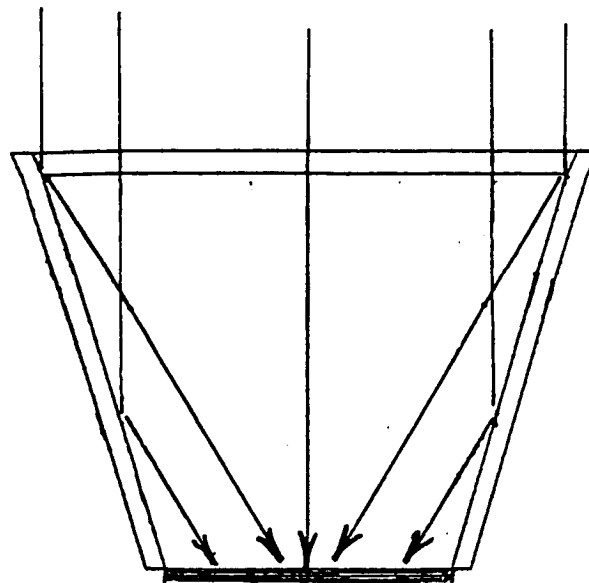
primaries and secondaries (portions of the SiO and SiO+Ag) were removed as well. Discussion with the vendors determined that the coating adhesion should have been much greater than the adhesion of the polymer, and that the failures were most likely attributable to insufficient surface cleaning prior to coating. The only fix available was to strip and then re-deposit the coatings. Since the effect of stripping on the mirror surface was unknown (such as potentially roughening the polished surface), and the damage was apparent on only a few optics, it was decided to leave the coatings as is without testing the remaining coatings. Temperature shock testing of a mirror already showing partial coating failure did not induce any further degradation or removal of the coatings. Coating failures from thermal cycling or other stress during NASA testing will not be considered as design failures since an in-place acceptance test would find coating manufacturing problems for any flight optics. The use of the polymer as an acceptance test is recommended for such acceptance testing.

- o Conic Mirror Coating Quality. All conic mirrors were visually inspected for coating defects such as missed or darkened sections or localized haziness. Coating quality in terms of absolute reflectance was not measured. After the measurement of offpoint performance of a large number of optics showed significantly high losses at small offpoint angles, test data was reevaluated to determine the cause. Data for output of the cell stacks with a cell sized mask was compared to output of the cone and cell combination with no secondary mirror (Figure 3-38). Since all light entering the cone would be absorbed by the cell, the reflectance of the cone could be backed out of the measurements as shown in Figure 3-39. Data for four optics showed that the conic mirror reflectance only achieved 65 to 70% in the 0.4 to 0.9 micrometers GaAs response range. The reasons for this were unknown. However, after questioning the coating vendors, it was found that a "proper" mounting procedure in the coating chamber to guarantee uniform coating quality was not used due to schedule and cost pressures from the electroforming vendor. The physical reason for the loss whether due to scatter or absorptance should be investigated. It is known that the loss is not caused by contamination. A series of cleaning fluids, acetone followed by freon followed by isopropyl alcohol, had negligible effect on most conic optics. Those improvements that were measured only increased total reflectance of the cone from 0.65 to 0.67 in a limited number of cases.

To check the extent of the low conic reflectance, all 180 optics to be mounted in the large deliverable panel were checked on an X25 solar simulator for total reflectance as measured by the GaAs cell in the



A CONE MASK
IN PLACE



B FULL SUN ON
MIRROR AND
CELL

FIGURE 3-38 METHOD FOR FINDING SPECULAR REFLECTANCE OF CONE.

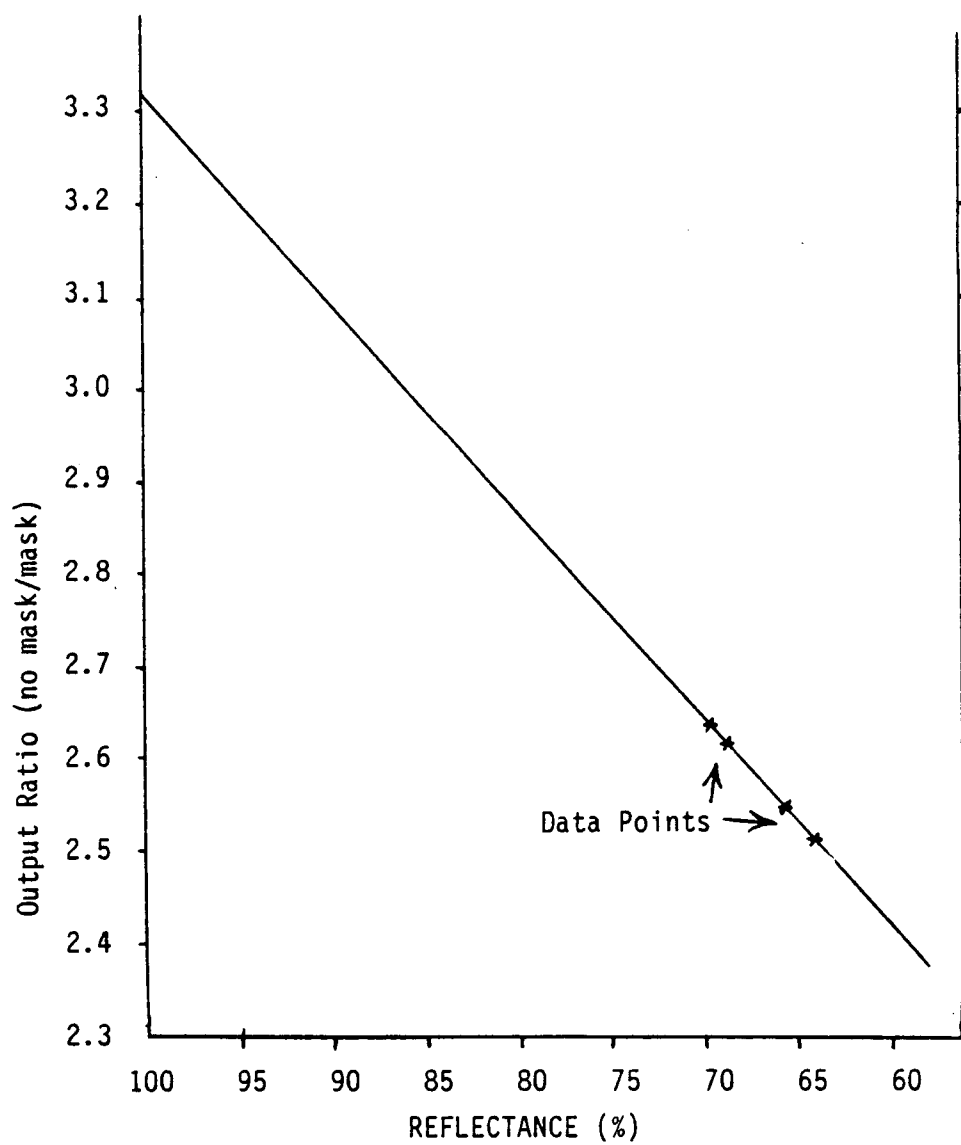


FIGURE 3-39 Conic mirror to cell output ratio as a function of cone reflectance.

subject optic using the same methods as outdoor sun tracking testing. The range of reflectance was measured to be 59 to 71% with an average of 66% and a standard deviation of 5%. The $\pm 5^\circ$ illumination angle from normal as is typical for the X25 due to geometry of the simulator did not skew the results since even 5° illumination angles for light rays would still reach the cell.

The effect of the low conic reflectance was checked in the previous tolerance analyses by looking at the total light reaching the cell via the cone for all pointing conditions. Figure 3-40 is a plot of the percent of light versus pointing angle for the new design which first bounces from the cone. It was obvious that the conic mirror was as important as the primary and secondary mirrors when considering the total system performance.

Using the average measured cone reflectance it was possible to recalculate from the test data the normalized offpoint characteristics of the MCC elements, substrings, and modules if the conic mirror had been 97% reflective. The absolute output of the onpointed and offpointed elements could be similarly corrected. All plots of output versus offpoint for the small and large panel strings were corrected accordingly. The plots showed very good agreement with the response as analyzed during the tolerance analysis. Variations due to other electrical effects are discussed in section 3.3.2.11.

3.3.2.11 Electrical/Optical Test Results of the Improved MCC Element

Measurements of individual optic/electrical performances, performance of strings of a single element in parallel by six elements in series, and 5 elements in parallel by six in series were made using the solar tracker and mounting hardware designed especially for this application (Figure 3-41). All measurements were corrected to 1 sun AMO exposure using a GaAs standard cell and were further corrected for temperature based upon readings from thermistors mounted on the back of two randomly selected elements.

Output Variation with Multiple Secondary Mirrors. The "proof" secondaries were tested for variations in offpointability using a single primary subassembly. Figure 3-42 shows the performance of each of the seven accepted secondary mirror samples from the separate electroforming tools as corrected for the cone reflectance losses discussed in the "Coatings" section. The variability is fairly significant in terms of expected offpoint

Total Fraction of Light to Reach Cell Which Is First Redirected by the Conic Mirror (Zero and Typical Tolerance Allowances Shown)

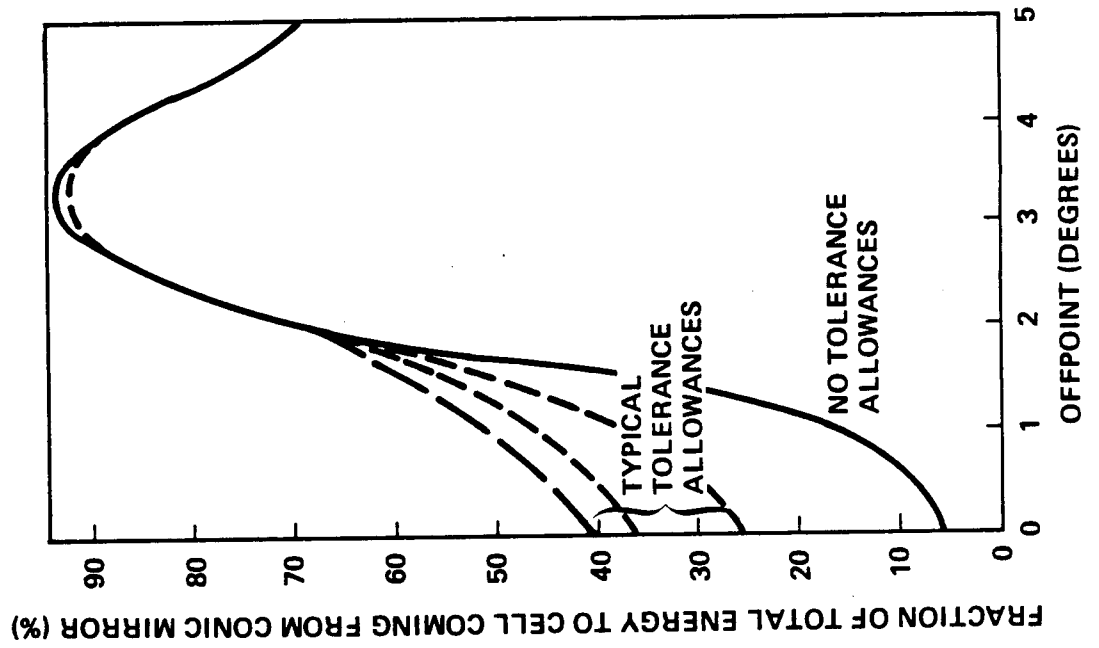


Figure 3-40

ORIGINAL PAGE IS
OF POOR QUALITY

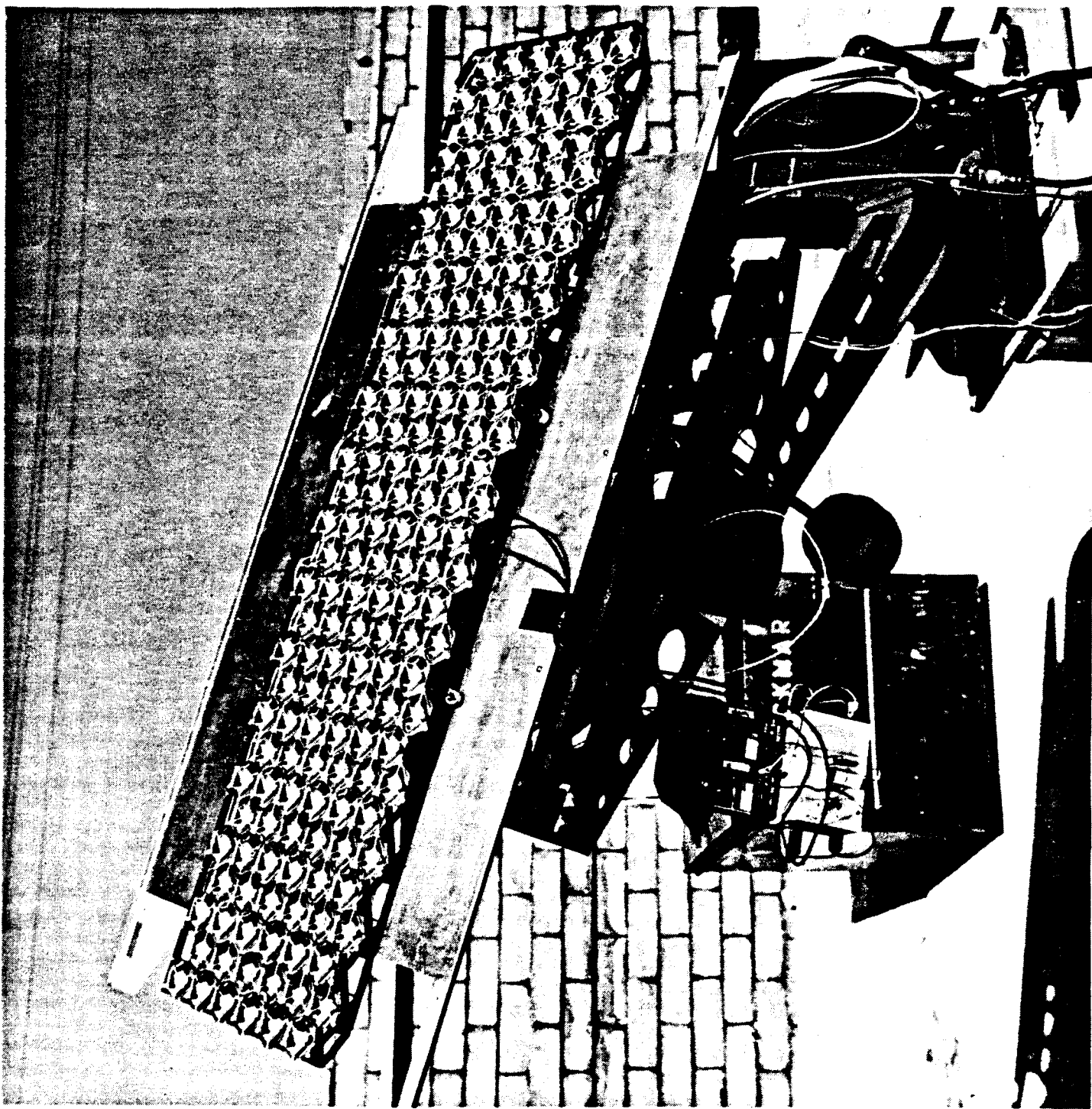


Figure 3-41. Both Deliverable Panels were Tested Using a Solar Tracker, Adapted from a Celestron Telescope Mount.

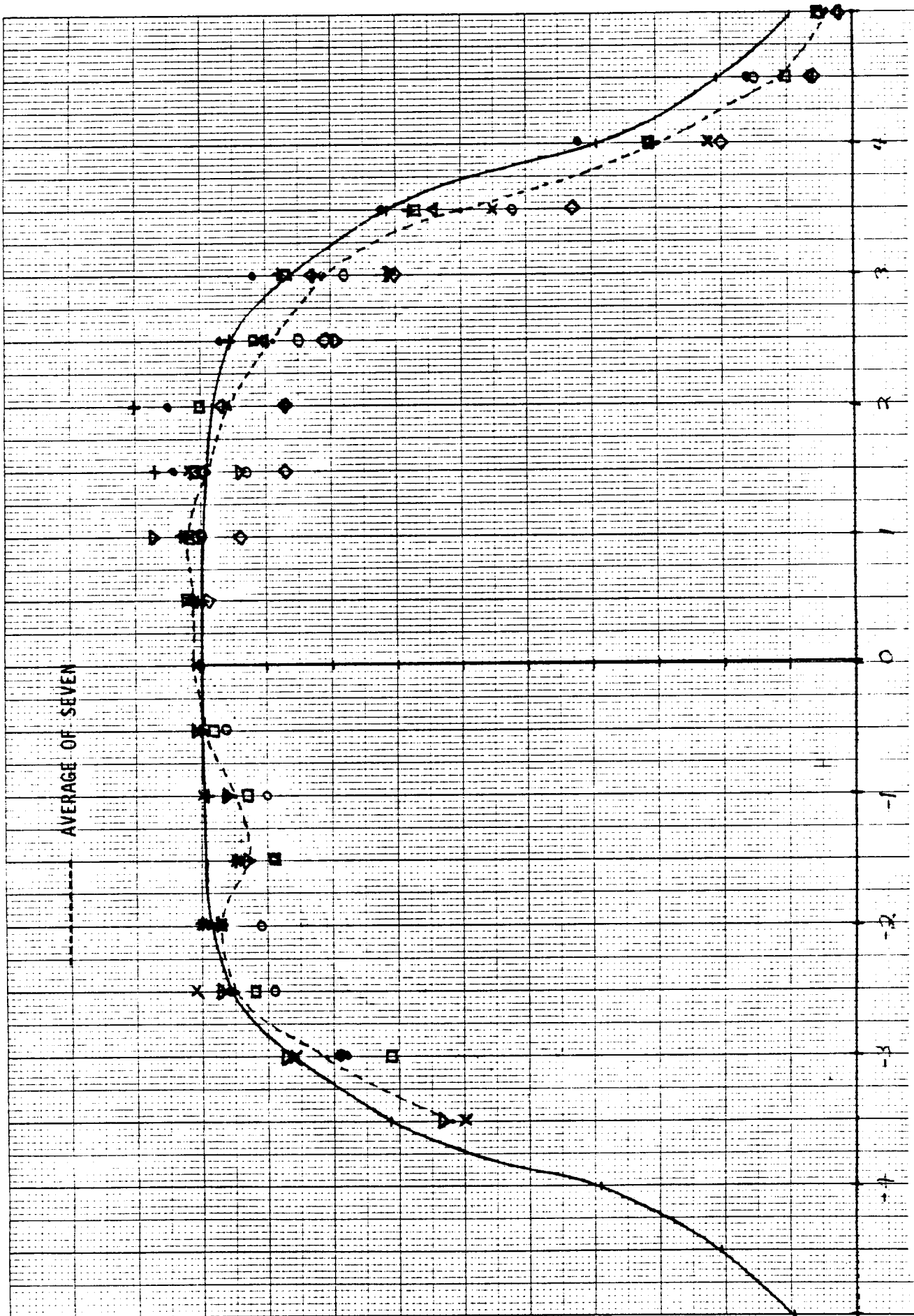


FIGURE 3-42: THE OPERATION OF THE SEVEN ACCEPTED SECONDARY PROOF ITEMS SHOWS HIGHER THAN DESIRED VARIATION, BUT STILL WITHIN REASON IN THE PROJECTED OPERATING MAXIMUM ANGLE OF 1.1 DEGREES.

performance of a mixture of the secondaries but it is important to note the relatively flat response each achieves for three degrees of total offpoint, near the center of the performance band.

3.3.2.12 Multi-Element String Measurements

Full current voltage (IV) curves were generated for each six cell in series substring located on the small and large deliverable panels. Zero degrees through three degrees and in some cases up to five degrees variation from normal sun were measured using a NORLAND 3001 data acquisition system with a fast load, and a concentrator one sun standard traceable to a balloon GaAs standard. The pertinent data from all measurements are located in Appendix A.

Offpoint Performance. The optics for the small 35 x 53 cm panel were chosen from optics with the initial high efficiency (>20.6%) cells available from ASEC. As expected, some loss due to matching of efficiency rather than matching of current at a set voltage was encountered. Essentially, each string is limited by the lowest MCC element current performance, which is in turn a combination of absolute cell output after assembly, mirror tolerance buildup effects on light collection efficiency and relative pointing of each of the elements. An ideal measurement of a well matched string is shown in Figure 3-43 for one substring. Figure 3-44 shows the effect of current limiting on the IV characteristic of another string. The sudden current increase near short circuit with a sharper knee indicates mismatching of output is occurring within the string. Figure 3-45 shows even greater mismatching to occur. A single MCC element which was found to be significantly low in output in string 3B was measured for the reverse voltage of the element as a function of string loading (Figure 3-46). The low output element ran quite hot in reverse as expected, but did not degrade after more than three minutes in the condition of approximately three volts at 300 mA across the cell.

The normalized offpoint performance of each of the strings of the small deliverable panel as corrected for conic mirror poor reflectance is shown graphed in Figures 3-47 and 3-48.

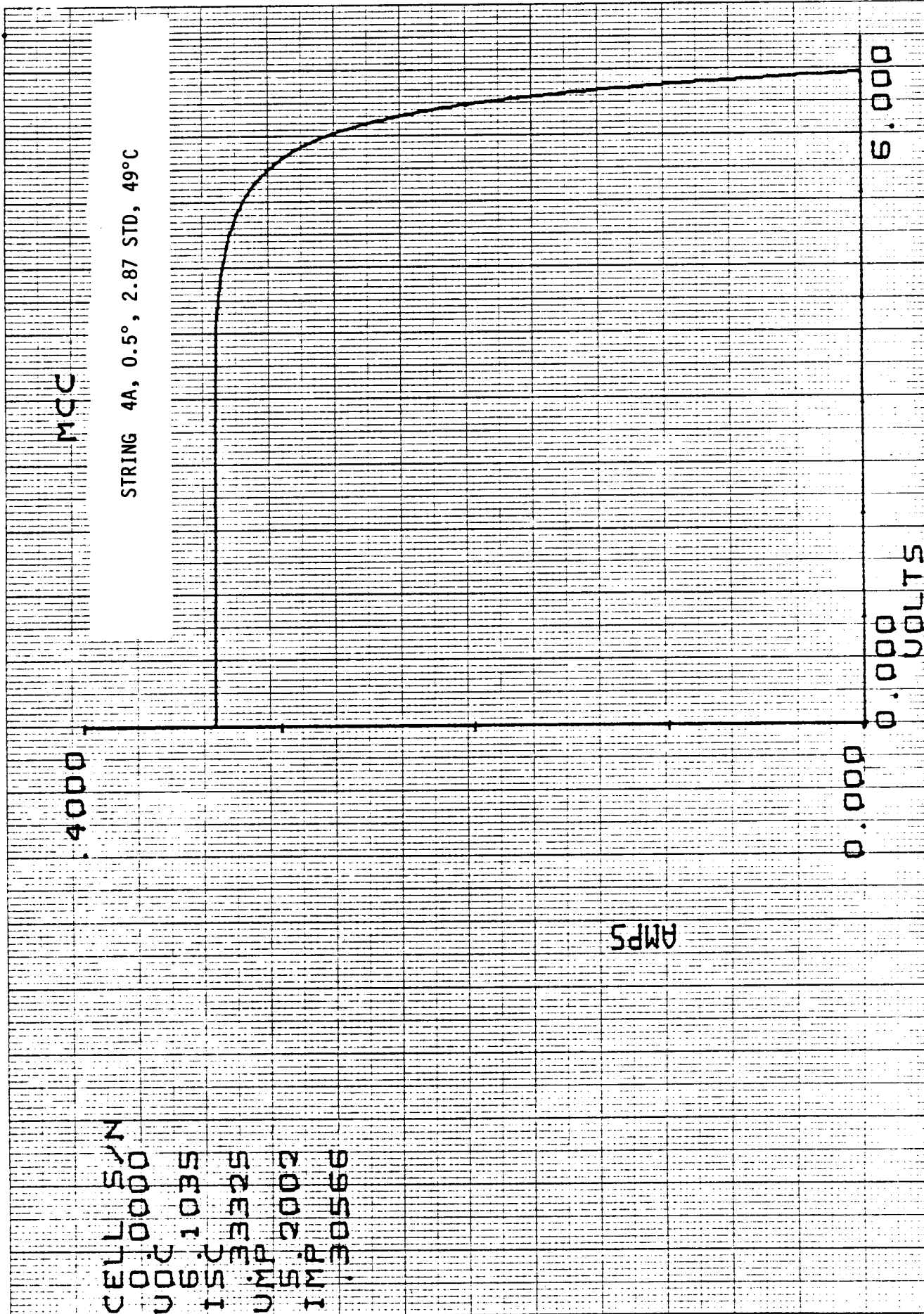


FIGURE 3-43: REASONABLE SHAPED I-V CURVES RESULT FROM OPERATION OF A SIX ELEMENT STRING NEAR NORMAL OFFPOINT.

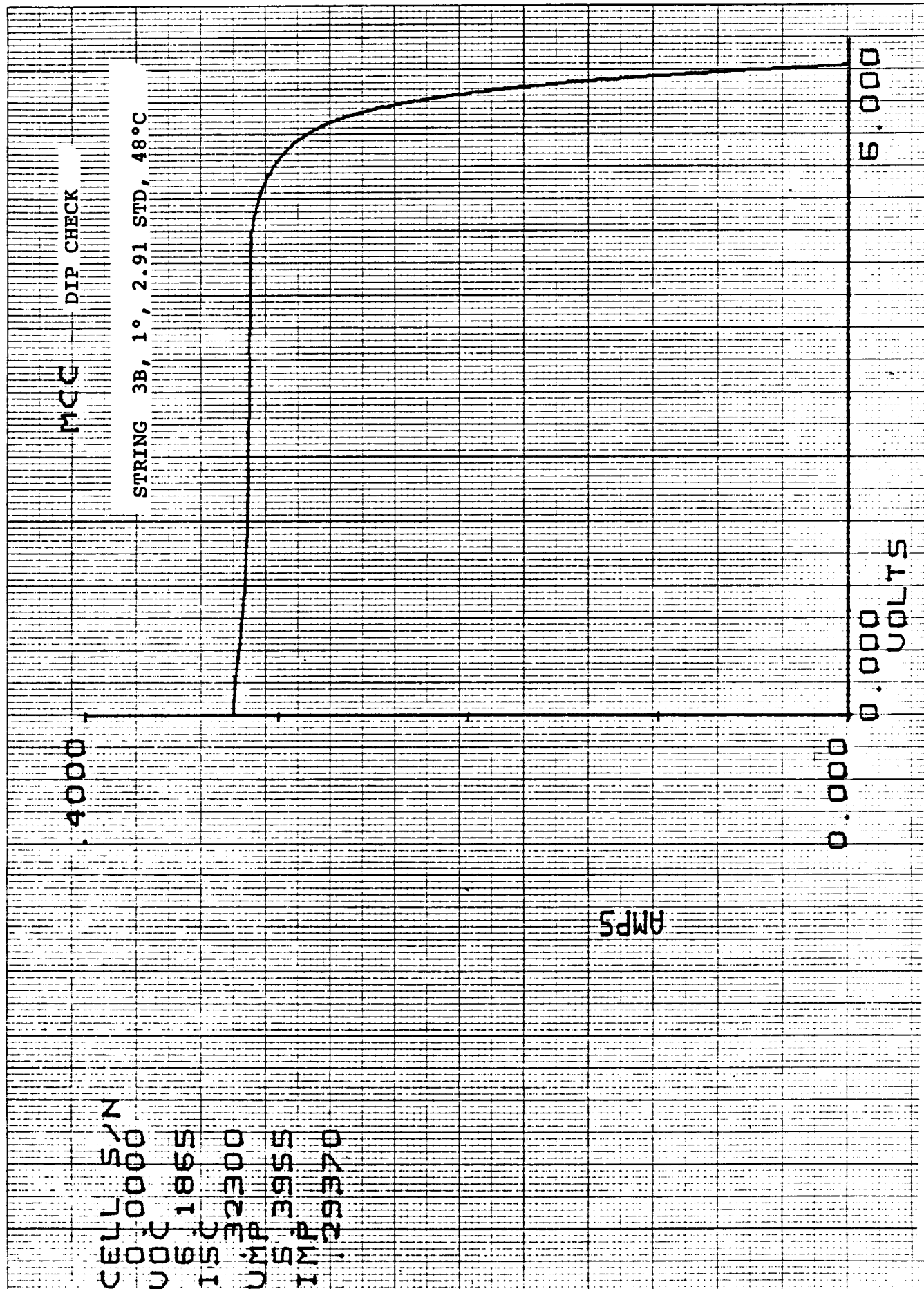


FIGURE 3-44: SOME MISMATCH PHENOMENA ARE VISIBLE IN THE STRING I-V PERFORMANCE.

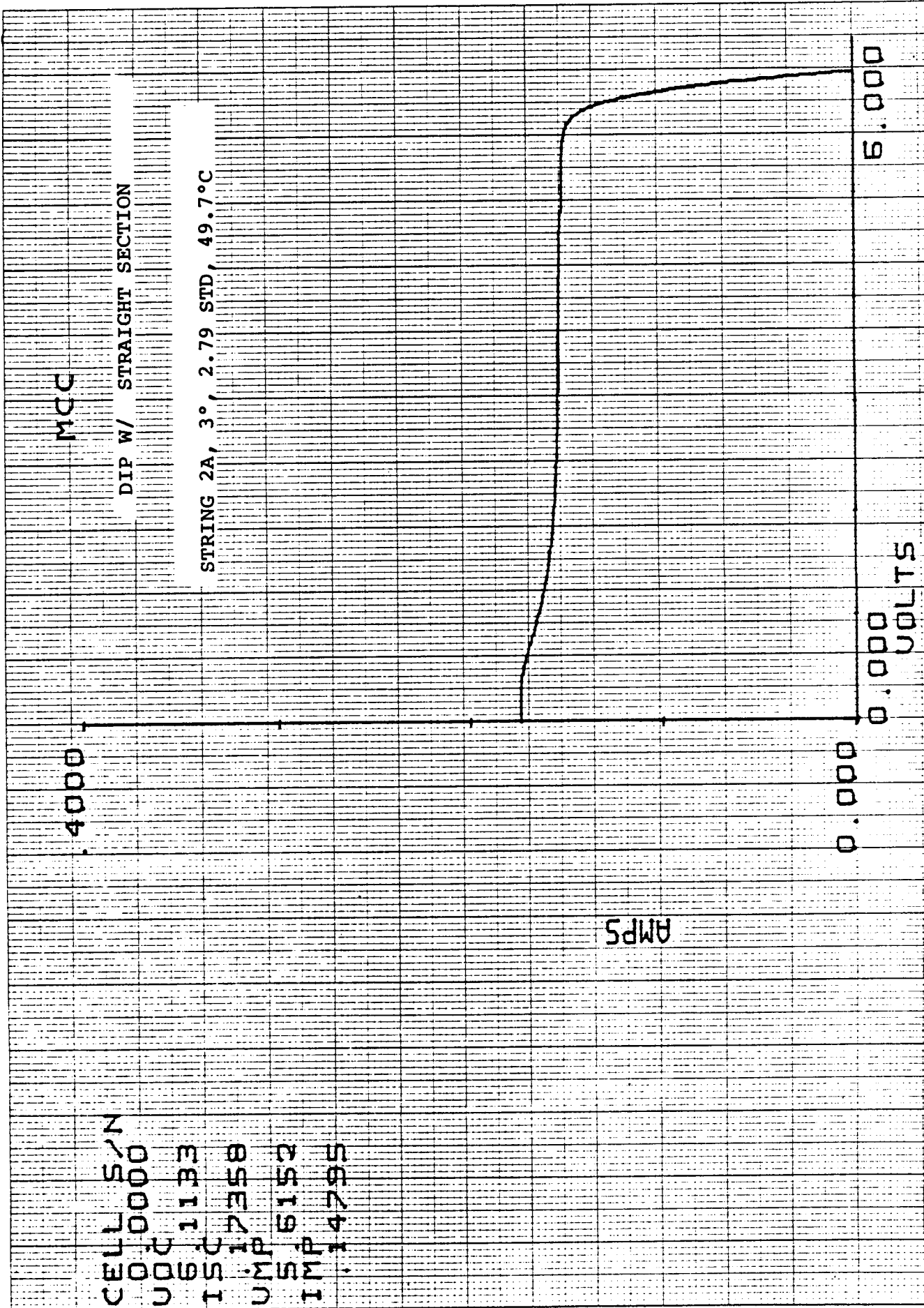


FIGURE 3-45: LARGE MISMATCH LOSSES ARE EASILY VISIBLE IN A NUMBER OF SEVERELY OFFPOINTED STRINGS.

FIGURE 3-46
 REVERSE BIAS TEST OF ELEMENT
 WITHIN STRING IN NATURAL SUNLIGHT (NO CORRECTIONS)

STRING 3B		<u>CONDITION</u>		
		<u>A</u>	<u>B</u>	<u>C</u>
String Voltage		1.50V	2.96V	4.95V
String Current		300mA	300mA	294mA
Voltage Element	7	.816	.790	.842
	8	.868	.840	.867
	9	.890	.880	.893
	10	.844	.780	.869
	11	-2.78	-1.23	-.589
	12	.886	.900	.915
Mismatch		5.5%	6%	4.2%
Excluding #11				

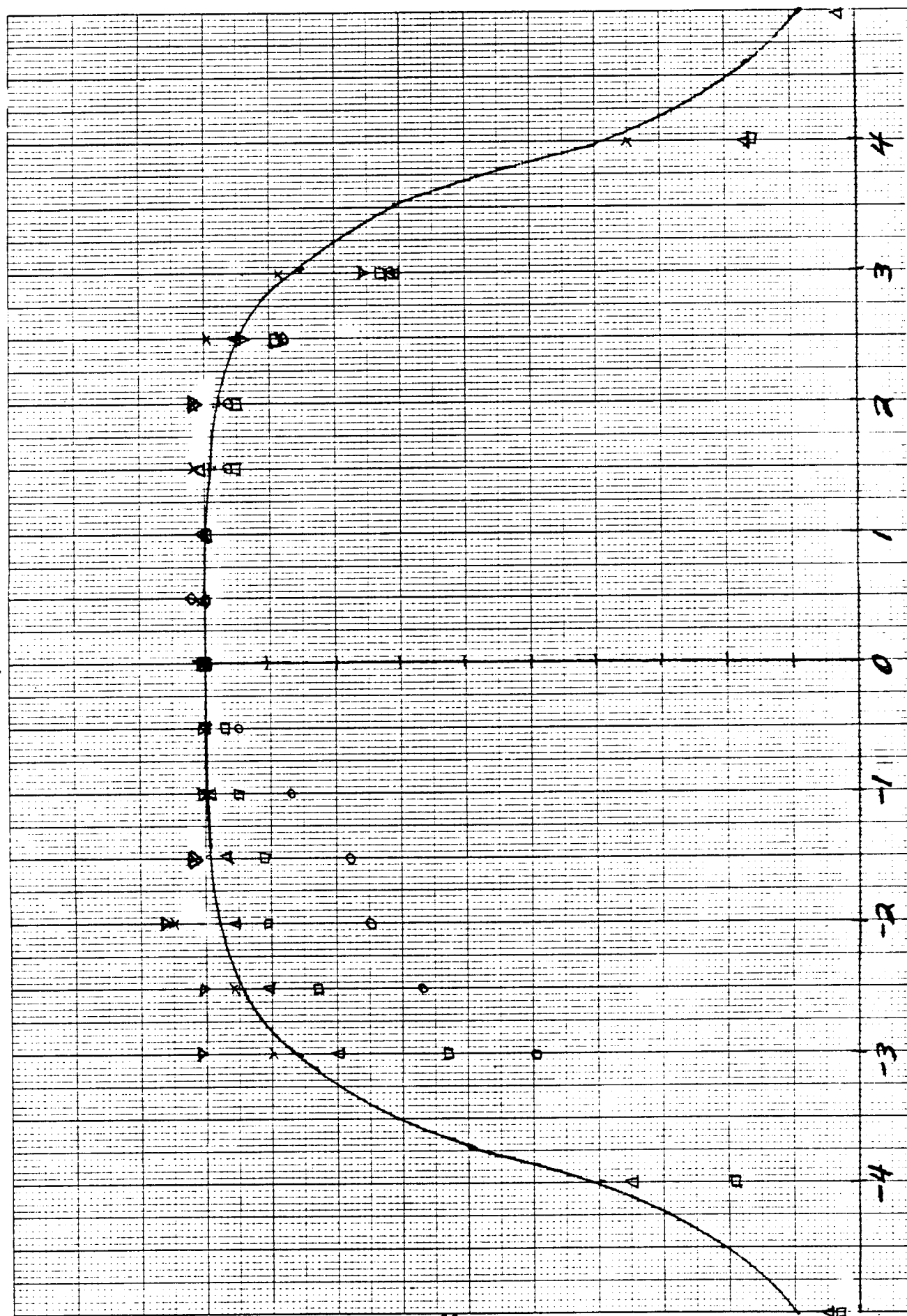


FIGURE 3-47: FIVE SIX-ELEMENT STRINGS OF A GROUP DESIGNATED "A" SHOW SOME VARIATION FROM IDEAL OUTPUT AFTER CORRECTION FOR THE CONIC MIRROR REFLECTANCE.

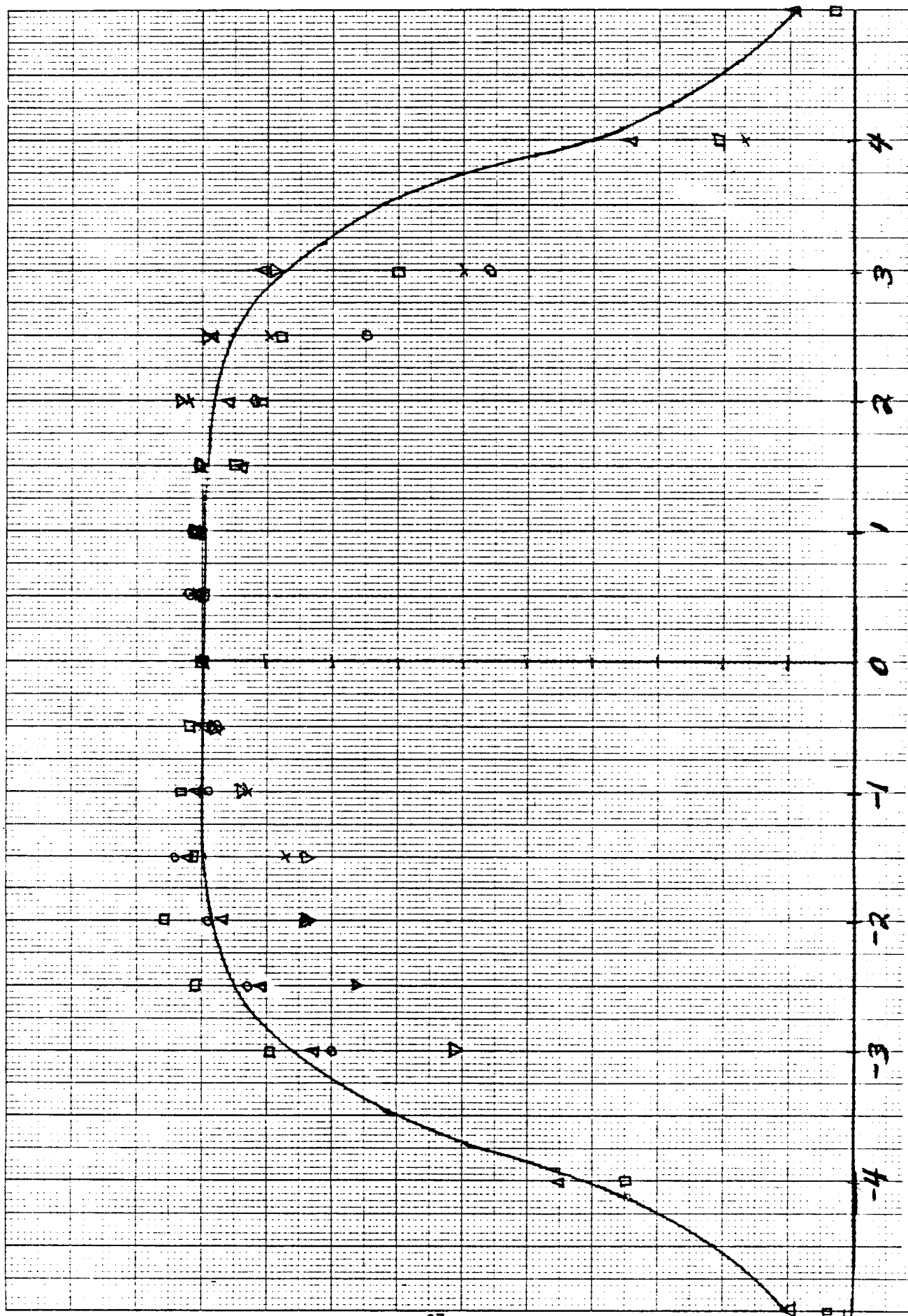


FIGURE 3-48: STRINGS OF GROUP "B" SHOW LESS VARIATION THAN GROUP "A".

Paralleling of two sets of substrings into two groups for measurements with five elements in parallel by six elements in series was performed. The measured output of the groups were compared to the expected output based upon the individual component substrings within the group. Excellent correlation was found (see Figure 3-49).

3.3.2.13 Correction Methods for MCC Element and String Test Data

All test data was corrected for known test conditions and test item deficiencies.

AMO Sun. The correction to AMO sunlight was simply accomplished by using test standard composed of a GaAs concentrator cell calibrated to a balloon flown GaAs primary standard. The GaAs test standard was monitored continuously during test of the test items.

$$\frac{\text{Std AMO}_{\text{cal. value}}}{\text{Std Test}_{\text{value}}} \times \text{test item reading} = \text{corrected reading}$$

Temperature. The correction for temperature for panel string tests was accomplished by mounting two thermistors to the back of randomly selected elements on the panel, and reading the resistances on Fluke 8060A calibrated meters. Each resistance was compared to a resistance versus temperature calibration chart (Figure 3-50) to define the base temperature, and then 6°C was added to the readings due to the known temperature difference between the cell and the thermistor mounting position including bond thermal resistance.

The current correction factor used was 0.045%/°C. The voltage correction factor was -1.6 mV/°C. The factors were derived from thermal testing of two elements on the panel while on the solar tracker. Both factors corresponds closely with data available from GaAs cell literature.

$$V_{\text{meas}} + (T-28)(-1.6 \text{ mV}/^{\circ}\text{C}) = V_{\text{correct}}$$

$$I_{\text{meas}} \times [1 + (T-28)(.0045)] = I_{\text{correct}}$$

Conic Mirror Reflectance

- o Based on Figure 3-40 and assuming typical tolerances apply to the onpointed MCC element output, the correction for conic mirror reflectance rho at 0° is:



**Offpoint Performance of Two Sub-Arrays (5 Parallel x 6 Series)
Compared to Perfect Optic Performance (Corrected for Cone Deficiency R=70%)**

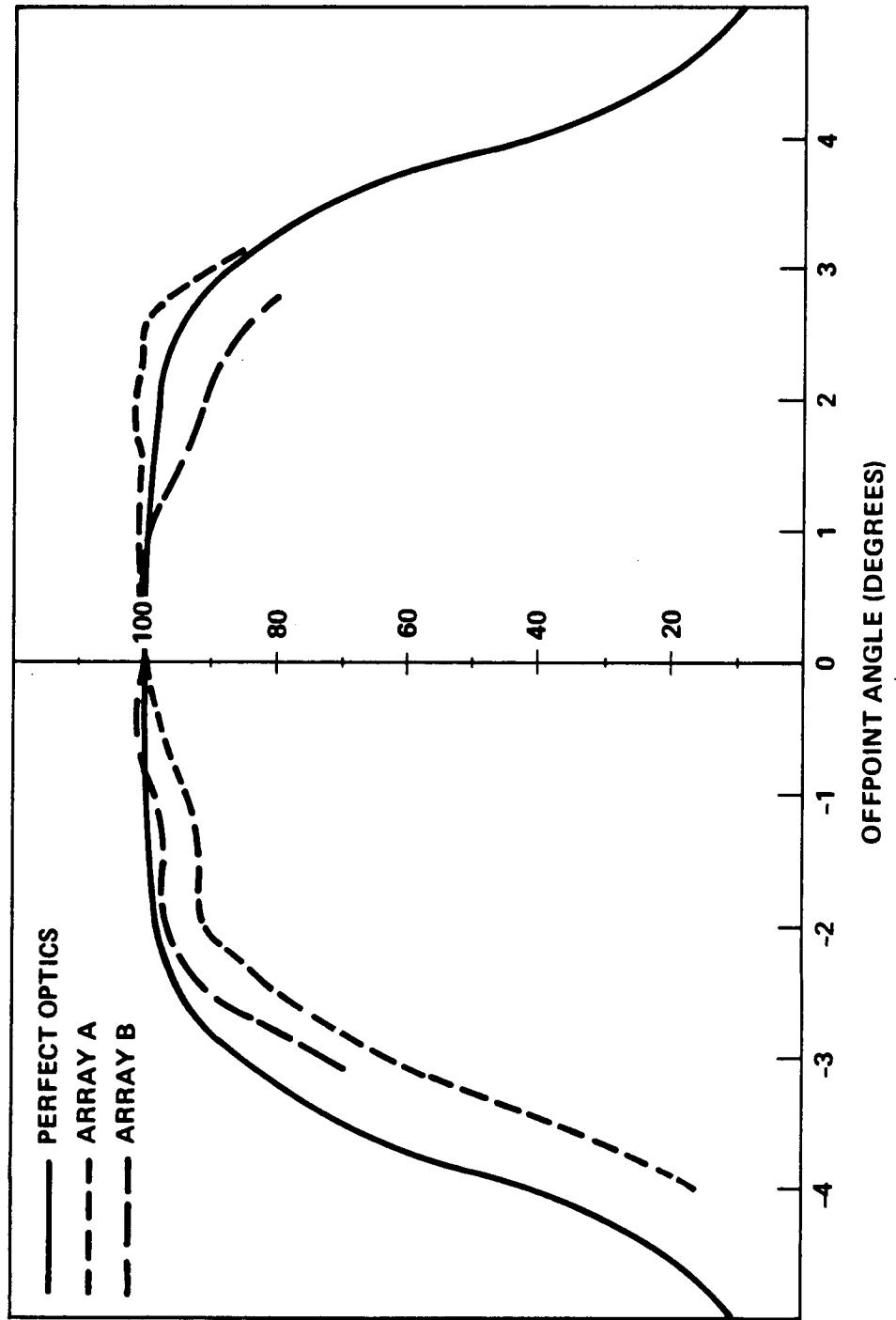


Figure 3-49



Temperature vs Resistance Reading for Mounted Thermistor 1M001-XXX

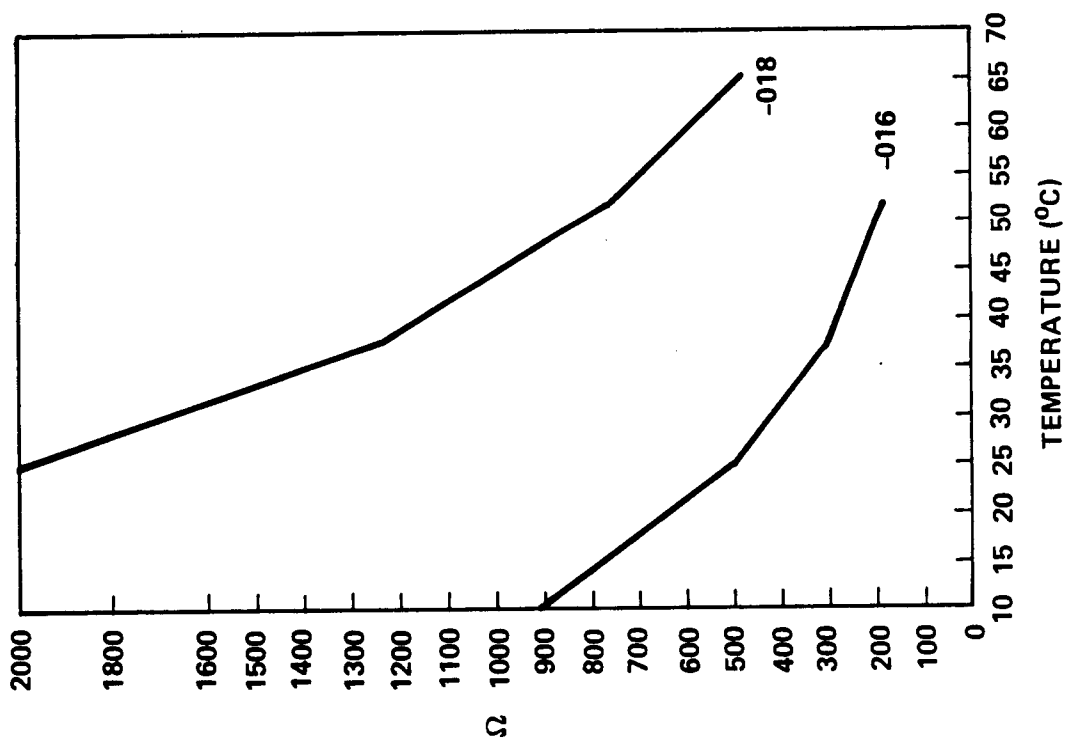


Figure 3-50

$$\frac{\text{current}}{(.41 \times \rho) + .59} = \text{corrected current}$$

- o For offpointing measurements, the perfectly aligned optic reflectance curve was used to correct the measurements.

Data presented for offpoint check was only corrected using the perfectly aligned optic correction. The result is that in many cases, the output at offpoint angles was corrected to be greater than the 0° offpoint condition.

For onpointed measurement for concentration ratio and absolute output of the elements, the 41% conic reflection represents a maximum and will vary between 25 and 41%. Similarly, the reflectance of the cones vary between 59 and 71% with an average of 66%. Therefore, the range of correction factors is as follows:

$$\begin{aligned} \frac{1}{(.41 \times .59) + .59} &= 1.202 && \text{high} \\ \frac{1}{(.25 \times .71) + .75} &= 1.078 && \text{low} \\ \frac{1}{(.36 \times .65) + .64} &= 1.144 && \text{average} \end{aligned}$$

Corrections for groups of elements in strings have a higher probability of being near the average values.

Mismatch Effects. Cell mismatch for the concentrator design is complicated by the additional consideration required due to variability of manufactured element tolerance effects. A high efficiency cell matched with a less quality optic may be equivalent to a lower efficiency cell in a high quality optic, but this would change as a function of offpoint. Conceptually, this is illustrated in Figure 3-51. Therefore, it can be expected that if low mismatch losses are desired, extensive testing and matching of a large population of MCC elements would be required.

Due to the small population of MCC elements available for this contract, the variability of the assembly tolerance effects, and the need for a dedicated grader for MCC element output which was not available, and the short time available for assembly and test, elements for the small deliverable panel were kitted into strings according to cell efficiency measured after the welding process used for electrical connection of the contacts.

Illustration of Mismatch Caused by Cell Efficiency Combined with Mirror Offpoint

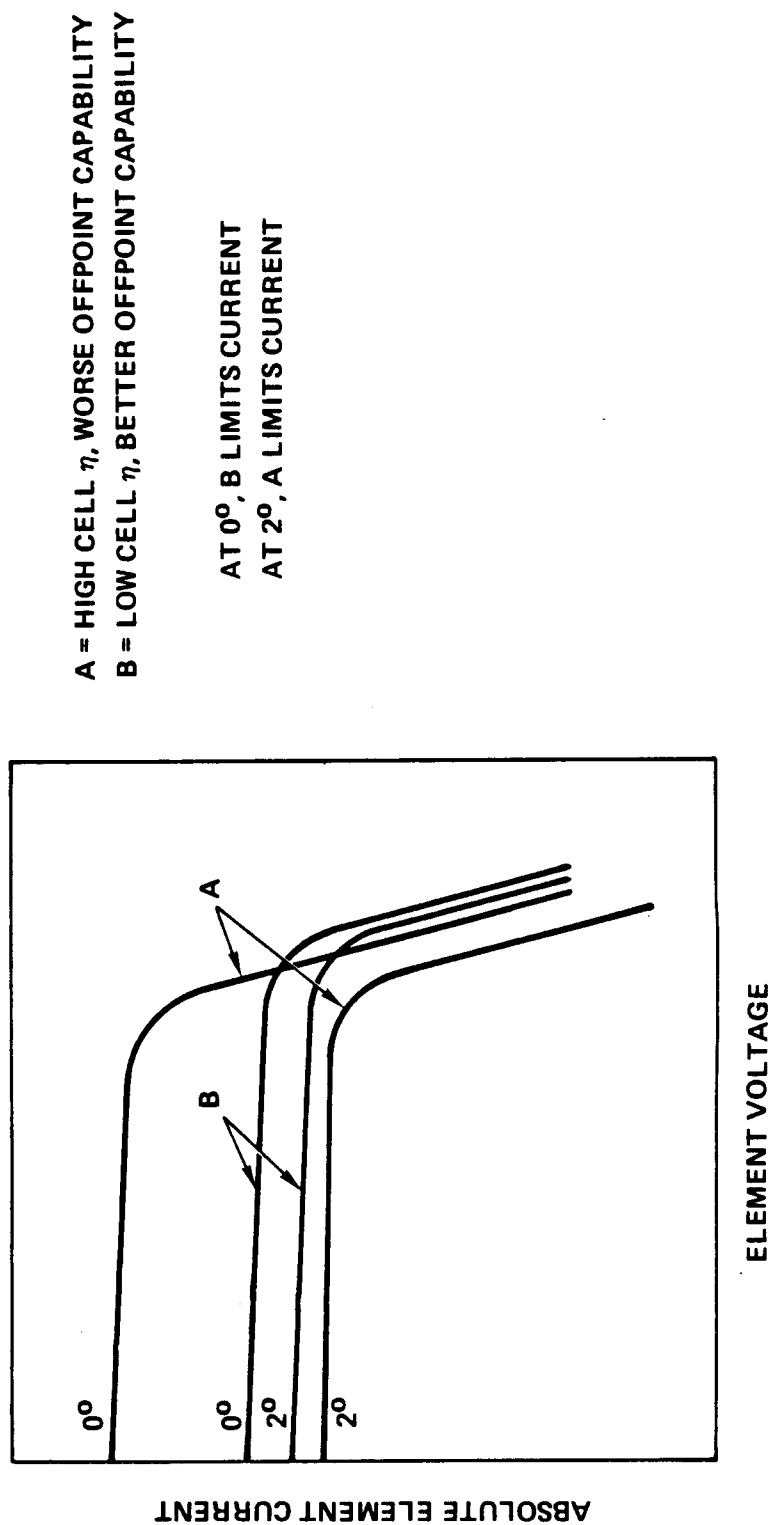


Figure 3-51

The MCC elements were mounted in the panel and tested. One shorted element was subsequently removed and replaced. Offpoint testing was performed. The panel was later tested for the output of each element at short circuit and open circuit. The results of that test, presented in 3-52, show a number of elements with substandard output at short circuit. The mismatch which results, especially due to current limiting as seen in the current voltage (IV) curves of Figures 3-44 and 3-45, directly reduces the maximum power of the tested string or strings.

As a rough approximation, the short circuit current of each of the elements in a string can be averaged to get an average string current which may then be divided into the lowest element short circuit current in a string to derive an effective mismatch, all assuming the open circuit voltage of the elements are very close in value.

Shown in Figure 3-52 are the average current for the six cell string, the calculation of mismatch for the string, and the calculation of average mismatch for all the strings, which is 7.7%.

For the larger deliverable panel, all 180 elements as completed were measured for current at 85% of open circuit voltage using the x25 solar simulator and matched as best as possible prior to assembly into the panel. As an additional complication, the cells from the three cell vendors were kept in separate strings. It was noted that the MCC elements with Varian cells were particularly poor in output due to the welding difficulties encountered (section 3.4.2.3).

Min/ Avg					Min/ Avg					Min/ Avg				
String	MCC	mV	mA		String	MCC	mV	mA		String	MCC	mV	mA	
1A	1	1054	424	.945	3A	1	1039	452	.915	5A	1	1048	427	.837
	2	1074	442			2	1066	438			2	1022	458	
	3	1078	430			3	1069	430			3	1052	425	
	4	1079	423			4	1079	389			4	1055	440	
	5	1085	422			5	1071	420			5	1058	350	
	6	1091	400			6	1056	422			6	1058	413	
	X		424			X		425			X		418	
1B	7	1048	426	.955	3B	7	1073	421	.936	5B	7	1056	447	.948
	8	1065	418			8	1074	392			8	1059	435	
	9	1073	445			9	1079	394			9	1057	445	
	10	1072	422			10	1073	432			10	1055	469	
	11	1062	414			11	1067	438			11	1033	418	
	12	1075	402			12	1082	438			12	1031	432	
	X		421			X		419			X		441	
2A	1	1069	441	.944	4A	1	1062	442	.835	AVERAGE OF MIN = .923 AVG				
	2	1070	444			2	1053	355						
	3	1017	403			3	1026	416						
	4	1075	422			4	1031	450						
	5	1086	434			5	1049	452						
	6	1082	419			6	1058	432						
	X		427			X		425						
2B	7	1080	439	.977	4B	7	1058	425	.942					
	8	1078	427			8	1051	405						
	9	1079	420			9	1061	445						
	10	1072	436			10	1055	437						
	11	1082	424			11	1053	435						
	12	1086	436			12	1053	435						
	X		430			X		430						

FIGURE 3-52: SMALL PANEL MISMATCH TALLY AND CALCULATION

3.4 CELL STACK DESIGN AND INVESTIGATION

The baseline design for electrical interconnection was soldering of both the top and the bottom connections as was performed for the MCC element designed under NAS8-35635. It was noted under that contract that significant degradation of the current and voltage was experienced by the cell after soldering. Measurements were performed under 1 sun AMO.

To determine the possible causes, various portions of the stack assembly process were investigated. Figure 3-53 records the investigation areas. A plan was developed to test the cells for gross effects. The bare cells were tested at one sun AMO. A number of configurations using solder versus no solder were run through heating cycles as used for the cell stack assembly. Samples were heated in both vapor phase solder station (VPS) and a hot plate. In most conditions the samples degraded similarly to those in contract NAS8-35635. The sample size was large enough to show that soldering was the degrading mechanism. The results are shown in Figure 3-54. Average losses were computed for the various processes by combining data of similar origin. For example all cells with solder on the front contact were grouped together, ignoring other factors in the process such as mounting method. This enabled gross judgements of defect mechanisms. As a second refinement, successively greater narrowing of the error band and grouping of the cells within the band, helped establish that it was the soldering process itself that was causing the degradation and probably the front contact solder bond.

Subsequent discussion with the vendors indicated that unlike silicon, GaAs will be wet by solder. Therefore, in any environment where the solder cannot be precisely controlled, a potential for solder flowing over the GaAs and shorting the junction exists. Both the hot plate and the vapor phase solder method are not precision controlled for solder placement.

The soldering process (front contacts versus rear contacts) was investigated by substituting another process for the soldering and checking the results. In parallel with this, the mechanism of degradation caused by the solder was investigated. Effort was concentrated to make connection on the front contact. The options were soldering, welding, and adhesive bonding.

TEST RESULT - ASSEMBLY LOSS (11%) INVESTIGATION



Engineering & Test Division
TRW Space & Technology Group

A. CELL JUNCTION DEGRADATION	TEST	Put cell stack in various stages of assembly through vapor phase reflow equipment. Use oven heated and unheated cells for control.	3 - 60%
B. TEST EQUIPMENT ERROR	TEST	Review test procedures for error propagation. Test cell output.	0
		Test cell output. Modify test fixture. Test cells again.	2.5% (I)
		Calibrate X25 simulator for uniformity in test area.	+1.5% (I)
C. TEMPERATURE UNCONTROLLED	TEST	Attach thermocouple to cell and MCC element back. Calibrate temperature gradient. Check output against temperature reading.	0.7% (V)
D. SPECTRAL SHIFT AFTER HEATING. USE OF SILICON STANDARD.	PROCUREMENT	Acquire balloon traceable GaAs standard cells.	N/A
	TEST	Compare output using Si standard vs output using GaAs standard.	+1.5%

FIGURE 3-53

FIGURE 3-54.

Initially, solder on the front contact and mounting to beryllia looked to be candidate causes. Fine tuning of the sample size by discarding very large loss cells showed that front contact soldering should be investigated

CELL NO.	IMP		VMP		ISC		VOC		PMP		FF		AVERAGE	
	BEFORE	AFTER	BEFORE	AFTER	BEFORE	AFTER	BEFORE	AFTER	BEFORE	AFTER	BEFORE	AFTER	BEFORE	AFTER
1	3.1399	3.0328	0.4582	0.4323	-0.0059	-0.0059	-0.0059	-0.0059	-0.0059	-0.0059	-0.0059	-0.0059	-0.0059	-0.0059
2	3.1399	3.0328	0.4582	0.4323	-0.0059	-0.0059	-0.0059	-0.0059	-0.0059	-0.0059	-0.0059	-0.0059	-0.0059	-0.0059
3	3.1399	3.0328	0.4582	0.4323	-0.0059	-0.0059	-0.0059	-0.0059	-0.0059	-0.0059	-0.0059	-0.0059	-0.0059	-0.0059
4	3.1399	3.0328	0.4582	0.4323	-0.0059	-0.0059	-0.0059	-0.0059	-0.0059	-0.0059	-0.0059	-0.0059	-0.0059	-0.0059
5	3.1399	3.0328	0.4582	0.4323	-0.0059	-0.0059	-0.0059	-0.0059	-0.0059	-0.0059	-0.0059	-0.0059	-0.0059	-0.0059
6	3.1399	3.0328	0.4582	0.4323	-0.0059	-0.0059	-0.0059	-0.0059	-0.0059	-0.0059	-0.0059	-0.0059	-0.0059	-0.0059
7	3.1399	3.0328	0.4582	0.4323	-0.0059	-0.0059	-0.0059	-0.0059	-0.0059	-0.0059	-0.0059	-0.0059	-0.0059	-0.0059
8	3.1399	3.0328	0.4582	0.4323	-0.0059	-0.0059	-0.0059	-0.0059	-0.0059	-0.0059	-0.0059	-0.0059	-0.0059	-0.0059
9	3.1399	3.0328	0.4582	0.4323	-0.0059	-0.0059	-0.0059	-0.0059	-0.0059	-0.0059	-0.0059	-0.0059	-0.0059	-0.0059
10	3.1399	3.0328	0.4582	0.4323	-0.0059	-0.0059	-0.0059	-0.0059	-0.0059	-0.0059	-0.0059	-0.0059	-0.0059	-0.0059
11	3.1399	3.0328	0.4582	0.4323	-0.0059	-0.0059	-0.0059	-0.0059	-0.0059	-0.0059	-0.0059	-0.0059	-0.0059	-0.0059
12	3.1399	3.0328	0.4582	0.4323	-0.0059	-0.0059	-0.0059	-0.0059	-0.0059	-0.0059	-0.0059	-0.0059	-0.0059	-0.0059
13	3.1399	3.0328	0.4582	0.4323	-0.0059	-0.0059	-0.0059	-0.0059	-0.0059	-0.0059	-0.0059	-0.0059	-0.0059	-0.0059
14	3.1399	3.0328	0.4582	0.4323	-0.0059	-0.0059	-0.0059	-0.0059	-0.0059	-0.0059	-0.0059	-0.0059	-0.0059	-0.0059
15	3.1399	3.0328	0.4582	0.4323	-0.0059	-0.0059	-0.0059	-0.0059	-0.0059	-0.0059	-0.0059	-0.0059	-0.0059	-0.0059
16	3.1399	3.0328	0.4582	0.4323	-0.0059	-0.0059	-0.0059	-0.0059	-0.0059	-0.0059	-0.0059	-0.0059	-0.0059	-0.0059
17	3.1399	3.0328	0.4582	0.4323	-0.0059	-0.0059	-0.0059	-0.0059	-0.0059	-0.0059	-0.0059	-0.0059	-0.0059	-0.0059
18	3.1399	3.0328	0.4582	0.4323	-0.0059	-0.0059	-0.0059	-0.0059	-0.0059	-0.0059	-0.0059	-0.0059	-0.0059	-0.0059
19	3.1399	3.0328	0.4582	0.4323	-0.0059	-0.0059	-0.0059	-0.0059	-0.0059	-0.0059	-0.0059	-0.0059	-0.0059	-0.0059
20	3.1399	3.0328	0.4582	0.4323	-0.0059	-0.0059	-0.0059	-0.0059	-0.0059	-0.0059	-0.0059	-0.0059	-0.0059	-0.0059
21	3.1399	3.0328	0.4582	0.4323	-0.0059	-0.0059	-0.0059	-0.0059	-0.0059	-0.0059	-0.0059	-0.0059	-0.0059	-0.0059
22	3.1399	3.0328	0.4582	0.4323	-0.0059	-0.0059	-0.0059	-0.0059	-0.0059	-0.0059	-0.0059	-0.0059	-0.0059	-0.0059
23	3.1399	3.0328	0.4582	0.4323	-0.0059	-0.0059	-0.0059	-0.0059	-0.0059	-0.0059	-0.0059	-0.0059	-0.0059	-0.0059
24	3.1399	3.0328	0.4582	0.4323	-0.0059	-0.0059	-0.0059	-0.0059	-0.0059	-0.0059	-0.0059	-0.0059	-0.0059	-0.0059
25	3.1399	3.0328	0.4582	0.4323	-0.0059	-0.0059	-0.0059	-0.0059	-0.0059	-0.0059	-0.0059	-0.0059	-0.0059	-0.0059
26	3.1399	3.0328	0.4582	0.4323	-0.0059	-0.0059	-0.0059	-0.0059	-0.0059	-0.0059	-0.0059	-0.0059	-0.0059	-0.0059
27	3.1399	3.0328	0.4582	0.4323	-0.0059	-0.0059	-0.0059	-0.0059	-0.0059	-0.0059	-0.0059	-0.0059	-0.0059	-0.0059
28	3.1399	3.0328	0.4582	0.4323	-0.0059	-0.0059	-0.0059	-0.0059	-0.0059	-0.0059	-0.0059	-0.0059	-0.0059	-0.0059
29	3.1399	3.0328	0.4582	0.4323	-0.0059	-0.0059	-0.0059	-0.0059	-0.0059	-0.0059	-0.0059	-0.0059	-0.0059	-0.0059
30	3.1399	3.0328	0.4582	0.4323	-0.0059	-0.0059	-0.0059	-0.0059	-0.0059	-0.0059	-0.0059	-0.0059	-0.0059	-0.0059
31	3.1399	3.0328	0.4582	0.4323	-0.0059	-0.0059	-0.0059	-0.0059	-0.0059	-0.0059	-0.0059	-0.0059	-0.0059	-0.0059
32	3.1399	3.0328	0.4582	0.4323	-0.0059	-0.0059	-0.0059	-0.0059	-0.0059	-0.0059	-0.0059	-0.0059	-0.0059	-0.0059
33	3.1399	3.0328	0.4582	0.4323	-0.0059	-0.0059	-0.0059	-0.0059	-0.0059	-0.0059	-0.0059	-0.0059	-0.0059	-0.0059
34	3.1399	3.0328	0.4582	0.4323	-0.0059	-0.0059	-0.0059	-0.0059	-0.0059	-0.0059	-0.0059	-0.0059	-0.0059	-0.0059
35	3.1399	3.0328	0.4582	0.4323	-0.0059	-0.0059	-0.0059	-0.0059	-0.0059	-0.0059	-0.0059	-0.0059	-0.0059	-0.0059
36	3.1399	3.0328	0.4582	0.4323	-0.0059	-0.0059	-0.0059	-0.0059	-0.0059	-0.0059	-0.0059	-0.0059	-0.0059	-0.0059

20 = all cells exposed to 410 F(210 C) for 20 seconds
 40 = all cells exposed to 410 F(210 C) for 40 seconds
 BeO = all cells mounted on BeO insulator/thermal conductor
 no BeO = all cells not mounted on BeO
 Cu = all cells mounted to BeO and copper plate
 no Cu = all cells not mounted to BeO and copper plate
 Back = all cells with solder melted onto back contact
 no Back = all cells with no solder melted onto back contact

Front = all cells with solder melted onto front contact
 no Front = all cells with no solder melted onto front contact
 Flux = all cells using flux during solder operation
 no Flux = all cells not using flux during solder operation
 Oven = all cells heated in solder reflow oven
 Plate = all cells heated on hot plate
 Process = all cells put through some part of soldering process
 no Process = all cells not put through some part of soldering process (except heating)

3.4.1 Solder Investigation

It was surmised that the solder was flowing over the top edges of the GaAs wafer and shorting the exposed junction at the edge of the cell. As a first attempt to control this perceived mechanism, a number of cells were sent back to the supplier, ASEC, and an SiO coating was applied to the sides of the cells.

Assembly of some of these cells in the VPS station yielded no better results than before. Since the back contact of the cell was required to make full-intimate contact with the heat sink, and solder was the best viable material, elimination of the uncontrolled VPS method was not considered practical. After success with another process (welding) was established, further process investigation was halted.

3.4.2 Alternate Bonding Methods

Any method to bond the top contacts had to be able to survive a vapor phase solder reflow process without debonding or shorting the cell. The reflow would be used for the bottom contact and/or the heat sink to primary bond.

3.4.2.1 Adhesive Bonding-Top Contacts

A silver filled adhesive was identified as a potential alternate to solder. Epoxies, polyimides, and even ceramics were considered. These processes were to be investigated in another ongoing program for which the results were made available. No effort was spent on this contract on these alternatives. The ceramic adhesive has good promise. The other adhesives degraded greater than 5% in thermal cycling. Scatter of the data was high.

3.4.2.2 Gold Germanium Eutectic

A gold germanium eutectic (350°C flow) was also considered but again results were available from another program. The bonds could not be made without significant degradation.

3.4.2.3 Welding

Since it was clear that soldering would not be viable with cell top contact installation, welding, a method with which TRW has had considerable development experience on silicon but not with GaAs was attempted. Initial trials developed good bonds but shorted the cell. The weld voltage was decreased until a good bond was retained and average cell maximum power point degradation was less than 1.2% (Figure 3-55). Testing was performed with a LAPSS moved to a range corresponding to 100 suns AMO exposure. The weld voltage range to maintain good electrical and mechanical bonding was more narrow than typically used ranges for silicon cells.

It was found that the weld schedule for GaAs was very specific to the cell manufacturer, most likely as a function of both cell construction and metallization method. For engineering purposes, an individual weld schedule was developed for each the ASEC, Spectrolab and Varian cells, without further investigation into exact weld metallurgy phenomena. The weld schedule for each vendor is shown in Figure 3-56.

Both the ASEC and Spectrolab cells had silver final metallization on the front and back contacts. The Varian cells had gold contacts. Contact metallization material was not specified for the cells for this application due partly to the original assumption that the cells would be soldered.

The silver interconnect to silver contact weld achieved the highest consistent weld strength of greater than 1 kilogram pull (shear only). An attempt to weld silver interconnects to the gold contacts was not successful due to the very low (<.05 kg) pull strength. Therefore, additional unplated interconnects were plated with gold of the same thickness as the silver interconnects and welding was again attempted. The resulting welds were significantly lower in strength (<.4 kg) and good adhesion was very difficult to attain without significant degradation of the cells (>10%) as evidenced by the extremely narrow weld schedule. Backing off of the time and increasing the voltage, and increasing time with decreased voltage compared to the baseline weld schedule yielded even worse results.

FIGURE 3-55: CELL PERFORMANCE TEST (100 SUN FLASHER INTENS., ROOM TEMPERATURE) BEFORE & AFTER WELD/SOLDER OF FRONT CELL CONTACT

GaAs CELL NO.	WELD SCHEDULE			ELECTR. BEFORE				ELECTR. AFTER				PA/PB
	VOLTAGE (V)	TIME (MS)	PRESS (Kg)	Isc (MA)	Voc (V)	Pop (MW)	PULL STRENGTH (lb.)	Isc (MA)	Voc (V)	Pop (MW)	PULL STRENGTH (lb.)	
27	.56	100	1			346.7		--	--	--		0
9	.56					341.7				335.3		.981
21	.56					338.7				342.9	5.0I	1.012
31	.56					348.0				347.7		.999
51	.58					343.0				337.5	2.8W	.984
80A	.58					341.6				336.8		.986
56	.58					342.9				342.7		.999
28	.58					347.7				335.9		.966
43A	.60					335.0				332.7		.993
88	.60					340.0				333.2	1.0C	.980
24	.60					344.2				345.4		1.003
23	.60					336.3				332.5	3.2W	.989
36	.60					332.4				329.3		.991
10	.60					346.9				341.3		.984
5	.60					335.2				329.7		.984
70	.60					338.3				335.9	4.5C	.993
49	.62					344.2				343.9		.999
41	.62					324.4				326.9	3.7W	1.008
83	.64					339.3				338.7	3.5W	.998
4	.70					341.6				337.0	5.5W	.987
95	.72	100	1			335.1		--	--	--		0
	DURAT (DIAL)	APLIT. (DIAL)	PRESS (lb.)					(9% Shorted) Average				.991
*94	8	5.5	1			345.2		--	--	--		0
*99						346.4				341.0	5.0I	.984
*13						349.2				335.3	5.5S	.960
*17				373.6	1.08	348.1		367.2	1.08	341.3		.983
*96A						344.2				250.7		(.728)
21						347.9		--	--	--		0
13						339.5		--	--	--		0
53						335.6				314.8		.938
55A						332.9				332.1	5.5I	.998
16	8	5.5	+			341.2				342.3		1.003
								(30% Shorted) Average				.978

* EDGE COATED CELLS/ (NO) = SHORTED CELLS

WELD SCHEDULES DEVELOPED FOR ALL VENDORS



Engineering & Test Division
TRW Space & Technology Group

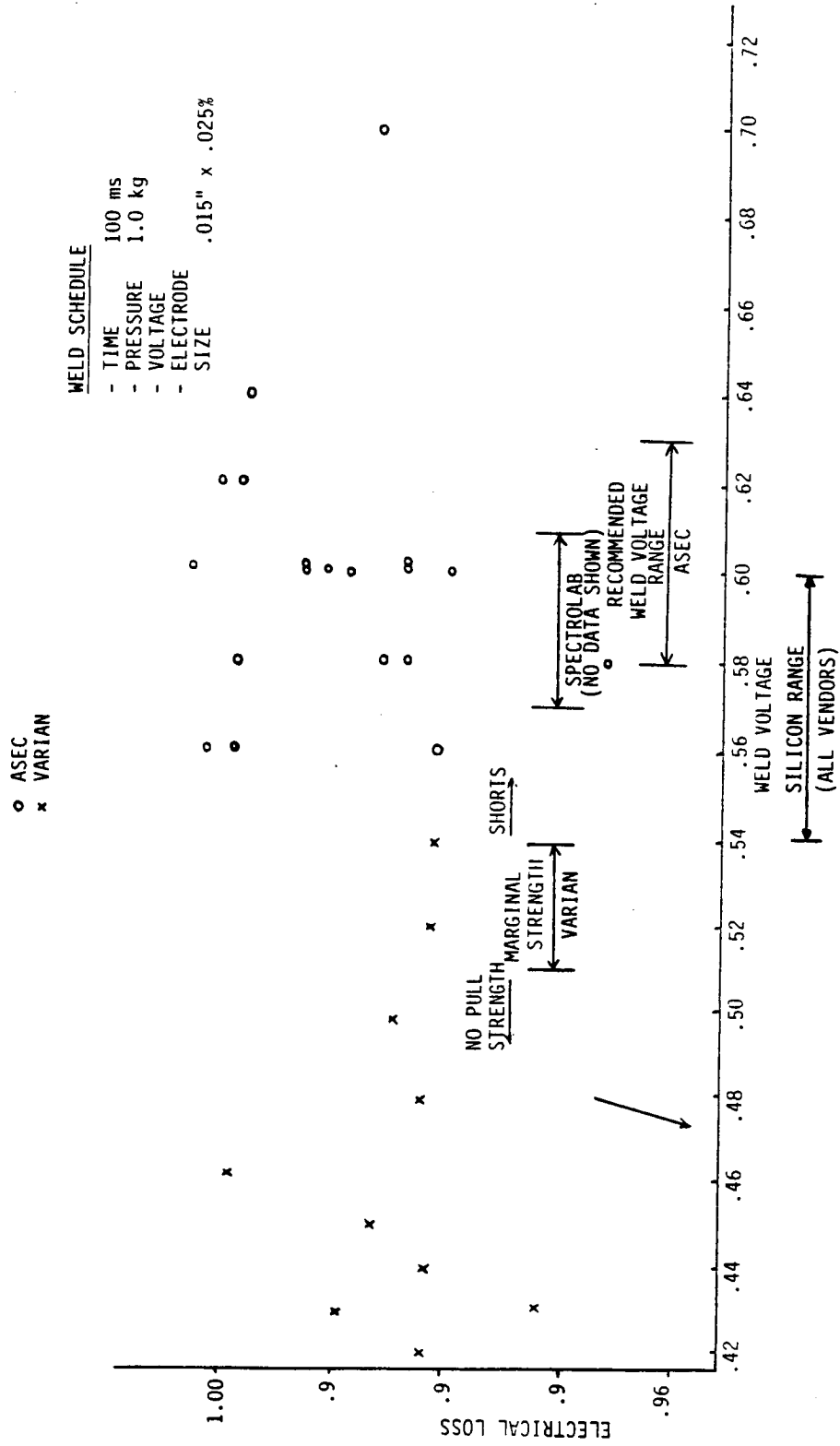


FIGURE 3-56

Although the degradation of output of the Spectrolab cells was slightly greater than the ASEC cells after welding, the sample size was insufficient to determine if this was significant. No more cells were available for these experimental purposes.

All future subcontracts to vendors will require the cell to be silver metallized since the silver welds were so successful and there is no compelling reason to retain gold contacts.

3.4.2.4 Stack Subassembly

Pretested welded cells were placed in a VPS fixture to bond the cell to the heat sink with a one mil solder preform between the cell and heat sink. The preform was slightly smaller than the cell. After soldering, the cells were tested. Degradation averaged only one percent (Figure 3-57). The welded front contact with VPS rear contact was made baseline.

Thermal shock testing (100 cycles, liquid nitrogen to 100°C) showed no additional degradation of the substacks.

3.4.3 Electrically Connected Versus Isolated Cell Stack-Heat Sink

The heat sink for the solar cell could be made either electrically conductive or insulative. The heat sink exists to isolate the brittle cell from the thermal expansion mismatched copper nickel mirror. The heat sink is required to have an expansion coefficient very near to that of the GaAs cell to minimize stress on the cell.

A molybdenum sink would provide a conductive path to the MCC mirror. An alumina or beryllia sink would provide insulation from the mirror.

In light of the goal of low cost and light weight a comparison was made between advantages and disadvantages as shown in Figure 3-58.

Clearly, an electrically insulated design is most desirable since it simplifies control of the electrical power without compromising the design of the conductive graphite substrate and mirror mounts.

CELL PERFORMANCE BEFORE AND AFTER VAPOR PHASE
SOLDERING OF CELL REAR CONTACT TO BE BeO SUBSTRATE



Engineering & Test Division
TRW Space & Technology Group

GaAs CELL No.	SOLDER			ELECTRICAL BEFORE			ELECTRICAL AFTER			P AFTER / P BEFORE
	TYPE	TEMP. (°F)	TIME (SEC)	Isc (mA)	Voc (V)	Pmp (mW)	Isc (mA)	Voc (V)	Pmp (mW)	
28	Sn62	419	15	364.4	1.073	335.2	363.1	1.075	332.7	.993
30				371.2	1.080	346.3	370.9	1.080	342.8	.990
10				370.4	1.076	342.1	368.8	1.076	339.6	.993
9				357.4	1.080	333.0	356.2	1.081	328.3	.986
80				359.3	1.082	336.5	358.5	1.082	331.8	.986
43	INDALLOY #2	320	15	371.3	1.066	331.2	370.9	1.066	326.7	.986
56				372.9	1.075	342.4	371.6	1.077	339.0	.990
36				366.6	1.080	328.0	364.5	1.080	321.0	.979
49				370.4	1.078	343.0	369.5	1.077	338.0	.985
24				375.7	1.076	344.7	373.3	1.077	342.8	.994
5	INDALLOY #3	428	70	357.7	1.082	325.0	353.4	1.079	316.0	.972

Sn62 Pavg = .990

Indalloy #2 Pavg = .987

FIGURE 3-57

	BeO	ALUMINA	MOLYBDENUM
THERMAL CONDUCTANCE $\frac{\text{Btu}}{\text{hr ft } ^\circ\text{F}}$	120	18	84.5
ELECTRICAL CONTROL	ISOLATED	ISOLATED	DIFFICULT
TEMP COEFFICIENT $(\frac{\text{cm}}{\text{cm } ^\circ\text{C}} \times 10^{-6})$	5.9	6.4	5.04
ELECTRICAL CONNECTION	Requires Metallizing	Requires Metallizing	Requires Metallizing
DENSITY $(\frac{\text{g}}{\text{cm}^3})$	3.9	3.94	10.2

FIGURE 3-58: CELL HEAT SPREADER TRADE

Beryllia was selected over alumina due to its high thermal conductivity and hence, lower effective operating temperature. The cost of alumina versus beryllia is not significant once the cost of metallization and high precision manufacturing are factored into the total cost.

The heat sink is shown in Figure 3-59. The two isolated metallized pads were provided before it was found that no mechanical attachment of the cone to the heat sink would be required. The pads will be eliminated in any future procurement.

3.4.3.1 Heat Sink Bond

The heat sink was bonded to the primary mirror using the vapor phase solder method. A pre-fluxed preform of 1 mil Sn62 solder was held tightly between the heat sink and the nickel surface of the mirror in a specially designed tool which was then lowered into the vapor phase station.

3.4.4 Coverglass

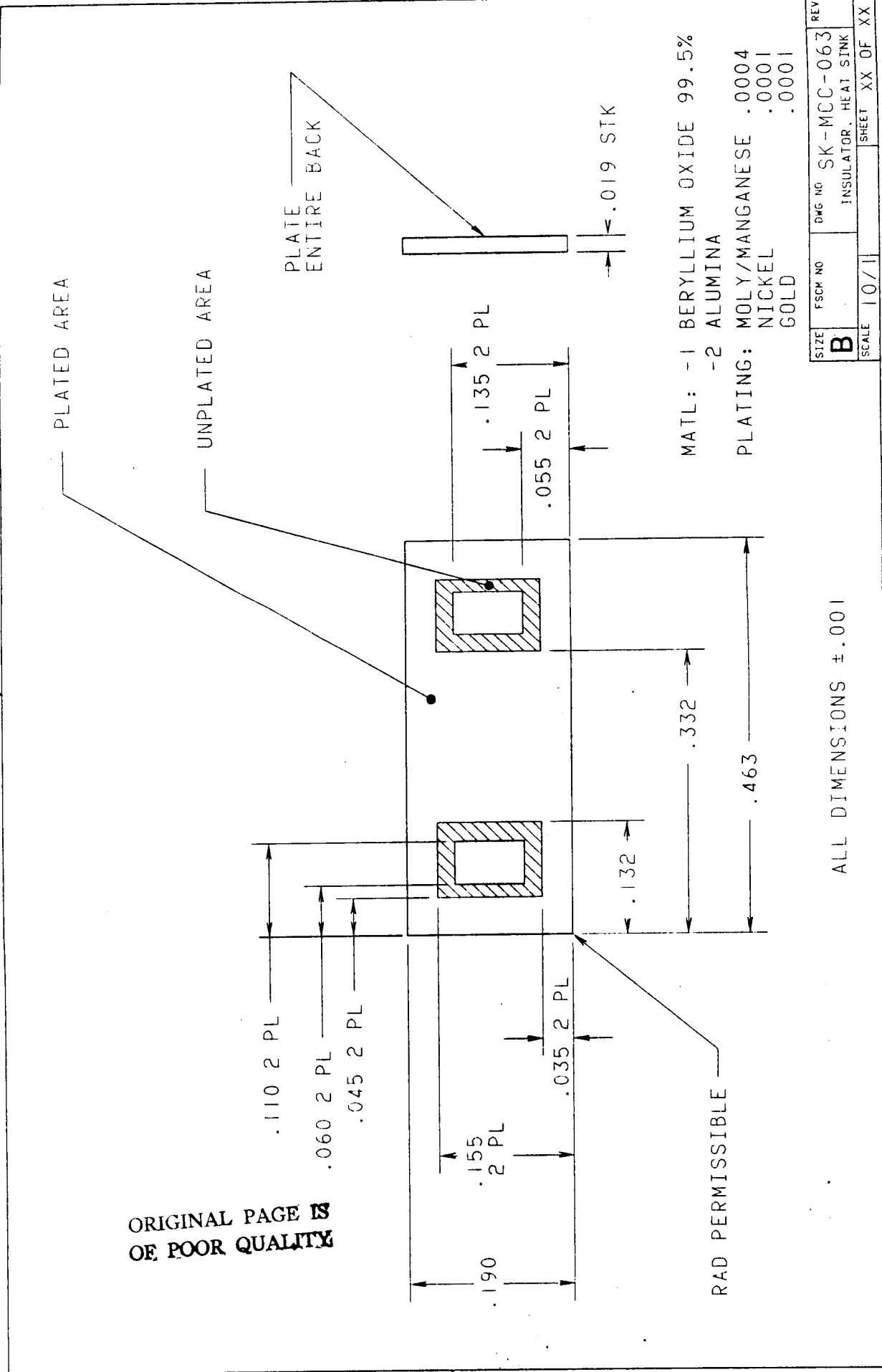
A coverglass (Figure 3-60) was incorporated into the cell stack to protect the cell from electron, proton, and other corpuscular radiation. Protection from atomic oxygen is also provided. The cover material was antireflection coated CMX, a ceria doped borosilicate glass manufactured by Pilkington, Great Britain. CMX was chosen over fused silica due to cost, wide use in other programs, and better thermal expansion match to GaAs, and to the nickel conic mirror.

3.4.5 Cover Adhesive

The cover adhesive is Dow Corning 93-500 silicone. This adhesive is standard to the solar array manufacturing industry. Adhesive bonding was chosen over mechanical capture of the cover over the cell. The darkening of this adhesive in this application should be investigated and is recommended for any future contract.

3.4.6 Conic Mirror

As defined in the Statement of Work for NAS8-36159, the conic mirror is considered part of the cell stack. A number of options were considered for mounting of this mirror to the cell



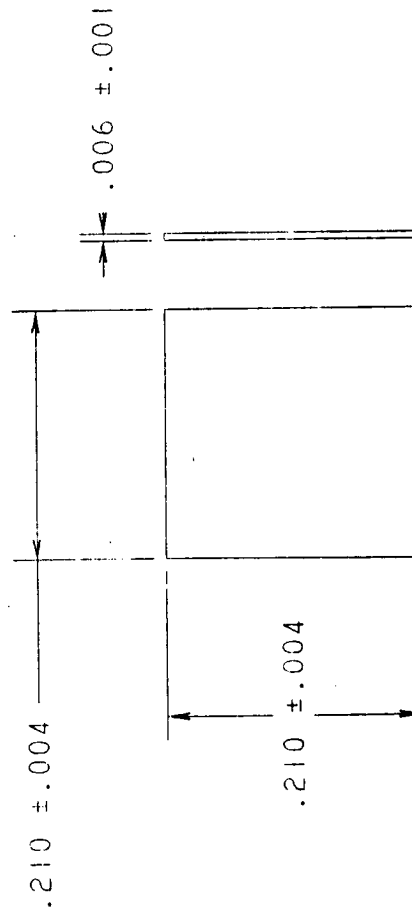
↑ CADAM

FIGURE 3-59



ACTUAL SIZE

ORIGINAL PAGE IS
OF POOR QUALITY.



-1 FUSED SILICA
-2 CMX

CELL COVER (PLAIN)

MCC 050

SCALE 10/1 09-04-85

stack (Figure 3-61). A cover with metallization could be used to solder from the cone to the cover. Potential thermal mismatch stresses, cost of the specialized metallization process (even for over 100,000 units), and loss of cone to cell optical centering flexibility, excluded this choice. The cone to heat sink solder bond was excluded due to added complexity of a new part and lack of precise positioning control in the soldering process. Direct soldering of the cone to the glass was considered. Indium solders wet well to glass but the process required (brushing with a metallic brush wet with the solder at elevated temperatures) made this impractical. Adhesives which were considered are shown in Figure 3-62.

DC93500 was a low strength candidate chosen chiefly for its low (around -120°C) glassing point, lower than the -80°C temperature minimum expected in a low earth orbit for the array. This would yield low glass to nickel strain and therefore little likelihood of failure under thermal cycling. DC61104 was chosen for its higher strength, and low temperature compliance. Lefkoweld epoxy was chosen for its resilience and availability as well as experience with flight space-craft. Another epoxy (EA934) was considered as a stronger material, but it had somewhat less resilience. Of the cone to cover adhesive bonding methods, the Dymax 628T ultraviolet curing acrylic adhesive was selected for high processibility, relative low thermal stress, and high strength. Considerable mechanical and thermal cycle stress testing was performed to assure the capability of withstanding a LEO environmental exposure.

3.4.7 Cell and MCC Element Electrical Interconnections

The cell stack electrical interconnect designs were patterned after similar TRW manufactured interconnects used on flight hardware. The cell top contact interconnect (Figure 3-63) was a plated kovar material chosen for thermal expansion match to GaAs. The physical configuration incorporated two bonding pads at the corners of the cell, and an out of plane thermal expansion loop.

The interconnect for the back contact (Figure 3-64) was designed to pick up the gold plating electrical path on the beryllia heat sink upon which the cell backside was soldered.

Cell Stack Mechanical Attachments Investigated

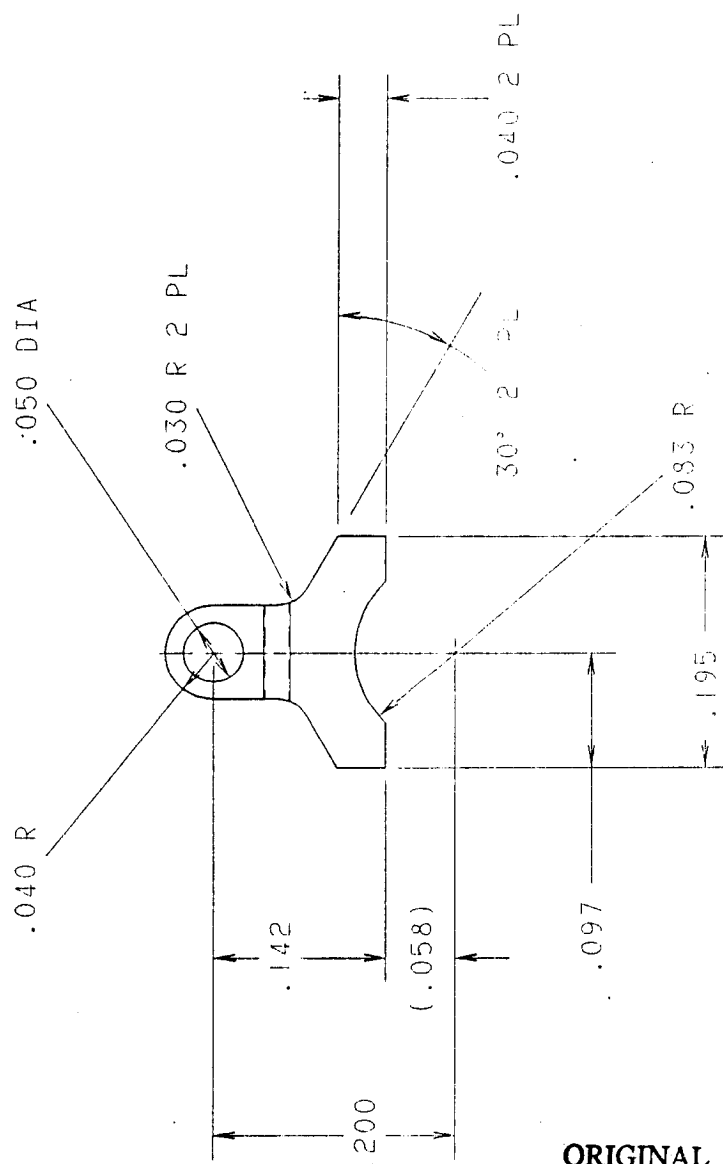


PARTS TO BE JOINED		OPTIONS	VIEW	PRESENT CHOICE
COVER	CELL	ADHESIVE		SELECTED
CONE	COVER	ADHESIVE		SELECTED
	-OR-			
CONE	BeO	SOLDER		N/A
BeO	PRIMARY	SOLDER		SELECTED
TERMINALS	PRIMARY	SOLDER		SELECTED

☐ CONSIDERED BEST MANUFACTURING OPTION

	MFG HANDLING	YIELD STRENGTH	TYPE OF BOND	RESILIENCE	ADHESION	OXYGEN ATOMIC	THERMAL CYCLE TEST	OUTGASSING	RADIATION RESISTANCE
RTV 3145	FAIR	450 PSI	TACK	GOOD	EXCELLENT	EXCELLENT	PASSED	POOR	EXCELLENT
DC93 500	GOOD	300 PSI	FULL FILLET	GOOD	FAIR TO POOR	EXCELLENT	PASSED	GOOD	EXCELLENT
DC6-1104	FAIR	400 PSI	TACK	GOOD	GOOD TO FAIR	EXCELLENT	PASSED	GOOD	EXCELLENT
LEFKOWELD EPOXY	FAIR	2200 PSI	TACK	VERY GOOD	EXCELLENT	?	PASSED	FAIR	GOOD
EA 934	FAIR	3500 PSI	TACK	FAIR (Brittle)	GOOD	?	PASSED	GOOD	GOOD
DYMAX 628T	EXCELLENT	1800 PSI	FULL FILLET	VERY GOOD	GOOD	?	PASSED	FAIR	?

FIGURE 3-62: ADHESIVE TRADE FOR CONE TO COVER BOND



MATERIAL: .001 THICK KOVAR
PLATING: -1 SILVER .0004
-2 GOLD .0004

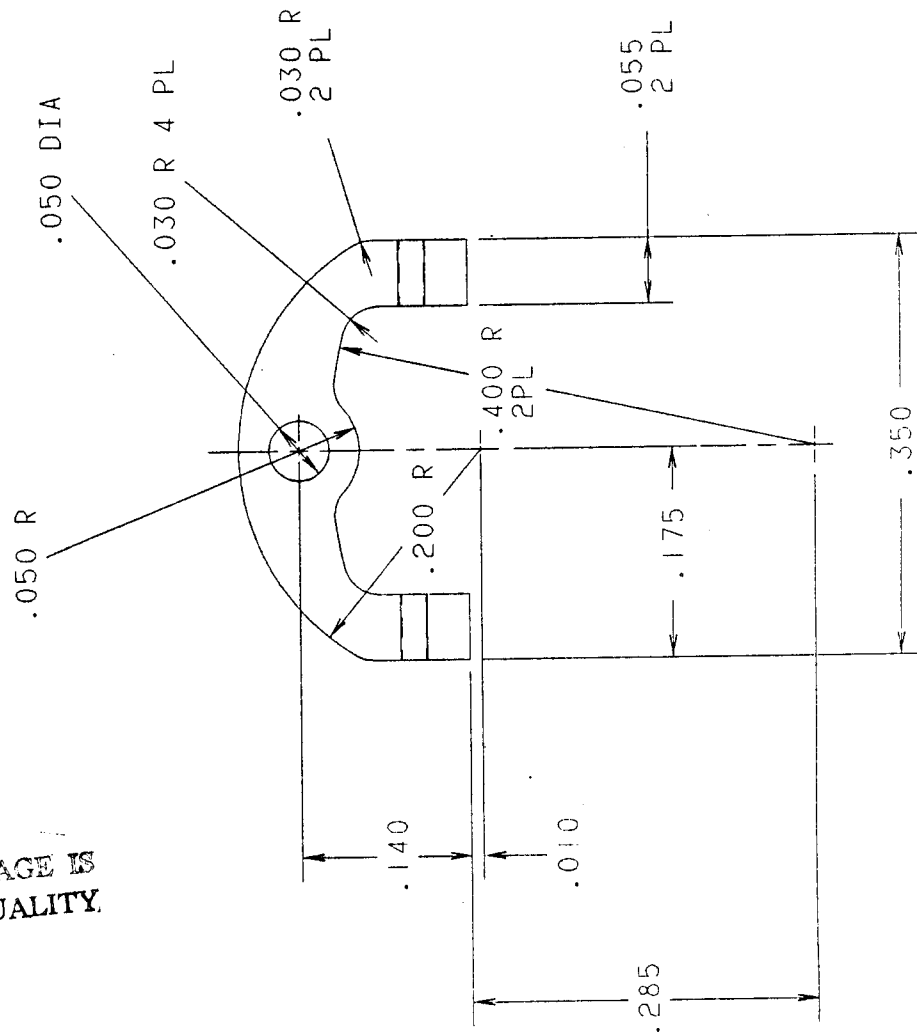
ORIGINAL PAGE IS
OF POOR QUALITY

SIZE	FORM NO	DWG NO	REV
B		MMC-092	
SCALE	10:1	SHEET	XX OF XX

CREAM

FIGURE 3-63: CELL TOP INTERCONNECT.

ORIGINAL PAGE IS
OF POOR QUALITY



SIZE	FSCM NO	DWG NO	REV
B		MCC-091	
SCALE	SHEET	XX OF	XX
10/11			

DRAWING = MCC-091
DATE = 12/10/85 TIME = 10.38 SCALE = 1.0000

↑ CADPAC

FIGURE 3-64 : INTERCONNECT TO HEAT SINK.

Two contact positions were provided on the interconnect which were then welded to the beryllia metallization. A gold to gold weld was chosen over soldering due to a manufacturing process desire to use vapor phase soldering for subsequent assembly steps. The interconnect has out of plane expansion loops to minimize the contact stresses. The weld schedule and strength are shown in Figure 3-65.

Each of the interconnects was mounted to special terminals using a standard SN62 solder. Posts on the terminals fit through holes in the interconnect as a mechanical bond (Figure 3-66).

The terminals are commercially available hermetically sealed feedthrough systems (HSC Series 1000 SP30, Hermetic Seal Corp.) which incorporate a glass bead to electrically isolate the electrical feedthrough post from the mechanical mounting. The glass perimeter is covered by metallization which may be used for solder mountings. In this application, the terminal is soldered to the feedthrough holes in the primary mirror cup. Electrical connection between optics is via wire soldered to the terminals showing on the backside of the cup (Figure 3-37).

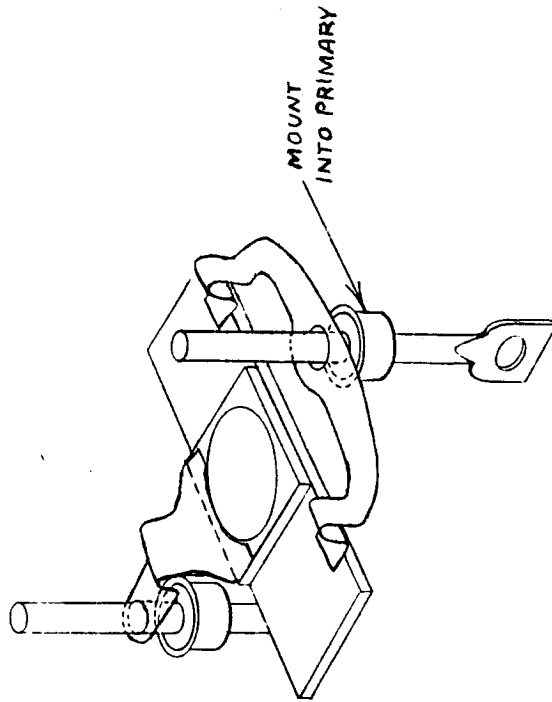
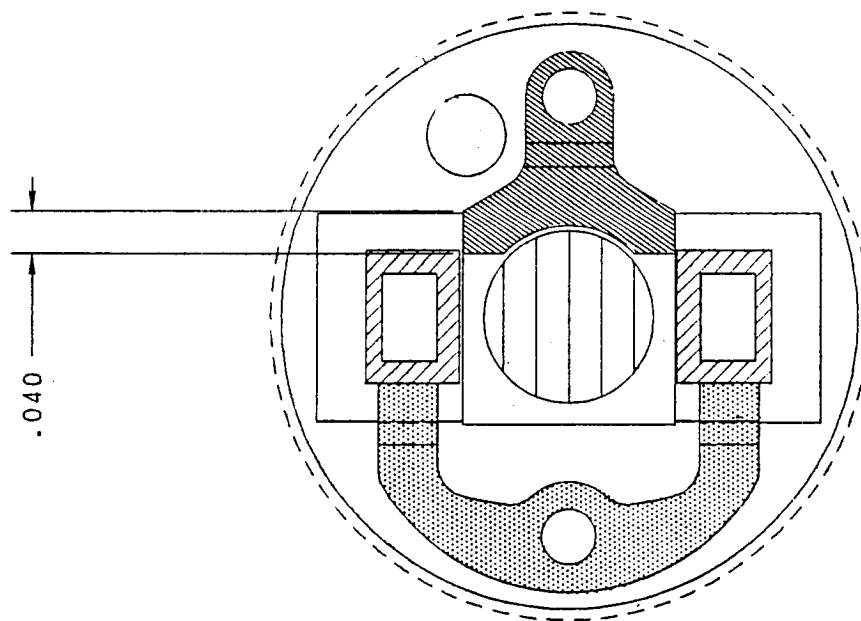
3.4.8 Summary

Figures 3-62 and 3-67 summarize the cell stack materials and bonding methods trades.

GaAs CELL No.	GOLD PLATED INTERCONN. TO BeO CHIF AFTER THERMAL CYCLING	
	VISUAL	PULL (lb.)
5	OK	1.4
9	*	---
10	OK	1.3
24	OK	2.1
30	OK	1.4
36	OK	1.5
43	OK	2.2
49	OK	2.1
56	OK	1.9
80	OK	2.0

FIGURE 3-65 INTERCONNECT TO HEAT SINK WELD TEST RESULTS

* Ribbon removed in therms.



CELL ELECTRICAL INTERCONNECT ASSEMBLY

FIGURE 3-66: CELL STACK ELECTRICAL INTERCONNECTION DESIGN.

Cell Stack Materials Trade



Part	Options	Choice based on:
Cell mounting pad	BeO Al ₂ O ₃ Mo	Electrical design, thermal conduction, coefficient of thermal expansion (CTE) match to GaAs
Cell coverglass	Fused Silica CMX	Cost, CTE match to nickel
Cell interconnect	2mil Ag wire formed Kovar	
Mounting pad metallization	AU AG CU	Solderability in manufacturing environment
Interconnect bonding agent	Ag filled adhesive solder, weld	
Feed through terminals	TRW design commercial	Cost, thermal design

3.5 STRUCTURAL DESIGN OF THE MCC

3.5.1 MCC Primary Mirror

The primary mirror built for contract NAS8-35635 was found to be less stiff than desirable as an unassembled piece. This resulted in unacceptable distortions when mounted to a structural assembly, as reflected by the tolerance analysis.

To stiffen the structure, two items were incorporated into the design. Stiffening rings were designed into the rim of the mirror and the edge of the flange to provide rigid right angle joints and minimize deflections.

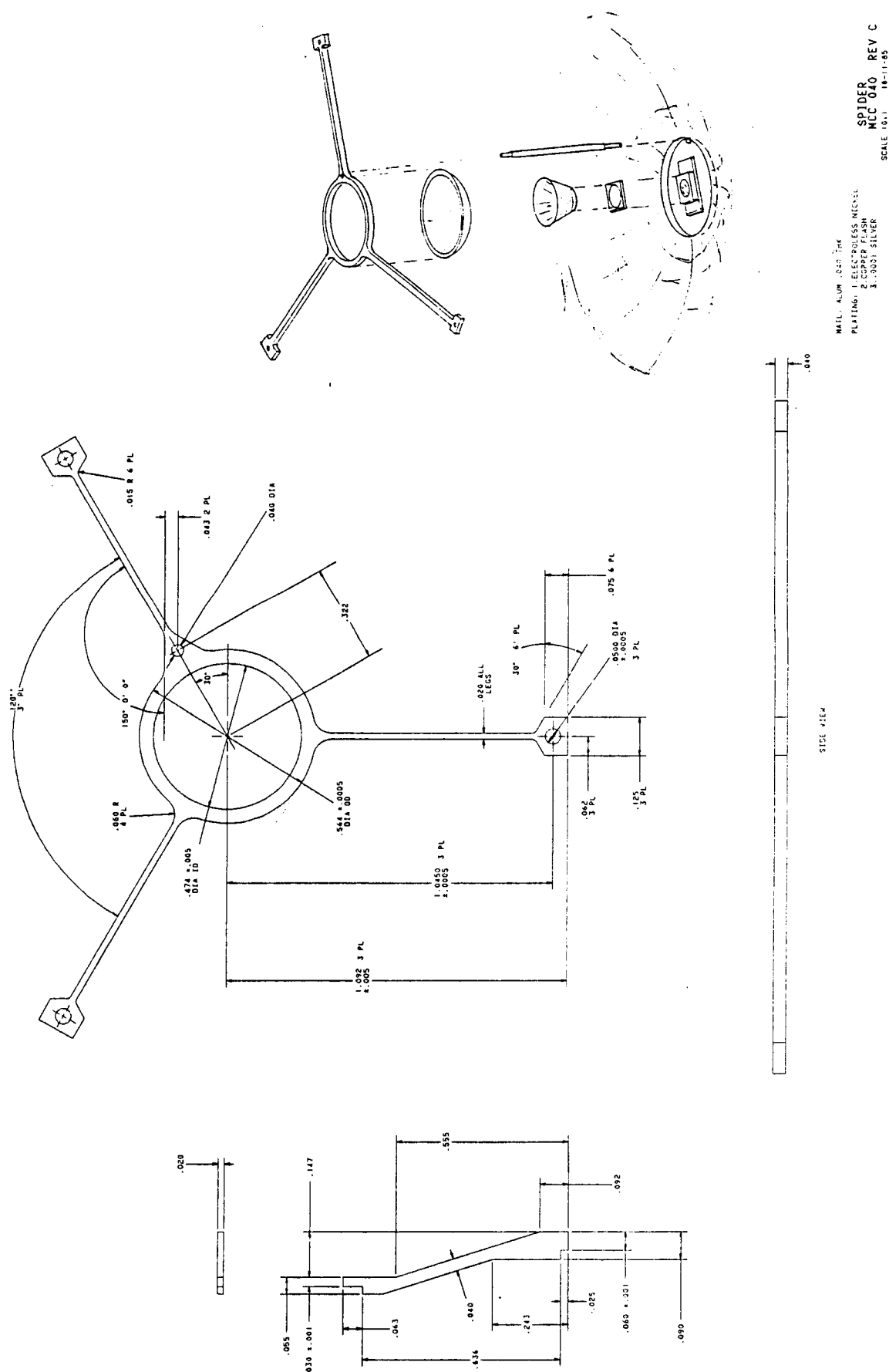
The spider structure mount for the secondary mirror acts as an additional stiffener across the bowl of the primary when the MCC is completely assembled.

3.5.2 MCC Secondary Mirror

The secondary mirror of contract NAS8-35635 was found to be sufficiently rigid. However, the new secondary design did not have a similar flat flange at the rim. A stiffening ring was therefore incorporated at the rim.

3.5.3 Secondary Mounting

The secondary mounting was changed from the "birdcage" approach (Figure 3-1) in NAS8-35635 to a "spider" approach (Figure 3-68). A leg was incorporated to provide stiffness in a third direction if necessary, but was later deleted after testing showed sufficient strength and stiffness to pass launch dynamic inputs. The change to a spider was made to decrease effective blockage of the collection aperture, to decrease the cost of the mounting system, and to improve the manufacturability of the MCC element (Figure 3-69). Mounting bosses were incorporated into the primary mirror flange to facilitate accurate assembly of the spider to the primary (Figure 3-70). The spider was produced by wire electrical discharge machining of a stack of plates with the correct dimensional characteristics.



Mechanical Design Options



- DESIGN FOR RIGID STRUCTURE, LIGHT WEIGHT, MINIMUM OBSCURATION

- SECONDARY SUPPORT

STRUCTURE	CONTRACTS	VIEW	OBSTRUCTION	COMMENTS
-----------	-----------	------	-------------	----------

BIRDCAGE	NAS8 35635		7%	COSTLY
----------	------------	---	----	--------

2-D SPIDER	NAS8 34131		14%	SIMPLE TO PRODUCE HEAVY
------------	------------	---	-----	----------------------------


3-D SPIDER	NAS8 36159		4%	SIMPLE TO PRODUCE ASSEMBLY MODERATELY DIFFICULT SECONDARY HEIGHT FINE TUNABLE
------------	------------	---	----	---

- PRIMARY DISTORTION

STIFFENING RING	VIEW	CONTRACT
-----------------	------	----------

ELECTROFORMED DOUBLE FLANGE		NAS8 36159
-----------------------------------	---	------------

SOME PACKING FACTOR LOSS.
BEST CHOICE FOR MANUFAC-
TURABILITY

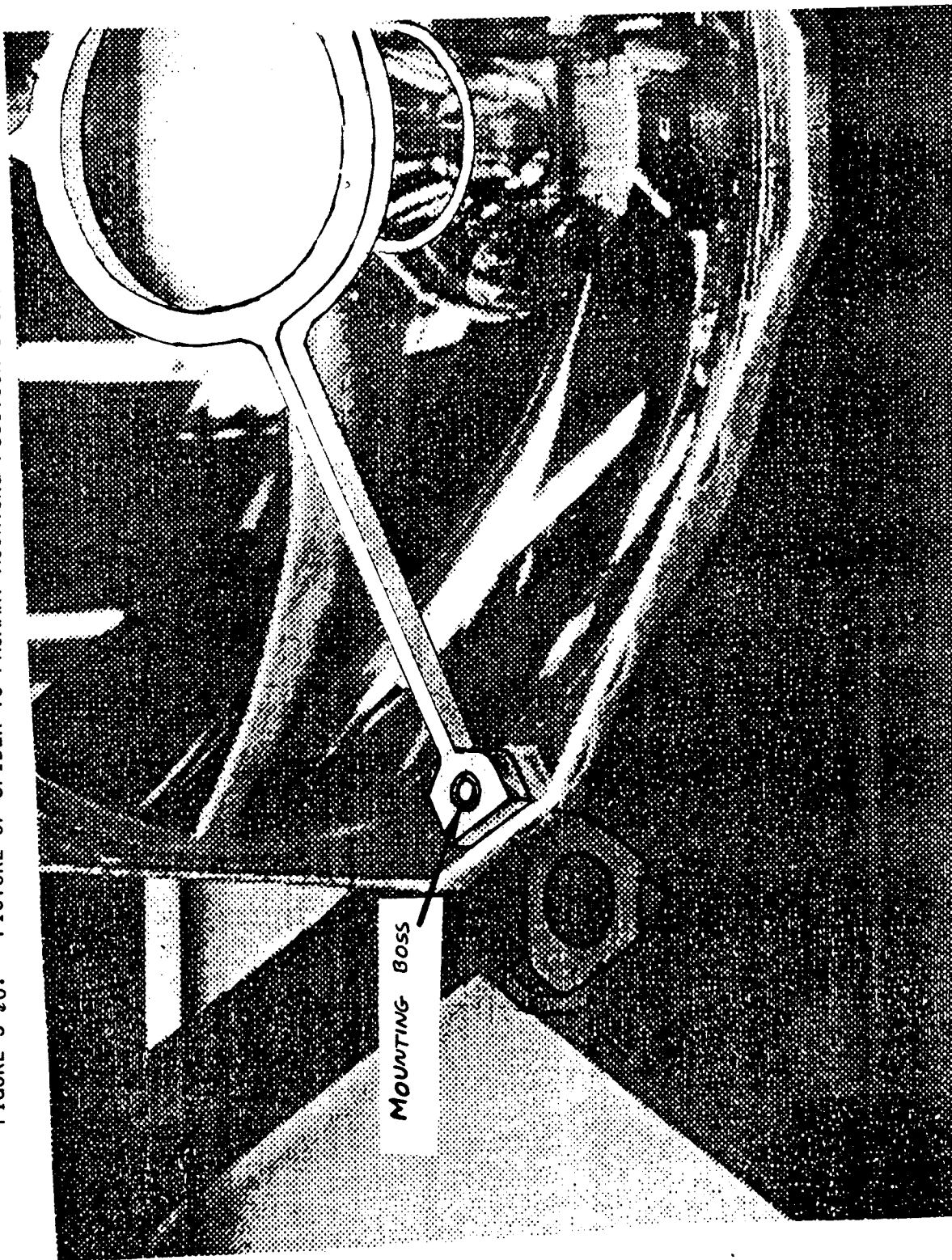
SECONDARY BONDED RING		N/A
--------------------------	---	-----

DIFFICULT TO IMPLEMENT. MAY NOT
ELIMINATE INITIAL MANUFACTURING
PROCESS

ELECTROFORMED FLANGE		NAS8 35635
-------------------------	---	------------

INSUFFICIENT TO PREVENT MIRROR
DISTORTION

FIGURE 3-70. PICTURE OF SPIDER TO PRIMARY MOUNTING POSITION SHOWING MOUNTING BOSS.



3.5.4 Mirror Manufacturing Methods

Methods for manufacture of the mirrors are shown in Figure 3-71. The baseline method of electroforming was chosen for direct comparison of the new design with the model developed in NAS8-35635 and because surface replication was known to be excellent.

3.5.5 MCC Element Bonding Methods

The joints for the cell, interconnects, cover and cone interfaces were considered under cell stack design. The joints for the secondary to spider and spider to primary were developed in parallel with that effort. The options for the secondary to spider bond are shown in Figure 3-72. Solder was chosen for its high thermal conduction path to the spider and the manufacturability inherent in the reflow design. Testing in acoustic and thermal cycling environments (Appendix A) confirmed the capability. The options for the spider to primary bond are also shown in Figure 3-72. Adhesive bonding with DYMAX 628T was chosen for good bond strength, good thermal cycling capability and ease in assembly.

3.5.6 Complete MCC Element Assembly

An assembly drawing of the MCC element is shown in Figure 3-73. Photographs of the assembly showing the assembly method to the support structure are shown in Figures 3-74 and 3-75. Manufacturing methods (Figure 3-76) employed for the production of MCC elements are described in Appendix B.



Mirror Material and Manufacturing Trade

MANUFACTURING METHOD	MATERIAL	RANK	SET ESTIMATE AND 100,000 PARTS	
ELECTROFORM	Ni, Cu	(1) BASELINE	15.00	SURFACE REPLICATION GOOD, SURFACE FINISH GOOD, NECESSARY FOR DESIGN COMPARISON WITH PREVIOUS CONTRACT
INJECTION MOLD, COMPRESSION MOLD	PLASTICS	(2) BEST CHANCE FOR SIGNIFICANT COST/WEIGHT REDUCTION	0.80	PREVIOUS USE FOR MIRRORS, SURFACE REPLICATION GOOD, UNKNOWN SURFACE QUALITY, UNKNOWN METALLIZATION ADHERENCE, REQUIRES REDESIGN, LIGHT WEIGHT
POWDERED METAL	Cu, Al, Be	(3) NEXT BEST CANDIDATE	12-20	GOOD SURFACE REPLICATION, ADDITIONAL POLISHING
STAMPING	Al	(8)	1-10	SURFACE QUALITY POOR, ACCURATE FIGURE REPLICATION POOR, REQUIRES ADDITIONAL POLISHING, MACHINING
SUPERPLASTIC FORMING	Ti, Al, Zn	(4)		NOT STUDIED
MACHINING (DIAMOND TURNING)	Al, Be	(6)	15-30	BEING STUDIED ON SEPARATE CONTRACT, RESULTS TO BE AVAILABLE IN FUTURE
BLOW MOLDING	GLASS	(5)	1-6	NOT STUDIED
SLURRY MOLDING	CERAMICS	(7)	1-20	NOT STUDIED
REPLICATION	NA	NA	Δ15	SURFACE MAY BE SECONDARILY BONDED TO ANY OF THE ABOVE BASE MATERIALS. AS ACCURATE AS ELECTROFORM

Optic Mechanical Attachments Investigated



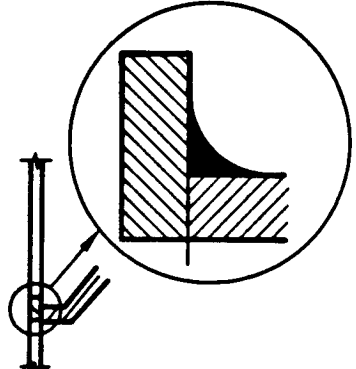
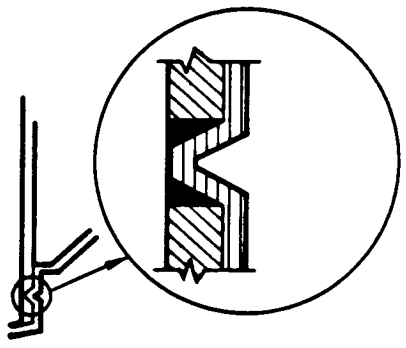
PARTS TO BE JOINED	OPTIONS	VIEW	PRESENT CHOICE
SECONDARY SPIDER	<div data-bbox="698 1270 755 1396">SOLDER</div> <div data-bbox="706 997 738 1165">ADHESIVES</div>		<div data-bbox="706 336 747 409"><input type="checkbox"/></div>
SPIDER PRIMARY	<div data-bbox="1079 1281 1120 1396">SOLDER</div> <div data-bbox="1079 987 1153 1186">ADHESIVES WELDING</div>		<div data-bbox="1079 336 1120 409"><input type="checkbox"/></div>

Figure 3-72

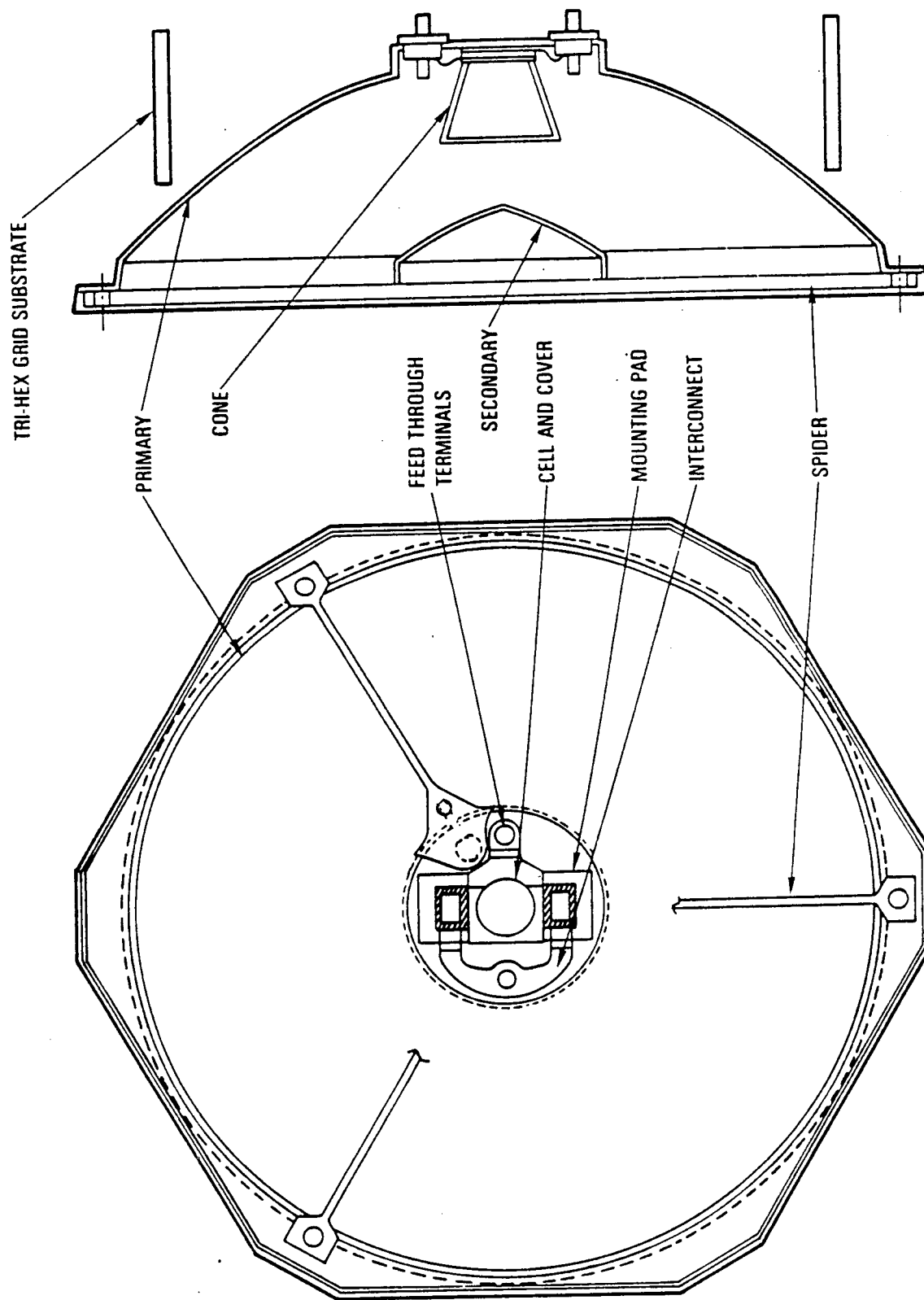


FIGURE 3-73: COMPLETE MINIATURE CASSEGRAINIAN CONCENTRATOR ASSEMBLY

Figure 3-73

ORIGINAL PAGE IS
OF POOR QUALITY

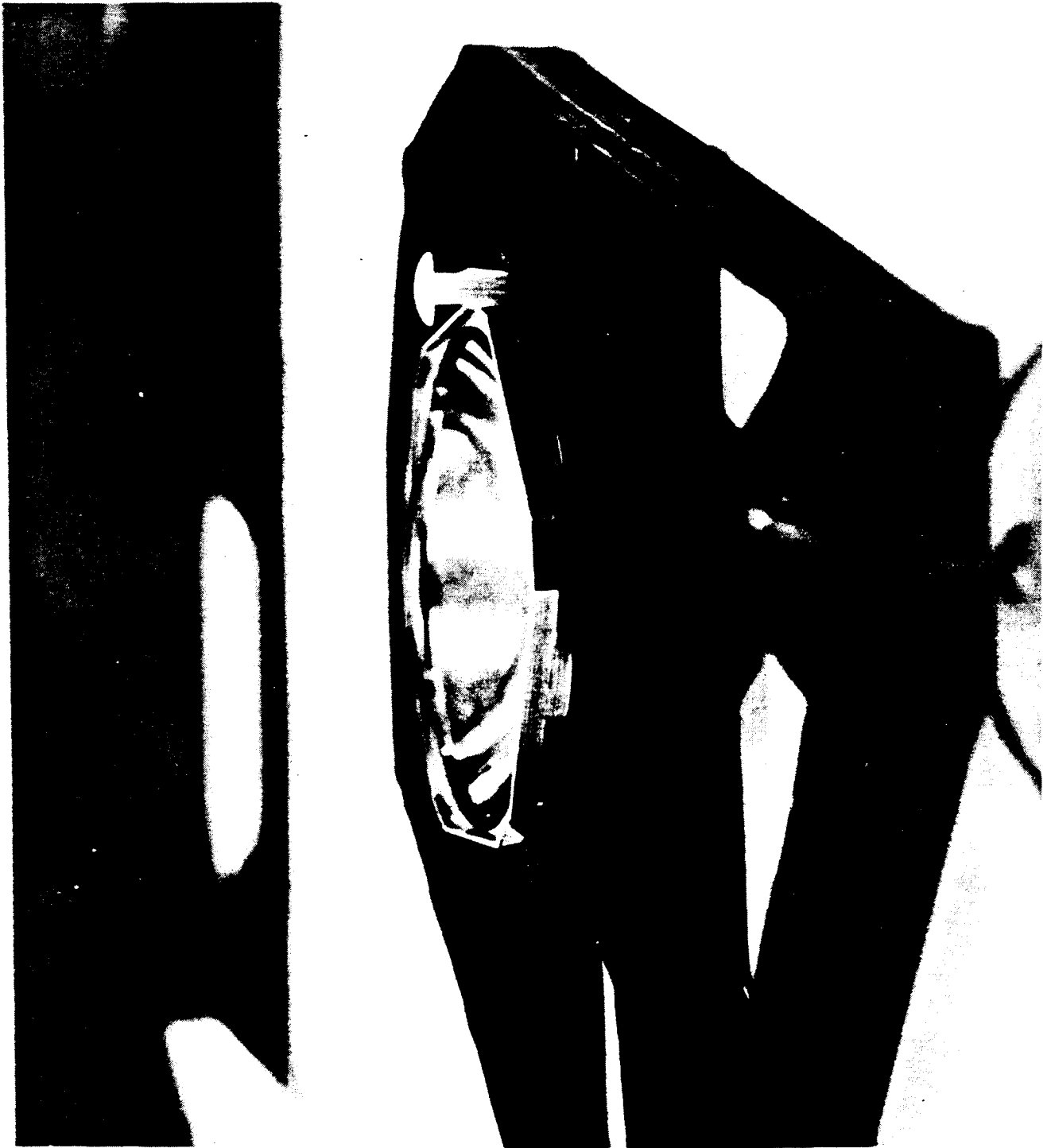


FIGURE 3-74: ASSEMBLY OF MCC ELEMENT INTO PANEL SHOWING
DETAIL OF SNAP INSERT.

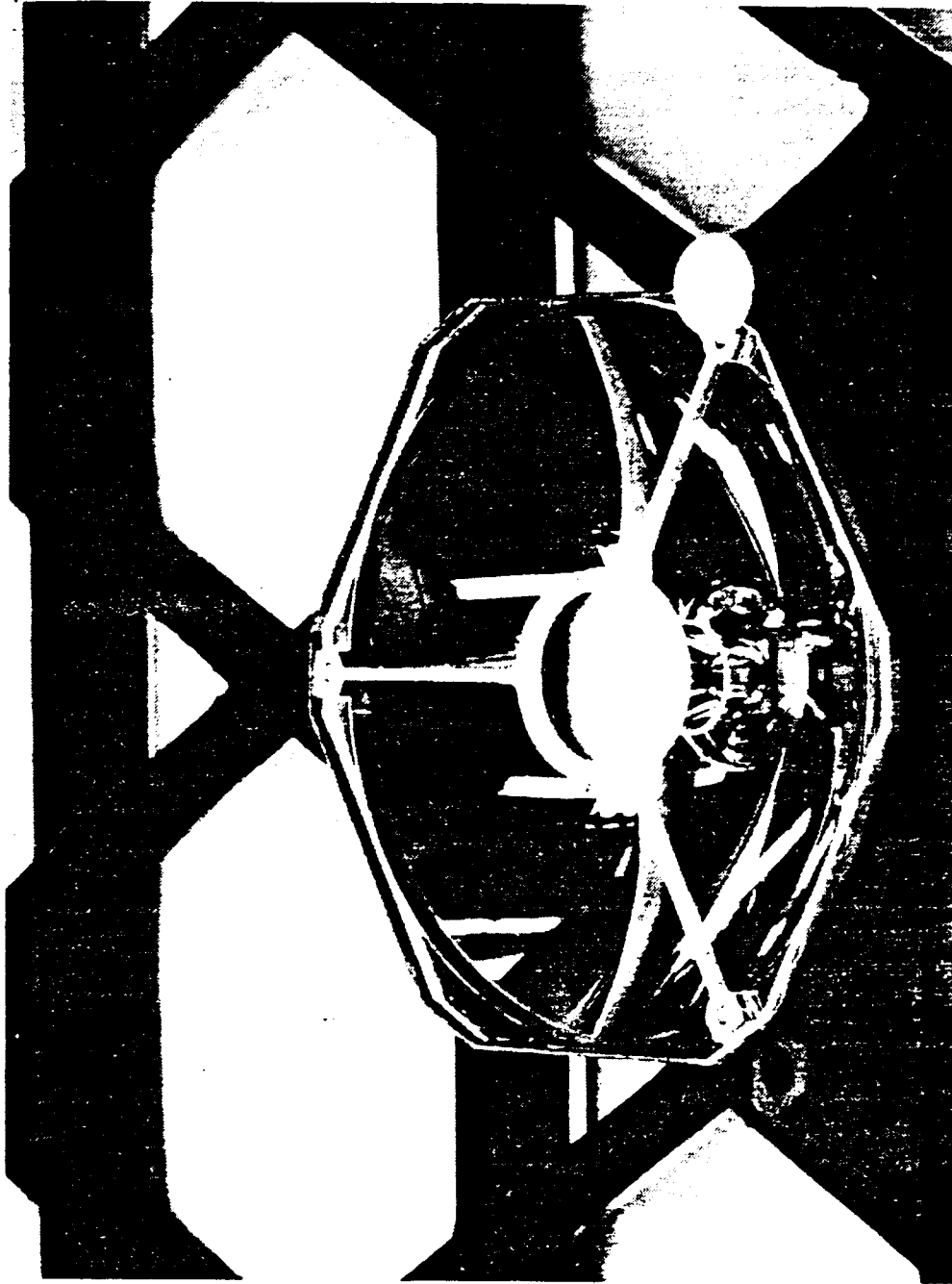


FIGURE 3-75: Third Generation NCC Hardware from the NAS8-36159 Contract

Figure 3-75

ORIGINAL PAGE IS
OF POOR QUALITY

3.6 MCC SUPPORT STRUCTURE

3.6.1 Frame Design

The main component of the structure, the tri hex grid design (THG) (Figure 3-77), was retained from NAS8-35635. This structure was compared with a competing hexagonal structure for stiffness and manufacturability. The significantly greater stiffness of the tri hex grid for unit weight (Figure 3-78) combined with the inherently simpler manufacturability confirmed the selection of this design as baseline to the program.

Potential materials were reviewed for cost and manufacturability (Figure 3-79). The Syalon ceramic material was rejected for difficult process control (shrinkage) which may have required secondary machining. A Beryllium structure was defined and found to be manufacturable at a reasonable cost for a large order of units. However, for potential low cost applications, a graphite fiber reinforced epoxy (GFRP) system was selected to explore manufacturability and cost. The inherent material cost was lower and overall fabrication cost was found to be less than that for beryllium. (For a more detailed discussion of processes see MFG-Panel in Appendix C.)

The GFRP layup methods used in previous contracts and TRW internal research resulted in a structure higher in resin content than desirable. Methods to compact the structure walls and achieve high fiber content (>60%) were considered (Figure 3-80).

The trapped rubber mold method had been used previously in commercial applications for squeezing resin from composite systems. Application to the array was believed to be the best choice for success.

As built, the small GFRP strips and a four element panel exceeded the goals for stiffness, fiber volume and void content.

The large 37 x 53 cm and 37 x 142 cm panels built under this contract met most or all requirements as initially manufactured. Some bowing of the larger panel out of specification was alleviated through a secondary cure process wherein the panel was heated to a higher temperature than that used for cure, stressed to counter any bowing and held for a specific time. After this, the panel was within specification.

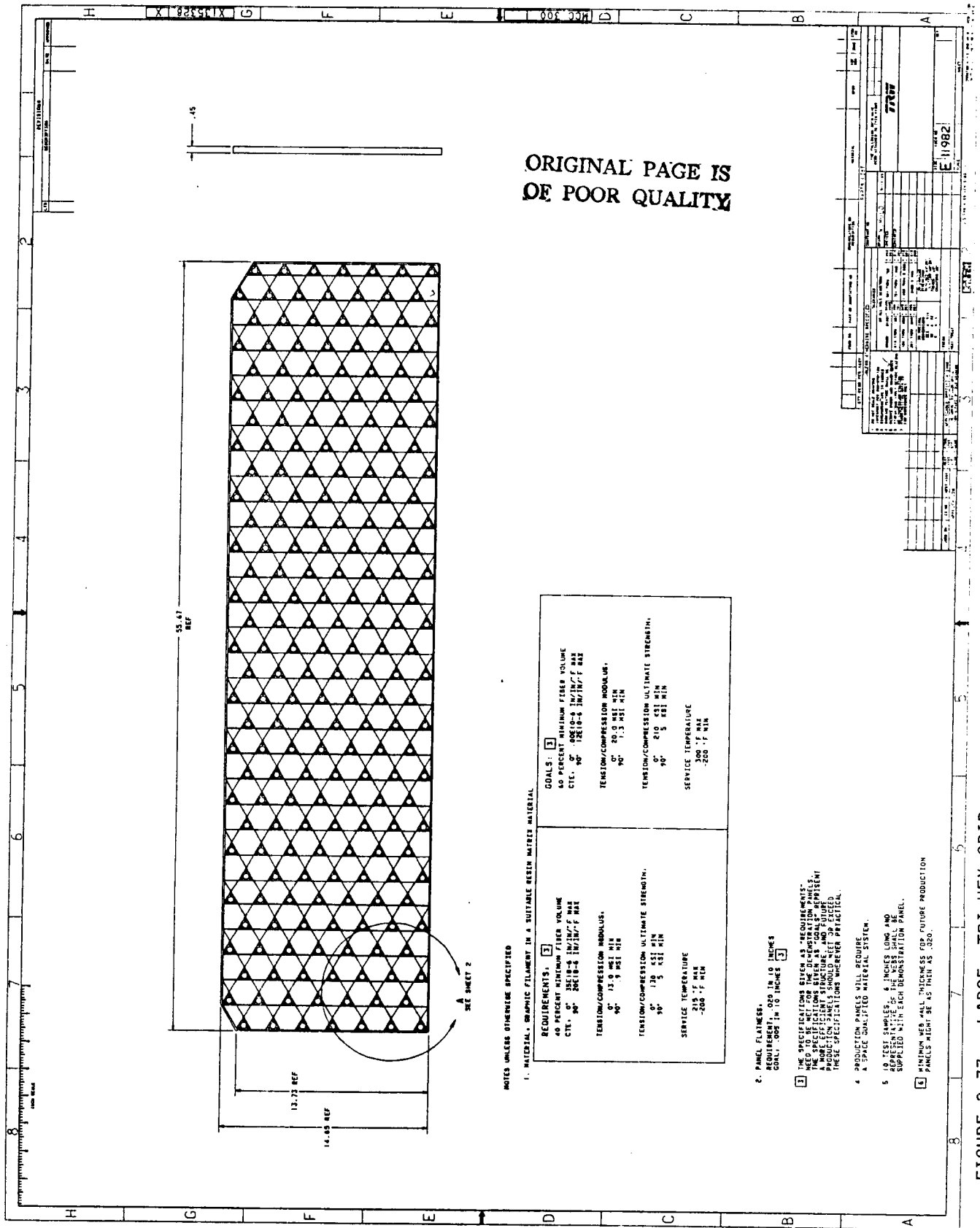
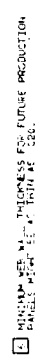


FIGURE 3-77a: LARGE TRI HEX GRID



ORIGINAL PAGE IS
OF POOR QUALITY

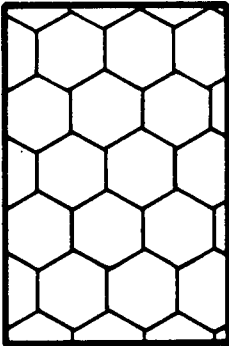
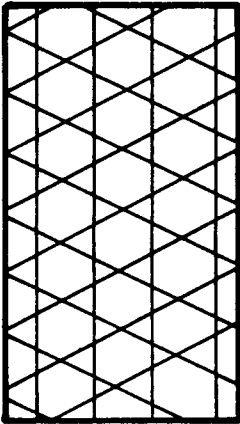
FIGURE 3-77b: SMALL TRI HEX GRID.



111

Hex versus Tri-Hex Trade



PARAMETER	HEX	TRI-HEX
CONFIGURATION		
SPECIFIC STIFFNESS FACTOR	BENDING 1.00 TORSION 1.00	BENDING 1.50 TORSION 9.60
FABRICATION OPTIONS	WINDING	WINDING
PROJECTED COST	MODERATE TO LOW	LOWEST
MCC ASSEMBLY TO PANEL	PRECLUDES USE OF ADJUSTABLE INSERTS	PERMITS USE OF ADJUSTABLE INSERTS

*KEY

Figure 3-78

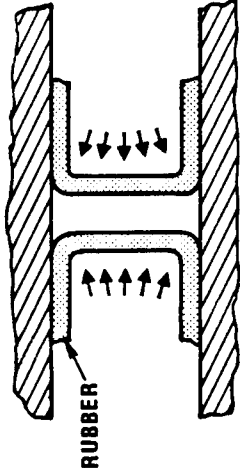
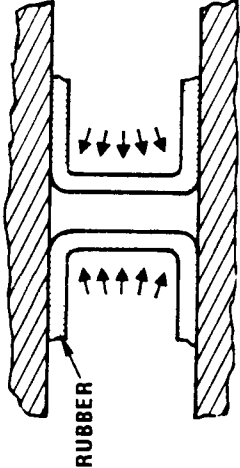
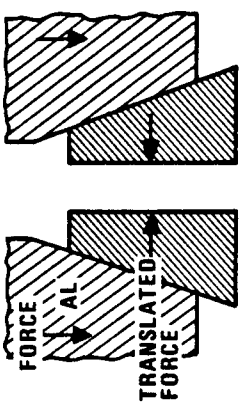
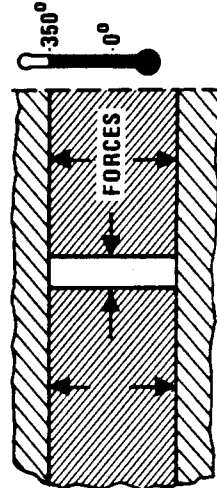
THG Fabrication Process Trades



MATERIAL AND PROCESS	VIEW	KEY FEATURES
<ul style="list-style-type: none"> CARBON FIBER REINFORCED PLASTIC (GFRP) WINDING RUBBER COMPACTION DURING CURE 		<ul style="list-style-type: none"> LIGHTEST WEIGHT POTENTIAL FOR LOW COST TECHNOLOGY STATE OF THE ART POTENTIAL 300 MSI/LB SPECIFIC STIFFNESS
<ul style="list-style-type: none"> BERYLLIUM FORMED STRIP BRAZED 		<ul style="list-style-type: none"> STIFFEST STRUCTURE WELL KNOWN TECHNOLOGY HINGE AND STRUCTURAL DETAIL JOINING SIMPLE 600 MSI/LB SPECIFIC STIFFNESS 10% ELONGATION MATERIAL (NON BRITTLE) AVAILABLE
<ul style="list-style-type: none"> SYALON (Si, Al, O, N-CERAMIC COMPOSITE) SLURRY MOLD SINTER 		<ul style="list-style-type: none"> WEIGHT \approx ALUMINUM NEW TECHNOLOGY MAY BE SLURRY MOLDED 300 MSI/LB SPECIFIC STIFFNESS

Compaction Methods



	METHOD	COMMENTS
 <p>RUBBER</p>	PNEUMATIC PRESS	COMPLEX TOOLING. DANGEROUS
 <p>RUBBER</p>	HYDRAULIC PRESS	COMPLEX TOOLING
 <p>FORCE AL TRANSLATED FORCE</p>	MECHANICAL PRESS	SIMPLE BUT CONFINEMENT AT TOP COMPLEX
 <p>FORCES</p> <p>-350° 0°</p>	BULK DIFFERENTIAL THERMAL EXPANSION	SELECTED BASED ON EASE OF IMPLEMENTATION IN MANUFACTURING

3.6.2 Insert Design

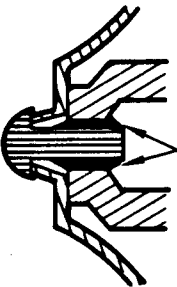
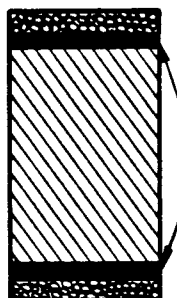
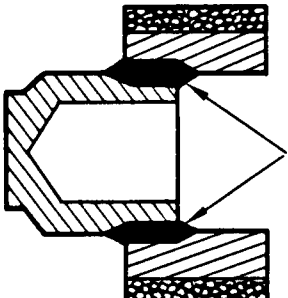
The tri hex grid panel required mounting provisions for the MCC elements. The natural location for the mounts were at the triangular sections formed by the THG geometry. The mounts were designated "inserts" which consisted of two or more components: a fixed insert in the panel; a fastener for the MCC element; a sliding insert for flatness control; a snubber for positive gripping of the MCC element. The design for the NAS8-35635 contract consisted of an aluminum female threaded part bonded in the THG, an aluminum male threaded part to fit in the female part allowing adjustment of the height above the panel and on which the MCC was positioned, a washer and a screw threaded for the interior of the male part which held the MCC in place.

To simplify assembly and manufacture, and decrease weight, a new part was designed with the intent to use a commercially available snap fastener to hold the MCC in place. The simplest process for bonding the fixed insert in place was to co-cure the insert with the THG manufacturing process. Since the flatness of the panel could not, at that time, be predicted, a sliding insert was designed to secondarily bond in place and minimize any out-of-tolerance flatness achieved during manufacturing (Figure 3-81).

A commercially available snap fastener was located which met overall dimensional requirements (Figure C-8). The fixed insert (Figure 3-82) was designed to be lightweight yet resistant to pressures developed in the trapped rubber mold manufacturing process. The insert was triangular and of a slightly large than nominal THG triangle size to ensure good bonding over the exterior surface with the graphite fibers. A triangular sliding insert (Figure 3-83) was designed to mount into the fixed insert and accurately slide within the hole provided with little rocking or offsetting. A snubber was designed which consisted of a washer-like 2 mil piece of kapton coated on one side with RTV silicone adhesive (General Electric RTV-142). The washer fit on the snap fastener such that the RTV faced the MCC element (away from the head of the fastener) (Figure C-8). The sliding insert mounting surface was modified with a groove to allow for MCC primary nickel material overgrowths (Figure 3-84).

THG Mechanical Attachments Investigated



PARTS TO BE JOINED	OPTIONS	VIEW	STATUS
MCC ADJUSTING INSERT	SCREWS SNAP PART	 ATTACHMENT AREA	SELECTED
FIXED INSERTS TRI HEX FRAME	CO CURE SECONDARY BOND	 ATTACHMENT AREA	SELECTED
ADJUSTING INSERTS FIXED INSERTS	BOND SCREW PIN	 ATTACHMENT AREA	SELECTED

ORIGINAL PAGE IS
OF POOR QUALITY

MATL. PLASTIC CARBON FIBER FILLED, 13K-40K
1 POLYETHYLENE SULFONE (VICTREX)
2 POLYETHYLENE SULFONE (VICTREX)
3 POLYETHYLENE SULFONE (VICTREX)
4 POLYETHYLENE SULFONE (VICTREX)

PANEL INSERT
12-10-85 SCALE: 10/1

MCC 135 REV A

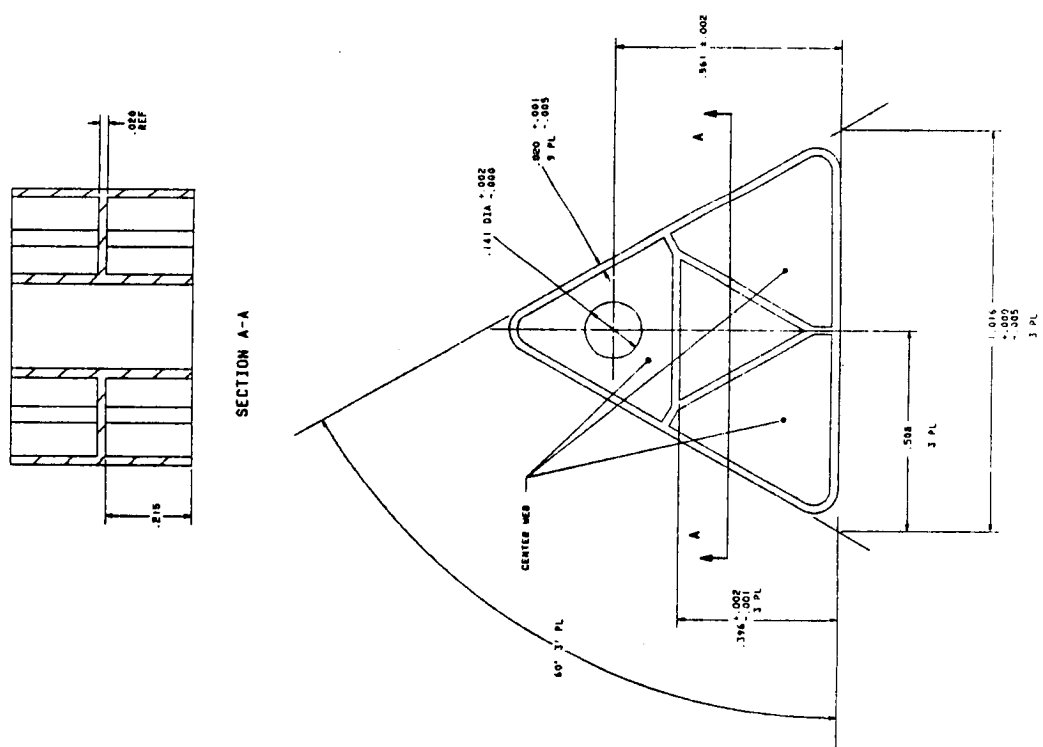
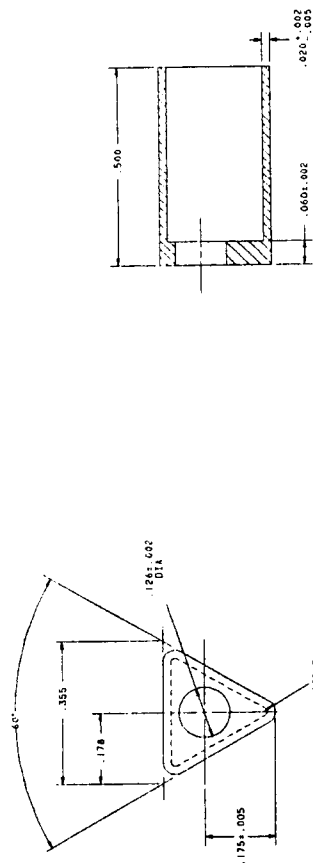


FIGURE 3-82: FIXED INSERT





ORIGINAL PAGE IS
OF POOR QUALITY


PANEL INSERT
12-10-85 SCALE: 10/1

MCC 147

BONDING MATERIAL POSITIONS

 A Interior Surface

 B Interior Edge Fillet

 C Exterior Edge Fillet

Groove to allow for primary
rough edge clearance.

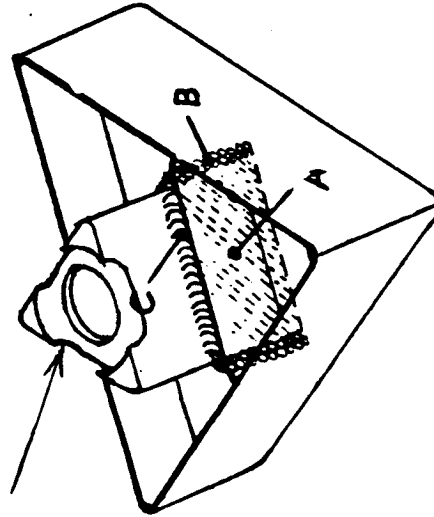


FIGURE 3-84: The sliding-to-fixed insert bond was tested with five bonding materials and three bonding positions as illustrated.

The sliding and fixed inserts were designed to meet requirements as shown in Figure 3-85. Materials considered were plastic, metal, and ceramic (Figure 3-86). Plastics were selected for easy, least cost manufacturing and best thermal expansion match to the THG GRFP material.

The plastic material choices needed both high (200°C) and low (<-170°C) temperature tolerance, low thermal expansion coefficients, and high tolerance to corpuscular radiation. Atomic oxygen susceptibility was an unknown, but coatings could be used if necessary. Of the four plastics finally considered (Figure 3-87), three were used to manufacture the inserts: polyetheretherketone, poly(amide)imide, and polyphenylene sulfide (PEEK, TORLON, RYTON).

Bonding Methods. Three methods for bonding the sliding to the fixed inserts were considered: adhesive, welding (plastic thermal reflow), and staking. The least effort method (adhesive bonding) was tried first.

The requirements of the bond were resilience, adequate strength for assembly (>3 lbs push force which was 50% above the snap fastener maximum push force), and good thermal cycling stability and reworkability.

A number of adhesives (Figure 3-88) were considered. The selected choice of Dymax 628T adhesive was based on adequate strength, good stability under thermal shock and deep thermal cycling environments, and reworkability with solvents. In addition, the fast 15 second set time made manufacturing a high productivity effort.

To provide an absolutely flat surface the THG panel was suspended by shims above a micro flat table, the inserts were carefully slid into place, the adhesive was applied, and quickly cured. The error was less than three mils on any insert.



THG Insert Design Requirements

- **Light weight**
- **Low cost**
- **Thermal expansion coefficient compatible with THG**
- **Environmentally stable under thermal cycling, UV, e⁻, P⁺, γ**
- **Easily manufactured**
- **Compatible with commercially available snap fastener**
- **Adjustable height from grid surface**
- **Compatible with THG fabrication method (co-curable)**

Insert Materials



Material	Comments
Plastic	<ul style="list-style-type: none">• May be filled with carbon fiber for characteristic modifications• Light weight• May be injection molded• Lowest cost (0.30 ea/1000)
Metal	<ul style="list-style-type: none">• Moderate weight• High strength• Tolerances hard to hold without machining• Powder metal process best option• Moderate cost
Ceramic	<ul style="list-style-type: none">• Brittle• Moderate weight• Tolerances hard to hold without machining• Slurry mold best option• High cost

Figure 3-86

Plastic Options For Baseline Insert Design



- Four engineering plastics, all carbon fiber filled
 - Polyethersulfone
 - Polyetheretherketone
 - Polyphenylene sulfide
 - Poly(amideimide)
- All plastics have
 - High (>400°F) temperature capability with no flow
 - High P+, e-, γ radiation resistance
 - High UV resistance
 - Have been used in low (near cryogenic) temperatures
- Best choice to be made after 30,000 thermal cycles performed by NASA

FIGURE 3-88
PUSH STRENGTH (LBS) FOR
ADHESIVES FOR SLIDING INSERT

	INSERT MATERIAL		
	<u>TORLON</u>	<u>RYTON</u>	<u>PEEK</u>
Dymax 628T*	6-22	4-6 M	6-11
DC93500	-	0-3 X	-
RTV 3145*	-	5-12	22-28
DC6 1104	-	2-10 X	4-12 M
Lefkowitz Type 46*	4-22 M	18-32	-
RTV 118	-	-	2-5 X
Cyanoacrylate*	>220	3.5 X	4.5 M
EA 934*	61-65	5-44	4-36 M

X = Cannot Use

M = Marginal

* = All adhesives tested in thermal cycling had greater than 4 lbs residual push strength.

4. ANALYSES

4.1 THERMAL CONSIDERATIONS

4.1.1 Thermal Performance For Cell Output

The new design of the MCC element was checked against thermal analyses for designs from previous NASA contracts. The essential components of an 8 mil copper optic/radiator have not changed. Thermal response in a low earth orbit for a typical element is as shown in Figure 4-1.

4.1.2 Secondary Mirror Temperatures

The temperature reached by the secondary mirror is important for both possible alignment distortions due to thermal mismatch and for long term stability of any materials used in the manufacture of the mirror and support structure.

A simplistic analysis assuming no fin cooling from the spider showed that the present design should run between 130 and 140°C. This is acceptable for the materials used. Consideration of the fin effect due to the aluminum spider should significantly reduce this range.

Thermally induced mismatch between the 80°C primary and a 138°C spider structure would cause a relative growth difference of only 0.8 mils which is much less than the 2 mil allowance at the local spider to primary bond interface. Very little optical distortion can be expected from this source.

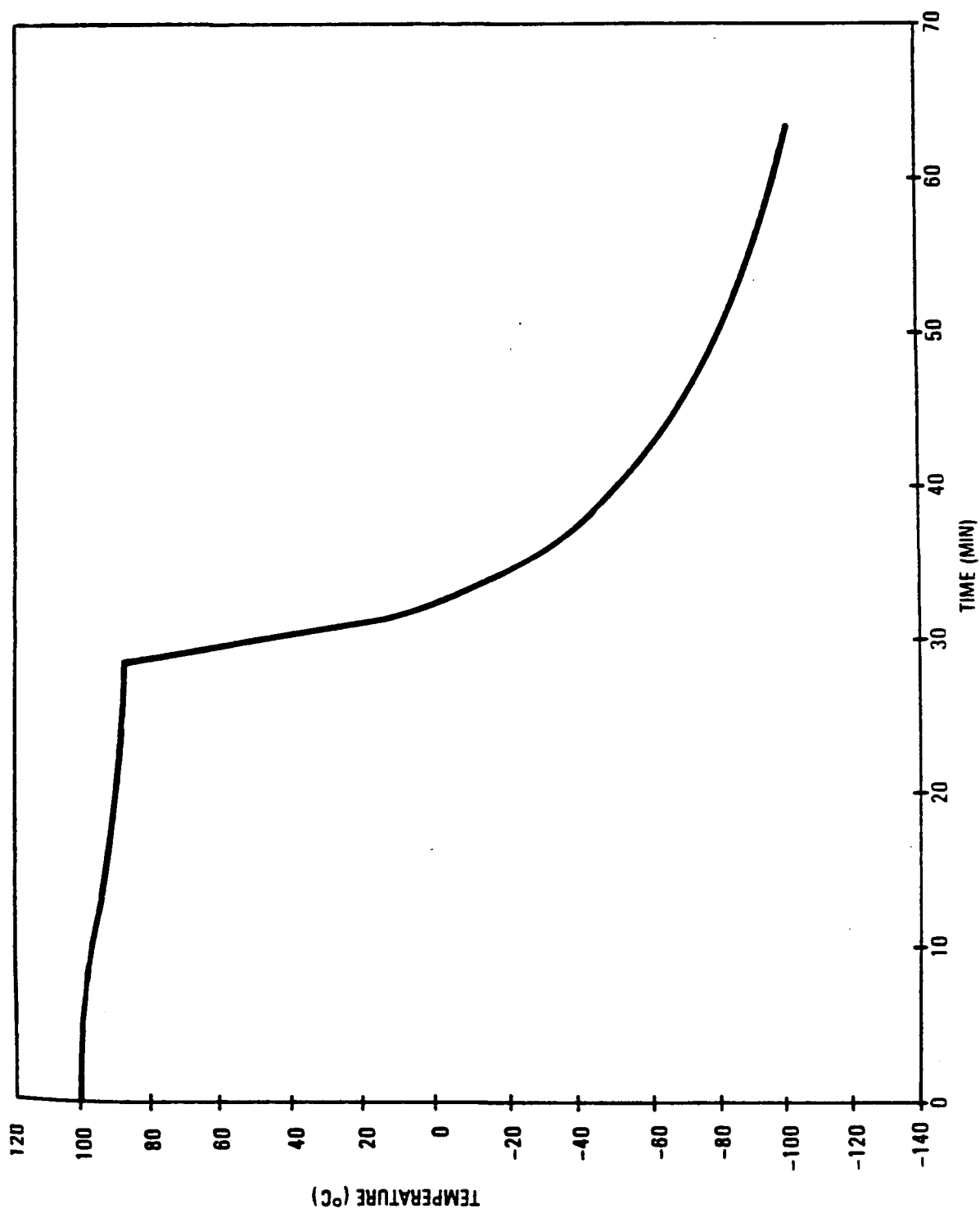


Figure 4-1 The latest temperature prediction for LEO operation shows the eclipse-exit temperature to be -100°C

4.2 WEIGHT

Shown in Figure 4-2 is the weight goal for a flight ready panel compared to the achieved weight of the NAS8-35635 contract and the new achieved weight of this contract.

Figure 4-3 displays the weight of each piece part of the MCC panel and summarizes the total average weight achieved per element.

The THG framework has reached the design weight goals originally set for it. The insert attachment hardware is greater than fifty-five percent decreased from the NAS8-35635 design but requires a two thirds reduction to meet the design goal. The MCC elements mounted on the large panel have achieved the flightweight design goal. The harnessing is 15% less than the flightweight goal. Altogether, the system weight per element as presently achieved is only 11% greater than the flightweight design, that is 14.17 g/element versus 12.60 g/element.

To achieve the design weight goal it is only necessary to order primary optics nominally 8 mils instead of nominally 9 mils thick as with the current manufacturing process. This has been discussed with the electroform vendor, Optical Radiation Corporation, and has been found to be easily achievable with only small risk of decreased yield. For example the 10 mil nominal thickness secondary mirrors were actually delivered as 4 to 6 mils thick and primary mirrors as delivered ranged from 6 to 11 mils thick.

MCC Panel Weight Analysis



COMPONENT	NAS8-35635			NAS8-31659 (Present Contract as built)						FLIGHTWEIGHT DESIGN*		
	Projected weight from as-built data (1 Panel)			Weight of large (15"x56") Demonstration Panel						WEIGHT FOR FULLY POPULATED QUARTER PANEL		
	UNIT MASS (g)	QUANTITY	TOTAL MASS (g)	UNIT MASS (g)	QUANTITY	TOTAL MASS (g)	UNIT MASS (g)	QUANTITY	TOTAL MASS (g)	UNIT MASS (g)	QUANTITY	TOTAL MASS (g)
TRI-HEX GRID PANEL AND FRAME	1509	1	1509	421	1	421	737	1	737	714	1	714
MCC ELEMENT (CELL STACK AND OPTICS)	9.6	330	3168	9.6	180	1730	9.6	330	3171	9.6	330**	3168
ELEMENT ATTACHMENT HARDWARE	3.3	372	1224	1.5	217	326	1.5	372	558	0.5	372	186
PANEL WIRING AND CONNECTOR	91	1	91	74	1	74	85	1	85	91	1	91
TOTAL PANEL MASS			5342			2550			4551			4159***

*PANEL DESIGN CONSISTENT WITH 28 W/Kg ARRAY SYSTEM PERFORMANCE (BEGINNING OF LIFE)

**330 ELEMENTS PRODUCE 137W AT THE ARRAY SYSTEM LEVEL

***ARRAY STRUCTURE ADDS AN ADDITIONAL 19.5% IN MASS

FIGURE 4-2: WEIGHT ANALYSIS SHOWING PREVIOUS CONTRACT CAPABILITY, PRESENT CONTRACT AS-BUILT WEIGHT FOR THE LARGE PANEL, PROJECTED WEIGHT FOR A QUARTER PANEL(26" X 56"), AND ULTIMATE FLIGHT GOAL.

FIGURE 4-3: WEIGHT OF PIECE PARTS AND WEIGHT SUMMARY

MCC ELEMENT COMPONENTS	AVERAGE WEIGHT (GRAMS)	ELEMENT ATTACHMENT COMPONENTS	AVERAGE WEIGHT (GRAMS)	MISCELLANEOUS ELECTRICAL	WEIGHT (GRAMS)
primary	7.538	fixed insert	1.080	wire 28 AWG large panel	45
secondary	.459	sliding insert	.281	wire 28 AWG small panel	12
cone	.116	snap fitting	.119	connector	26
cell	.047	snubber	.005	bonds & ties large panel	3
glass	.011	adhesive	.014	small panel	2
insulator (BeO)	.098				
interconnect top	.007	TOTAL	1.50		
interconnect bottom	.018	(GOAL 0.50)			
terminals (2)	.084				
spider	.350				
solder	.320				
adhesive	.112				
paint	.450				
		STRUCTURE (THG)	WEIGHT (GRAMS)	DENSITY g/cm ³	
TOTAL	9.61	141.4cm x 37.7 cm	421.4	.069gcm ³ (0.67g/cm ³ goal)	LARGE
(GOAL 9.60)		52.5cm x 37.7 cm	159.7	.071g/cm ³ (.067g cm ³ goal)	SMALL

TOTAL WEIGHT (ESTIMATE)

SMALL (9.61 x 66) + (84 x 1.5) + 159.7 + 12 + 26 + 2 = 968g

LARGE (9.61 x 180) + (217 x 1.5) + 421.4 + 45 + 26 + 3 = 2550g

MEASURED

2.55 + .01g

OVERALL

14.67g/element

14.17g/element

(GOAL 12.60g/element)

4.3 PERFORMANCE ANALYSIS

4.3.1 Overall Electrical Achievement

Figure 4-4 shows the capability of the as-built MCC element configuration for this contract, compared to the goals set for the MCC technology. Also shown is the projected capability of the current design when the effect of known manufacturing defects is eliminated.

4.3.2 Electrical Output Corrected for Known Defects

The outputs for the substrings of the 37 cm x 53 cm panel are shown in Appendix A. At 0° offpoint the average power for a six element in series substring is 2.14 W after AMO and temperature correction. This amounts to 0.357 W/element. When corrected for the poor reflectance of the conic mirror (from 0.66 to 0.98), using the method specified in 3.3.2.13, the power jumps to 0.419 W. When corrected for mismatch also as described in section 3.3.2.13, the power achieved is 0.453 W. Performance at 85°C would be 0.419 W.

An element under 1 sun AMO, 85°C should be capable of $0.162 \times .1353 \text{ W/cm}^2 \times \pi(2.54 \text{ cm})^2 = 0.444 \text{ W}$ with a 20% efficient at 85°C cell in the present design. Correction to 28°C is $[1 + (57^\circ\text{C}) \times (.13\%/^\circ\text{C})] \times 0.444 = \underline{0.478 \text{ W}}$.

The cells used for this small panel were initially 20.6% efficient at 28°C or 19.1% efficient at 85°C. Allowing for an increase to 20% efficiency cells at operating temperature, the current design would achieve $(20/19.1) \times .453 = \underline{.475 \text{ W}}$ at 28°C at the element level which is very close to the 0.478 W as expected from the above calculations.

The corrected measurements achieve the capability goals of the design. There are no unexplained losses in the system.

FIGURE 4.4: MCC ELEMENT CAPABILITY

	NASA 35635	NASA 36159		
	ACHIEVED	ACHIEVED	CORRECTED ⁺	GOAL
OPTIC TRAIN				
BLOCKAGE	.86	.91	.91	.89
PRIMARY REFLECTANCE	.97	.98	.98	.98
SECONDARY REFLECTANCE	.97	.98	.98	.98
CONIC REFLECTANCE	.97	.86*	.99	.99**
SCATTER LOSS	.93	.96	.96	.96
GLASSING LOSS	--	1.0	1.0	1.0
MISALIGNMENT	.96	.99	.99	.99
TOTAL	.70(.79)	.714(.81)	.822	.80
CELL STACK				
CELL EFFICIENCY @ 85 ⁺⁺ °C	.138	.194	.194	.200
FABRICATION LOSS	.89	.98	.98	N/A
TOTAL	.123	.190	.190	.200
PANEL LEVEL				
MISMATCH	N/A	.94	.99	.98
ELEMENT PACKING	.79	.82	.82	.79
WIRING & DIODE LOSS***	.97	.97	.97	.97
OFFPOINT ERROR (1.1°)	.98	.99	.99	.98
TOTAL	.75	.74	.78	.74
OVERALL SYSTEM EFFICIENCY	.067 (.130)	.100	.122	.118
w/ element	.184	.277	.334	.324
o APPLIES IN MEASURED CONDITION	(.357)			
w/m ²	90.8	136	165	160

⁺⁺Conversion 28°C to 85°C is .955 factor. Cell average on small panel was .203 @ 28°C.

⁻Applies in the measured condition.

⁺Corrected for known manufacturing deficiencies.

*Based on 66% cone reflectance, $0.60 + (0.40 \times 0.66)$.86

**Based on 98% cone reflectance, $0.60 + (0.40 \times 0.98)$.99

***Actual losses were negligible. This is shown for comparison to a system design only.

Based on the achieved weight calculated per element in section 4.2, the specific power of the design is 29.6 W/kg at the panel level and 24.7 W/kg at the array system level using the 100 kW array parameters from NAS8-34131, and the corrected performance values shown above.

4.4 ADVANCED DESIGNS

To surpass the weight goal of 28 W/kg there are many categories of change which can have significant impact.

4.4.1 Material Thickness Change

The optics may be changed from the present 9 mil thickness to 4.5 mils thickness. Counting only the primary mirror, this would be equivalent to a 3.8 g per optic drop or 1244 g per quarter panel for a total of 3307 g remaining or 35.2 W/kg at the array level.

4.4.2 Material Type Change

With the proviso that the mirror surface could be replicated and secondarily bonded into place, a 30 mil magnesium casting could be used to achieve 3.5 g optic drop or nearly that of the 5 mil copper optic.

The best candidate is to compression mold graphite fiber cloth whose thermal conductivity is near that of aluminum structure (66 Btu/hr ft²F) such that no secondary radiator would be required. Five mils of this material at 1.7 g/cm³ would total only 0.8 g per primary for a savings over the baseline of 6.8 g/optic or 2244 g of element weight. Subtracting from 3168 nominal element weight leaves 924 g. Combined with the other articles and a 0.5 g element attachment hardware, the total weight would be 1915 g with .444 W element x 330 = 146.6 W. With 19.5% backup structure, the system watt/kg is

$$\frac{146.6}{1915 \text{ g} \times 1.195}$$

or 64 W/kg

4.4.3 Coatings

The coverglass may be coated with an infrared reflecting filter for a potential of 11°C drop or 1.43% improvement.

4.4.4 Advanced Cells

The concentrator may use any advanced cells as they become available and in a size which may be relatively easy to produce. A twenty-seven percent efficient cell which has been reported would increase power to 197.9 W on a quarter panel or 39.8 W/kg.

4.4.5 Combined

The combined potential of the above design changes could make the MCC concentrator achieve $1.35 \times 1.0143 \times 64 \text{ W/kg} = 87 \text{ W/kg}$.

4.4.6 Manufacturing

If compression molding were implemented, the piece part price could be reduced to less than two dollars a part depending on final complexity.

4.4.7 Offpoint Performance

Quick research into historical analyses discovered that a focusing refracting lens placed on top of the cone would increase offpointability by an extra degree. This remains to be seen with the new element optical design. The lens could be used in place of the protective glass cover.

5. CONCLUSIONS

The optical design of the miniature Cassegrainian concentrator (MCC) element has been improved for both offpoint and onpoint power capability. The cell stack design has shown no losses under the high short term thermal stresses imposed by component level test and is projected to be capable of greater than five years thermal cycle life in low earth orbit. The structural design met all requirements for stiffness and flatness and requires adjustable inserts for fine tuning of the GFRP structure to meet flatness goals. The completed, fully populated small and large MCC panels deliverable under this contract perform electrically as expected.

A solid acceptance inspection program to guarantee quality of all purchased parts, and continued manufacturing process improvements will make the MCC design a viable low cost alternative to standard flat panel technology. Minor improvements to the cell stack design of the MCC element can make significant improvements in both the performance and manufacturability of the MCC system.

6. RECOMMENDED FOLLOW-ON WORK

The following schedule shows recommended follow-on work to be accomplished prior to acceptance of the MCC array system as a low risk alternative to flat panel technology arrays.



Recommended Follow-On Development Plan

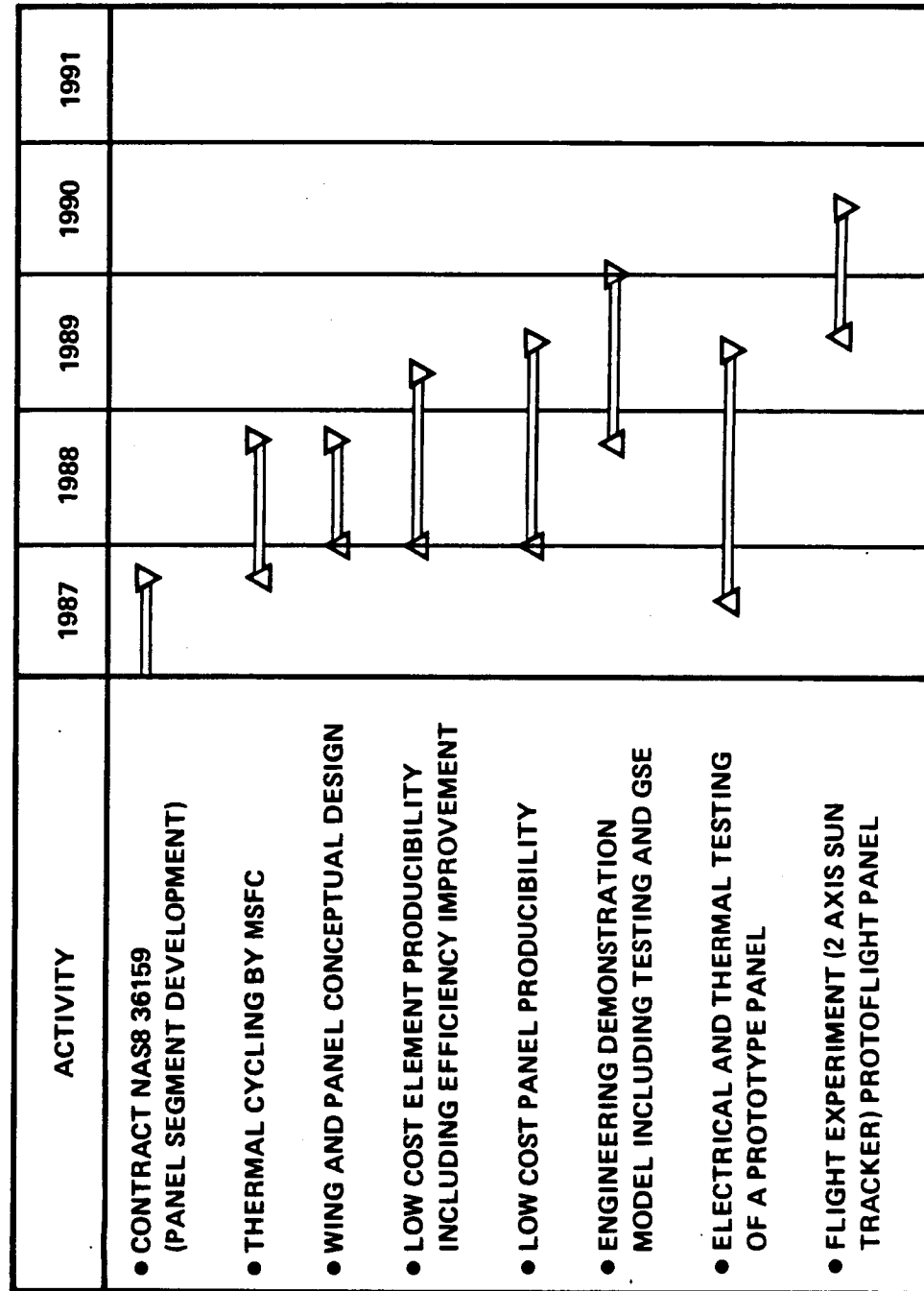


Figure 6-1

APPENDIX A
ENVIRONMENTAL AND ELECTRICAL TEST RESULTS

1. INTRODUCTION

This section presents the parameters and results of selected environmental and electrical testing performed to support this contract.

2. ENVIRONMENTAL TESTING

2.1 THERMAL CYCLING

The following tests were performed.

CONDITIONS	TEST ARTICLES	RESULTS
A. 200 cycles -160 to 10°C	20 weld joints to cell, 20 solder joints to cell, 6 weld joints to BeO, 6 solder joints to BeO	1 failure due to incipient cell crack failure no failures 1 failure due to Au metal- lization failure no failures
B. 120 cycles (shock) -65 to +124°C	10 cells mounted on BeO, 10 silver welds of cells, 15 gold welds to BeO, 3 each Torlon, Ryton, Peek sliding insert to fixed insert epoxy bond	no failures no cracks
C. 470 cycles -150 to +65°C *(-170 to +80°C)	small tri-hex panel with bonded inserts, *small parts from (B) above	no failures, partial loss of epoxy strength but no effect on capability
D. 100 cycles (shock) -80 to +100°C	Plastic parts as in (B) except with UV628 bonds, cone to cover UV bonds, 2 completed unpainted optic element with spider bond with UV 628, sliding inserts with epoxy 9321	no failures, no visible degradation
E. 100 cycles -80 to +80°C	5 cones with covers, UV cure adhesive	no failures, no visible degradation, bond strength greater than glass
F. 5 cycles (shock-LN ₂ Dip) -196 to 66°C	2 completed optic elements with S13GLO paint (bonds-Dymax	no bond failures, no Ag, SiO coating failures, no paint failures (passed UV628, DC93500) tape test)
G. 100 cycles +80 to -80°C (3 openings)	See Figure A-1	See Figure A-2

PLATE METAL	ALUMINUM	ALUMINUM	ALUMINUM
SPIDER METAL	ALUMINUM	ALUMINUM	ALUMINUM
SPIDER-TO-PLATE BOND	93-500	93-500	93-500
SECONDARY METAL	STAINLESS	STAINLESS	STAINLESS
SPIDER-TO-SECONDARY BOND	93-500	93-500	93-500
CONE METAL	NICKEL	NICKEL	NICKEL
CONE-TO-GLASS BOND	93-500	93-500	93-500
PLATE METAL	ALUMINUM	NICKEL	NICKEL
SPIDER METAL	NICKEL	ALUMINUM	ALUMINUM
SPIDER-TO-PLATE BOND	93-500	93-500	142
SECONDARY METAL	STAINLESS	NICKEL	NICKEL
SPIDER-TO-SECONDARY BOND	93-500	93-500	INDIUM #2
PLATE METAL	NICKEL	NICKEL	NICKEL
SPIDER METAL	NICKEL	NICKEL	NICKEL
SPIDER-TO-PLATE BOND	93-500 W/CABOSIL	LEFKOWELD	INDIUM #2
SECONDARY METAL	NICKEL	NICKEL	NICKEL
SPIDER-TO-SECONDARY BOND	99-500 W/CABOSIL	LEFKOWELD	INDIUM #2
CONE METAL	STAINLESS	STAINLESS	STAINLESS
CONE-TO-GLASS BOND	93-500	93-500	93-500
CONE METAL	STAINLESS	STAINLESS	STAINLESS
CONE-TO-GLASS BOND	LEFKOWELD	LEFKOWELD	LEFKOWELD

Figure A1 MATERIALS USED ON TEST PLATE FOR ACOUSTIC EXPOSURE AND THERMAL CYCLING

TEMPERATURE RANGE

- +80 to -80°C
(+176 to -112°F)

MAY 1, 1986 (0 CYCLES)

- Initial inspection & photo. Cone accidentally debonded by technician.

MAY 5, 1986 (30 CYCLES)

- No change

MAY 12, 1986 (76 CYCLES)

Additional (unplanned) cold temp exposure; ~180°C/15 hrs.

- Additional cone debonded (adhesive failure to cone; 93-500)

MAY 14, 1986 (100 CYCLES)

Spider debonded by technician upon removing from chamber; 93-500 failed adhesively to spider

NO APPARENT CHANGE WAS NOTED ON TEST PANEL BEFORE ACCIDENTAL COLD TEMPERATURE SOAK AT LIQUID NITROGEN TEMPERATURES. EVEN AFTER COLD SOAK LITTLE DAMAGE WAS APPARENT.

Figure A2 THERMAL CYCLING RESULTS

2.2 ACOUSTIC EXPOSURE

The test panel from 2.1G above was subjected to an acoustic exposure prior to thermal cycling. The acoustic spectrum is plotted in Figure A-3. Overall pressure level was 146 dB. No failures were observed as a result of the test.

3. ELECTRICAL TESTING

3.1 CELL ELECTRICAL OUTPUT

The cell data curves for forward one sun, 100 sun, dark forward, and dark reverse testing are too numerous to present here. All data is held at the contractor. A summary of the data is provided.

All efficiencies reported below are at 100 AMO sun intensity.

The cells from ASEC all performed between nineteen and twenty one percent at 28°C with a few stragglers above and below this range. An additional 100 cells from ASEC produced and received as replacements for those with contact problems had efficiencies all above 20% at 28°C. As noted in the text, the Spectrolab cells averaged 18% efficient with a range of 17.5% to 18.5%. The Varian solar cells averaged 16% with a range of 11% to 18.5%. (Known contact and batch problems with the delivered lot caused the low efficiency, but time constraints precluded waiting for another batch. Cells received for another TRW program all ranged near 20% at 80°C.)

The dark forward characteristics showed no notable changes from the 100 sun data.

The dark reverse testing for the cells revealed significantly different characteristics from typical measurements of silicon cells. The reverse breakdown voltage ranged between 1 and 2 volts for most samples. No samples exhibited breakdown at any greater than 6 volts. No damage was apparent after reverse testing. For comparison, 2x4 data for silicon cells typically shows a breakdown >20V with a range between 5 and 50 V.

3.2 SMALL PANEL STRING OUTPUT DATA

The small panel contains MCC elements with copper nickel sandwich primary mirrors. The best cells of the ASEC quantity were reserved for this panel. All matching was performed based upon pre-welded outputs. No equipment was available to match elements outputs. The MCC elements were arranged in strings of twelve in series. Measurements were performed on half strings (6 in series) to avoid some equipment limitations in voltage. After data was gained on each of the 11 half strings, five of the "A" half strings were put in parallel and measured. The same was done for the "B" half strings. All data was corrected for solar intensity using a GaAs concentrator cell transfer standard at 1 sun and corrected for temperature using the average of two thermistors mounted on the back of elements and including a known steady state temperature drop of 3°C. Some data may be off by 3 to 5°C at random due to some transient wind cooling but effort was made to wait for steady state conditions.

Data for the strings was then corrected for the conic mirror coating defects as discussed in section 3.3.2.10 using an average reflectance of 0.70.

Both the data corrected to 28°C and standard conditions and corrected for the average conic reflectance loss are reproduced here in figures A4 and A6.

Data for the combined strings are contained in Figures A5 and A6.

3.3 LARGE PANEL STRING OUTPUT DATA

The large panel contains all nickel MCC elements with various strings composed entirely of cells from each of ASEC, Spectrolab, and Varian solar cell manufacturers. Specific kitting may be found in Appendix B.

Data was measured for individual six element in series half strings as in 3.2. However a 3 month time lag between measurements occurred between measurements of elements 1A through 4D and 5A

TEST: _____ DATE: 4/23/86

SPECIMEN: MCC TEST PANEL

S/N: NA

SPL 146 db O/A

RESPONSE OF: AVERAGE MICROPHONE

ANALYSIS BANDWIDTH: 1/3 OCTAVE

NOTES: _____

ACOUSTIC SPECTRUM

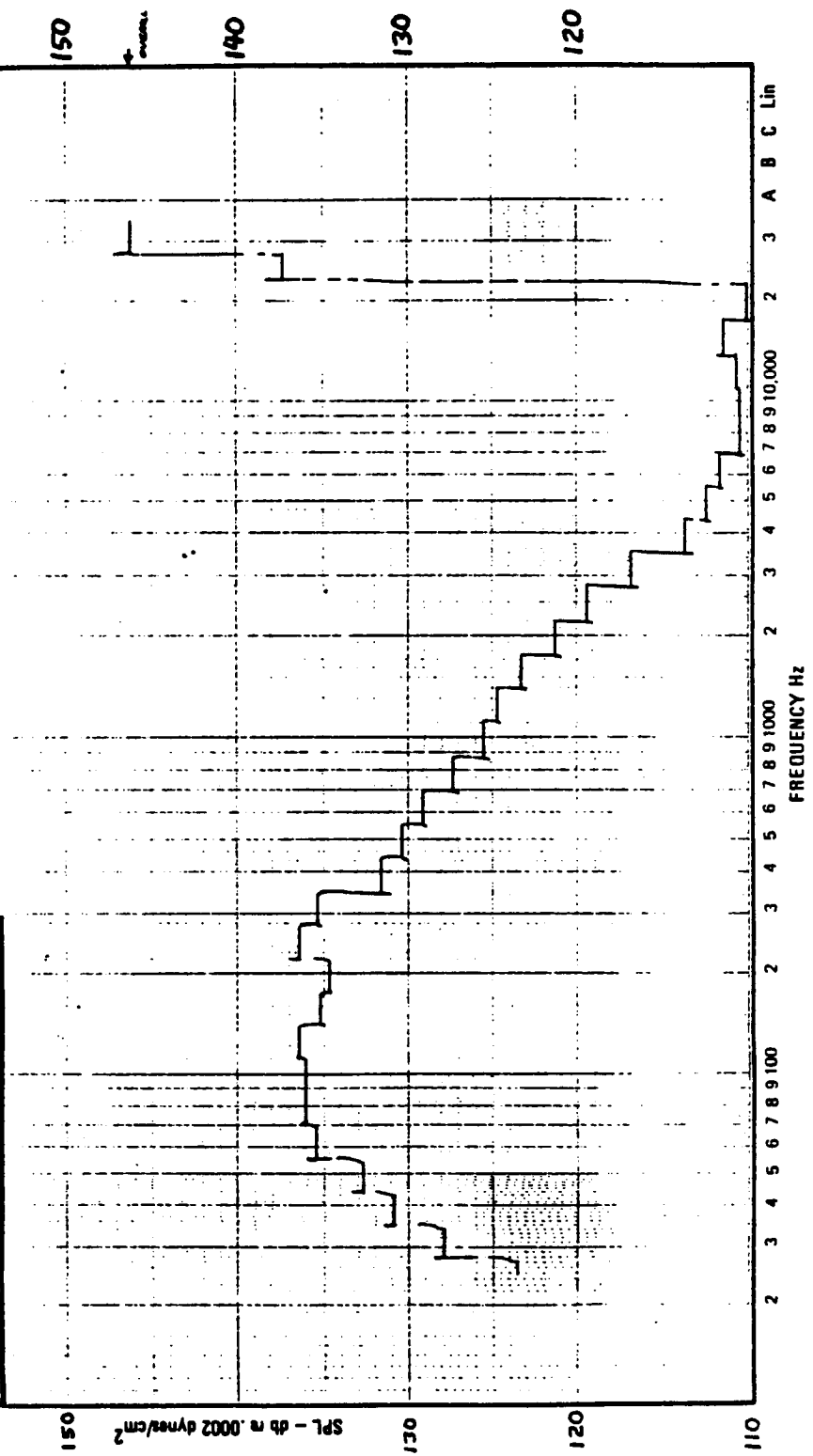


Figure A3

1A 28°C corrected

θ	Voc	Isc	Vmp	Imp	Pmp	FF	norm case Pmp	norm case Isc	STD	EST
3	6.33	.208	5.54	.273	1.51	.80	.712	.69	1.81	34
2.5	6.36	.332	5.49	.312	1.71	.81	.807	.77	1.85	36
2	6.38	.382	5.37	.355	1.91	.78	.901	.88	1.88	37
1.5	6.41	.412	5.40	.384	2.07	.79	.976	.95	1.89	38
1	6.42	.419	5.43	.385	2.09	.78	.986	.97	2.01	39
.5	6.42	.422	5.49	.389	2.13	.79	1.01	.98	2.05	40
0	6.39	.432	5.44	.390	2.12	.78	1.00	1.00	2.15	41
1 0	6.40	.421	5.35	.390	2.09	.77	.99	.97	1.70	41
1.5	6.42	.411	5.40	.379	2.05	.78	.97	.95	1.81	40
2	6.38	.371	5.46	.337	1.84	.78	.87	.86	1.80	39
2.5	6.38	.341	5.48	.311	1.70	.78	.80	.77	1.99	38
3	6.37	.293	5.51	.264	1.45	.78	.68	.68	1.98	37
3.5	6.30	.208	5.59	.182	1.02	.78	.48	.48	2.00	36
4	6.15	.115	5.35	.105	.56	.79	.26	.27	2.07	34

NEEDS
1° SHIFT
↓

1B 28°C corrected

θ	Voc	Isc	Vmp	Imp	Pmp	FF	norm case Pmp	norm case Isc	STD	EST
2	6.26	.306	5.66	.281	1.59	.83	.74	.71	2.19	34
1.5	6.29	.347	5.53	.329	1.82	.84	.86	.81	2.18	36
1	6.30	.392	5.43	.368	2.00	.81	.94	.91	2.15	37
.5	6.32	.417	5.43	.387	2.10	.80	.99	.97	2.16	38
0	6.34	.429	5.50	.388	2.14	.79	1.00	1.00	2.17	39
.5	6.35	.430	5.47	.395	2.16	.79	1.01	1.00	2.17	40
1 0	6.33	.420	5.47	.388	2.13	.79	1.00	.98	2.15	41
1.5	6.37	.419	5.50	.388	2.13	.80	1.00	.98	2.19	42
2	6.33	.398	5.48	.371	2.03	.80	.95	.93	2.19	41
2.5	6.33	.371	5.55	.337	1.87	.80	.88	.86	2.23	41
3	6.31	.311	5.71	.265	1.51	.77	.71	.72	2.00	39
3.5	6.24	.198	5.75	.159	.91	.74	.43	.46	1.91	36
4	6.16	.121	5.59	.098	.55	.74	.26	.28	1.89	34
4.5	5.98	.055	5.08	.052	.27	.81	.13	.13	1.87	32

NEEDS
1° SHIFT
↓

2A 28°C corrected

θ	Voc	Isc	Vmp	Imp	Pmp	FF	norm case Pmp	norm case Isc	STD	T1	T2
5	5.95	.011	5.174	.010	.051	.784	.024	.026	2.64	46.3	41.6
4	6.192	.062	5.830	.053	.307	.793	.143	.147	2.62	49.2	43.7
3	6.364	.204	5.959	.175	1.041	.803	.484	.485	2.62	49.4	45
2.5	6.397	.279	5.906	.244	1.441	.807	.670	.670	2.66	49.4	46
2	6.405	.324	5.839	.287	1.677	.808	.780	.770	2.65	48.5	46
1.5	6.402	.361	5.650	.321	1.868	.808	.869	.857	2.60	49.8	
1	6.413	.390	5.627	.360	2.028	.811	.943	.926	2.60	51.5	
.5	6.431	.405	5.621	.377	2.117	.812	.985	.962	2.50	52	
0	6.437	.420	5.623	.382	2.145	.792	.998	1.00	2.48	51.5	
0	6.484	.421	5.634	.382	2.154	.791	1.002	.998	2.77	58.3	46
.5	6.454	.416	5.624	.377	2.121	.790	.987	.988	2.77	54.5	46
1	6.436	.405	5.586	.370	2.069	.793	.962	.962	2.77	53	44
1.5	6.410	.371	5.541	.348	1.926	.809	.896	.881	2.78	51.2	45
2	6.402	.337	5.674	.311	1.766	.818	.821	.800	2.79	49.2	44
2.5	6.402	.301	5.747	.265	1.636	.848	.761	.715	2.79	49.2	44
3	6.371	.236	5.873	.201	1.180	.786	.549	.561	2.79	49.7	45.5
4	6.160	.052	5.662	.048	.273	.850	.127	.124	2.79	43.5	43

2B 28°C corrected

θ	Voc	Isc	Vmp	Imp	Pmp	FF	norm case Pmp	norm case Isc	STD	T1	T2
5	5.887	.016	5.199	.015	.075	.811	.033	.037	2.94	40.5	34
4	6.332	.117	5.863	.102	.599	.807	.264	.273	2.94	46.6	34
3	6.442	.293	5.914	.258	1.528	.810	.672	.683	2.93	49	35
2.5	6.451	.346	5.738	.333	1.909	.855	.840	.807	2.91	50	41.5
2	6.451	.382	5.552	.353	1.962	.796	.863	.890	2.91	50.5	43.5
1.5	6.460	.404	5.586	.372	2.078	.795	.914	.942	2.91	50	46
1	6.471	.430	5.617	.392	2.217	.798	.975	1.002	2.89	50.7	44.5
.5	6.475	.433	5.660	.402	2.275	.817	.970	1.007	2.88	50	46
0	6.481	.430	5.660	.402	2.275	.817	1.001	1.002	2.85	49.5	43
0	6.491	.428	5.656	.402	2.271	.818	.999	.998	2.95	49.5	44
.5	6.475	.428	5.626	.380	2.140	.772	.941	.998	2.95	50.5	46
1	6.469	.421	5.590	.386	2.159	.793	.950	.981	2.93	51	45
1.5	6.455	.380	5.571	.349	1.942	.792	.854	.886	2.96	51	46
2	6.446	.327	5.806	.296	1.717	.814	.755	.762	2.95	50	44.5
2.5	6.436	.301	5.787	.293	1.693	.874	.715	.702	2.96	50	46.5
3	6.384	.230	5.778	.244	1.292	.880	.568	.536	2.96	48	46
4	6.196	.070	5.596	.066	.371	.860	.163	.163	2.97	44.5	42.5
5	5.745	.010	5.057	.009	.048	.825	.021	.023	2.96	40	37

FIGURE A4 HALF STRING OUTPUTS FOR 15" x 21" PANEL . CORRECTED FOR INSULATION AND TEMPERATURE.

ORIGINAL PAGE IS
OF POOR QUALITY

3A 28°C corrected
4A 28°C corrected

θ	Voc	Isc	Vmp	Imp	Pmp	FF	norm. I _{sc}	norm. P _{mp}	STD	T1	T2
5	5.648	.017	5.043	.015	.073	.746	.035	.746	.040	2.94	34.5
4	6.257	.116	5.671	.105	.593	.821	.283	.821	.276	2.95	32.5
3	6.368	.260	5.855	.218	1.276	.771	.608	.771	.618	2.95	41
2.5	6.374	.306	5.783	.262	1.517	.777	.723	.777	.727	2.96	48.5
2	6.373	.342	5.612	.305	1.709	.784	.814	.784	.812	2.96	49.5
1.5	6.374	.379	5.524	.343	1.896	.786	.904	.786	.900	2.91	50.7
1	6.398	.406	5.538	.367	2.035	.783	.970	.783	.964	2.85	49.5
.5	6.397	.417	5.535	.379	2.097	.787	.999	.787	.990	2.84	50
0	6.391	.423	5.498	.384	2.113	.782	1.007	.782	1.005	2.94	51
0	6.403	.419	5.529	.377	2.084	.776	.993	.776	.995	2.95	49
.5	6.403	.417	5.452	.380	2.073	.776	.988	.776	.990	2.94	47.5
1	6.359	.406	5.413	.371	2.009	.778	.957	.778	.964	2.94	47
1.5	6.375	.387	5.403	.353	1.909	.774	.910	.774	.919	2.94	47
2	6.365	.356	5.374	.339	1.822	.803	.868	.803	.846	2.94	47.5
2.5	6.352	.319	5.417	.302	1.633	.807	.778	.807	.758	2.94	45
3	6.300	.227	5.631	.203	1.141	.798	.544	.798	.539	2.94	49.5
4	6.054	.052	5.624	.042	.236	.752	.112	.752	.124	2.93	39
5	5.202	.007	4.343	.006	.026	.743	.012	.743	.017	2.93	38.2

3B 28°C corrected

θ	Voc	Isc	Vmp	Imp	Pmp	FF	norm. I _{sc}	norm. P _{mp}	STD	T1	T2
5	6.105	.034	5.690	.029	.164	.794	.076	.794	.080	2.81	36
4	6.311	.150	5.818	.136	.790	.837	.364	.837	.351	2.88	47
3	6.370	.296	5.749	.274	1.573	.835	.726	.835	.642	2.89	47
2.5	6.370	.329	5.613	.312	1.749	.833	.807	.833	.731	2.89	47.5
2	6.364	.373	5.485	.347	1.901	.800	.877	.800	.813	2.91	48
1.5	6.379	.406	5.524	.373	2.061	.796	.951	.796	.951	2.91	48
1	6.394	.421	5.603	.383	2.147	.797	.990	.797	.986	2.91	48
.5	6.399	.426	5.638	.393	2.213	.811	1.021	.811	.998	2.91	47.5
0	6.396	.429	5.610	.387	2.170	.791	1.001	.791	1.005	2.92	45.5
.5	6.376	.427	5.576	.389	2.166	.798	.999	.798	.998	2.93	45.5
1	6.372	.418	5.523	.387	2.199	.803	1.014	.803	1.000	2.93	45
1.5	6.367	.373	5.610	.333	1.875	.790	.965	.790	.979	2.92	44
2	6.364	.344	5.741	.305	1.744	.798	.804	.798	.806	2.96	42.5
2.5	6.358	.334	5.675	.306	1.734	.817	.800	.817	.762	2.97	43
3	6.340	.278	5.759	.269	1.550	.820	.715	.820	.698	2.98	42
4	6.211	.113	5.777	.094	.545	.775	.251	.775	.265	2.69	37.5
5	5.886	.018	5.270	.016	.084	.790	.059	.790	.042	2.70	35.5

θ	Voc	Isc	Vmp	Imp	Pmp	FF	norm. I _{sc}	norm. P _{mp}	STD	T1	T2
3	6.217	.163	5.758	.135	.776	.767	.362	.767	.374	2.86	49
2.5	6.261	.233	5.704	.206	1.173	.803	.548	.803	.534	2.87	49
2	6.271	.275	5.651	.249	1.404	.814	.655	.814	.631	2.86	49
1.5	6.275	.315	5.542	.295	1.635	.829	.763	.829	.722	2.85	50
1	6.285	.371	5.494	.336	1.849	.792	.863	.792	.851	2.85	49
.5	6.311	.413	5.500	.374	2.058	.789	.961	.789	.947	2.85	47.5
0	6.316	.435	5.408	.395	2.138	.779	.998	.779	.998	2.84	47.5
0	6.300	.437	5.353	.401	2.145	.779	1.001	.779	1.002	2.87	49
.5	6.320	.441	5.416	.404	2.189	.786	1.022	.786	1.011	2.87	49
1	6.281	.426	5.334	.390	2.076	.777	.969	.777	.977	2.86	48
1.5	6.277	.388	5.374	.360	1.934	.794	.903	.794	.890	2.85	47
2	6.264	.354	5.385	.334	1.745	.788	.815	.788	.812	2.85	45
2.5	6.247	.307	5.563	.279	1.554	.811	.725	.811	.704	2.82	48
3	6.217	.237	5.645	.209	1.181	.802	.557	.802	.544	2.81	43

4B 28°C corrected

θ	Voc	Isc	Vmp	Imp	Pmp	FF	norm. I _{sc}	norm. P _{mp}	STD	T1	T2
3	6.312	.264	5.838	.208	1.212	.727	.568	.727	.568	2.66	46.5
2.5	6.305	.318	5.772	.259	1.492	.744	.699	.744	.746	2.67	45.7
2	6.310	.356	5.568	.318	1.772	.790	.831	.790	.836	2.69	46.3
1.5	6.332	.410	5.493	.369	2.025	.780	.949	.780	.962	2.71	45
1	6.338	.411	5.537	.370	2.051	.787	.962	.787	.965	2.71	44.5
.5	6.358	.414	5.486	.371	2.038	.774	.955	.774	.972	2.69	44.5
0	6.363	.428	5.546	.387	2.197	.789	1.007	.789	1.005	2.73	45.7
0	6.349	.424	5.553	.382	2.120	.787	.994	.787	.995	2.61	44.7
.5	6.346	.431	5.487	.394	2.161	.790	1.013	.790	1.012	2.60	46.5
1	6.335	.421	5.563	.375	2.084	.783	.977	.783	.988	2.59	46.3
1.5	6.331	.397	5.540	.366	2.025	.806	.949	.806	.932	2.58	47
2	6.320	.331	5.617	.296	1.664	.795	.780	.795	.777	2.59	46.3
2.5	6.308	.256	5.884	.233	1.367	.847	.641	.847	.601	2.59	45
3	6.290	.183	5.962	.164	.975	.849	.457	.849	.430	2.57	43

ORIGINAL PAGE IS
OF POOR QUALITY

FIGURE A4 (CONTINUED)

SC 28° corrected

SA 28°C corrected

θ	Voc	Isc	Vmp	Imp	Pmp	FF	norm Amp	code	norm Isc	STD	T1	T2
3	6.19	.215	5.43	.207	1.12	.845	.569	TD	.540	1.45	34	
2.5	6.22	.290	5.43	.272	1.48	.818	.751	TD	.729	1.44	33.5	
2	6.23	.332	5.43	.305	1.66	.803	.843	SD	.834	1.33	33	
1.5	6.21	.356	5.45	.309	1.69	.763	.858	SD	.844	1.16	33	
1	6.25	.375	5.35	.355	1.90	.808	.964	G	.912	1.43	34	
.5	6.27	.394	5.46	.358	1.96	.792	.915	SD	.99	1.43	34	
0	6.268	.398	5.49	.358	1.96	.787	.995	SD	1.00	1.42	33.5	
0	6.27	.399	5.51	.358	1.97	.788	1.00	SD	1.003	1.49	35	
.5	6.28	.392	5.47	.363	1.98	.807	1.005	SD	.985	1.49	34	
1	6.26	.379	5.45	.349	1.90	.803	.964	SD	.952	1.51	34	
1.5	6.24	.340	5.57	.304	1.70	.800	.863	D	.854	1.50	34.5	
2	6.23	.299	5.62	.266	1.50	.803	.761	D	.751	1.50	34.5	
2.5	6.22	.253	5.67	.222	1.26	.799	.640	D	.636	1.51	34	
3	6.20	.199	5.71	.172	.98	.796	.497	D	.500	1.54	33	

28

5B 28°C

θ	Voc	Isc	Vmp	Imp	Pmp	FF	norm Amp	code	norm Isc	STD	T1	T2
3	6.156	.198	5.334	.180	1.012	.831	.486	SD	.470	1.30	32.5	
2.5	6.211	.257	5.668	.234	1.324	.828	.635	SD	.610	1.44	32.5	
2	6.220	.296	5.644	.269	1.520	.825	.729	SD	.703	1.36	32.5	
1.5	6.216	.328	5.614	.299	1.678	.822	.805	SD	.779	1.30	32.5	
1	6.259	.385	5.468	.358	1.960	.813	.940	TD	.914	1.43	33	
.5	6.263	.410	5.418	.379	2.051	.799	.984	TD	.974	1.43	34	
0	6.253	.423	5.379	.389	2.095	.792	1.005	TD	1.005	1.51	34	
0	6.245	.420	5.342	.388	2.073	.790	.995	G	.988	1.35	31.5	
.5	6.236	.420	5.352	.383	2.050	.783	.984	TD	.978	1.15	31.0	
1	6.241	.414	5.362	.379	2.029	.786	.974	TD	.963	1.24	31.5	
1.5	6.241	.396	5.328	.362	1.931	.782	.927	TD	.941	1.29	31.5	
2	6.216	.366	5.303	.335	1.779	.783	.854	G	.869	1.22	31.5	
2.5	6.216	.335	5.342	.311	1.664	.778	.788	G	.796	1.33	31.5	
3	6.168	.289	5.289	.252	1.335	.748	.641	G	.626	1.13	30.5	

ORIGINAL PAGE 43
OF POOR QUALITY

FIGURE 43 (CONTINUED)

θ	Voc	Isc	Vmp	Imp	Pmp	FF	norm Amp	code	norm Isc	STD	T1	T2
3	1.019	.317	.891	.299	.267	.827	.681		.665	2.62	40	
2.5	1.018	.342	.884	.317	.280	.805	.714		.717	2.61	41	
2	1.020	.378	.871	.342	.298	.774	.760		.792	2.61	42	
1.5	1.024	.408	.873	.375	.327	.784	.834		.855	2.62	43	
1	1.025	.441	.885	.412	.365	.807	.921		.925	2.59	44	
.5	1.027	.470	.885	.436	.386	.799	.985		.985	2.61	44.5	
0	1.027	.476	.895	.444	.393	.804	1.003		.978	2.60	45	
0	1.024	.477	.881	.444	.392	.802	1.000		1.000	2.59	45	
0	1.024	.477	.875	.439	.384	.786	.980		1.000	2.65	45	
.5	1.021	.461	.878	.426	.374	.795	.957		.966	2.63	44.5	
1	1.025	.410	.877	.378	.331	.788	.844		.960	2.67	52	
1.5	1.022	.344	.888	.320	.284	.810	.724		.721	2.64	49	
2	1.023	.310	.890	.288	.256	.806	.653		.650	2.66	48	
2.5	1.024	.269	.900	.254	.228	.828	.582		.564	2.69	50	
3	1.020	.167	.892	.157	.140	.825	.357		.350	2.68	52	

CELL 73-7 OFFPOINT 45°C @ Orange 19.76 hours estimated

STRINGS 1 THROUGH 5 "A" IN PARALLEL (28°C CORRECTION)

θ	Voc	Isc	Vmp	Imp	Pmp	FF	norm cos Inc	norm Age	STD	T1	T2
4	5.88	.16	5.14	.13	.67	.71	.07	.08	2.38	33	37.5
35	6.13	.45	5.46	.39	2.14	.78	.21	.22	2.34	33	39
3	6.26	.87	5.55	.78	4.31	.77	.42	.42	2.47	37	48
25	6.31	1.29	5.51	1.16	6.42	.79	.63	.63	2.47	40	44
2	6.34	1.57	5.47	1.47	8.04	.81	.79	.76	2.46	43	45
15	6.33	1.73	5.36	1.63	8.75	.80	.86	.84	2.53	43	47
1	6.35	1.89	5.33	1.76	9.36	.78	.92	.92	2.54	43	47
.5	6.38	2.01	5.33	1.88	9.99	.78	.98	.98	2.52	45	46
0	6.390	1.936	5.336	1.897	10.10	.82	.99	.94	2.65	42	44.5
0	6.37	2.06	5.34	1.91	10.19	.78	1.00	1.00	2.39	41.5	43.5
.5	6.39	2.05	5.40	1.90	10.24	.78	1.00	1.00	2.43	45	45
1	6.37	1.93	5.40	1.85	10.04	.78	.99	.98	2.38	46	47
1.5	6.36	1.78	5.40	1.76	9.48	.77	.93	.94	2.39	42.5	45
2	6.35	1.61	5.44	1.61	8.71	.77	.85	.86	2.40	41	43
2.5	6.33	1.43	5.50	1.45	7.88	.77	.77	.78	2.40	39	41
3	6.30	1.16	5.50	1.26	6.91	.76	.68	.69	2.34	37.5	39
3.5	6.26	.81	5.50	.99	5.44	.75	.53	.56	2.28	40	39
4	6.26	.81	5.50	.68	3.75	.74	.37	.39	2.26	40	37

STRINGS 1 THROUGH 5 "A" IN PARALLEL ROTATED 90° (28°C CORRECTION)

θ	Voc	Isc	Vmp	Imp	Pmp	FF	norm cos Inc	norm Age	STD	T1	T2
4.5	5.70	.11	4.92	.09	.43	.66	.04	.05	2.20	32.5	33.5
4	5.97	.28	5.17	.22	1.14	.68	.11	.13	1.93	32	33
35	6.19	.64	5.50	.54	2.97	.75	.28	.30	2.04	34	35.5
3	6.26	1.03	5.56	.90	5.03	.78	.48	.49	1.99	35	36.5
25	6.30	1.38	5.52	1.23	6.77	.78	.64	.65	1.91	35	36.5
2	6.31	1.63	5.54	1.45	8.05	.78	.76	.77	1.89	36	38
15	6.33	1.80	5.45	1.63	8.88	.78	.84	.85	2.09	37	39.5
1	6.37	1.95	5.47	1.78	9.75	.78	.92	.92	2.07	40	39
.5	6.37	2.04	5.43	1.88	10.21	.78	.97	.97	2.02	40.5	39.5
.5	6.39	2.04	5.45	1.88	10.22	.79	.97	.97	2.30	36.5	36
0	6.40	2.11	5.45	1.94	10.57	.78	1.00	1.00	2.30	43	42.5
.5	6.39	2.10	5.43	1.92	10.43	.78	.97	.97	2.32	41.5	42.5
1	6.39	2.07	5.46	1.90	10.37	.78	.98	.98	2.35	43	43
1.5	6.38	1.97	5.37	1.82	9.80	.78	.93	.93	2.39	43	43
2	6.34	1.81	5.41	1.67	9.03	.79	.85	.86	2.34	42	45.5
2.5	6.34	1.68	5.50	1.54	8.49	.80	.90	.90	2.36	41.5	44.5
3	6.33	1.43	5.53	1.32	7.28	.80	.69	.68	2.31	42	43.5
3.5	6.28	.99	5.58	.90	5.03	.81	.48	.47	2.38	39	41

STRINGS 1 THROUGH 5 "B" IN PARALLEL (28°C CORRECTION)

θ	Voc	Isc	Vmp	Imp	Pmp	FF	norm cos Inc	norm Age	STD	T1	T2
4	6.07	.28	5.23	.25	1.29	.77			2.08	30.5	33
35	6.29	.97	5.59	.86	4.80	.79	.98		2.14	32	35
3	6.35	1.64	5.52	1.50	8.29	.79	.82		2.12	34.5	36
25	6.35	1.55	5.52	1.41	7.81	.77	.77		2.25	34.5	35
2	6.36	1.73	5.48	1.55	8.51	.78	.86		2.14	33.5	34
15	6.34	1.78	5.43	1.63	8.87	.79	.89		1.86	36	36
1	6.37	2.04	5.32	1.88	9.98	.77	1.01		2.18	35	35.5
.5	6.37	2.01	5.31	1.83	9.70	.76	1.00		2.21	34.5	35
0	6.36	1.99	5.38	1.82	9.81	.77	.99		1.83	32	32.5
.5	6.37	2.06	5.35	1.88	10.04	.77	1.02		2.02	28.5	29.5
1	6.28	1.96	5.33	1.81	9.63	.78	.98		1.08	28.5	29
1.5											
2											
2.5											
3											
3.5											
4											

STRINGS 1 THROUGH 5 "B" IN PARALLEL ROTATED 90° (28°C CORRECTION)

θ	Voc	Isc	Vmp	Imp	Pmp	FF	norm cos Inc	norm Age	STD	T1	T2
4.5	5.93	.16	5.24	.13	.66	.72	.06	.08	2.08	31	32
4	6.24	.75	5.62	.66	3.69	.79	.35	.36	1.98	34	36
35	6.30	1.19	5.60	1.06	5.93	.79	.57	.56	1.95	34	36
3	6.33	1.57	5.57	1.43	7.95	.80	.76	.74	1.98	34.5	36
25	6.33	1.73	5.53	1.59	8.80	.80	.84	.82	1.91	35	37
2	6.35	1.89	5.48	1.74	9.51	.79	.91	.90	1.91	35	36
15	6.36	2.03	5.43	1.89	10.28	.79	.98	.96	1.89	35	36
1	6.36	2.11	5.43	1.92	10.41	.78	.99	.99	1.88	35.5	37.5
.5	6.36	2.11	5.39	1.92	10.36	.77	.99	.99	2.11	36	39
.5	6.37	2.11	5.44	1.92	10.48	.78	1.00	1.00	2.13	35.5	37.5
0	6.36	2.11	5.39	1.91	10.32	.77	.98	.98	2.21	36	39
.5	6.35	2.02	5.39	1.86	10.02	.78	.96	.96	2.17	36.5	39
1	6.35	1.83	5.47	1.66	9.07	.78	.87	.87	2.13	37	40
1.5	6.33	1.61	5.53	1.49	8.24	.81	.79	.76	2.13	37	39
2	6.33	1.44	5.63	1.31	7.38	.81	.70	.68	1.98	36	37
2.5	6.24	.72	5.62	.66	3.68	.82	.35	.34	2.01	33.5	35
3	6.24	.72	5.62	.66	3.68	.82	.35	.34	2.01	33.5	35

FIGURE A5 COMBINED STRINGS CORRECTED FOR INSULATION AND TEMPERATURE

OFF-AXIS ANGLE	INDIVIDUAL HALF STRINGS										COMBINED PARALLEL STRINGS					
	1A	1B	2A	2B	3A	3B	4A	4B	5A	5B	5C	0° A	0° B	90° A	90° B	90° B
5			.03	.04	.05	.10						.75	.79	.17		
4			.19	.35	.35	.45						.87	.91	.81		
3	.90		.63	.89	.90	.83	.49	.80	1.01	.61	.70	.55	.73	.64		
2.5	.96		.83	1.01	.91	.91	.67	.93	1.01	.76	.91	.79	.91	.81		
2	1.05	.84	.91	1.06	.96	.97	.75	.99	1.06	.84	.99	.90	.95	.91		
1.5	1.02	.87	.92	1.01	.97	1.02	.78	1.04	1.02	.84	.96	.90	.96	.92		
1	1.00	.93	.95	1.03	.99	1.01	.87	.99	1.01	.94	.97	.94	.98	.94		
.5	.99	.98	.97	1.02	1.00	1.00	.95	.98	1.00	.98	1.00	.99	.99	.98		
0	1.00	1.00	1.00	1.00	1.00	1.00	1.00	1.00	1.00	1.00	1.00	1.00	1.00	1.00		
0	1.00	1.00	1.00	1.00	1.00	1.00	1.00	1.00	1.00	1.00	1.00	1.00	1.00	1.00		
.5	—	1.01	.99	1.00	1.00	1.01	1.02	1.02	1.00	1.00	.99	1.01	1.01	1.01		
1	1.00	1.01	.99	1.01	1.00	1.01	1.00	1.01	.99	1.01	.98	1.01	1.01	1.01		
1.5	1.02	1.00	.95	.95	1.00	.94	.96	1.00	.99	1.01	.92	1.01	.98	1.00		
2	1.02	1.02	.95	.91	1.01	.96	.96	.92	1.02	1.03	.89	1.02	.96	1.02		
2.5	.99	.90	.89	.88	.95	.98	.88	.75	.95	.99	.79	.92	.90	1.00		
3	.88	.60	.73	.70	.71	.91	.71	.56	.76	.89	.65	.75	.73	.88		
4	.35	.17	.16	.20	.17	.34						.90		.88		
5	—		.03	.03	.03	.05						.50				

* BASED ON AVERAGE CURRENT OF ALL STRINGS AT ISC

FIGURE A6 COMBINED AND INDIVIDUAL HALF STRING DATA NORMALIZED FOR OUTPUT AT ISC AND CORRECTED FOR CONIC MIRROR REFLECTANCE OF 0.75

ORIGINAL PAGE IS OF POOR QUALITY

through 10D. During that time the panel was stored but not bagged in the array manufacturing area as well as the test stand. It was noted that additional contamination of the mirrors was evident. Strings 1A through 1D and 2D were remeasured to see this effect. An apparent 1 to 12% loss in output was recorded compared to earlier readings. The average was near 5%. Also noted was additional conic mirror coating degradation in terms of actual increases in defect areas. It was not possible to determine the relative contributions of the contamination and conic mirror degradation to the total loss recorded. Data for the remeasured mirrors is noted as strings 1A2 through 1D2 and 2D2.

As with the small panel data, the large panel data is shown corrected to standard conditions in Figure A7 and corrected for conic mirror average loss (0.70) in Figure A8. Note that with reference to efficiency in Figure A8, an efficiency of 15.5% would represent a 20% efficient cell in an optic with nominal capabilities as defined in the main text figure 4-4 "corrected".

3.4 SECONDARY MIRROR TESTING

The secondary proof mirrors (bare nickel) were checked by bonding each to a dedicated nickel spider and then successively measuring the short circuit current output of two primary subassemblies at various pointing angles. Figure A09 shows the current and normalized output recorded for eight proof secondaries corrected for intensity only. Figure A-10 shows the normalized data corrected for conic mirror reflectance of 0.70.

DATA FOR STRING 1A CORRECTED FOR TEMPERATURE AND INSOLATION												
BUT NOT CONIC MIRROR QUALITY												
ANGLE (DEG)	VOC	ISC	VMP	IMP	PMP	FILL FACTOR	ORIG TEMP	TEMP ERROR	ORIG TEMP	TEMP ERROR	ORIG TEMP	TEMP ERROR
0.0	4.981	440	4.207	394	1.658	.757	45.0	4.2	45.0	4.2	45.0	4.2
1.0	5.084	432	4.310	392	1.688	.768	38.9	1.3	38.9	1.3	38.9	1.3
2.0	5.046	380	4.233	355	1.503	.784	38.7	1.1	38.7	1.1	38.7	1.1
2.5	5.066	366	4.341	346	1.502	.811	38.4	1.5	38.4	1.5	38.4	1.5
3.0	5.074	323	4.393	314	1.378	.840	37.8	1.0	37.8	1.0	37.8	1.0
0.0	5.039	434	4.250	391	1.662	.760	40.3	0.2	40.3	0.2	40.3	0.2
-1.0	5.066	411	4.240	374	1.584	.761	39.0	0.4	39.0	0.4	39.0	0.4
-2.0	5.032	328	4.407	312	1.374	.832	40.7	2.2	40.7	2.2	40.7	2.2
-2.5	5.018	285	4.418	272	1.202	.840	41.4	2.2	41.4	2.2	41.4	2.2
-3.0	5.043	213	4.479	188	0.844	.787	38.5	1.4	38.5	1.4	38.5	1.4

DATA FOR STRING 1B CORRECTED FOR TEMPERATURE AND INSOLATION												
BUT NOT CONIC MIRROR QUALITY												
ANGLE (DEG)	VOC	ISC	VMP	IMP	PMP	FILL FACTOR	ORIG TEMP	TEMP ERROR	ORIG TEMP	TEMP ERROR	ORIG TEMP	TEMP ERROR
0.0	6.090	414	5.206	381	1.983	.786	37.3	2.7	37.3	2.7	37.3	2.7
1.0	6.090	394	5.213	366	1.906	.794	37.6	0.4	37.6	0.4	37.6	0.4
2.0	6.071	346	5.316	303	1.612	.768	36.8	0.6	36.8	0.6	36.8	0.6
2.5	6.055	327	5.403	279	1.505	.760	37.6	1.7	37.6	1.7	37.6	1.7
3.0	6.040	254	5.435	205	1.112	.724	36.9	0.5	36.9	0.5	36.9	0.5
0.0	6.107	414	5.211	381	1.985	.785	36.1	2.4	36.1	2.4	36.1	2.4
-1.0	6.095	407	5.172	376	1.936	.780	35.8	2.2	35.8	2.2	35.8	2.2
-2.0	6.098	362	5.178	335	1.734	.784	34.7	1.0	34.7	1.0	34.7	1.0
-2.5	6.134	314	5.314	293	1.557	.809	31.7	0.8	31.7	0.8	31.7	0.8
-3.0	6.111	232	5.413	207	1.118	.787	31.5	1.9	31.5	1.9	31.5	1.9

ORIGINAL PAGE IS
OF POOR QUALITY

DATA FOR STRING 1C CORRECTED FOR TEMPERATURE AND INSOLATION												
BUT NOT CONIC MIRROR QUALITY												
ANGLE (DEG)	VOC	ISC	VMP	IMP	PMP	FILL FACTOR	ORIG TEMP	TEMP ERROR	ORIG TEMP	TEMP ERROR	ORIG TEMP	TEMP ERROR
0.0	6.050	415	5.198	371	1.929	.768	39.7	1.5	39.7	1.5	39.7	1.5
1.0	6.063	390	5.182	363	1.883	.796	38.6	0.7	38.6	0.7	38.6	0.7
2.0	6.095	353	5.282	333	1.761	.819	36.8	0.8	36.8	0.8	36.8	0.8
2.5	6.057	299	5.473	278	1.520	.840	38.0	0.8	38.0	0.8	38.0	0.8
3.0	6.067	198	5.649	181	1.024	.850	36.4	0.8	36.4	0.8	36.4	0.8
0.0	6.095	410	5.255	366	1.922	.769	36.5	0.1	36.5	0.1	36.5	0.1
-1.0	6.099	353	5.410	308	1.668	.775	35.6	0.7	35.6	0.7	35.6	0.7
-2.0	6.107	213	5.602	119	0.667	.513	32.2	0.5	32.2	0.5	32.2	0.5
-2.5	5.974	114	5.486	036	0.197	.288	35.1	3.0	35.1	3.0	35.1	3.0
-3.0	5.866	087	2.873	033	0.094	.184	34.1	3.3	34.1	3.3	34.1	3.3

DATA FOR STRING 1D CORRECTED FOR TEMPERATURE AND INSOLATION												
BUT NOT CONIC MIRROR QUALITY												
ANGLE (DEG)	VOC	ISC	VMP	IMP	PMP	FILL FACTOR	ORIG TEMP	TEMP ERROR	ORIG TEMP	TEMP ERROR	ORIG TEMP	TEMP ERROR
0.0	6.140	415	5.339	370	1.977	.776	34.4	2.2	34.4	2.2	34.4	2.2
1.0	6.083	391	5.213	369	1.921	.808	37.3	0.5	37.3	0.5	37.3	0.5
2.0	6.057	336	5.359	313	1.679	.826	37.9	1.0	37.9	1.0	37.9	1.0
2.5	6.054	288	5.483	264	1.448	.831	37.7	0.9	37.7	0.9	37.7	0.9
3.0	6.023	235	5.486	214	1.177	.832	38.1	1.3	38.1	1.3	38.1	1.3
0.0	6.145	415	5.330	371	1.978	.776	34.3	0.5	34.3	0.5	34.3	0.5
-1.0	6.206	376	5.449	335	1.823	.781	28.7	1.0	28.7	1.0	28.7	1.0
-2.0	6.145	309	5.530	264	1.461	.768	30.6	0.1	30.6	0.1	30.6	0.1
-2.5	6.138	249	5.599	204	1.142	.748	31.2	1.1	31.2	1.1	31.2	1.1
-3.0	6.063	138	5.509	113	0.621	.741	30.9	1.5	30.9	1.5	30.9	1.5

DATA FOR STRING 2A CORRECTED FOR TEMPERATURE AND INSOLATION												
BUT NOT CONIC MIRROR QUALITY												
ANGLE (DEG)	VOC	ISC	VMP	IMP	PMP	FILL FACTOR	ORIG TEMP	TEMP ERROR	ORIG TEMP	TEMP ERROR	ORIG TEMP	TEMP ERROR
0.0	6.175	336	5.585	302	1.684	.811	30.7	0.6	30.7	0.6	30.7	0.6
1.0	6.184	413	5.340	384	2.051	.803	30.8	0.1	30.8	0.1	30.8	0.1
2.0	6.134	416	5.251	376	1.973	.773	33.4	0.4	33.4	0.4	33.4	0.4
2.5	6.090	387	5.231	351	1.837	.780	36.0	0.2	36.0	0.2	36.0	0.2
3.0	6.094	354	5.310	323	1.713	.794	35.9	0.4	35.9	0.4	35.9	0.4
0.0	6.131	334	5.552	299	1.663	.813	33.8	0.2	33.8	0.2	33.8	0.2
-1.0	6.083	284	5.605	234	1.312	.816	34.9	0.4	34.9	0.4	34.9	0.4
-2.0	6.050	128	5.731	108	0.618	.795	32.2	1.1	32.2	1.1	32.2	1.1
-2.5	6.053	069	5.655	058	0.329	.782	31.5	0.3	31.5	0.3	31.5	0.3
-3.0	5.953	038	5.413	030	0.165	.737	30.0	1.5	30.0	1.5	30.0	1.5

DATA FOR STRING 2B CORRECTED FOR TEMPERATURE AND INSOLATION												
BUT NOT CONIC MIRROR QUALITY												
ANGLE (DEG)	VOC	ISC	VMP	IMP	PMP	FILL FACTOR	ORIG TEMP	TEMP ERROR	ORIG TEMP	TEMP ERROR	ORIG TEMP	TEMP ERROR
0.0	6.185	434	5.414	403	2.182	.812	29.6	1.1	29.6	1.1	29.6	1.1
1.0	6.170	425	5.386	394	2.124	.810	30.0	0.0	30.0	0.0	30.0	0.0
2.0	6.146	360	5.504	320	1.761	.796	30.0	0.5	30.0	0.5	30.0	0.5
2.5	6.126	329	5.557	286	1.590	.790	31.0	1.2	31.0	1.2	31.0	1.2
3.0	6.099	272	5.562	241	1.342	.809	31.3	0.4	31.3	0.4	31.3	0.4
0.0	6.082	435	5.313	404	2.146	.812	35.1	1.2	35.1	1.2	35.1	1.2
-1.0	6.059	430	5.232	403	2.109	.810	36.9	0.6	36.9	0.6	36.9	0.6
-2.0	6.013	389	5.161	362	1.870	.800	38.5	1.3	38.5	1.3	38.5	1.3
-2.5	6.010	347	5.302	330	1.749	.838	38.7	0.2	38.7	0.2	38.7	0.2
-3.0	5.954	262	5.395	240	1.293	.830	41.0	0.7	41.0	0.7	41.0	0.7

DATA FOR STRING 2C CORRECTED FOR TEMPERATURE AND INSOLATION												
BUT NOT CONIC MIRROR QUALITY												
ANGLE (DEG)	VOC	ISC	VMP	IMP	PMP	FILL FACTOR	ORIG TEMP	TEMP ERROR	ORIG TEMP	TEMP ERROR	ORIG TEMP	TEMP ERROR
0.0	5.924	443	4.994	410	2.046	.780	42.1	0.9	42.1	0.9	42.1	0.9
1.0	5.924	409	5.014	379	1.899	.785	42.8	0.8	42.8	0.8	42.8	0.8
2.0	5.933	330	5.149	311	1.601	.817	41.4	1.1	41.4	1.1	41.4	1.1
2.5	5.953	282	5.335	252	1.343	.799	38.9	1.4	38.9	1.4	38.9	1.4
3.0	6.004	198	5.496	166	0.915	.771	33.6	1.5	33.6	1.5	33.6	1.5
0.0	6.081	434	5.161	398	2.056	.779	33.4	0.9	33.4	0.9	33.4	0.9
-1.0	6.082	424	5.135	391	2.007	.779	32.8	0.6	32.8	0.6	32.8	0.6
-2.0	6.056	359	5.253	331	1.738	.800	33.5	0.1	33.5	0.1	33.5	0.1
-2.5	6.045	307	5.386	274	1.474	.795	33.5	0.4	33.5	0.4	33.5	0.4
-3.0	6.018	227	5.427	203	1.099	.803	33.4	0.5	33.4	0.5	33.4	0.5

DATA FOR STRING 2D CORRECTED FOR TEMPERATURE AND INSOLATION												
BUT NOT CONIC MIRROR QUALITY												
ANGLE (DEG)	VOC (V)	ISC (A)	VMP (V)	IMP (A)	PMP (W)	FILL FACTOR	ORIG TEMP	TEMP ERROR	ORIG TEMP	TEMP ERROR	ORIG TEMP	TEMP ERROR
0.0	6.080	425	5.140	399	2.050	.794	34.5	2.6	34.5	2.6	34.5	2.6
1.0	6.091	403	5.192	374	1.942	.792	33.4	1.3	33.4	1.3	33.4	1.3
2.0	6.069	324	5.420	283	1.536	.780	33.1	1.7	33.1	1.7	33.1	1.7
2.5	6.061	268	5.526	227	1.256	.772	32.7	1.2	32.7	1.2	32.7	1.2
3.0	6.008	187	5.576	154	0.859	.766	32.6	0.2	32.6	0.2	32.6	0.2
0.0	6.140	423	5.200	397	2.064	.795	30.3	0.1	30.3	0.1	30.3	0.1
-1.0	6.119	402	5.142	373	1.920	.781	31.0	3.0	31.0	3.0	31.0	3.0
-2.0	6.081	329	5.383	313	1.647	.823	32.7	1.9	32.7	1.9	32.7	1.9
-2.5	6.062	294	5.515	280	1.462	.820	32.8	2.6	32.8	2.6	32.8	2.6
-3.0	6.035	219	5.515	193	1.045	.795	31.7	0.4	31.7	0.4	31.7	0.4

DATA FOR STRING 4A CORRECTED FOR TEMPERATURE AND INSOLATION										
BUT NOT CONIC MIRROR QUALITY										
ANGLE (DEG)	VOC (V)	ISC (A)	IMP (W)	PMP (W)	FILL FACTOR (%)	ORIG TEMP	TEMP ERROR	ORIG TEMP	TEMP ERROR	ORIG TEMP
0.0	5.860	4.15	4.883	367	1.793	737	32.3	737	32.3	737
0.0	5.836	3.90	4.842	352	1.706	749	33.5	749	33.5	749
1.0	5.841	3.14	4.986	298	1.484	808	31.2	808	31.2	808
2.0	5.822	2.18	5.228	203	1.062	837	28.1	837	28.1	837
2.5	5.822	2.18	5.228	203	1.062	837	28.1	837	28.1	837
3.0	5.786	1.61	5.275	149	0.787	844	28.6	844	28.6	844
0.0	5.843	4.15	4.876	365	1.779	733	33.5	733	33.5	733
-1.0	5.781	3.79	4.778	345	1.647	752	35.6	752	35.6	752
-2.0	5.810	3.21	4.816	302	1.454	779	31.1	779	31.1	779
-2.5	5.771	2.62	4.838	249	1.204	797	29.4	797	29.4	797
-3.0	5.724	1.67	4.942	162	0.801	836	24.4	836	24.4	836

DATA FOR STRING 4B CORRECTED FOR TEMPERATURE AND INSOLATION										
BUT NOT CONIC MIRROR QUALITY										
ANGLE (DEG)	VOC (V)	ISC (A)	IMP (W)	PMP (W)	FILL FACTOR (%)	ORIG TEMP	TEMP ERROR	ORIG TEMP	TEMP ERROR	ORIG TEMP
0.0	6.148	4.08	4.915	346	1.701	678	29.7	678	29.7	678
0.0	6.091	4.07	4.832	327	1.579	637	32.8	637	32.8	637
1.0	6.012	3.44	4.803	309	1.483	716	36.3	716	36.3	716
2.0	6.012	3.44	4.803	309	1.483	716	36.3	716	36.3	716
2.5	6.015	3.15	4.904	287	1.407	743	36.7	743	36.7	743
3.0	5.994	2.78	5.015	255	1.279	766	37.1	766	37.1	766
0.0	6.079	4.05	4.922	342	1.703	692	34.4	692	34.4	692
-1.0	6.104	3.67	5.154	342	1.765	787	33.3	787	33.3	787
-2.0	6.098	2.71	5.485	245	1.343	814	31.4	814	31.4	814
-2.5	6.106	2.17	5.577	194	1.083	818	29.5	818	29.5	818
-3.0	6.113	1.57	5.677	137	0.777	812	26.5	812	26.5	812

DATA FOR STRING 4C CORRECTED FOR TEMPERATURE AND INSOLATION										
BUT NOT CONIC MIRROR QUALITY										
ANGLE (DEG)	VOC (V)	ISC (A)	IMP (W)	PMP (W)	FILL FACTOR (%)	ORIG TEMP	TEMP ERROR	ORIG TEMP	TEMP ERROR	ORIG TEMP
0.0	6.182	3.83	5.615	346	1.945	821	23.6	821	23.6	821
1.0	6.171	4.10	5.433	381	2.073	820	24.3	820	24.3	820
2.0	6.161	3.72	5.402	350	1.888	823	24.3	823	24.3	823
2.5	6.134	3.31	5.387	319	1.716	845	25.5	845	25.5	845
3.0	6.119	2.87	5.479	278	1.521	867	25.6	867	25.6	867
0.0	6.113	3.75	5.566	341	1.895	826	27.8	826	27.8	826
-1.0	6.113	2.84	5.644	254	1.433	826	26.8	826	26.8	826
-2.0	6.141	2.15	5.675	189	1.073	812	23.3	812	23.3	812
-2.5	6.139	1.83	5.685	160	0.909	809	22.0	809	22.0	809
-3.0	6.121	1.51	5.630	132	0.745	804	20.4	804	20.4	804

DATA FOR STRING 4D CORRECTED FOR TEMPERATURE AND INSOLATION										
BUT NOT CONIC MIRROR QUALITY										
ANGLE (DEG)	VOC (V)	ISC (A)	IMP (W)	PMP (W)	FILL FACTOR (%)	ORIG TEMP	TEMP ERROR	ORIG TEMP	TEMP ERROR	ORIG TEMP
0.0	6.199	4.19	5.399	402	2.171	836	23.9	836	23.9	836
1.0	6.240	4.09	5.422	388	2.106	824	19.9	824	19.9	824
2.0	6.172	3.27	5.535	307	1.802	843	21.9	843	21.9	843
2.5	6.120	2.90	5.561	270	1.502	847	24.5	847	24.5	847
3.0	6.090	2.54	5.543	237	1.313	849	26.1	849	26.1	849
0.0	6.172	4.05	5.372	385	2.069	828	23.9	828	23.9	828
-1.0	6.173	3.82	5.384	362	1.948	826	23.1	826	23.1	826
-2.0	6.153	3.01	5.508	277	1.526	823	21.9	823	21.9	823
-2.5	6.137	2.44	5.529	235	1.300	866	19.9	866	19.9	866
-3.0	6.116	1.58	5.681	122	0.806	864	19.6	864	19.6	864

DATA FOR STRING 5A CORRECTED FOR TEMPERATURE AND INSOLATION										
BUT NOT CONIC MIRROR QUALITY										
ANGLE (DEG)	VOC (V)	ISC (A)	IMP (W)	PMP (W)	FILL FACTOR (%)	ORIG TEMP	TEMP ERROR	ORIG TEMP	TEMP ERROR	ORIG TEMP
0.0	6.325	4.17	5.229	376	1.968	747	17.4	747	17.4	747
1.0	6.287	4.22	5.191	389	2.021	762	19.8	762	19.8	762
2.0	6.248	3.62	5.220	331	1.750	773	21.4	773	21.4	773
2.5	6.255	3.19	5.288	301	1.592	798	20.1	798	20.1	798
3.0	6.228	2.79	5.429	260	1.414	815	21.2	815	21.2	815
0.0	6.239	4.16	5.186	372	1.929	743	22.8	743	22.8	743
-1.0	6.215	3.13	5.195	289	1.500	771	21.2	771	21.2	771
-2.0	6.126	1.79	5.384	162	0.873	794	20.3	794	20.3	794
-2.5	6.045	1.37	5.259	124	0.650	787	21.6	787	21.6	787
-3.0	5.947	1.06	4.921	102	0.451	718	20.4	718	20.4	718

DATA FOR STRING 5B CORRECTED FOR TEMPERATURE AND INSOLATION										
BUT NOT CONIC MIRROR QUALITY										
ANGLE (DEG)	VOC (V)	ISC (A)	IMP (W)	PMP (W)	FILL FACTOR (%)	ORIG TEMP	TEMP ERROR	ORIG TEMP	TEMP ERROR	ORIG TEMP
0.0	6.005	3.84	5.087	365	1.856	804	43.1	804	43.1	804
1.0	6.043	3.81	5.152	354	1.826	794	41.0	794	41.0	794
2.0	5.994	3.24	5.156	311	1.606	827	42.7	827	42.7	827
2.5	5.975	2.88	5.153	274	1.413	821	42.4	821	42.4	821
3.0	5.968	2.55	5.155	242	1.250	822	42.1	822	42.1	822
0.0	6.055	3.93	5.146	364	1.874	809	39.4	809	39.4	809
-1.0	6.044	3.57	5.143	334	1.718	795	39.3	795	39.3	795
-2.0	6.010	2.79	5.250	262	1.373	820	39.3	820	39.3	820
-2.5	6.007	2.28	5.255	216	1.137	828	38.1	828	38.1	828
-3.0	5.878	0.92	5.363	087	0.466	860	37.2	860	37.2	860

DATA FOR STRING 5C CORRECTED FOR TEMPERATURE AND INSOLATION										
BUT NOT CONIC MIRROR QUALITY										
ANGLE (DEG)	VOC (V)	ISC (A)	IMP (W)	PMP (W)	FILL FACTOR (%)	ORIG TEMP	TEMP ERROR	ORIG TEMP	TEMP ERROR	ORIG TEMP
0.0	5.963	3.83	5.236	356	1.864	816	40.3	816	40.3	816
1.0	5.966	3.85	5.231	355	1.858	808	40.1	808	40.1	808
2.0	5.958	3.45	5.233	324	1.698	826	39.8	826	39.8	826
2.5	6.016	3.00	5.345	283	1.511	838	36.6	838	36.6	838
3.0	5.972	2.53	5.354	242	1.295	857	37.9	857	37.9	857
0.0	5.947	3.83	5.242	356	1.868	821	41.0	821	41.0	821
-1.0	5.940	3.52	5.207	334	1.737	831	40.8	831	40.8	831
-2.0	5.924	2.39	5.404	223	1.208	853	39.3	853	39.3	853
-2.5	5.904	1.91	5.399	177	0.955	849	37.6	849	37.6	849
-3.0	5.907	1.31	5.368	122	0.654	847	33.9	847	33.9	847

DATA FOR STRING 5D CORRECTED FOR TEMPERATURE AND INSOLATION										
BUT NOT CONIC MIRROR QUALITY										
ANGLE (DEG)	VOC (V)	ISC (A)	IMP (W)	PMP (W)	FILL FACTOR (%)	ORIG TEMP	TEMP ERROR	ORIG TEMP	TEMP ERROR	ORIG TEMP
0.0	5.829	4.03	4.884	340	1.660	707	51.0	707	51.0	707
1.0	5.839	3.55	4.902	302	1.479	714	49.2	714	49.2	714
2.0	5.782	2.77	4.799	240	1.150	718	49.0	718	49.0	718
2.5	5.738	2.25	4.764	188	0.897	695	48.5	695	48.5	695
3.0	5.726	2.25	4.751	188	0.895	695	49.8	695	49.8	695
0.0	5.889	3.98	4.920	338	1.662	709	47.5	709	47.5	709
-1.0	5.864	3.95	4.885	346	1.688	729	49.1	729	49.1	729
-2.0	5.877	3.15	4.902	294	1.443	780	46.3	780	46.3	780
-2.5	5.832	2.71	4.916	257	1.262	798	46.9	798	46.9	798
-3.0	5.814	2.22	5.032	211	1.062	823	46.2	823	46.2	823

DATA FOR STRING 6A CORRECTED FOR TEMPERATURE AND INSOLATION										
BUT NOT CONIC MIRROR QUALITY										
ANGLE (DEG)	VOC (V)	ISC (A)	IMP (W)	PMP (W)	FILL FACTOR	ORIG TEMP	TEMP ERROR	ORIG TEMP	TEMP ERROR	ORIG TEMP
0.0	5.895	3.81	5.016	357	1.793	798	51.5	798	51.5	798
1.0	5.860	3.18	4.974	305	1.517	815	51.3	815	51.3	815
2.0	5.903	2.50	5.051	240	1.214	821	47.1	821	47.1	821
2.5	5.905	1.92	5.177	184	0.952	839	44.4	839	44.4	839
3.0	5.831	1.21	5.130	116	0.598	844	42.6	844	42.6	844
0.0	6.033	3.78	5.142	354	1.821	799	43.5	799	43.5	799
-1.0	6.019	3.61	5.216	339	1.767	812	44.5	812	44.5	812
-2.0	5.971	2.76	5.380	257	1.380	839	45.4	839	45.4	839
-2.5	5.919	2.49	5.314	231	1.228	833	47.2	833	47.2	833
-3.0	5.917	2.04	5.395	184	0.995	826	46.1	826	46.1	826

DATA FOR STRING 102 CORRECTED FOR TEMPERATURE AND INSOLATION													
BUT NOT CONIC MIRROR QUALITY													
ANGLE (DEG)	VOC (V)	ISC (A)	VMP (V)	IMP (A)	PMP (W)	FILL FACTOR	ORIG TEMP	TEMP ERROR	FILL FACTOR	ORIG TEMP	TEMP ERROR	FILL FACTOR	ORIG TEMP
0.0	6.034	391	5.006	345	1.727	.733	36.5	0.1					
1.0	5.972	366	4.910	337	1.655	.757	38.9	0.6					
2.0	6.077	302	5.249	282	1.480	.807	31.5	1.2					
2.5	6.045	247	5.368	228	1.229	.823	32.1	0.3					
3.0	6.007	200	5.333	185	0.989	.823	33.0	0.9					
0.0	6.061	398	5.039	343	1.727	.717	34.2	1.0					
-1.0	6.041	309	5.028	312	1.570	.708	34.5	0.4					
-2.0	6.049	309	5.060	253	1.283	.685	32.2	0.7					
-2.5	6.001	248	4.988	202	1.008	.677	32.1	0.3					
-3.0	5.873	157	4.845	126	0.610	.660	32.0	0.3					

DATA FOR STRING 202 CORRECTED FOR TEMPERATURE AND INSOLATION													
BUT NOT CONIC MIRROR QUALITY													
ANGLE (DEG)	VOC (V)	ISC (A)	VMP (V)	IMP (A)	PMP (W)	FILL FACTOR	ORIG TEMP	TEMP ERROR	FILL FACTOR	ORIG TEMP	TEMP ERROR	FILL FACTOR	ORIG TEMP
0.0	6.093	396	5.144	370	1.905	.789	30.6	3.8					
1.0	6.086	392	5.136	371	1.903	.798	31.3	3.2					
2.0	6.031	337	5.343	299	1.600	.787	33.2	3.1					
2.5	6.033	293	5.415	254	1.373	.778	30.3	0.8					
3.0	6.049	231	5.539	194	1.077	.771	27.5	0.8					
0.0	6.115	394	5.156	370	1.907	.791	29.6	3.0					
-1.0	6.097	342	5.213	320	1.666	.800	28.0	0.5					
-2.0	6.075	277	5.248	260	1.365	.812	28.6	2.3					
-2.5	6.058	213	5.345	190	1.015	.787	26.6	0.8					
-3.0	5.983	121	5.353	104	0.556	.767	23.8	1.1					

ORIGINAL PAGE IS
OF POOR QUALITY

DATA FOR STRING 10B CORRECTED FOR TEMPERATURE AND INSOLATION													
BUT NOT CONIC MIRROR QUALITY													
ANGLE (DEG)	VOC (V)	ISC (A)	VMP (V)	IMP (A)	PMP (W)	FILL FACTOR	ORIG TEMP	TEMP ERROR	FILL FACTOR	ORIG TEMP	TEMP ERROR	FILL FACTOR	ORIG TEMP
0.0	3.887	250	2.899	243	0.704	.723	42.2	1.9					
1.0	3.950	341	2.920	307	0.897	.665	42.8	0.6					
2.0	3.972	334	2.952	310	0.914	.689	41.2	0.1					
2.5	3.967	290	3.071	275	0.843	.732	39.8	0.6					
3.0	3.915	246	3.131	234	0.787	.759	41.6	0.3					
0.0	3.882	261	3.125	252	0.787	.775	45.3	0.1					
-1.0	3.852	259	3.083	251	0.775	.776	47.7	0.3					
-2.0	3.851	234	3.033	224	0.681	.754	41.4	0.4					
-2.5	3.782	216	2.844	204	0.581	.712	43.0	1.7					
-3.0	3.704	153	2.837	148	0.421	.743	40.7	2.3					

DATA FOR STRING 1A2 CORRECTED FOR TEMPERATURE AND INSOLATION													
BUT NOT CONIC MIRROR QUALITY													
ANGLE (DEG)	VOC (V)	ISC (A)	VMP (V)	IMP (A)	PMP (W)	FILL FACTOR	ORIG TEMP	TEMP ERROR	FILL FACTOR	ORIG TEMP	TEMP ERROR	FILL FACTOR	ORIG TEMP
0.0	4.042	422	3.441	404	1.390	.814	38.1	1.5					
1.0	4.026	406	3.435	379	1.302	.797	38.5	1.0					
2.0	4.022	361	3.446	346	1.191	.821	38.3	1.0					
2.5	4.029	326	3.484	315	1.096	.834	37.1	0.7					
3.0	4.042	279	3.515	267	0.940	.833	34.9	0.5					
0.0	4.043	421	3.433	387	1.329	.792	37.4	0.0					
-1.0	4.014	401	3.418	373	1.276	.781	38.4	1.3					
-2.0	4.028	323	3.547	310	1.099	.846	37.2	0.7					
-2.5	4.010	291	3.514	281	0.989	.848	37.8	0.3					
-3.0	3.997	246	3.489	227	0.790	.804	37.1	0.7					

DATA FOR STRING 1B2 CORRECTED FOR TEMPERATURE AND INSOLATION													
BUT NOT CONIC MIRROR QUALITY													
ANGLE (DEG)	VOC (V)	ISC (A)	VMP (V)	IMP (A)	PMP (W)	FILL FACTOR	ORIG TEMP	TEMP ERROR	FILL FACTOR	ORIG TEMP	TEMP ERROR	FILL FACTOR	ORIG TEMP
0.0	5.993	363	5.168	338	1.746	.802	38.7	0.0					
1.0	6.003	334	5.012	314	1.571	.783	36.2	0.0					
2.0	5.943	305	5.017	286	1.436	.791	39.9	0.5					
2.5	5.970	263	5.089	228	1.160	.740	37.6	0.1					
3.0	5.937	193	5.109	168	0.856	.746	37.5	0.4					
0.0	5.996	366	5.173	340	1.758	.801	38.9	0.0					
-1.0	6.015	362	5.148	338	1.743	.800	37.7	0.1					
-2.0	6.031	321	5.192	299	1.555	.804	35.0	1.7					
-2.5	5.976	280	5.200	260	1.350	.808	37.5	1.5					
-3.0	6.020	223	5.265	206	1.086	.809	33.2	0.4					

DATA FOR STRING 1C2 CORRECTED FOR TEMPERATURE AND INSOLATION													
BUT NOT CONIC MIRROR QUALITY													
ANGLE (DEG)	VOC (V)	ISC (A)	VMP (V)	IMP (A)	PMP (W)	FILL FACTOR	ORIG TEMP	TEMP ERROR	FILL FACTOR	ORIG TEMP	TEMP ERROR	FILL FACTOR	ORIG TEMP
0.0	6.160	403	5.251	373	1.956	.789	31.1	0.5					
1.0	6.131	389	5.252	366	1.920	.805	33.1	0.4					
2.0	6.108	350	5.332	330	1.759	.823	33.9	0.7					
2.5	6.115	285	5.553	264	1.467	.841	32.4	1.1					
3.0	6.083	181	5.692	165	0.937	.852	32.7	0.5					
0.0	6.085	406	5.167	376	1.944	.787	36.3	0.4					
-1.0	6.061	382	5.226	338	1.768	.764	36.7	1.1					
-2.0	6.033	298	5.281	271	1.431	.797	37.6	1.6					
-2.5	5.985	237	5.287	191	1.008	.709	38.5	0.5					
-3.0	5.914	151	5.318	082	0.435	.486	37.1	0.2					

DATA FOR STRING 8A CORRECTED FOR TEMPERATURE AND INSOLATION BUT NOT CONIC MIRROR QUALITY													
ANGLE (DEG)	VOC (V)	ISC (A)	VMP (V)	IMP (A)	PMP (W)	FILL FACTOR	ORIG TEMP	TEMP ERROR	FILL FACTOR	ORIG TEMP	TEMP ERROR	FILL FACTOR	ORIG TEMP
0.0	5.861	.392	4.396	.342	1.505	.656	45.6	1.8					
1.0	5.816	.391	4.349	.335	1.458	.691	48.0	2.2					
2.0	5.812	.280	4.418	.257	1.134	.681	42.8	3.1					
2.5	5.729	.259	4.294	.227	0.973	.655	45.6	2.8					
3.0	5.728	.228	4.300	.196	0.844	.646	43.9	1.8					
0.0	5.868	.392	4.427	.343	1.518	.660	45.4	3.0					
-1.0	5.832	.347	4.472	.321	1.435	.710	45.6	3.6					
-2.0	5.803	.246	4.684	.231	1.083	.760	43.8	3.5					
-2.5	5.817	.210	4.658	.201	0.936	.765	40.5	4.7					
					0.920	.763	41.3	5.2					

ORIGINAL PAGE IS
OF POOR QUALITY

DATA FOR STRING 1A CORRECTED FOR ALL CONDITIONS INCLUDING CONIC MIRROR QUALITY (REFLECTANCE SET TO .7)

NORMALIZED TO 0 DEGREES FOR ISC, IMP, AND PMP

ANGLE VDC (DEG)	ISC (V)	IMP (V)	PMP (V)	ISC (%)	IMP (%)	PMP (%)	NORM ISC	NORM IMP	NORM PMP
0.0	4.98	4.93	4.21	4.42	1.859	13.56	1.00	1.00	1.00
1.0	5.08	5.00	4.31	4.53	1.951	14.23	1.01	1.02	1.05
2.0	5.05	4.74	4.23	4.43	1.874	13.67	0.96	1.00	1.01
2.5	5.07	4.83	4.34	4.43	1.985	14.48	0.98	1.03	1.07
3.0	5.07	4.45	4.39	4.31	1.895	13.83	0.90	0.98	1.02
3.0	5.04	4.86	4.25	4.38	1.863	13.59	1.00	1.00	1.00
-1.0	5.07	4.75	4.24	4.32	1.832	13.36	0.98	0.99	0.98
-2.0	5.03	4.09	4.41	3.89	1.714	12.50	0.84	0.89	0.92
-2.5	5.02	3.77	4.42	3.60	1.588	11.58	0.77	0.82	0.85
-3.0	5.04	2.93	4.48	2.59	1.161	8.47	0.60	0.59	0.62

NORMALIZED TO THE MAXIMUM OF ISC, IMP, OR PMP WITH ANGLE RESET WITH RESPECT TO ISC

ANGLE VDC (DEG)	ISC (V)	IMP (V)	PMP (V)	ISC (%)	IMP (%)	PMP (%)	NORM ISC	NORM IMP	NORM PMP
0.0	4.98	4.93	4.21	4.42	1.859	13.56	0.99	0.97	0.94
-1.0	4.98	4.93	4.21	4.42	1.859	13.56	0.99	0.97	0.94
0.0	5.08	5.00	4.31	4.53	1.951	14.23	1.00	0.99	0.98
1.0	5.05	4.74	4.23	4.43	1.874	13.67	0.95	0.97	0.94
1.5	5.07	4.83	4.34	4.43	1.985	14.48	0.97	1.00	1.00
2.0	5.07	4.45	4.39	4.31	1.895	13.83	0.89	0.94	0.96
-1.0	5.04	4.86	4.25	4.38	1.863	13.59	0.97	0.96	0.94
-2.0	5.07	4.75	4.24	4.32	1.832	13.36	0.95	0.94	0.92
-3.0	5.03	4.09	4.41	3.89	1.714	12.50	0.82	0.85	0.86
-3.5	5.02	3.77	4.42	3.60	1.588	11.58	0.75	0.79	0.80
-4.0	5.04	2.93	4.48	2.59	1.161	8.47	0.59	0.57	0.58

DATA FOR STRING 1B CORRECTED FOR ALL CONDITIONS INCLUDING CONIC MIRROR QUALITY (REFLECTANCE SET TO .7)

NORMALIZED TO 0 DEGREES FOR ISC, IMP, AND PMP

ANGLE VDC (DEG)	ISC (V)	IMP (V)	PMP (V)	ISC (%)	IMP (%)	PMP (%)	NORM ISC	NORM IMP	NORM PMP
0.0	6.09	4.65	5.21	4.27	2.223	13.51	1.00	1.00	1.00
1.0	6.09	4.56	5.21	4.23	2.203	13.39	0.98	0.99	0.99
2.0	6.07	4.31	5.32	3.78	2.010	12.22	0.93	0.89	0.90
2.5	6.05	4.32	5.40	3.68	1.988	12.08	0.93	0.86	0.89
3.0	6.04	3.50	5.43	2.81	1.598	9.29	0.75	0.66	0.69
0.0	6.11	4.64	5.21	4.27	2.226	13.53	1.00	1.00	1.00
-1.0	6.09	4.70	5.14	4.35	2.238	13.60	1.01	1.02	1.01
-2.0	6.10	4.52	5.18	4.18	2.162	13.14	0.97	0.98	0.97
-2.5	6.13	4.14	5.31	3.87	2.057	12.50	0.89	0.91	0.92
-3.0	6.11	3.20	5.41	2.84	1.538	9.35	0.69	0.67	0.69

NORMALIZED TO THE MAXIMUM OF ISC, IMP, OR PMP WITH ANGLE RESET WITH RESPECT TO ISC

ANGLE VDC (DEG)	ISC (V)	IMP (V)	PMP (V)	ISC (%)	IMP (%)	PMP (%)	NORM ISC	NORM IMP	NORM PMP
0.0	6.09	4.65	5.21	4.27	2.223	13.51	0.99	0.98	0.99
1.0	6.09	4.56	5.21	4.23	2.203	13.39	0.97	0.97	0.98
2.0	6.07	4.31	5.32	3.78	2.010	12.22	0.92	0.87	0.90
3.0	6.05	4.32	5.40	3.68	1.988	12.08	0.92	0.85	0.89
4.0	6.04	3.50	5.43	2.81	1.529	9.29	0.74	0.65	0.68
0.0	6.11	4.64	5.21	4.27	2.226	13.53	0.99	0.98	0.99
-1.0	6.11	4.64	5.21	4.27	2.226	13.53	0.99	0.98	0.99
0.0	6.09	4.70	5.14	4.35	2.238	13.60	1.00	1.00	1.00
-1.0	6.10	4.52	5.18	4.18	2.162	13.14	0.96	0.96	0.97
-1.5	6.13	4.14	5.31	3.87	2.057	12.50	0.88	0.89	0.92
-2.0	6.11	3.20	5.41	2.84	1.538	9.35	0.68	0.65	0.69

DATA FOR STRING 2A CORRECTED FOR ALL CONDITIONS INCLUDING CONIC MIRROR QUALITY (REFLECTANCE SET TO .7)

NORMALIZED TO 0 DEGREES FOR ISC, IMP, AND PMP

ANGLE VDC (DEG)	ISC (V)	IMP (V)	PMP (V)	ISC (%)	IMP (%)	PMP (%)	NORM ISC	NORM IMP	NORM PMP
0.0	6.18	3.77	5.58	3.38	1.888	11.48	1.00	1.00	1.00
1.0	6.18	4.78	5.34	4.44	2.371	14.41	1.27	1.31	1.26
2.0	6.13	5.18	5.25	4.68	2.460	14.95	1.37	1.39	1.30
2.5	6.09	5.11	5.23	4.64	2.427	14.75	1.35	1.37	1.29
3.0	6.09	4.87	5.31	4.44	2.356	14.32	1.29	1.31	1.25
0.0	6.13	3.74	5.55	3.36	1.864	11.33	1.00	1.00	1.00
-1.0	6.08	3.06	5.60	2.71	1.516	9.22	0.82	0.81	0.81
-2.0	6.09	3.59	5.73	3.14	1.770	4.68	0.43	0.40	0.41
-2.5	6.05	0.92	5.65	0.77	0.435	2.64	0.25	0.23	0.23
-3.0	5.95	0.52	5.41	0.42	0.227	1.38	0.14	0.12	0.12

NORMALIZED TO THE MAXIMUM OF ISC, IMP, OR PMP WITH ANGLE RESET WITH RESPECT TO ISC

ANGLE VDC (DEG)	ISC (V)	IMP (V)	PMP (V)	ISC (%)	IMP (%)	PMP (%)	NORM ISC	NORM IMP	NORM PMP
0.0	6.18	3.77	5.58	3.38	1.888	11.48	1.00	1.00	1.00
-1.0	6.18	4.78	5.34	4.44	2.371	14.41	1.00	1.00	1.00
0.0	6.13	4.68	5.25	4.21	2.211	13.44	0.98	0.95	0.93
1.0	6.13	4.68	5.25	4.21	2.211	13.44	0.98	0.95	0.93
1.5	6.09	4.38	5.23	3.98	2.080	12.64	0.92	0.90	0.88
2.0	6.09	4.09	5.31	3.73	1.980	12.03	0.85	0.84	0.84
-1.0	6.13	4.16	5.55	3.73	2.073	12.60	0.87	0.84	0.87
-2.0	6.08	3.64	5.60	3.22	1.804	10.97	0.76	0.73	0.76
-3.0	6.09	1.73	5.73	1.46	0.839	5.10	0.36	0.33	0.35
-3.5	6.05	0.90	5.65	0.76	0.428	2.60	0.19	0.17	0.18
-4.0	5.95	0.47	5.41	0.38	0.208	1.26	0.10	0.09	0.09

DATA FOR STRING 2B CORRECTED FOR ALL CONDITIONS INCLUDING CONIC MIRROR QUALITY (REFLECTANCE SET TO .7)

NORMALIZED TO 0 DEGREES FOR ISC, IMP, AND PMP

ANGLE VDC (DEG)	ISC (V)	IMP (V)	PMP (V)	ISC (%)	IMP (%)	PMP (%)	NORM ISC	NORM IMP	NORM PMP
0.0	6.19	4.87	5.41	4.52	2.447	14.87	1.00	1.00	1.00
1.0	6.17	4.92	5.39	4.56	2.456	14.93	1.01	1.01	1.00
2.0	6.15	4.49	5.50	3.99	2.196	13.35	0.92	0.88	0.90
2.5	6.13	4.34	5.56	3.78	2.101	12.77	0.89	0.84	0.86
3.0	6.10	3.74	5.56	3.32	1.845	11.22	0.77	0.73	0.75
0.0	6.08	4.87	5.31	4.53	2.406	14.62	1.00	1.00	1.00
-1.0	6.06	4.97	5.23	4.66	2.438	14.82	1.02	1.03	1.01
-2.0	6.01	4.85	5.16	4.52	2.332	14.17	0.99	1.00	0.97
-2.5	6.01	4.58	5.30	4.36	2.310	14.04	0.94	0.96	0.96
-3.0	5.95	3.60	5.39	3.30	1.778	10.81	0.74	0.73	0.74

NORMALIZED TO THE MAXIMUM OF ISC, IMP, OR PMP WITH ANGLE RESET WITH RESPECT TO ISC

ANGLE VDC (DEG)	ISC (V)	IMP (V)	PMP (V)	ISC (%)	IMP (%)	PMP (%)	NORM ISC	NORM IMP	NORM PMP
0.0	6.19	4.87	5.41	4.52	2.447	14.87	1.00	1.00	1.00
1.0	6.17	4.92	5.39	4.56	2.456	14.93	0.98	0.97	1.00
2.0	6.15	4.49	5.50	3.99	2.196	13.35	0.99	0.98	1.00
3.0	6.15	4.49	5.50	3.99	2.196	13.35	0.99	0.98	1.00
3.5	6.13	4.34	5.56	3.78	2.101	12.77	0.87	0.81	0.86
4.0	6.10	3.74	5.56	3.32	1.845	11.22	0.75	0.71	0.75
0.0	6.08	4.87	5.31	4.53	2.406	14.62	0.98	0.97	0.97
0.0	6.06	4.97	5.23	4.66	2.438	14.82	1.00	1.00	0.99
-1.0	6.01	4.85	5.16	4.52	2.332	14.17	0.98	0.97	0.95
-1.5	6.01	4.58	5.30	4.36	2.310	14.04	0.92	0.93	0.94
-2.0	5.95	3.60	5.39	3.30	1.778	10.81	0.72	0.71	0.72

FIGURE A8 DATA FROM 15 x 56 PANEL CORRECTED FOR CONIC MIRROR REFLECTANCE OF 0.70

[illegible][illegible]

DATA FOR STRING 2C CORRECTED FOR ALL CONDITIONS INCLUDING CONIC MIRROR QUALITY (REFLECTANCE SET TO .7)														
NORMALIZED TO 0 DEGREES FOR ISC, IMP, AND PMP														
ANGLE VOC	ISC	VMP	IMP	PMP	EFFCY	NORM	ISC	IMP	PMP	EFFCY	NORM	ISC	IMP	PMP
(DEG) (V)	(A)	(V)	(A)	(W)	(%)		(A)	(V)	(A)	(W)	(%)	(A)	(V)	(A)
0.0	5.92	496	4.99	459	2.294	13.94	1.00	1.00	1.00	1.00	1.00	1.00	1.00	1.00
1.0	5.92	472	5.01	438	2.196	13.35	0.95	0.95	0.95	0.95	0.95	0.95	0.95	0.96
2.0	5.93	412	5.15	388	1.977	12.14	0.83	0.84	0.87	0.83	0.84	0.87	0.83	0.87
2.5	5.95	373	5.33	333	1.775	10.79	0.75	0.75	0.72	0.77	0.75	0.72	0.77	0.75
3.0	6.00	272	5.50	229	1.259	7.65	0.55	0.55	0.50	0.55	0.55	0.50	0.55	0.55
3.0	6.08	486	5.16	447	2.305	14.01	1.00	1.00	1.00	1.00	1.00	1.00	1.00	1.00
4.0	6.08	490	5.13	452	2.321	14.11	1.01	1.01	1.01	1.01	1.01	1.01	1.01	1.01
4.2	6.06	447	5.25	412	2.167	13.73	0.92	0.92	0.94	0.92	0.94	0.92	0.94	0.94
4.5	6.05	405	5.39	361	1.947	11.83	0.83	0.83	0.81	0.84	0.83	0.81	0.84	0.84
4.8	6.02	313	5.43	279	1.512	9.19	0.64	0.62	0.66	0.64	0.62	0.66	0.64	0.66
NORMALIZED TO THE MAXIMUM OF ISC,IMP,OR PMP WITH ANGLE RESET WITH RESPECT TO ISC														
ANGLE VOC	ISC	VMP	IMP	PMP	EFFCY	NORM	ISC	IMP	PMP	EFFCY	NORM	ISC	IMP	PMP
(DEG) (V)	(A)	(V)	(A)	(W)	(%)		(A)	(V)	(A)	(W)	(%)	(A)	(V)	(A)
0.0	5.92	496	4.99	459	2.294	13.94	1.00	1.00	1.00	0.99	0.99	1.00	1.00	0.99
1.0	5.92	472	5.01	438	2.196	13.35	0.95	0.95	0.95	0.95	0.95	0.95	0.95	0.95
2.0	5.93	412	5.15	388	1.997	12.14	0.83	0.84	0.86	0.83	0.84	0.86	0.83	0.86
2.5	5.95	373	5.33	333	1.775	10.79	0.75	0.75	0.76	0.75	0.76	0.75	0.76	0.75
3.0	6.00	272	5.50	229	1.259	7.65	0.55	0.50	0.54	0.55	0.50	0.54	0.55	0.50
3.0	6.08	486	5.16	447	2.305	14.01	0.98	0.97	0.99	0.97	0.99	0.98	0.97	0.99
4.0	6.08	490	5.13	452	2.321	14.11	0.99	0.98	1.00	0.99	0.98	1.00	0.99	0.93
4.2	6.06	447	5.25	412	2.167	13.17	0.90	0.90	0.93	0.90	0.93	0.90	0.90	0.84
4.5	6.05	405	5.39	361	1.947	11.83	0.82	0.79	0.84	0.82	0.79	0.84	0.82	0.79
4.8	6.02	313	5.43	279	1.512	9.19	0.63	0.61	0.65	0.63	0.61	0.65	0.63	0.65
DATA FOR STRING 2D CORRECTED FOR ALL CONDITIONS INCLUDING CONIC MIRROR QUALITY (REFLECTANCE SET TO .7)														
NORMALIZED TO 0 DEGREES FOR ISC, IMP, AND PMP														
ANGLE VOC	ISC	VMP	IMP	PMP	EFFCY	NORM	ISC	IMP	PMP	EFFCY	NORM	ISC	IMP	PMP
(DEG) (V)	(A)	(V)	(A)	(W)	(%)		(A)	(V)	(A)	(W)	(%)	(A)	(V)	(A)
0.0	6.08	476	5.14	447	2.298	13.97	1.00	1.00	1.00	1.00	1.00	1.00	1.00	1.00
1.0	6.09	466	5.19	432	2.245	13.65	0.98	0.97	0.98	0.97	0.98	0.97	0.97	0.98
2.0	6.07	405	5.42	353	1.915	11.64	0.85	0.79	0.83	1.915	11.64	0.85	0.79	0.83
2.5	6.06	354	5.53	300	1.660	10.09	0.74	0.67	0.72	1.660	10.09	0.74	0.67	0.72
3.0	6.01	257	5.58	212	1.181	7.18	0.54	0.47	0.51	1.181	7.18	0.54	0.47	0.51
3.0	6.14	474	5.20	445	2.314	14.06	1.00	1.00	1.00	1.00	1.00	1.00	1.00	1.00
4.0	6.12	465	5.14	432	2.220	13.48	0.98	0.97	0.96	2.220	13.48	0.98	0.97	0.96
-1.0	6.08	410	5.25	391	2.053	12.48	0.87	0.88	0.89	2.053	12.48	0.87	0.88	0.89
-2.0	6.06	389	5.21	370	1.931	11.74	0.82	0.83	0.83	1.931	11.74	0.82	0.83	0.83
-2.5	6.06	389	5.21	370	1.931	11.74	0.82	0.83	0.83	1.931	11.74	0.82	0.83	0.83
-3.0	6.03	300	5.42	266	1.438	8.74	0.63	0.60	0.62	1.438	8.74	0.63	0.60	0.62
NORMALIZED TO THE MAXIMUM OF ISC,IMP,OR PMP WITH ANGLE RESET WITH RESPECT TO ISC														
ANGLE VOC	ISC	VMP	IMP	PMP	EFFCY	NORM	ISC	IMP	PMP	EFFCY	NORM	ISC	IMP	PMP
(DEG) (V)	(A)	(V)	(A)	(W)	(%)		(A)	(V)	(A)	(W)	(%)	(A)	(V)	(A)
0.0	6.08	476	5.14	447	2.298	13.97	1.00	1.00	1.00	0.99	0.99	1.00	1.00	0.99
1.0	6.09	466	5.19	432	2.245	13.65	0.98	0.97	0.97	0.97	0.98	0.97	0.97	0.97
2.0	6.07	405	5.42	353	1.915	11.64	0.85	0.79	0.83	1.915	11.64	0.85	0.79	0.83
2.5	6.06	354	5.53	300	1.660	10.09	0.74	0.67	0.72	1.660	10.09	0.74	0.67	0.72
3.0	6.01	257	5.58	212	1.181	7.18	0.54	0.47	0.51	1.181	7.18	0.54	0.47	0.51
3.0	6.14	474	5.20	445	2.314	14.06	1.00	1.00	1.00	1.00	1.00	1.00	1.00	1.00
4.0	6.12	465	5.14	432	2.220	13.48	0.98	0.97	0.96	2.220	13.48	0.98	0.97	0.96
-1.0	6.08	410	5.25	391	2.053	12.48	0.87	0.88	0.89	2.053	12.48	0.87	0.88	0.89
-2.0	6.06	389	5.21	370	1.931	11.74	0.82	0.83	0.83	1.931	11.74	0.82	0.83	0.83
-2.5	6.06	389	5.21	370	1.931	11.74	0.82	0.83	0.83	1.931	11.74	0.82	0.83	0.83
-3.0	6.03	300	5.42	266	1.438	8.74	0.63	0.60	0.62	1.438	8.74	0.63	0.60	0.62
NORMALIZED TO THE MAXIMUM OF ISC,IMP,OR PMP WITH ANGLE RESET WITH RESPECT TO ISC														
ANGLE VOC	ISC	VMP	IMP	PMP	EFFCY	NORM	ISC	IMP	PMP	EFFCY	NORM	ISC	IMP	PMP
(DEG) (V)	(A)	(V)	(A)	(W)	(%)		(A)	(V)	(A)	(W)	(%)	(A)	(V)	(A)
0.0	6.08	476	5.14	447	2.298	13.97	1.00	1.00	1.00	0.99	0.99	1.00	1.00	0.99
1.0	6.09	466	5.19	432	2.245	13.65	0.98	0.97	0.97	0.97	0.98	0.97	0.97	0.97
2.0	6.07	405	5.42	353	1.915	11.64	0.85	0.79	0.83	1.915	11.64	0.85	0.79	0.83
2.5	6.06	354	5.53	300	1.660	10.09	0.74	0.67	0.72	1.660	10.09	0.74	0.67	0.72
3.0	6.01	257	5.58	212	1.181	7.18	0.54	0.47	0.51	1.181	7.18	0.54	0.47	0.51
3.0	6.14	474	5.20	445	2.314	14.06	1.00	1.00	1.00	1.00	1.00	1.00	1.00	1.00
4.0	6.12	465	5.14	432	2.220	13.48	0.98	0.97	0.96	2.220	13.48	0.98	0.97	0.96
-1.0	6.08	410	5.25	391	2.053	12.48	0.87	0.88	0.89	2.053	12.48	0.87	0.88	0.89
-2.0	6.06	389	5.21	370	1.931	11.74	0.82	0.83	0.83	1.931	11.74	0.82	0.83	0.83
-2.5	6.06	389	5.21	370	1.931	11.74	0.82	0.83	0.83	1.931	11.74	0.82	0.83	0.83
-3.0	6.03	300	5.42	266	1.438	8.74	0.63	0.60	0.62	1.438	8.74	0.63	0.60	0.62
NORMALIZED TO THE MAXIMUM OF ISC,IMP,OR PMP WITH ANGLE RESET WITH RESPECT TO ISC														
ANGLE VOC	ISC	VMP	IMP	PMP	EFFCY	NORM	ISC	IMP	PMP	EFFCY	NORM	ISC	IMP	PMP
(DEG) (V)	(A)	(V)	(A)	(W)	(%)		(A)	(V)	(A)	(W)	(%)	(A)	(V)	(A)
0.0	6.08	476	5.14	447	2.298	13.97	1.00	1.00	1.00	0.99	0.99	1.00	1.00	0.99
1.0	6.09	466	5.19	432	2.245	13.65	0.98	0.97	0.97	0.97	0.98	0.97	0.97	0.97
2.0	6.07	405	5.42	353	1.915	11.64	0.85	0.79	0.83	1.915	11.64	0.85	0.79	0.83
2.5	6.06	354	5.53	300	1.660	10.09	0.74	0.67	0.72	1.660	10.09	0.74	0.67	0.72
3.0	6.01	257	5.58	212	1.181	7.18	0.54	0.47	0.51	1.181	7.18	0.54	0.47	0.51
3.0	6.14	474	5.20	445	2.314	14.06	1.00	1.00	1.00	1.00	1.00	1.00	1.00	1.00
4.0	6.12	465	5.14	432	2.220	13.48	0.98	0.97	0.96	2.220	13.48	0.98	0.97	0.96
-1.0	6.08	410	5.25	391	2.053	12.48	0.87	0.88	0.89	2.053	12.48	0.87	0.88	0.89
-2.0	6.06	389	5.21	370	1.931	11.74	0.82	0.83	0.83	1.931	11.74	0.82	0.83	0.83
-2.5	6.06	389	5.21	370	1.931	11.74	0.82	0.83	0.83	1.931	11.74	0.82	0.83	0.83
-3.0	6.03	300	5.42	266	1.438	8.74	0.63	0.60	0.62	1.438	8.74	0.63	0.60	0.62
NORMALIZED TO THE MAXIMUM OF ISC,IMP,OR PMP WITH ANGLE RESET WITH RESPECT TO ISC														
ANGLE VOC	ISC	VMP	IMP	PMP	EFFCY	NORM	ISC	IMP	PMP	EFFCY	NORM	ISC	IMP	PMP
(DEG) (V)	(A)	(V)	(A)	(W)	(%)		(A)	(V)	(A)	(W)	(%)	(A)	(V)	(A)
0.0	6.08	476	5.14	447	2.298	13.97	1.00	1.00	1.00	0.99	0.99	1.00	1.00	0.99
1.0	6.09	466	5.19	432	2.245	13.65	0.98	0.97	0.97	0.97	0.98	0.97	0.97	0.97
2.0	6.07	405	5.42	353	1.915	11.64	0.85	0.79	0.83	1.915	11.64	0.85	0.79	0.83
2.5	6.06	354	5.53	300	1.660	10.09	0.74	0.67	0.72	1.660	10.09	0.74	0.67	0.72
3.0	6.01	257	5.58	212	1.181	7.18	0.54	0.47	0.51	1.181	7.18	0.54	0.47	0.51
3.0	6.14	474	5.20	445	2.314	14.06	1.00	1.00	1.00	1.00	1.00	1.00	1.00	1.00
4.0	6.12	465	5.14	432	2.220	13.48	0.98	0.97	0.96	2.220	13.48	0.98	0.97	0.96
-1.0	6.08	410	5.25	391	2.053	12.48	0.87	0.88	0.89	2.053	12.48	0.87	0.88	0.89
-2.0	6.06	389	5.21	370	1.931	11.74	0.82	0.83	0.83	1.931	11.74	0.82	0.83	0.83
-2.5	6.06	389	5.21	370	1.931	11.74	0.82	0.83	0.83	1.931	11.74	0.82	0.83	0.83
-3.0	6.03	300	5.42	266	1.438	8.74	0.63	0.60	0.62	1.438	8.74	0.63	0.60	0.62
NORMALIZED TO THE MAXIMUM OF ISC,IMP,OR PMP WITH ANGLE RESET WITH RESPECT TO ISC														
ANGLE VOC	ISC	VMP	IMP	PMP	EFFCY	NORM	ISC	IMP	PMP	EFFCY	NORM	ISC	IMP	PMP
(DEG) (V)	(A)	(V)	(A)	(W)	(%)		(A)	(V)	(A)	(W)	(%)	(A)	(V)	(A)
0.0	6.08	476	5.14	447	2.298	13.97	1.00	1						

*DATA FOR STRING 2D CORRECTED FOR ALL CONDITIONS INCLUDING											
*CONIC MIRROR QUALITY (REFLECTANCE SET TO .7)											
*NORMALIZED TO 0 DEGREES FOR ISC, IMP, AND PMP											
NORMALIZED TO THE MAXIMUM OF ISC,IMP,OR PMP WITH ANGLE RESET											
WITH RESPECT TO ISC											
ANGLE VOC	ISC	VMP	IMP	PMP	EFFCY	NORM	ISC	IMP	PMP	EFFCY	NORM
(DEG) (V)	(A)	(V)	(A)	(W)	(%)	(A)	(A)	(W)	(%)	(A)	(A)
0.0	6.08	.476	5.14	4.47	2.298	13.97	1.00	1.00	1.00	1.00	1.00
1.0	6.09	.466	5.19	.432	2.245	13.65	0.98	0.97	0.98	0.97	0.98
2.0	6.07	.405	5.42	.353	1.915	11.64	0.85	0.79	0.83	0.79	0.83
2.5	6.06	.354	5.53	.300	1.660	10.09	0.74	0.67	0.72	0.67	0.72
3.0	6.01	.257	5.58	.212	1.181	7.18	0.54	0.47	0.51	0.47	0.51
4.0	6.14	.474	5.20	.445	2.314	14.06	1.00	1.00	1.00	1.00	1.00
-1.0	6.12	.465	5.14	.432	2.220	13.49	0.98	0.97	0.96	0.97	0.96
-2.0	6.08	.410	5.25	.391	2.053	12.48	0.87	0.88	0.83	0.88	0.83
-2.5	6.06	.389	5.21	.370	1.931	11.74	0.82	0.83	0.79	0.83	0.79
-3.0	6.03	.300	5.42	.266	1.438	8.74	0.63	0.60	0.62	0.60	0.62
NORMALIZED TO THE MAXIMUM OF ISC,IMP,OR PMP WITH ANGLE RESET											
WITH RESPECT TO ISC											
ANGLE VOC	ISC	VMP	IMP	PMP	EFFCY	NORM	ISC	IMP	PMP	EFFCY	NORM
(DEG) (V)	(A)	(V)	(A)	(W)	(%)	(A)	(A)	(W)	(%)	(A)	(A)
0.0	6.08	.476	5.14	4.47	2.298	13.97	1.00	1.00	0.99	0.99	0.99
1.0	6.09	.466	5.19	.432	2.245	13.65	0.98	0.97	0.97	0.97	0.97
2.0	6.07	.405	5.42	.353	1.915	11.64	0.85	0.79	0.83	0.79	0.83
2.5	6.06	.354	5.53	.300	1.660	10.09	0.74	0.67	0.72	0.67	0.72
3.0	6.01	.257	5.58	.212	1.181	7.18	0.54	0.47	0.51	0.47	0.51
4.0	6.14	.474	5.20	.445	2.314	14.06	1.00	1.00	1.00	1.00	1.00
-1.0	6.12	.465	5.14	.432	2.220	13.49	0.98	0.97	0.96	0.97	0.96
-2.0	6.08	.410	5.25	.391	2.053	12.48	0.86	0.87	0.89	0.87	0.89
-2.5	6.06	.389	5.21	.370	1.931	11.74	0.82	0.83	0.83	0.83	0.83
-3.0	6.03	.300	5.42	.266	1.438	8.74	0.63	0.59	0.62	0.59	0.62

FIGURE A8 (CONTINUED)

ORIGINAL PAGE IS
OF POOR QUALITY

ORIGINAL PAGE IS OF POOR QUALITY

DATA FOR STRING 4A CORRECTED FOR ALL CONDITIONS INCLUDING CONIC MIRROR QUALITY (REFLECTANCE SET TO .7) NORMALIZED TO 0 DEGREES FOR ISC, IMP, AND PMP

ANGLE VDC (DEG)	ISC (V)	IMP (A)	PMP (W)	ISC (%)	IMP (%)	PMP (%)	NORM ISC	NORM IMP	NORM PMP
0.0	5.86	466	4.88	412	2.010	12.22	1.00	1.00	1.00
1.0	5.84	451	4.84	407	1.972	11.99	0.97	0.99	0.98
2.0	5.84	392	4.99	371	1.850	11.24	0.84	0.90	0.92
2.5	5.82	288	5.23	268	1.403	8.53	0.62	0.65	0.70
3.0	5.79	222	5.28	205	1.083	6.58	0.48	0.50	0.54
0.0	5.84	466	4.88	409	1.994	12.12	1.00	1.00	1.00
-1.0	5.78	438	4.78	399	1.904	11.57	0.94	0.97	0.95
-2.0	5.81	401	4.82	376	1.813	11.02	0.86	0.92	0.91
-2.5	5.77	346	4.84	329	1.591	9.67	0.74	0.80	0.80
-3.0	5.72	230	4.94	223	1.102	6.70	0.49	0.55	0.55

NORMALIZED TO THE MAXIMUM OF ISC, IMP, OR PMP WITH ANGLE RESET WITH RESPECT TO ISC

ANGLE VDC (DEG)	ISC (V)	IMP (A)	PMP (W)	ISC (%)	IMP (%)	PMP (%)	NORM ISC	NORM IMP	NORM PMP
0.0	5.86	466	4.88	412	2.010	12.22	1.00	1.00	1.00
1.0	5.84	451	4.84	407	1.972	11.99	0.97	0.99	0.98
2.0	5.84	392	4.99	371	1.850	11.24	0.84	0.90	0.92
2.5	5.82	288	5.23	268	1.403	8.53	0.62	0.65	0.70
3.0	5.79	222	5.28	205	1.083	6.58	0.48	0.50	0.54
0.0	5.84	466	4.88	409	1.994	12.12	1.00	0.99	0.99
-1.0	5.78	438	4.78	399	1.904	11.57	0.94	0.97	0.95
-2.0	5.81	401	4.82	376	1.813	11.02	0.86	0.91	0.90
-2.5	5.77	346	4.84	329	1.591	9.67	0.74	0.80	0.79
-3.0	5.72	230	4.94	223	1.102	6.70	0.49	0.54	0.55

DATA FOR STRING 4B CORRECTED FOR ALL CONDITIONS INCLUDING CONIC MIRROR QUALITY (REFLECTANCE SET TO .7) NORMALIZED TO 0 DEGREES FOR ISC, IMP, AND PMP

ANGLE VDC (DEG)	ISC (V)	IMP (A)	PMP (W)	ISC (%)	IMP (%)	PMP (%)	NORM ISC	NORM IMP	NORM PMP
0.0	6.15	458	4.92	388	1.907	11.59	1.00	1.00	1.00
1.0	6.09	470	4.83	378	1.825	11.09	1.03	0.97	0.96
2.0	6.01	429	4.80	385	1.849	11.24	0.94	0.99	0.97
2.5	6.02	416	4.90	379	1.859	11.30	0.91	0.98	0.97
3.0	5.99	383	5.02	351	1.759	10.69	0.84	0.90	0.92
0.0	6.08	454	4.92	388	1.909	11.61	1.00	1.00	1.00
-1.0	6.10	425	5.15	396	2.040	12.40	0.93	1.02	1.07
-2.0	6.10	337	5.48	305	1.675	10.18	0.74	0.79	0.88
-2.5	6.11	286	5.58	257	1.431	8.70	0.63	0.66	0.75
-3.0	6.11	215	5.67	189	1.069	6.50	0.47	0.49	0.56

NORMALIZED TO THE MAXIMUM OF ISC, IMP, OR PMP WITH ANGLE RESET WITH RESPECT TO ISC

ANGLE VDC (DEG)	ISC (V)	IMP (A)	PMP (W)	ISC (%)	IMP (%)	PMP (%)	NORM ISC	NORM IMP	NORM PMP
0.0	6.15	458	4.92	388	1.907	11.59	1.00	1.00	1.00
1.0	6.09	470	4.83	378	1.825	11.09	1.03	0.97	0.96
2.0	6.01	429	4.80	385	1.849	11.24	0.94	0.99	0.97
2.5	6.02	416	4.90	379	1.859	11.30	0.91	0.98	0.97
3.0	5.99	383	5.02	351	1.759	10.69	0.84	0.90	0.92
0.0	6.08	454	4.92	388	1.909	11.61	1.00	1.00	1.00
-1.0	6.10	425	5.15	396	2.040	12.40	0.93	1.02	1.07
-2.0	6.10	337	5.48	305	1.675	10.18	0.74	0.79	0.88
-2.5	6.11	286	5.58	257	1.431	8.70	0.63	0.66	0.75
-3.0	6.11	215	5.67	189	1.069	6.50	0.47	0.49	0.56

DATA FOR STRING 4C CORRECTED FOR ALL CONDITIONS INCLUDING CONIC MIRROR QUALITY (REFLECTANCE SET TO .7) NORMALIZED TO 0 DEGREES FOR ISC, IMP, AND PMP

ANGLE VDC (DEG)	ISC (V)	IMP (A)	PMP (W)	ISC (%)	IMP (%)	PMP (%)	NORM ISC	NORM IMP	NORM PMP
0.0	6.18	430	5.62	388	2.180	13.25	1.00	1.00	1.00
1.0	6.17	474	5.43	441	2.396	14.56	1.10	1.14	1.10
2.0	6.16	464	5.40	436	2.354	14.31	1.08	1.12	1.08
2.5	6.13	438	5.39	421	2.267	13.78	1.02	1.08	1.04
3.0	6.12	394	5.48	382	2.092	12.71	0.92	0.98	0.96
0.0	6.11	421	5.57	382	2.125	12.92	1.00	1.00	1.00
-1.0	6.11	328	5.64	294	1.657	10.07	0.78	0.77	0.78
-2.0	6.14	268	5.67	236	1.338	8.13	0.64	0.62	0.63
-2.5	6.14	242	5.68	211	1.201	7.30	0.57	0.55	0.57
-3.0	6.12	208	5.63	182	1.024	6.23	0.49	0.48	0.48

NORMALIZED TO THE MAXIMUM OF ISC, IMP, OR PMP WITH ANGLE RESET WITH RESPECT TO ISC

ANGLE VDC (DEG)	ISC (V)	IMP (A)	PMP (W)	ISC (%)	IMP (%)	PMP (%)	NORM ISC	NORM IMP	NORM PMP
0.0	6.18	430	5.62	388	2.180	13.25	1.00	1.00	1.00
1.0	6.17	474	5.43	441	2.396	14.56	1.10	1.14	1.10
2.0	6.16	464	5.40	436	2.354	14.31	1.08	1.12	1.08
2.5	6.13	438	5.39	421	2.267	13.78	1.02	1.08	1.04
3.0	6.12	394	5.48	382	2.092	12.71	0.92	0.98	0.96
0.0	6.11	421	5.57	382	2.125	12.92	1.00	1.00	1.00
-1.0	6.11	328	5.64	294	1.657	10.07	0.78	0.77	0.78
-2.0	6.14	268	5.67	236	1.338	8.13	0.64	0.62	0.63
-2.5	6.14	242	5.68	211	1.201	7.30	0.57	0.55	0.57
-3.0	6.12	208	5.63	182	1.024	6.23	0.49	0.48	0.48

DATA FOR STRING 4D CORRECTED FOR ALL CONDITIONS INCLUDING CONIC MIRROR QUALITY (REFLECTANCE SET TO .7) NORMALIZED TO 0 DEGREES FOR ISC, IMP, AND PMP

ANGLE VDC (DEG)	ISC (V)	IMP (A)	PMP (W)	ISC (%)	IMP (%)	PMP (%)	NORM ISC	NORM IMP	NORM PMP
0.0	6.20	470	5.40	451	2.434	14.79	1.00	1.00	1.00
1.0	6.24	473	5.42	449	2.434	14.80	1.01	1.00	1.00
2.0	6.17	408	5.53	383	2.122	12.90	0.87	0.85	0.87
2.5	6.12	383	5.56	357	1.985	12.06	0.81	0.79	0.82
3.0	6.09	349	5.54	326	1.806	10.98	0.74	0.72	0.74
0.0	6.17	454	5.37	432	2.319	14.10	1.00	1.00	1.00
-1.0	6.17	441	5.38	418	2.232	13.69	0.97	0.97	0.97
-2.0	6.15	376	5.51	345	1.902	11.56	0.83	0.80	0.82
-2.5	6.14	323	5.53	311	1.717	10.44	0.71	0.72	0.74
-3.0	6.12	218	5.68	195	1.109	6.74	0.48	0.45	0.48

NORMALIZED TO THE MAXIMUM OF ISC, IMP, OR PMP WITH ANGLE RESET WITH RESPECT TO ISC

ANGLE VDC (DEG)	ISC (V)	IMP (A)	PMP (W)	ISC (%)	IMP (%)	PMP (%)	NORM ISC	NORM IMP	NORM PMP
0.0	6.20	470	5.40	451	2.434	14.79	1.00	1.00	1.00
1.0	6.24	473	5.42	449	2.434	14.80	1.01	1.00	1.00
2.0	6.17	408	5.53	383	2.122	12.90	0.87	0.85	0.87
2.5	6.12	383	5.56	357	1.985	12.06	0.81	0.79	0.82
3.0	6.09	349	5.54	326	1.806	10.98	0.74	0.72	0.74
0.0	6.17	454	5.37	432	2.319	14.10	1.00	1.00	1.00
-1.0	6.17	441	5.38	418	2.232	13.69	0.97	0.97	0.97
-2.0	6.15	376	5.51	345	1.902	11.56	0.83	0.80	0.82
-2.5	6.14	323	5.53	311	1.717	10.44	0.71	0.72	0.74
-3.0	6.12	218	5.68	195	1.109	6.74	0.48	0.45	0.48

DATA FOR STRING 5A CORRECTED FOR ALL CONDITIONS INCLUDING CONIC MIRROR QUALITY (REFLECTANCE SET TO .7) NORMALIZED TO 0 DEGREES FOR ISC, IMP, AND PMP

ANGLE VDC (DEG)	ISC (V)	IMP (A)	PMP (W)	ISC (%)	IMP (%)	PMP (%)	NORM ISC	NORM IMP	NORM PMP
0.0	6.33	467	5.23	422	2.506	13.41	1.00	1.00	1.00
1.0	6.29	488	5.19	450	2.337	14.20	1.04	1.07	1.06
2.0	6.25	452	5.22	418	2.182	13.26	0.97	0.99	0.99
2.5	6.25	421	5.29	398	2.104	12.79	0.90	0.94	0.95
3.0	6.23	383	5.43	358	1.944	11.82	0.82	0.85	0.88
0.0	6.24	467	5.19	417	2.162	13.14	1.00	1.00	1.00
-1.0	6.13	424	5.38	334	1.734	10.54	0.78	0.80	0.80
-2.0	6.12	362	5.19	282	1.588	9.61	0.68	0.70	0.70
-2.5	6.05	188	5.26	163	1.088	6.61	0.48	0.48	0.50
-3.0	5.95	145	4.92	126	0.859	5.22	0.39	0.39	0.40

NORMALIZED TO THE MAXIMUM OF ISC, IMP, OR PMP WITH ANGLE RESET WITH RESPECT TO ISC

ANGLE VDC (DEG)	ISC (V)	IMP (A)	PMP (W)	ISC (%)	IMP (%)	PMP (%)	NORM ISC	NORM IMP	NORM PMP
0.0	6.33	467	5.23	422	2.506	13.41	1.00	1.00	1.00
1.0	6.29	488	5.19	450	2.337	14.20	1.04	1.07	1.06
2.0	6.25	452	5.22	418	2.182	13.26	0.97	0.99	0.99
2.5	6.25	421	5.29	398	2.104	12.79	0.90	0.94	0.95
3.0	6.23	383	5.43	358	1.944	11.82	0.82	0.85	0.88
0.0	6.24	467	5.19	417	2.162	13.14	1.00	1.00	1.00
-1.0	6.13	424	5.38	334	1.734	10.54	0.78	0.80	0.80
-2.0	6.12	362	5.19	282	1.588	9.61	0.68	0.70	0.70
-2.5	6.05	188	5.26	163	1.088	6.61	0.48	0.48	0.50
-3.0	5.95	145	4.92	126	0.859	5.22	0.39	0.39	0.40

ANGLE (DEG)	VOC	ISC (V)	VMP (V)	IMP (A)	PMP (W)	EFFCY (%)	NORM ISC	NORM IMP	NORM PMP
0.0	6.33	.482	5.23	.435	2.275	13.83	1.00	1.00	1.00
1.0	6.29	.473	5.19	.437	2.266	13.77	0.98	1.00	1.00
2.0	6.25	.419	5.22	.358	2.023	12.29	0.87	0.89	0.89
2.5	6.25	.381	5.29	.359	1.900	11.55	0.79	0.82	0.84
3.0	6.23	.347	5.43	.325	1.763	10.71	0.72	0.74	0.77
0.0	6.24	.481	5.19	.430	2.230	13.55	1.00	0.98	0.98
-1.0	6.22	.391	5.19	.360	1.871	11.37	0.81	0.82	0.82
-2.0	6.13	.247	5.28	.223	1.200	7.30	0.51	0.51	0.53
-2.5	6.05	.189	5.35	.171	0.898	5.46	0.39	0.39	0.39
-3.0	5.95	.143	4.92	.124	0.612	3.72	0.30	0.28	0.27

ORIGINAL PAGE IS OF POOR QUALITY

DATA FOR STRING 5C CORRECTED FOR ALL CONDITIONS INCLUDING
CONIC MIRROR QUALITY (REFLECTANCE SET TO .7)
NORMALIZED TO 0 DEGREES FOR ISC, IMP, AND PMP

ANGLE (DEG)	ISC (V)	IMP (V)	PMP (V)	ISC (%)	IMP (%)	PMP (%)	NORM ISC	NORM IMP	NORM PMP
0.0	5.96	4.30	5.24	399	2.089	12.70	1.00	1.00	1.00
1.0	5.97	4.45	5.23	411	2.148	13.06	1.04	1.03	1.03
2.0	5.96	4.30	5.23	404	2.117	12.87	1.00	1.01	1.01
2.5	6.02	3.96	5.34	373	1.996	12.13	0.92	0.94	0.96
3.0	5.97	3.48	5.35	333	1.782	10.83	0.81	0.83	0.85
0.0	5.95	4.29	5.24	366	2.095	12.73	1.00	1.00	1.00
-1.0	5.94	4.07	5.21	386	2.008	12.21	0.95	0.97	0.96
-2.0	5.90	2.98	5.40	279	1.506	9.75	0.69	0.70	0.72
-2.5	5.90	2.52	5.40	234	1.261	7.67	0.59	0.58	0.60
-3.0	5.91	1.80	5.37	168	0.900	5.47	0.42	0.42	0.43

NORMALIZED TO THE MAXIMUM OF ISC, IMP, OR PMP WITH ANGLE RESET WITH RESPECT TO ISC

ANGLE (DEG)	ISC (V)	IMP (V)	PMP (V)	ISC (%)	IMP (%)	PMP (%)	NORM ISC	NORM IMP	NORM PMP
0.0	5.96	4.43	5.24	411	2.154	13.09	1.00	0.99	0.99
1.0	5.97	4.32	5.23	398	2.083	12.66	0.98	0.96	0.96
2.0	5.96	3.99	5.23	375	1.962	11.93	0.90	0.90	0.91
2.5	6.02	3.58	5.34	337	1.803	10.96	0.81	0.81	0.83
3.0	5.97	3.15	5.35	302	1.615	9.82	0.71	0.73	0.75
0.0	5.95	4.43	5.24	412	2.160	13.13	1.00	0.99	1.00
-1.0	5.94	4.39	5.21	416	2.166	13.16	0.99	1.00	1.00
-2.0	5.92	3.23	5.40	307	1.661	10.10	0.74	0.74	0.77
-2.5	5.90	2.69	5.40	244	1.319	8.02	0.59	0.59	0.61
-3.0	5.91	1.78	5.37	166	0.889	5.40	0.40	0.40	0.41

DATA FOR STRING 5D CORRECTED FOR ALL CONDITIONS INCLUDING
CONIC MIRROR QUALITY (REFLECTANCE SET TO .7)
NORMALIZED TO 0 DEGREES FOR ISC, IMP, AND PMP

ANGLE (DEG)	ISC (V)	IMP (V)	PMP (V)	ISC (%)	IMP (%)	PMP (%)	NORM ISC	NORM IMP	NORM PMP
0.0	5.83	4.52	4.88	381	1.861	11.31	1.00	1.00	1.00
1.0	5.84	4.10	4.90	349	1.710	10.39	0.91	0.92	0.92
2.0	5.78	3.45	4.80	299	1.434	8.72	0.76	0.78	0.77
2.5	5.74	2.97	4.76	249	1.185	7.20	0.65	0.66	0.64
3.0	5.73	3.10	4.75	259	1.231	7.48	0.69	0.68	0.66
0.0	5.89	4.46	4.92	379	1.863	11.32	1.00	1.00	1.00
-1.0	5.86	4.57	4.89	399	1.951	11.86	1.02	1.05	1.05
-2.0	5.88	3.92	4.90	367	1.799	10.94	0.88	0.97	0.97
-2.5	5.83	3.58	4.92	339	1.667	10.13	0.80	0.90	0.89
-3.0	5.81	3.05	5.03	290	1.460	8.88	0.68	0.77	0.78

NORMALIZED TO THE MAXIMUM OF ISC, IMP, OR PMP WITH ANGLE RESET WITH RESPECT TO ISC

ANGLE (DEG)	ISC (V)	IMP (V)	PMP (V)	ISC (%)	IMP (%)	PMP (%)	NORM ISC	NORM IMP	NORM PMP
0.0	5.83	4.52	4.88	381	1.861	11.31	0.99	0.95	0.95
1.0	5.84	4.10	4.90	349	1.710	10.39	0.90	0.87	0.88
2.0	5.78	3.45	4.80	299	1.434	8.72	0.76	0.75	0.73
2.5	5.74	2.97	4.76	249	1.185	7.20	0.65	0.62	0.61
3.0	5.73	3.10	4.75	259	1.231	7.48	0.68	0.65	0.63
0.0	5.89	4.46	4.92	379	1.863	11.32	0.98	0.95	0.95
-1.0	5.89	4.46	4.92	379	1.863	11.32	0.98	0.95	0.95
-2.0	5.86	4.57	4.89	399	1.951	11.86	1.00	1.00	1.00
-2.5	5.83	3.58	4.92	339	1.667	10.13	0.80	0.90	0.89
-3.0	5.81	3.05	5.03	290	1.460	8.88	0.68	0.77	0.78

DATA FOR STRING 6A CORRECTED FOR ALL CONDITIONS INCLUDING
CONIC MIRROR QUALITY (REFLECTANCE SET TO .7)
NORMALIZED TO 0 DEGREES FOR ISC, IMP, AND PMP

ANGLE (DEG)	ISC (V)	IMP (V)	PMP (V)	ISC (%)	IMP (%)	PMP (%)	NORM ISC	NORM IMP	NORM PMP
0.0	5.90	4.27	5.02	401	2.010	12.22	1.00	1.00	1.00
1.0	5.86	3.67	4.97	352	1.753	10.66	0.86	0.88	0.87
2.0	5.90	3.12	5.05	300	1.514	9.20	0.73	0.75	0.75
2.5	5.90	2.54	5.18	243	1.257	7.64	0.59	0.61	0.63
3.0	5.83	1.67	5.13	160	0.822	5.00	0.39	0.40	0.41
0.0	6.03	4.23	5.14	397	2.041	12.41	1.00	1.00	1.00
-1.0	6.02	4.18	5.22	392	2.042	12.41	0.99	0.99	1.00
-2.0	5.97	3.44	5.38	320	1.721	10.46	0.81	0.81	0.84
-2.5	5.92	3.29	5.31	305	1.622	9.86	0.78	0.77	0.79
-3.0	5.92	2.80	5.39	254	1.369	8.32	0.66	0.64	0.67

NORMALIZED TO THE MAXIMUM OF ISC, IMP, OR PMP WITH ANGLE RESET WITH RESPECT TO ISC

ANGLE (DEG)	ISC (V)	IMP (V)	PMP (V)	ISC (%)	IMP (%)	PMP (%)	NORM ISC	NORM IMP	NORM PMP
0.0	5.90	4.27	5.02	401	2.010	12.22	1.00	1.00	0.98
1.0	5.86	3.67	4.97	352	1.753	10.66	0.86	0.88	0.86
2.0	5.90	3.12	5.05	300	1.514	9.20	0.73	0.75	0.74
2.5	5.90	2.54	5.18	243	1.257	7.64	0.59	0.61	0.62
3.0	5.83	1.67	5.13	160	0.822	5.00	0.39	0.40	0.40
0.0	6.03	4.23	5.14	397	2.041	12.41	0.99	0.99	1.00
-1.0	6.02	4.18	5.22	392	2.042	12.41	0.99	0.99	1.00
-2.0	5.97	3.44	5.38	320	1.721	10.46	0.80	0.80	0.84
-2.5	5.92	3.29	5.31	305	1.622	9.86	0.77	0.76	0.79
-3.0	5.92	2.80	5.39	254	1.369	8.32	0.66	0.63	0.67

DATA FOR STRING 6B CORRECTED FOR ALL CONDITIONS INCLUDING
CONIC MIRROR QUALITY (REFLECTANCE SET TO .7)
NORMALIZED TO 0 DEGREES FOR ISC, IMP, AND PMP

ANGLE (DEG)	ISC (V)	IMP (V)	PMP (V)	ISC (%)	IMP (%)	PMP (%)	NORM ISC	NORM IMP	NORM PMP
0.0	5.76	4.43	4.68	394	1.843	11.20	1.00	1.00	1.00
1.0	5.73	3.86	4.70	361	1.698	10.32	0.87	0.92	0.92
2.0	5.78	2.96	4.99	283	1.410	8.57	0.67	0.72	0.77
2.5	5.71	2.44	5.06	231	1.168	7.10	0.55	0.59	0.63
3.0	5.63	1.72	5.09	162	0.822	4.99	0.39	0.41	0.45
0.0	5.81	4.38	4.72	392	1.851	11.25	1.00	1.00	1.00
-1.0	5.79	4.48	4.73	394	1.866	11.34	1.02	1.01	1.01
-2.0	5.74	3.93	4.67	358	1.670	10.15	0.90	0.91	0.90
-2.5	5.73	3.33	4.72	319	1.506	9.15	0.76	0.81	0.81
-3.0	5.69	2.84	4.88	273	1.330	8.09	0.65	0.70	0.72

NORMALIZED TO THE MAXIMUM OF ISC, IMP, OR PMP WITH ANGLE RESET WITH RESPECT TO ISC

ANGLE (DEG)	ISC (V)	IMP (V)	PMP (V)	ISC (%)	IMP (%)	PMP (%)	NORM ISC	NORM IMP	NORM PMP
0.0	5.76	4.43	4.68	394	1.843	11.20	0.99	1.00	0.99
1.0	5.73	3.86	4.70	361	1.698	10.32	0.86	0.92	0.91
2.0	5.78	2.96	4.99	283	1.410	8.57	0.66	0.72	0.76
2.5	5.71	2.44	5.06	231	1.168	7.10	0.54	0.59	0.63
3.0	5.63	1.72	5.09	162	0.822	4.99	0.38	0.41	0.44
0.0	5.81	4.38	4.72	392	1.851	11.25	0.98	0.99	0.99
-1.0	5.81	4.38	4.72	392	1.851	11.25	0.98	0.99	0.99
-2.0	5.74	3.93	4.67	358	1.670	10.15	0.88	0.91	0.90
-2.5	5.73	3.33	4.72	319	1.506	9.15	0.74	0.81	0.81
-3.0	5.69	2.84	4.88	273	1.330	8.09	0.63	0.69	0.71

DATA FOR STRING 7A CORRECTED FOR ALL CONDITIONS INCLUDING
CONIC MIRROR QUALITY (REFLECTANCE SET TO .7)
NORMALIZED TO 0 DEGREES FOR ISC, IMP, AND PMP

ANGLE (DEG)	ISC (V)	IMP (V)	PMP (V)	ISC (%)	IMP (%)	PMP (%)	NORM ISC	NORM IMP	NORM PMP
0.0	4.80	4.08	4.18	389	1.627	11.87	1.00	1.00	1.00
1.0	4.74	4.23	4.03	407	1.639	11.95	1.04	1.05	1.01
2.0	4.77	4.01	4.02	377	1.517	11.06	0.98	0.97	0.93
2.5	4.82	3.81	4.14	347	1.434	10.46	0.93	0.89	0.88
3.0	4.85	2.99	4.20	285	1.197	8.73	0.73	0.73	0.74
0.0	4.85	4.13	4.21	392	1.651	12.04	1.00	1.00	1.00
-1.0	4.84	3.68	4.28	354	1.515	11.05	0.89	0.90	0.92
-2.0	4.78	2.70	4.38	260	1.138	8.30	0.65	0.66	0.69
-2.5	4.78	2.38	4.41	228	1.003	7.31	0.58	0.58	0.61
-3.0	4.78	1.83	4.44	176	0.780	5.69	0.44	0.45	0.47

NORMALIZED TO THE MAXIMUM OF ISC, IMP, OR PMP WITH ANGLE RESET WITH RESPECT TO ISC

ANGLE (DEG)	ISC (V)	IMP (V)	PMP (V)	ISC (%)	IMP (%)	PMP (%)	NORM ISC	NORM IMP	NORM PMP
0.0	4.80	4.08	4.18	389	1.627	11.87	0.96	0.96	0.99
1.0	4.74	4.23	4.03	407	1.639	11.95	1.00	1.00	0.99
2.0	4.77	4.01	4.02	377	1.517	11.06	0.95	0.93	0.92
2.5	4.82	3.81	4.14	347	1.434	10.46	0.90	0.85	0.87
3.0	4.85	2.99	4.20	285	1.197	8.73	0.71	0.70	0.73
0.0	4.85	4.13	4.21	392	1.651	12.04	0.98	0.96	1.00
-1.0	4.84	3.68	4.28	354	1.515	11.05	0.87	0.87	0.92
-2.0	4.78	2.70	4.38	260	1.138	8.30	0.64	0.64	0.69
-2.5	4.78	2.38	4.41	228	1.003	7.31	0.56	0.56	0.61
-3.0	4.78	1.83	4.44	176	0.780	5.69	0.43	0.43	0.47

DATA FOR STRING 7B CORRECTED FOR ALL CONDITIONS INCLUDING CONIC MIRROR QUALITY (REFLECTANCE SET TO .7) NORMALIZED TO 0 DEGREES FOR ISC, IMP, AND PMP.									
ANGLE (DEG)	ISC (V)	IMP (V)	PMP (V)	ISC (%)	IMP (%)	PMP (%)	NORM ISC	NORM IMP	NORM PMP
0.0	5.64	4.13	4.69	373	1.749	10.63	1.00	1.00	1.00
1.0	5.60	4.00	4.69	372	1.746	10.62	0.97	1.00	1.00
2.0	5.56	3.19	4.80	296	1.421	8.64	0.77	0.79	0.81
2.5	5.52	2.85	4.83	266	1.284	7.81	0.69	0.71	0.73
3.0	5.51	2.38	4.84	227	1.102	6.70	0.58	0.61	0.63
0.0	5.69	4.11	4.76	370	1.760	10.70	1.00	1.00	1.00
-1.0	5.66	3.96	4.75	380	1.808	10.99	0.96	1.03	1.03
-2.0	5.60	3.58	4.69	337	1.578	9.59	0.87	0.91	0.90
-2.5	5.59	3.36	4.71	316	1.491	9.06	0.82	0.86	0.85
-3.0	5.58	2.77	4.91	240	1.178	7.16	0.67	0.65	0.67
NORMALIZED TO THE MAXIMUM OF ISC, IMP, OR PMP WITH ANGLE RESET WITH RESPECT TO ISC									
ANGLE (DEG)	ISC (V)	IMP (V)	PMP (V)	ISC (%)	IMP (%)	PMP (%)	NORM ISC	NORM IMP	NORM PMP
0.0	5.64	4.13	4.69	373	1.749	10.63	1.00	0.98	0.97
1.0	5.60	4.00	4.69	372	1.746	10.62	0.97	0.98	0.97
2.0	5.56	3.19	4.80	296	1.421	8.64	0.69	0.70	0.79
2.5	5.52	2.85	4.83	266	1.284	7.81	0.67	0.70	0.71
3.0	5.51	2.38	4.84	227	1.102	6.70	0.58	0.60	0.61
0.0	5.69	4.11	4.76	370	1.760	10.70	1.00	0.97	0.97
-1.0	5.66	3.96	4.75	380	1.808	10.99	0.96	1.00	1.00
-2.0	5.60	3.58	4.69	337	1.578	9.59	0.87	0.89	0.87
-2.5	5.59	3.36	4.71	316	1.491	9.06	0.81	0.83	0.82
-3.0	5.58	2.77	4.91	240	1.178	7.16	0.67	0.63	0.65

ORIGINAL PAGE IS
OF POOR QUALITY

DATA FOR STRING 8A CORRECTED FOR ALL CONDITIONS INCLUDING CONIC MIRROR QUALITY (REFLECTANCE SET TO .7)

NORMALIZED TO 0 DEGREES FOR ISC, IMP, AND PMP

ANGLE VOC (DEG)	ISC (V)	IMP (V)	PMP (V)	ISC (%)	IMP (%)	PMP (%)	NORM ISC	NORM IMP	NORM PMP
0.0	5.86	4.39	4.40	384	1.687	10.26	1.00	1.00	1.00
1.0	5.82	4.52	4.35	388	1.686	10.25	1.03	1.01	1.00
2.0	5.81	349	4.42	320	1.414	8.60	0.80	0.83	0.84
2.5	5.73	342	4.29	299	1.286	7.82	0.78	0.78	0.76
3.0	5.73	314	4.30	270	1.162	7.06	0.71	0.70	0.69
0.0	5.87	439	4.43	384	1.702	10.35	1.00	1.00	1.00
-1.0	5.83	401	4.47	371	1.658	10.08	0.91	0.95	0.97
-2.0	5.80	306	4.68	288	1.350	8.21	0.70	0.75	0.79
-2.5	5.82	278	4.66	265	1.236	7.51	0.63	0.69	0.73
-3.0	5.64	198	4.54	188	0.853	5.18	0.45	0.49	0.50

NORMALIZED TO THE MAXIMUM OF ISC, IMP, OR PMP WITH ANGLE RESET WITH RESPECT TO ISC

ANGLE VOC (DEG)	ISC (V)	IMP (V)	PMP (V)	ISC (%)	IMP (%)	PMP (%)	NORM ISC	NORM IMP	NORM PMP
0.0	5.86	439	4.40	384	1.687	10.26	0.97	0.99	0.99
-1.0	5.82	432	4.35	388	1.686	10.25	1.00	1.00	0.99
1.0	5.81	349	4.42	320	1.414	8.60	0.77	0.83	0.83
1.5	5.73	342	4.29	299	1.286	7.82	0.76	0.77	0.76
2.0	5.73	314	4.30	270	1.162	7.06	0.69	0.70	0.68
-1.0	5.87	439	4.43	384	1.702	10.35	0.97	0.99	1.00
-2.0	5.83	401	4.47	371	1.658	10.08	0.89	0.96	0.97
-3.0	5.80	306	4.68	288	1.350	8.21	0.68	0.74	0.79
-3.5	5.82	278	4.66	265	1.236	7.51	0.61	0.68	0.73
-4.0	5.64	198	4.54	188	0.853	5.18	0.44	0.49	0.50

DATA FOR STRING 8B CORRECTED FOR ALL CONDITIONS INCLUDING CONIC MIRROR QUALITY (REFLECTANCE SET TO .7)

NORMALIZED TO 0 DEGREES FOR ISC, IMP, AND PMP

ANGLE VOC (DEG)	ISC (V)	IMP (V)	PMP (V)	ISC (%)	IMP (%)	PMP (%)	NORM ISC	NORM IMP	NORM PMP
0.0	4.87	400	4.12	367	1.512	11.03	1.00	1.00	1.00
1.0	4.88	408	4.11	384	1.576	11.50	1.02	1.04	1.04
2.0	4.88	386	3.99	360	1.440	10.50	0.97	0.98	0.95
2.5	4.89	353	4.02	328	1.320	9.62	0.88	0.89	0.87
3.0	4.88	304	3.82	278	1.062	7.75	0.76	0.76	0.70
0.0	4.95	398	3.99	364	1.453	10.59	1.00	1.00	1.00
-1.0	4.92	377	3.94	359	1.414	10.32	0.95	0.99	0.97
-2.0	4.86	255	4.26	250	1.064	7.76	0.64	0.69	0.73
-2.5	4.83	224	4.31	216	0.934	6.81	0.56	0.59	0.64
-3.0	4.82	182	4.29	177	0.758	5.53	0.46	0.48	0.52

NORMALIZED TO THE MAXIMUM OF ISC, IMP, OR PMP WITH ANGLE RESET WITH RESPECT TO ISC

ANGLE VOC (DEG)	ISC (V)	IMP (V)	PMP (V)	ISC (%)	IMP (%)	PMP (%)	NORM ISC	NORM IMP	NORM PMP
0.0	4.87	400	4.12	367	1.512	11.03	0.98	0.96	0.96
-1.0	4.87	400	4.12	367	1.512	11.03	1.00	1.00	1.00
0.0	4.88	408	4.11	384	1.576	11.50	1.00	1.00	1.00
1.0	4.88	386	3.99	360	1.440	10.50	0.95	0.94	0.91
1.5	4.89	353	4.02	328	1.320	9.62	0.87	0.86	0.84
2.0	4.88	304	3.82	278	1.062	7.75	0.75	0.72	0.67
-1.0	4.95	398	3.99	364	1.453	10.59	0.98	0.95	0.92
-2.0	4.92	377	3.94	359	1.414	10.32	0.92	0.94	0.90
-3.0	4.86	255	4.26	250	1.064	7.76	0.62	0.65	0.68
-3.5	4.83	224	4.31	216	0.934	6.81	0.55	0.56	0.59
-4.0	4.82	182	4.29	177	0.758	5.53	0.45	0.46	0.48

DATA FOR STRING 9A CORRECTED FOR ALL CONDITIONS INCLUDING CONIC MIRROR QUALITY (REFLECTANCE SET TO .7)

NORMALIZED TO 0 DEGREES FOR ISC, IMP, AND PMP

ANGLE VOC (DEG)	ISC (V)	IMP (V)	PMP (V)	ISC (%)	IMP (%)	PMP (%)	NORM ISC	NORM IMP	NORM PMP
0.0	5.83	390	4.92	328	1.612	9.80	1.00	1.00	1.00
1.0	5.77	321	4.89	280	1.372	8.34	0.82	0.86	0.85
2.0	5.83	270	5.11	235	1.202	7.31	0.69	0.72	0.75
2.5	5.87	203	5.21	160	0.833	5.06	0.52	0.49	0.52
3.0	5.78	142	5.10	106	0.542	3.29	0.37	0.32	0.34
0.0	5.88	387	5.03	317	1.596	9.70	1.00	1.00	1.00
-1.0	5.90	374	4.80	247	1.183	7.19	0.97	0.78	0.74
-2.0	5.86	367	4.82	315	1.520	9.24	0.95	1.00	0.95
-2.5	5.84	328	4.88	288	1.389	8.45	0.85	0.90	0.87
-3.0	5.81	289	4.83	256	1.235	7.50	0.75	0.81	0.77

NORMALIZED TO THE MAXIMUM OF ISC, IMP, OR PMP WITH ANGLE RESET WITH RESPECT TO ISC

ANGLE VOC (DEG)	ISC (V)	IMP (V)	PMP (V)	ISC (%)	IMP (%)	PMP (%)	NORM ISC	NORM IMP	NORM PMP
0.0	5.83	390	4.92	328	1.612	9.80	1.00	1.00	1.00
1.0	5.77	321	4.89	280	1.372	8.34	0.82	0.86	0.85
2.0	5.83	270	5.11	235	1.202	7.31	0.69	0.72	0.75
2.5	5.87	203	5.21	160	0.833	5.06	0.52	0.49	0.52
3.0	5.78	142	5.10	106	0.542	3.29	0.37	0.32	0.34
0.0	5.88	387	5.03	317	1.596	9.70	0.99	0.97	0.99
-1.0	5.90	374	4.80	247	1.183	7.19	0.96	0.75	0.73
-2.0	5.86	367	4.82	315	1.520	9.24	0.94	0.96	0.94
-2.5	5.84	328	4.88	288	1.389	8.45	0.84	0.87	0.86
-3.0	5.81	289	4.83	256	1.235	7.50	0.74	0.78	0.77

DATA FOR STRING 9B CORRECTED FOR ALL CONDITIONS INCLUDING CONIC MIRROR QUALITY (REFLECTANCE SET TO .7)

NORMALIZED TO 0 DEGREES FOR ISC, IMP, AND PMP

ANGLE VOC (DEG)	ISC (V)	IMP (V)	PMP (V)	ISC (%)	IMP (%)	PMP (%)	NORM ISC	NORM IMP	NORM PMP
0.0	3.94	421	3.01	346	1.043	9.51	1.00	1.00	1.00
1.0	3.96	447	3.00	362	1.086	9.90	1.06	1.04	1.04
2.0	3.91	368	2.90	303	0.879	8.01	0.87	0.88	0.84
2.5	3.83	341	2.83	261	0.739	6.73	0.81	0.75	0.71
3.0	3.75	316	2.17	205	0.635	5.32	0.75	0.59	0.53
0.0	3.89	419	2.93	349	1.020	9.30	1.00	1.00	1.00
-1.0	3.84	363	2.95	225	0.664	6.05	0.87	0.65	0.65
-2.0	3.64	237	2.91	132	0.383	3.49	0.56	0.38	0.38
-2.5	3.46	187	2.77	087	0.240	2.19	0.45	0.25	0.24
-3.0	3.28	125	1.80	087	0.156	1.42	0.30	0.25	0.15

NORMALIZED TO THE MAXIMUM OF ISC, IMP, OR PMP WITH ANGLE RESET WITH RESPECT TO ISC

ANGLE VOC (DEG)	ISC (V)	IMP (V)	PMP (V)	ISC (%)	IMP (%)	PMP (%)	NORM ISC	NORM IMP	NORM PMP
0.0	3.94	421	3.01	346	1.043	9.51	1.00	0.99	1.00
1.0	3.96	447	3.00	362	1.086	9.90	1.00	0.98	0.98
2.0	3.91	368	2.90	303	0.879	8.01	0.87	0.78	0.76
2.5	3.83	341	2.83	261	0.739	6.73	0.81	0.66	0.62
3.0	3.75	316	2.17	205	0.635	5.32	0.66	0.52	0.50
0.0	3.89	419	2.93	349	1.020	9.30	1.00	1.00	0.98
-1.0	3.84	363	2.95	225	0.664	6.05	0.87	0.68	0.67
-2.0	3.64	237	2.91	132	0.383	3.49	0.56	0.40	0.39
-2.5	3.46	187	2.77	087	0.240	2.19	0.45	0.25	0.23
-3.0	3.28	125	1.80	087	0.156	1.42	0.30	0.25	0.14

DATA FOR STRING 10B CORRECTED FOR ALL CONDITIONS INCLUDING CONIC MIRROR QUALITY (REFLECTANCE SET TO .7)

NORMALIZED TO 0 DEGREES FOR ISC, IMP, AND PMP

ANGLE VOC (DEG)	ISC (V)	IMP (V)	PMP (V)	ISC (%)	IMP (%)	PMP (%)	NORM ISC	NORM IMP	NORM PMP
0.0	3.89	281	2.90	272	0.789	7.19	1.00	1.00	1.00
1.0	3.95	395	2.92	355	1.037	9.45	1.41	1.30	1.31
2.0	3.97	416	2.95	386	1.140	10.39	1.48	1.42	1.45
2.5	3.97	384	3.07	363	1.114	10.15	1.37	1.33	1.41
3.0	3.91	339	3.13	321	1.006	9.17	1.21	1.18	1.28
0.0	3.88	293	3.12	282	0.882	8.04	1.00	1.00	1.00
-1.0	3.85	300	3.08	280	0.896	8.17	1.02	1.03	1.02
-2.0	3.85	292	3.03	280	0.849	7.74	1.00	0.99	0.96
-2.5	3.78	285	2.84	270	0.767	6.99	0.97	0.95	0.87
-3.0	3.70	210	2.84	204	0.579	5.28	0.72	0.72	0.66

NORMALIZED TO THE MAXIMUM OF ISC, IMP, OR PMP WITH ANGLE RESET WITH RESPECT TO ISC

ANGLE VOC (DEG)	ISC (V)	IMP (V)	PMP (V)	ISC (%)	IMP (%)	PMP (%)	NORM ISC	NORM IMP	NORM PMP
0.0	3.89	281	2.90	272	0.789	7.19	1.00	1.00	1.00
-1.0	3.85	293	3.12	282	0.882	8.04	1.00	1.00	1.00
1.0	3.95	395	2.92	355	1.037	9.45	0.99	0.96	0.95
2.0	3.97	416	2.95	386	1.140	10.39	1.00	1.00	1.00
2.5	3.97	384	3.07	363	1.114	10.15	0.90	0.91	0.86
3.0	3.91	339	3.13	321	1.006	9.17	0.80	0.81	0.86
-1.0	3.88	293	3.12	282	0.882	8.04	0.78	0.81	0.86
-2.0	3.85	292	3.03	280	0.849	7.74	0.84	0.87	0.91
-3.0	3.78	285	2.84	270	0.767	6.99	0.85	0.86	0.89
-4.5	3.78	298	2.84	282	0.802	7.31	0.77	0.79	0.76
-5.0	3.70	208	2.84	201	0.572	5.21	0.54	0.56	0.54

DATA FOR STRING 1A2 CORRECTED FOR ALL CONDITIONS INCLUDING CONIC MIRROR QUALITY (REFLECTANCE SET TO .7) NORMALIZED TO 0 DEGREES FOR ISC, IMP, AND PMP									
ANGLE VOC	ISC	VMP	IMP	(A)	(V)	(W)	PMP	EFFCY	NORM
DEG)	(V)	(V)	(A)	(A)	(V)	(W)	(W)	(%)	ISC
0.0	4.04	473	3.44	453	1.558	14.21	1.00	1.00	1.00
1.0	4.03	469	3.43	438	1.505	13.72	0.99	0.97	0.97
2.0	4.02	450	3.45	431	1.484	13.53	0.95	0.95	0.95
2.5	4.03	431	3.48	416	1.448	13.20	0.91	0.92	0.93
3.0	4.04	384	3.52	368	1.293	11.79	0.81	0.81	0.83
0.0	4.04	472	3.43	434	1.490	13.58	1.00	1.00	1.00
-1.0	4.01	464	3.42	432	1.475	13.45	0.98	0.99	0.99
-2.0	4.03	402	3.55	386	1.370	12.49	0.85	0.89	0.92
-2.5	4.01	384	3.51	372	1.306	11.91	0.81	0.86	0.88
-3.0	4.00	338	3.49	312	1.087	9.91	0.72	0.72	0.73
NORMALIZED TO THE MAXIMUM OF ISC, IMP, OR PMP WITH ANGLE RESET WITH RESPECT TO ISC									
ANGLE VOC	ISC	VMP	IMP	(A)	(V)	(W)	PMP	EFFCY	NORM
DEG)	(V)	(V)	(A)	(A)	(V)	(W)	(W)	(%)	ISC
0.0	4.04	473	3.44	453	1.558	14.21	1.00	1.00	1.00
1.0	4.03	469	3.43	438	1.505	13.72	0.99	0.97	0.97
2.0	4.02	450	3.45	431	1.484	13.53	0.95	0.95	0.95
2.5	4.03	431	3.48	416	1.448	13.20	0.91	0.92	0.93
3.0	4.04	384	3.52	368	1.293	11.79	0.81	0.81	0.83
0.0	4.04	472	3.43	434	1.490	13.58	1.00	0.96	0.96
-1.0	4.01	464	3.42	432	1.475	13.45	0.98	0.95	0.95
-2.0	4.03	402	3.55	386	1.370	12.49	0.85	0.85	0.88
-2.5	4.01	384	3.51	372	1.306	11.91	0.81	0.82	0.84
-3.0	4.00	338	3.49	312	1.087	9.91	0.71	0.69	0.70

DATA FOR STRING 1B2 CORRECTED FOR ALL CONDITIONS INCLUDING CONIC MIRROR QUALITY (REFLECTANCE SET TO .7)
NORMALIZED TO 0 DEGREES FOR ISC, IMP, AND PMP

ANGLE VDC (DEG)	ISC (V)	VMP (V)	IMP (A)	PMP (W)	EFFCY (%)	NORM ISC	NORM VMP	NORM IMP	NORM PMP
0.0	5.99	407	5.17	379	1.957	11.90	1.00	1.00	1.00
1.0	6.00	386	5.01	362	1.817	11.04	0.95	0.96	0.93
2.0	5.94	381	5.02	357	1.791	10.88	0.94	0.94	0.91
2.5	5.97	347	5.09	301	1.533	9.32	0.85	0.80	0.78
3.0	5.94	266	5.11	230	1.178	7.16	0.65	0.61	0.60
0.0	6.00	410	5.17	381	1.971	11.98	1.00	1.00	1.00
-1.0	6.02	419	5.15	391	2.015	12.25	1.02	1.03	1.02
-2.0	6.03	400	5.19	373	1.939	11.78	0.97	0.98	0.98
-2.5	5.98	369	5.20	343	1.784	10.84	0.90	0.90	0.90
-3.0	6.02	307	5.27	284	1.493	9.08	0.75	0.74	0.76

NORMALIZED TO THE MAXIMUM OF ISC, IMP, OR PMP WITH ANGLE RESET WITH RESPECT TO ISC

ANGLE VDC (DEG)	ISC (V)	VMP (V)	IMP (A)	PMP (W)	EFFCY (%)	NORM ISC	NORM VMP	NORM IMP	NORM PMP
0.0	5.99	407	5.17	379	1.957	11.90	0.97	0.97	0.97
1.0	6.00	386	5.01	362	1.817	11.04	0.92	0.93	0.90
2.0	5.94	381	5.02	357	1.791	10.88	0.91	0.91	0.89
3.0	5.97	347	5.09	301	1.533	9.32	0.83	0.77	0.76
4.0	5.94	266	5.11	230	1.178	7.16	0.63	0.59	0.58
1.0	6.00	410	5.17	381	1.971	11.98	0.98	0.97	0.98
0.0	6.02	419	5.15	391	2.015	12.25	1.00	1.00	1.00
-1.0	6.03	400	5.19	373	1.939	11.78	0.96	0.95	0.96
-1.5	5.98	369	5.20	343	1.784	10.84	0.88	0.88	0.89
-2.0	6.02	307	5.27	284	1.493	9.08	0.73	0.72	0.74

DATA FOR STRING 1C2 CORRECTED FOR ALL CONDITIONS INCLUDING CONIC MIRROR QUALITY (REFLECTANCE SET TO .7)
NORMALIZED TO 0 DEGREES FOR ISC, IMP, AND PMP

ANGLE VDC (DEG)	ISC (V)	VMP (V)	IMP (A)	PMP (W)	EFFCY (%)	NORM ISC	NORM VMP	NORM IMP	NORM PMP
0.0	6.16	451	5.25	418	2.193	13.33	1.00	1.00	1.00
1.0	6.13	450	5.25	423	2.220	13.49	1.00	1.01	1.01
2.0	6.11	436	5.33	411	2.193	13.33	0.97	0.98	1.00
2.5	6.11	377	5.55	349	1.937	11.78	0.83	0.84	0.88
3.0	6.08	249	5.69	226	1.289	7.83	0.55	0.54	0.59
0.0	6.08	455	5.17	422	2.180	13.25	1.00	1.00	1.00
-1.0	6.06	441	5.23	391	2.044	12.43	0.97	0.93	0.94
-2.0	6.03	371	5.28	338	1.785	10.85	0.81	0.80	0.82
-2.5	5.99	314	5.29	252	1.331	8.09	0.69	0.60	0.61
-3.0	5.91	208	5.32	113	0.599	3.64	0.46	0.27	0.27

NORMALIZED TO THE MAXIMUM OF ISC, IMP, OR PMP WITH ANGLE RESET WITH RESPECT TO ISC

ANGLE VDC (DEG)	ISC (V)	VMP (V)	IMP (A)	PMP (W)	EFFCY (%)	NORM ISC	NORM VMP	NORM IMP	NORM PMP
0.0	6.16	451	5.25	418	2.193	13.33	0.99	0.99	0.99
1.0	6.13	450	5.25	423	2.220	13.49	0.99	1.00	1.00
2.0	6.11	436	5.33	411	2.193	13.33	0.96	0.97	0.99
2.5	6.11	377	5.55	349	1.937	11.78	0.83	0.83	0.87
3.0	6.08	249	5.69	226	1.289	7.83	0.55	0.54	0.58
0.0	6.08	455	5.17	422	2.180	13.25	1.00	1.00	1.00
-1.0	6.06	441	5.23	391	2.044	12.43	0.97	0.93	0.92
-2.0	6.03	371	5.28	338	1.785	10.85	0.81	0.80	0.80
-2.5	5.99	314	5.29	252	1.331	8.09	0.69	0.60	0.61
-3.0	5.91	208	5.32	113	0.599	3.64	0.46	0.27	0.27

DATA FOR STRING 1D2 CORRECTED FOR ALL CONDITIONS INCLUDING CONIC MIRROR QUALITY (REFLECTANCE SET TO .7)
NORMALIZED TO 0 DEGREES FOR ISC, IMP, AND PMP

ANGLE VDC (DEG)	ISC (V)	VMP (V)	IMP (A)	PMP (W)	EFFCY (%)	NORM ISC	NORM VMP	NORM IMP	NORM PMP
0.0	6.03	438	5.01	387	1.936	11.77	1.00	1.00	1.00
1.0	5.97	423	4.91	390	1.913	11.63	0.97	1.01	0.99
2.0	6.08	377	5.25	352	1.846	11.22	0.86	0.91	0.95
2.5	6.04	326	5.39	301	1.623	9.86	0.74	0.78	0.84
3.0	6.01	275	5.33	255	1.360	8.27	0.63	0.66	0.70
0.0	6.06	446	5.04	384	1.936	11.77	1.00	1.00	1.00
-1.0	6.04	424	5.03	361	1.815	11.03	0.95	0.94	0.94
-2.0	6.05	386	5.06	316	1.599	9.72	0.87	0.82	0.83
-2.5	6.02	328	4.99	267	1.332	8.09	0.73	0.69	0.69
-3.0	5.87	216	4.84	173	0.839	5.10	0.49	0.45	0.43

NORMALIZED TO THE MAXIMUM OF ISC, IMP, OR PMP WITH ANGLE RESET WITH RESPECT TO ISC

ANGLE VDC (DEG)	ISC (V)	VMP (V)	IMP (A)	PMP (W)	EFFCY (%)	NORM ISC	NORM VMP	NORM IMP	NORM PMP
0.0	6.03	438	5.01	387	1.936	11.77	0.98	0.99	1.00
1.0	5.97	423	4.91	390	1.913	11.63	0.95	1.00	0.99
2.0	6.08	377	5.25	352	1.846	11.22	0.84	0.90	0.95
2.5	6.04	326	5.39	301	1.623	9.86	0.73	0.77	0.84
3.0	6.01	275	5.33	255	1.360	8.27	0.62	0.65	0.70
0.0	6.06	446	5.04	384	1.936	11.77	1.00	0.99	1.00
-1.0	6.04	424	5.03	361	1.815	11.03	0.95	0.93	0.94
-2.0	6.05	386	5.06	316	1.599	9.72	0.87	0.81	0.83
-2.5	6.00	328	4.99	267	1.332	8.09	0.73	0.69	0.69
-3.0	5.87	216	4.84	173	0.839	5.10	0.49	0.44	0.43

DATA FOR STRING 2D2 CORRECTED FOR ALL CONDITIONS INCLUDING CONIC MIRROR QUALITY (REFLECTANCE SET TO .7)
NORMALIZED TO 0 DEGREES FOR ISC, IMP, AND PMP

ANGLE VDC (DEG)	ISC (V)	VMP (V)	IMP (A)	PMP (W)	EFFCY (%)	NORM ISC	NORM VMP	NORM IMP	NORM PMP
0.0	6.09	444	5.14	415	2.135	12.98	1.00	1.00	1.00
1.0	6.09	453	5.14	428	2.200	13.37	1.02	1.03	1.03
2.0	6.03	420	5.34	373	1.995	12.12	0.95	0.90	0.93
2.5	6.03	387	5.42	335	1.814	11.03	0.87	0.81	0.85
3.0	6.05	318	5.54	267	1.481	9.00	0.72	0.64	0.69
0.0	6.12	442	5.16	415	2.138	12.99	1.00	1.00	1.00
-1.0	6.10	395	5.21	370	1.927	11.71	0.89	0.89	0.90
-2.0	6.08	345	5.25	324	1.702	10.34	0.78	0.78	0.80
-2.5	6.06	281	5.35	251	1.341	8.15	0.64	0.60	0.63
-3.0	5.98	167	5.35	143	0.765	4.65	0.38	0.34	0.36

NORMALIZED TO THE MAXIMUM OF ISC, IMP, OR PMP WITH ANGLE RESET WITH RESPECT TO ISC

ANGLE VDC (DEG)	ISC (V)	VMP (V)	IMP (A)	PMP (W)	EFFCY (%)	NORM ISC	NORM VMP	NORM IMP	NORM PMP
-1.0	6.09	444	5.14	415	2.135	12.98	0.98	0.97	0.97
0.0	6.09	453	5.14	428	2.200	13.37	1.00	1.00	1.00
1.0	6.03	420	5.34	373	1.995	12.12	0.93	0.87	0.91
1.5	6.03	387	5.42	335	1.814	11.03	0.85	0.78	0.82
2.0	6.05	318	5.54	267	1.481	9.00	0.70	0.62	0.67
2.0	6.12	442	5.16	415	2.138	12.99	0.98	0.97	0.97
-1.0	6.10	395	5.21	370	1.927	11.71	0.87	0.86	0.88
-2.0	6.08	345	5.25	324	1.702	10.34	0.76	0.76	0.77
-2.5	6.06	281	5.35	251	1.341	8.15	0.62	0.59	0.61
-3.0	5.98	167	5.35	143	0.765	4.65	0.37	0.33	0.35

ORIGINAL PAGE IS
OF POOR QUALITY

FIGURE A8 (CONTINUED)

SECONDARY PROOF MIRRORS

OFFPOINT DATA CORRECTED TO AMO AND 28°C ONLY



Engineering & Test Division
TRW Space & Technology Group

Angle Offset	1	2	3	5	6	7	8	9				
3	139	.48	164	.61	134	.55	199	.66	187	.62	139	.60
2.5	195	.67	212	.78	180	.74	224	.75	232	.77	176	.77
2	228	.78	228	.84	198	.82	241	.80	247	.82	192	.83
1.5	238	.82	238	.88	202	.83	257	.86	256	.85	200	.87
1	252	.86	259	.96	220	.91	271	.90	282	.94	217	.94
.5	274	.94	268	.99	234	.97	290	.97	292	.97	228	.99
0	292	1.00	270	1.00	239	.99	297	.99	297	.99	229	1.00
0	292	1.00	271	1.00	242	1.00	300	1.00	300	1.00	230	1.00
.5	298	1.02	267	.99	244	1.01	295	.98	301	1.00	230	1.00
1	293	1.00	272	1.00	240	.99	277	.92	299	.98	231	1.00
1.5	303	1.04	267	.99	227	.94	243	.81	279	.93	224	.97
2	254	.87	253	.93	204	.84	219	.73	247	.82	203	.88
2.5	212	.73	209	.77	178	.74	195	.65	217	.72	179	.78
3	185	.63	183	.68	163	.67	163	.54	192	.64	164	.71
3.5	161	.55	140	.52	124	.51	98	.33	147	.49	126	.55
4					58	.24	47	.16	71	.24	75	.33
4.5					19	.08	16	.05	17	.06	30	.13
5					9	.04	5	.02	7	.02		
10									1.30	.0043		
15									.91	.0030		
Shadowed *												
Offpoint > 15**												

NOTES: * Shadowed output is shadow equal in size to optic. This represents background.

* Offpoint > 15 represents output due to scatter from primary and secondary.

FIGURE A9

SECONDARY PROOF NORMALIZATION AND CONVERSION



Engineering & Test Division
TRW Space & Technology Group

	1	2	3	5	6	7	8	9	AVG
3.5	.63		.60						.62
3	.87	.79	.86	.79	.71	.86	.80	.78	.81
2.5	.97	.97	1.01	.89	.92	.94	.96	.96	.95
2	.97	1.00	1.00	.91	.97	.96	.97	.99	.97
1.5	.93	.95	.95	.89	.89	.94	.92	.94	.93
1	.96	.99	1.00	.90	.93	.93	.96	.96	.95
.5	1.01	1.00	1.01	.96	.98	.99	.98	1.00	.99
0	1.02	1.00	1.01	1.00	1.00	1.00	1.01	1.01	1.01
0	1.02	1.00	1.01	1.00	1.00	1.00	1.00	1.00	1.00
.5	1.01	1.00	1.02	1.01	1.02	.99	1.01	1.01	1.01
1	1.07	1.03	1.02	1.00	1.02	.94	1.01	1.03	1.02
1.5	.94	1.07	1.02	.93	1.01	.87	1.00	1.04	.99
2	.87	1.10	.96	.87	1.00	.87	.97	1.05	.96
2.5	.79	.96	.91	.85	.92	.81	.90	.97	.89
3	.71	.88	.82	.78	.87	.70	.83	.92	.81
3.5		.68	.53	.52	.67	.43	.64	.72	.60
4			.23	.31	.31	.20	.31	.42	.30
4.5				.15	.10	.06	.07	.16	.11
5				.05	.05	.02	.02		.04

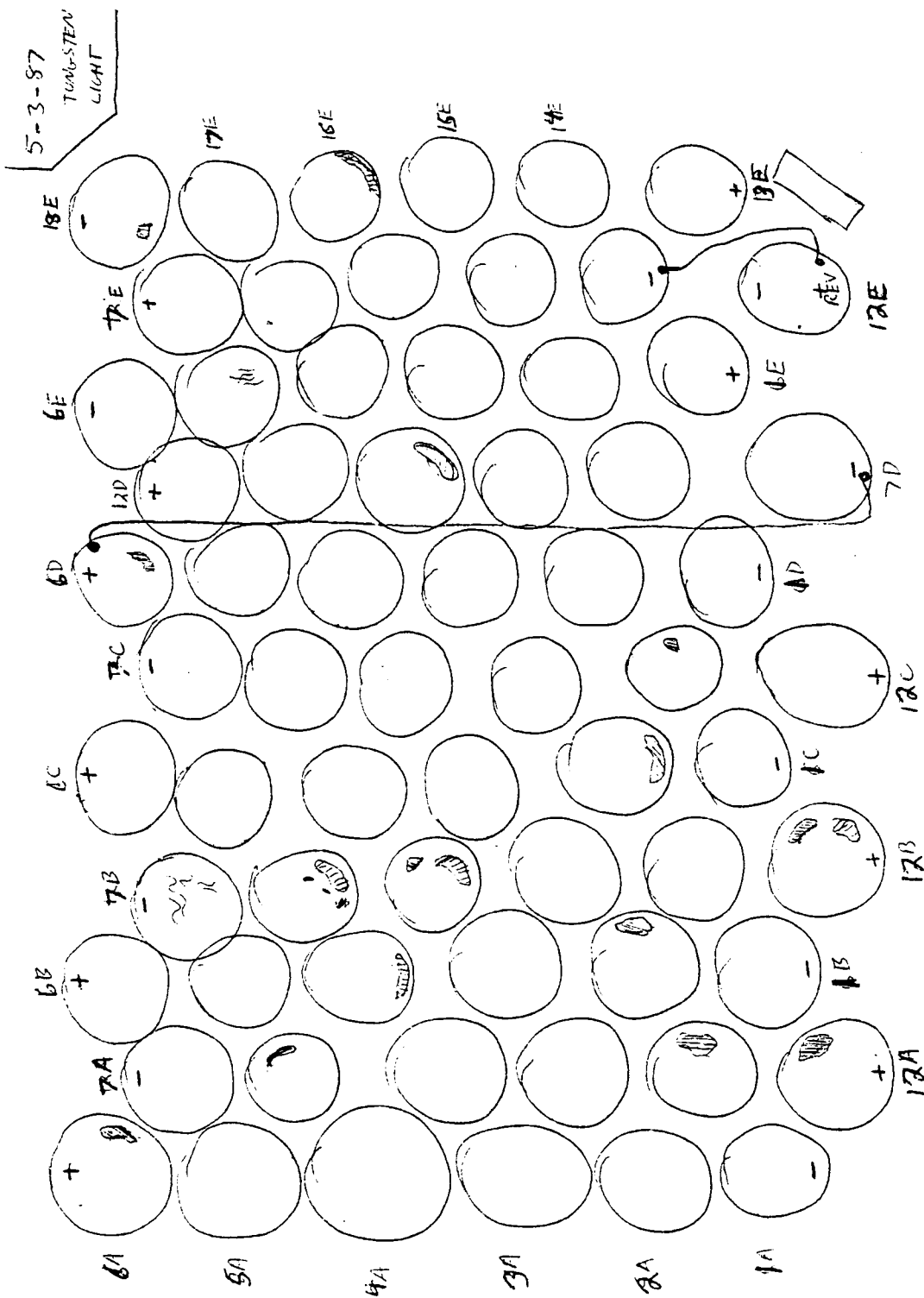
4.0 INSPECTION RESULTS

The small panel was checked and mapped for defects in the primary mirror coating and for weld joint integrity. Figure A11 is a sketch of the defects found.

The large panel was inspected in the same manner as the small panel. It was noted that 5 mechanically produced nickel conic mirrors originally machined as test articles with no coatings or polish found their way onto the panel as noted in Figure A12. What is surprising is that the machined parts had relatively small effect on output of the strings involved. Apparently the coating degradation is approximately equal in effect to a bare nickel machined part.

Lack of schedule precluded replacing these machined conic parts.

Figure A13 presents electrical inspection remarks as determined during output testing. A number of elements were found to be open or shorted as shown. The Varian string 10A was not possible to electrically measure due to the characteristics of the string. Some elements had essentially 0 current but full voltage capability and acted as reverse diodes in series with the string. It was not practical to jumper the effected elements as only 1 element was actually producing power correctly. This string will be monitored only for mechanical degradations.



COATING- DEFECT NOTATIONS

- COATING DISCOLORATION
- COATING REMOVAL
- SCRATCHES

ABOUT 2% CONTAM 1% ADDITIONAL SCATTER GOES?

FIGURE A11 COATING AND PART DEFECTS IN SMALL 15" x 21" PANEL.

ORIGINAL PAGE IS
OF POOR QUALITY

ORIGINAL PAGE IS
OF POOR QUALITY

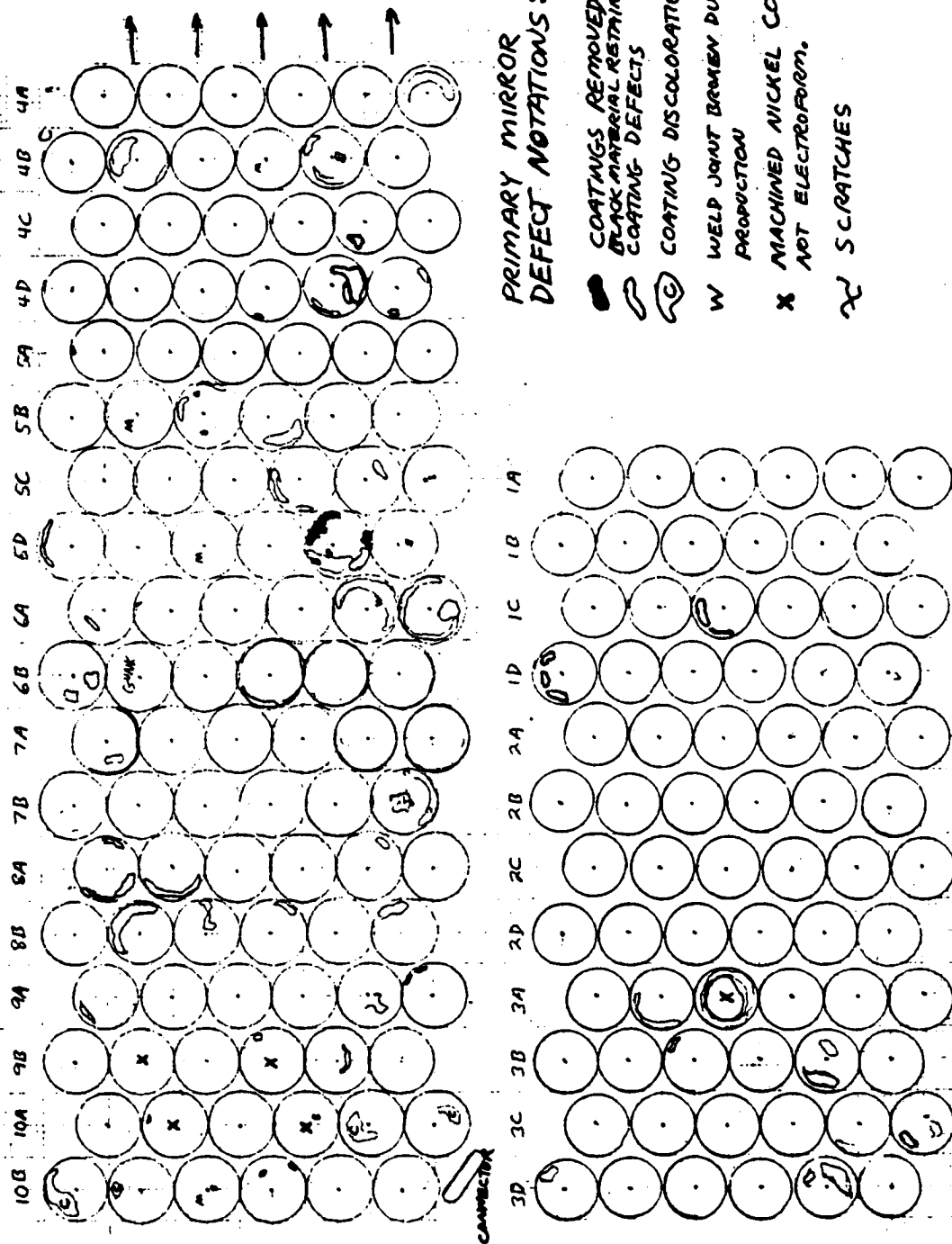


FIGURE A12 INSPECTION RESULTS OF 15" x 56" PANEL.

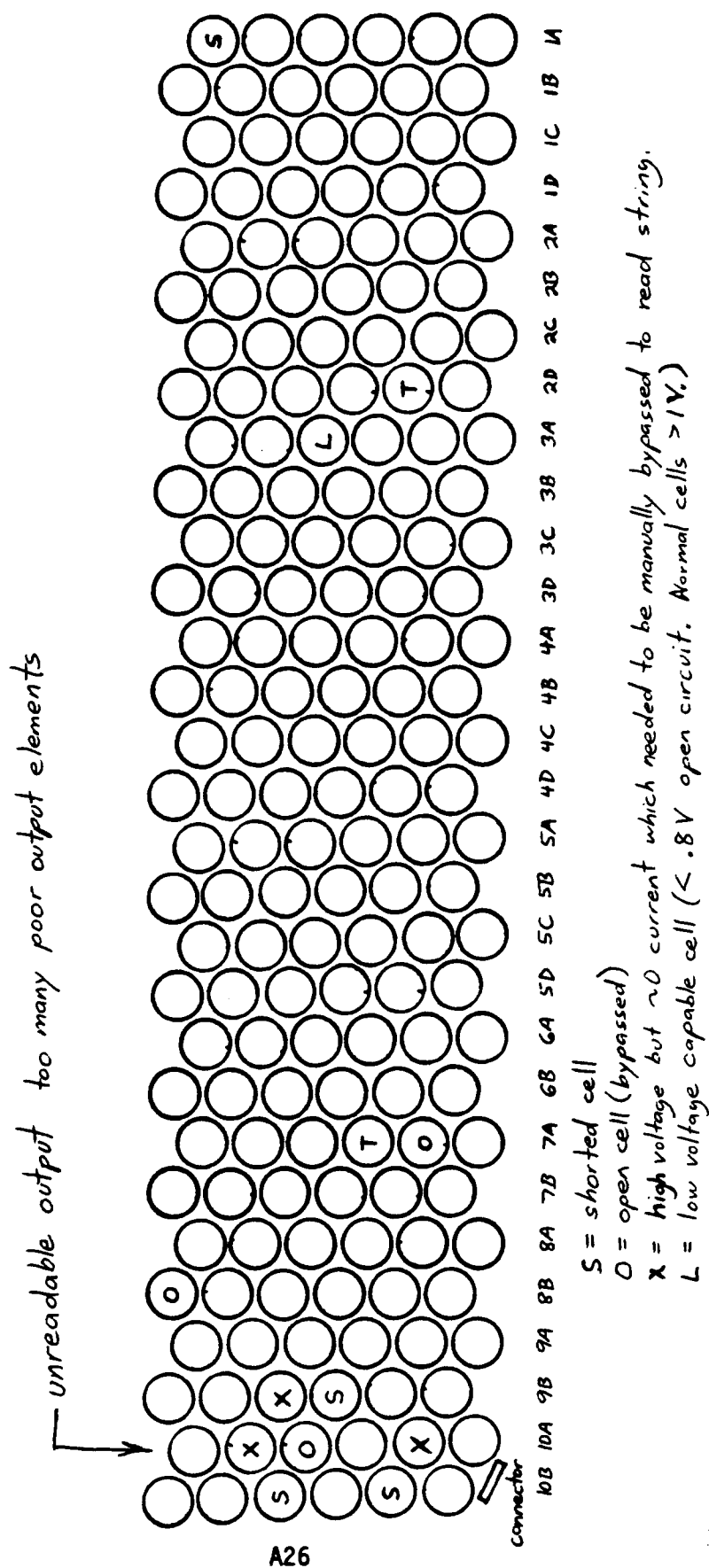


FIGURE A-13. Electrical Test notes showing locations of shorted and open cells as well as thermistor locations.

Appendix B - MCC
ELECTRICAL MANUFACTURING

1. FABRICATION

Items required for fabrication:

CELL I/C

BeO I/C

Spider

Washers

1.1 CELL AND BeO INTERCONNECTS

Approximately 300 interconnects for the cell and BeO cell mounting were required for the MCC job. Kovar was chosen as base material due to close match in CTE with the GaAs cell, and by availability. The Kovar was cut into 0.001" x 1" x 6" strips which were plated with nickel, copper and either silver or gold as required. Plated strips were then stacked and machined using a wire electro-discharge process. Cut rates were extremely slow to avoid fusing strips together and alloying of base material with platings. Final cut stacks were then separated as individual piece parts. Stress relief loops were formed in each part using a two piece die; five parts were formed per cycle. Completed parts were then cleaned in a solvent bath and protective packaged for later use.

1.2 SPIDER

Approximately 270 spiders were required. Fabrication techniques were almost identical to those used for the interconnects. Base material for the spider was chosen as Aluminum; weight was a major driver. The aluminum plates were stacked as limited by the machine wire tolerance and, again, a slow burn rate was used to avoid fusing parts and/or alloying of plating and base material. Cut stacks were separated and sent to a silver plating bath. The silver plate allowed the use of solder to bond the secondary mirror to the spider. The parts were then protective packaged for later use.

1.3 WASHERS

Approximately 250 Kapton/RTV washers were required for the MCC job. These washers are used at installation of the MCC element into the Tri-Hex grid. Commercially available pop-pins (snap inserts) were used to hold the MCC elements in place. An uneven top surface of the three elements held by the pop-pins created non-uniform pressure on the elements, tending to distort the surface or the pin. Therefore, it was desirable to have a pliable surface between the element and the pop-pin surface.

This surface was created by making washers the size of the the pop-pin head. These washers were made from Kapton and RTV. A 0.002" Kapton sheet was covered with a thin layer 0.001-0.002" of RTV 142. After cure, the outside diameter of the washers were punched, one unit at a time. Concentric with the O.D., an inner circle of material was removed that matched the pin shaft O.D., completing the washer.

2. SUBASSEMBLIES REQUIRED

Washer to Pop-pin

Cell I/C to Cell

BeO I/C to BeO

Coverglass to Cone

Secondary to Spider

2.1 WASHER TO POP-PIN

The completed washer was installed to the pop-pin. Since the pop-pin shaft O.D. is much larger at the pressure fitting than the washer I.D., tooling was required to compress the pop-pin shaft. This avoided splits to the Kapton washer during installation. The completed pin washer assembly was then stored for later use.

2.2 CELL AND BeO INTERCONNECT ATTACHMENT

As discussed in section 3.4.2.3, welding was selected for joining I/Cs to both the cell and BeO pads. Tooling was fabricated for both of these operations. The cell or BeO were loaded into a cavity and solvent cleaned. The interconnects as made in section 1.1 of this appendix were centered over a locating pin and rotated over the cell and/or BeO until desired location was achieved (Figure B1, Left tool). The weld was then made in two places for each interconnect. The completed joints were then cleaned and the completed assembly was boxed for later use.

For the cells, all were measured for I/V characteristics prior to the welding and identified. After a weld schedule had been developed for each vendor, the cells were then grouped by performance and welded. It was assumed that performance degradation would be relatively constant for all cells, by vendor. The cells were re-grouped by "performance prior to welding," after welding. These groups were selected to develop a kitting plan to group similar performance cells at the panel level.



FIGURE B-1. BeO welding tool (left) and conic mirror coarse alignment tool (right).

ORIGINAL PAGE IS
OF POOR QUALITY

2.3 COVERGLASS TO CONE BONDING

As discussed in section 3.4.6, several options were evaluated for joining the cone to the coverglass. This joint was critical in that the cone must be perpendicular to the glass and that no bonding material could be allowed on the interior of the cone. Reduced viscosity bonding materials were ideal for good filleting but "leaked" under cone to inside surfaces. Higher viscosity materials did not provide filleting, or the force required for filleting caused mis-mating of the two components. Dymax 628, a UV curing adhesive was chosen. This material has a very low viscosity but can be kept from "leaking" by accelerated cure under intense UV exposure.

A multiple place tool was constructed for this operation (Figure B2) Five coverglasses were loaded into cavities for locating and cleaning. Five cones were then loaded onto the tool and centered by estimation. Centering spindles made of nylon and match ground to the base ID of the cone were lowered into the cone and brought down flush to the glass. The centering nylon could touch only the base of the ID of the cone. This locked the two components for bonding. A small dot (5 mg) of the UV adhesive was placed on the side wall of the cone. As the material ran down the wall of the cone and filleted the coverglass, it was exposed to high intensity UV light for 10-15 seconds. This operation was repeated for all four corners of the coverglass. The resulting bond was then baked for 30 minutes at 100°C in air to ensure full cure.

Cleanup and rework was accomplished by flushing the bond with acetone and IPA. Care was taken to avoid contamination of the interior cone surface.

This bond was tested by thermal cycling sample components in air from +100°C to -100°C, 200 cycles in duration. Also, sample components were exposed to acoustic protoqual pressure levels. No joints showed evidence of delamination or failure.

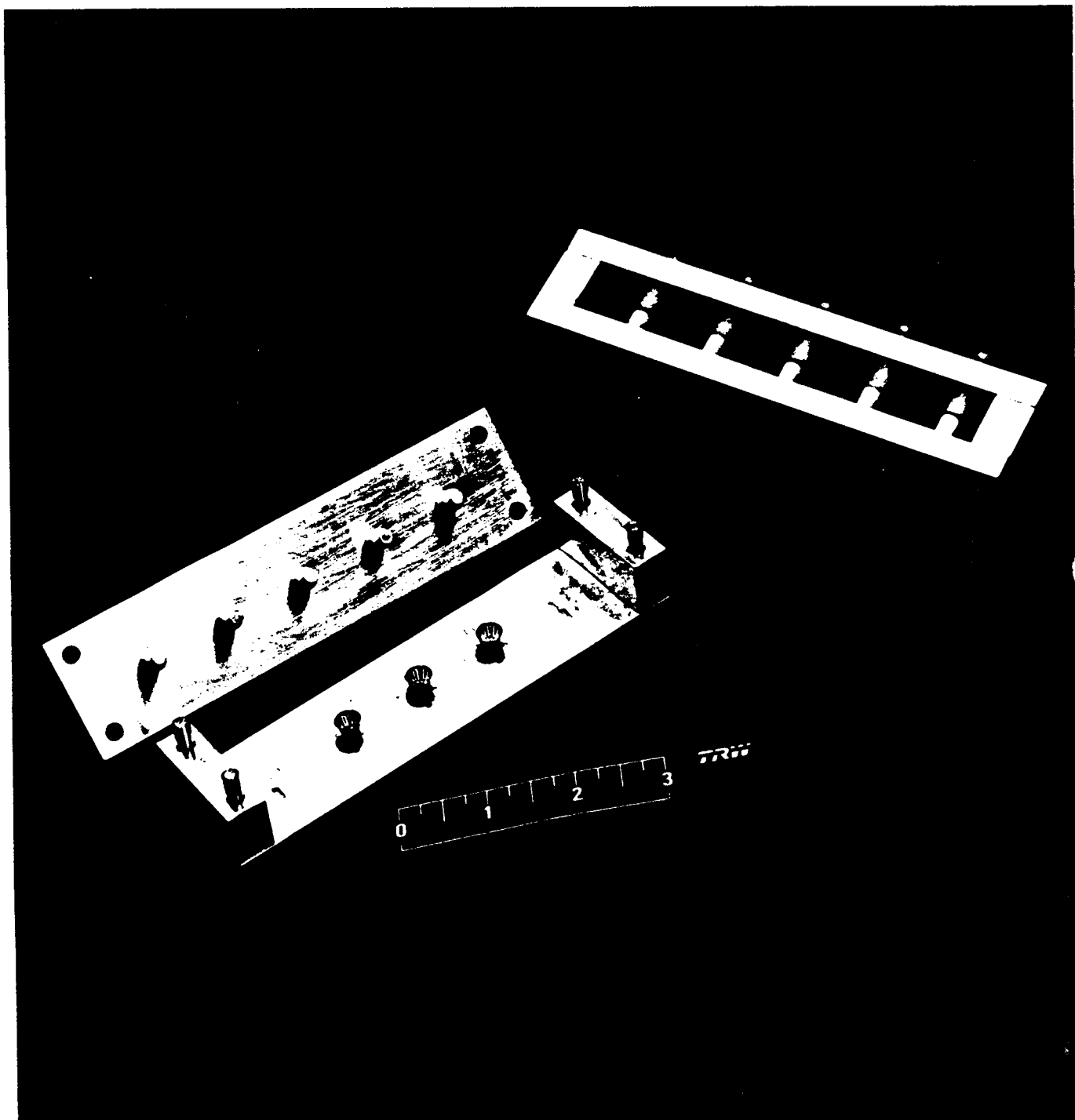


FIGURE B-2. Conic mirror to coverglass bonding tool.

ORIGINAL PAGE IS
OF POOR QUALITY

2.4 SECONDARY TO SPIDER JOINTS

Adhesive bonding was selected as a baseline process for joining the secondary mirror to the spider support. This baseline was a very difficult method. To keep the secondary pointed and true to the cone, the adhesive layer had to be perfectly flat and continuous. Low viscosity materials were investigated, however, bond strength was marginal. Paste adhesives resulted in inconsistent bond thickness. Attempts to eliminate the interface bond and fillet the joint with paste adhesives were equally unsatisfactory as well as extremely time consuming to complete.

A secondary system was developed to solder the secondary mirror to the spider. The aluminum spider was silver plated with nickel-copper base. The interior surface of the secondary, electroformed nickel, was not prepared. A silver filled solder, preform was made by wrapping a rod sized slightly larger than the inside diameter of the secondary with solder wire. Preforms were then cut from the rod. The spider was located on a solder fixture (Figure B-3, right tool) on its outside diameter. The solder preform was then fluxed in Alpha flux diluted with isopropyl alcohol. The preform was then located over the spider outside diameter on the fixture. Installation of the secondary mirror on top of the preform capped the assembly. The preform was then pushed inside the secondary mirror and held by "spring action" to the inside surface. The secondary was pressed firm to the spider by slight pressure of a teflon pad.

The fixture containing secondary, spider and preform were then soldered via Vapor Phase soldering on a controlled elevator for time at temperature. Solder schedules were developed for producing 100% filleting to the inside surface. Pressure and flux were critical to achieve wetting to the nickel interior.

None of these subassemblies required rework.

3. OPTIC ASSEMBLY

Cell Stack Installation

Feed Through Post, Installation

Cone/Core Installation

Painting

Secondary/Spider Installation

3.1 CELL STACK INSTALLATION TO PRIMARY MIRROR

The original proposal for installation of the cell stack was to make one joint at a time, using vapor phase solder techniques. However, each subsequent joint had to utilize higher temperature solders to prevent reflow (and misalignment) of the prior joint. This quickly proved unworkable and expensive. A secondary approach called for joining the cell to the BeO and the BeO to the primary mirror in a single vapor phase operation. This method was much more difficult to tool due to the extremely tight tolerance for placement of the cell but was chosen over the method above for cost constraints.

Solder preforms were experimented with and selected at 70% of the total interface area and at 0.001" thick of silver filled solder (to avoid gold migration from the BeO). Tooling fabrication was made to locate the BeO pad and the cell into the Primary. This tool had a two step cavity (Figure B-3, left tool small cylinder with cavity). The first cavity held the solar cell, active surface down with its interconnect. The cell solder preform was then dipped in flux and placed on the back cell surface. Excess flux here broke cells and was minimized. The cavity was made slightly less deep than the cell. The BeO was then placed in the second cavity, over the cell solder preform. The BeO solder preform was then fluxed and added to the back of the BeO. This cavity was also slightly less deep than the BeO.

The outside diameter was match ground to the inside diameter of the primary mirror. A through locating pin aligned the tool to the primary mirror, where the tool was inserted and pushed flush with the base of the primary. The undersized cavity created pressure between all components and the preforms. The tool was then clamped to the primary by a mating shell with spring loaded tension (Figure B-3, left tool, hexagonal, with coil interior and leaf exterior springs).

ORIGINAL PAGE IS
OF POOR QUALITY

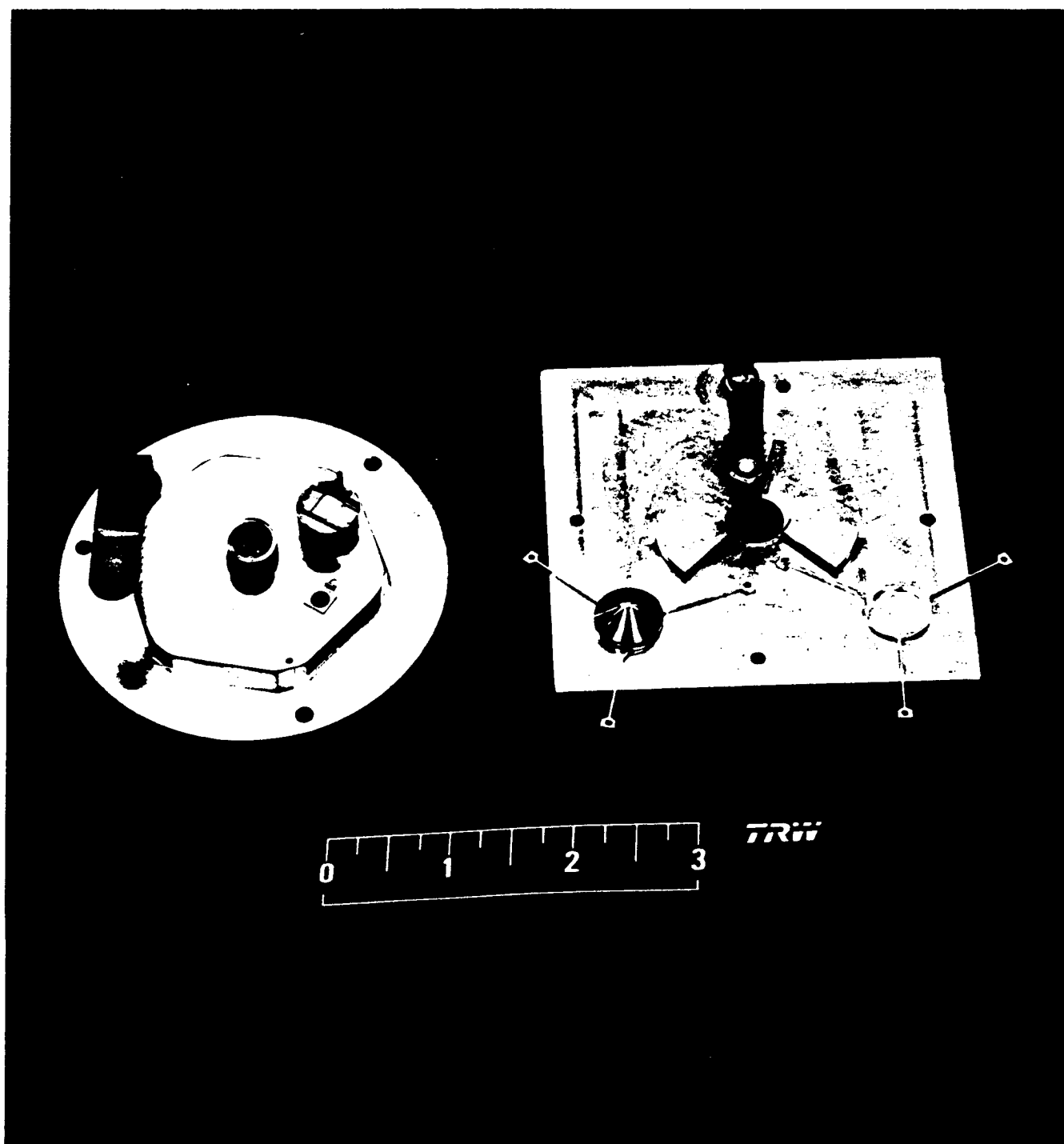


FIGURE B-3. Cell and BeO insulator to primary vapor phase solder tool (left) and secondary to spider vapor phase solder tool (right).

The primary with tool clamped in place, was then soldered in the vapor phase solder machine. A schedule was developed to ensure good wetting of the cell and BeO to each other and to the primary. To maintain schedule, soldering of the cell stacks was done concurrent with the soldering of the spider assemblies noted in B.4.

The soldered primary was then removed from the vapor phase and allowed to cool. A vapor degreaser was used to remove the flux from the tool and completed primary subassembly after soldering and removal of the clamp. The locating tool was then removed. The primary was then identified with the cell and electrical group contained within.

This operation caused the worst cell breakage as the GaAs cell was very brittle and had to be held to the center of the primary. Vent and flux cleaning holes were added to the tool which improved throughput yields, see attached Figure B-4. This area will be further evaluated in follow-on contracts.

The completed cell stacks were then protective packaged, identified, and stored.

3.2 FEED THROUGH POST INSTALLATION

To this point, the interconnected cell and BeO (-)N and (+)P contacts were floating freely in the primary mirror. Hermetically sealed feed through posts as used by the printed circuit board industry were acquired and used to connect the contacts and feed through the base of the primary to form terminations.

Before assembly, the base of the terminals (ground) were coated with encapsulant to prevent shorting of the soldered joints. The back surface of the primary was lightly abraded and cleaned with acetone to prepare it for soldering. The post was then inserted from the backside and soldered to the primary mirror using a hand held iron and silver filled solder. A 50% fillet was required. The joints were tested for isolation between pin and mirror at 500 V. Any failures were reworked. Flux was used as required to activate the surface.

The positive and negative contacts were then made on each assembly using a hand held iron and a mild flux. The assembly was held in a fixture so that the operator could make both joints required without contacting ground (mirror or pin body).

MCC VAPOR PHASE YIELDS Primary and Cell Joint

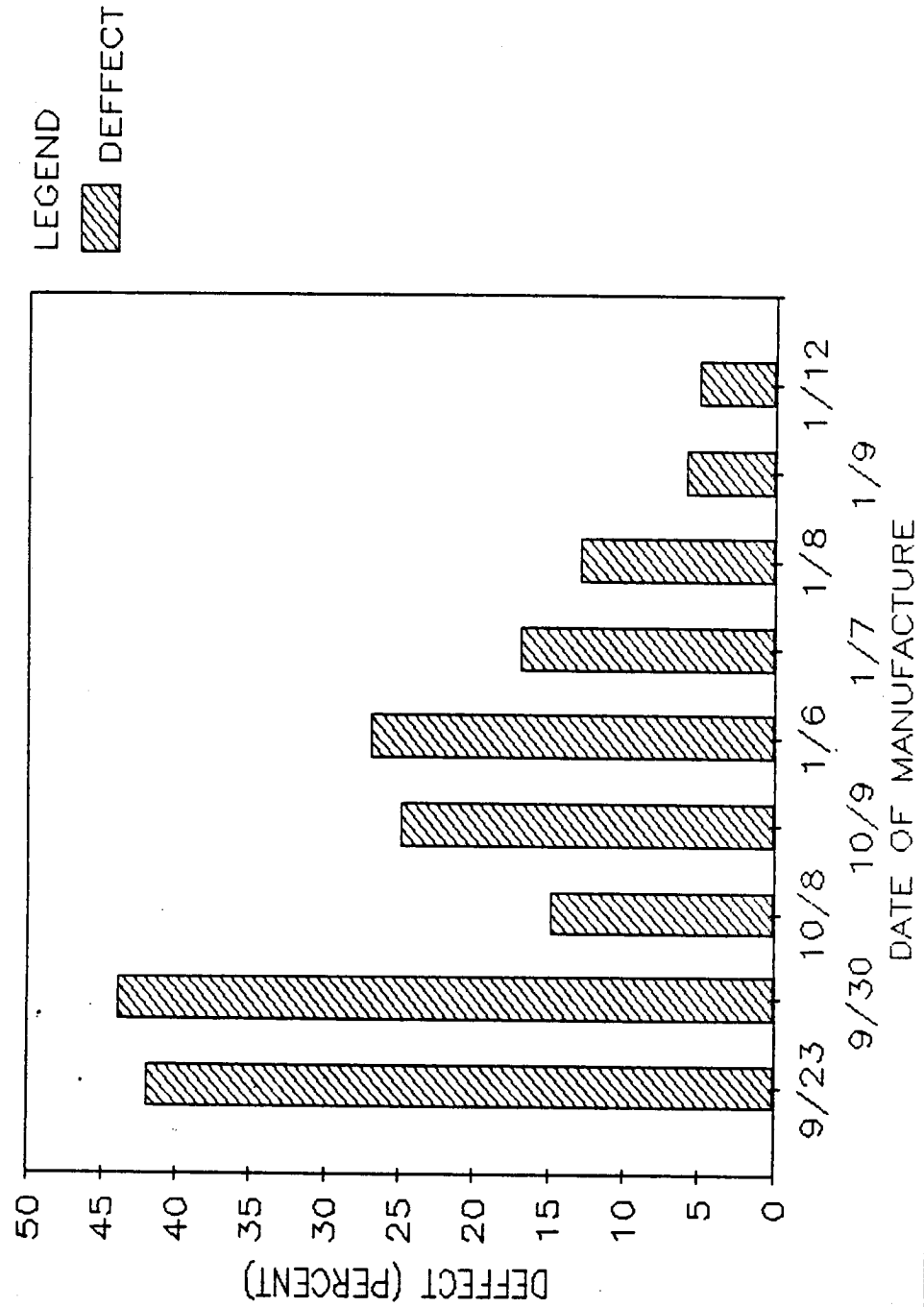


FIGURE B-4

Because the heated flux tended to splatter and contaminate the primary mirror, prior to soldering, the mirror was coated with X59 optic cleaner. The cleaner was recommended for use by the TRW optic lab as its residue is measured in angstroms and it is easily removed. The toluene base material was coated on the interior of all optics and removed after soldering with a touch of masking tape applied to a non mirror surface.

Removal of this material revealed severe plating problems with the primary mirror plating adhesion.

3.3 CONE AND COVER INSTALLATION

The cone and cover assembly was bonded to the cell using a small drop of optical adhesive DC93-500. The rightmost tool in Fig. B-1 was used to install and rough center the cone assembly to the primary. The cone was centered on the cell by visual alignment and tacked in place by using an elevated temperature cure lamp. After tacking, the assembly was baked at 100°C for 90 minutes to full cure the adhesive.

Rework for misalignment was easily performed by swelling the cover adhesive with a chlorinated solvent, manually cleaning, and rebonding.

3.4 PAINTING

Painting of the optics was probably one of the most difficult tasks. The paint, S13GLO a white RTV paint, is difficult to work with and does not adhere well to nickel or silver plating. Two surfaces required application of paint - the backside of the primary mirror and the top side of the spider/secondary assembly.

The primary mirror was placed on a painting aid and bonded in place with double sided tape. Positions of the optics were mapped to show identification and the tags were removed. Surface prep included wipes with acetone and alcohol with one half hour dry times in between. The posts and the mirror support hole were then masked with painting aids and the surface was primed with a thin coat of the vendor supplied primer. The primer was air brushed on in a box coat to a thickness of less than 0.0003". S13GLO paint was then mixed and sprayed per the vendor instructions. Approximately 0.001" of paint was applied per session, with an overnight dry between applications. The total paint thickness was targeted at 0.003" to 0.004".

The painted primaries were then removed from the double back tape by cutting an edge in the tape with an "X-Acto" knife. The plugs were removed and the flaking paint at these edges was cleaned with the knife. The part was then bagged and identified from the map.

Secondary mirror subassemblies were loaded into a custom fabricated aid for painting. A sheet of neoprene rubber with a best fit packing factor was cut with through holes that allowed the secondary mirror outside diameter to "press fit" through. The neoprene sheet was supported by "lexan" plastic. The spider assemblies, when placed in the aid, were then masked with masking tape dots at the to be bonded ends of the spider legs. Cleaning, priming and painting were achieved using the same procedure as noted above. The sole exception was that the upper edge of the interior diameter of the secondary was hard brushed with primer and paint.

The spider assemblies were removed and cleaned using a sharp knife to remove excess and flaking paint. Special care was taken not to damage the legs of the spider in removal. The painted parts were then protective packaged for the next assembly.

3.5 SECONDARY/SPIDER INSTALLATION TO PRIMARY

The secondary/spider assembly self aligned to the primary on three mounting posts. The interface between the surfaces was cleaned with acetone and allowed to dry for one half hour. The secondary was then placed on the primary and three small dots of lightweld 628 adhesive were added. The spiders were quickly tacked in place with the UV lightsource used in section 2.3 of this appendix. Final cure was accomplished in an oven at 100°C for 30 minutes. After cure, the completed optic was bagged and identified.

4. PANEL ASSEMBLY

Installation of the Floating Inserts

Optic Installation

Harness Fabrication

Series Stringing and Harnessing

Testing and Rework

4.1 INSTALLATION OF PANEL INSERTS

Three candidate materials were installed to the Tri-Hex grid in the development phase as discussed in the report body. All three candidates were included on the 66 and 180 optic panels.

Installation of the inserts creates the plane that the optics rest on and therefore is critical for electrical performance. This work demonstrated that even though the panel was bowed significantly, the inserts could create a new plane. The panel was placed on a granite table with the optic side down. Spacer shims were then added between the panel and the table rather at random. The inserts were then slid through the panel from the back side of the panel until they located on the granite table. (Note: inserts had to be deburred prior to installation. Burrs were made by the mirror vendor.)

After insertion, three inserts were selected in the middle of the panel that made the largest possible triangle. These three inserts were bonded with UV adhesive noted above, thus creating the optic plane. With great care not to touch or distort the panel, the next intersecting and bisecting triangles were selected and bonded. Soon the panel was sturdy and rested on the bonded inserts; the shims were removed. The remaining inserts were bonded as these first triangles, row by row.

The panel was then inverted and epoxy bond (EA9321) added as a fillet around the top of the insert to add strength to the bond. The panel was then cured at 100°C for two hours. Rework was accomplished by solvent and heat gun removal and subsequent rebonding of the insert on the micro flat granite.

4.2 OPTIC INSTALLATION

The first step towards optic installation was development of a kitting plan. The optics had been identified throughout manufacture with the original cell output data as well as optic type (several optics were of Ni/Cu/Ni sandwich construction). Based on original cell performance data, the optics were kitted to the panel per attached Figure B-5. Roadmaps were made showing the pedigree of each optic as it was loaded to the Tri-Hex grid.

After loading, the optic was fastened to the Tri-Hex with the pop-pin/washer assembly detailed in section 2.1 of this appendix. Each optic was held by three such pins. Pins were all loaded to the floating insert and then pressed into position, one at a time such that the RTV washer captured the lip of the optic. the optics were all oriented so that the feedthrough terminals were aligned for ease of series wiring.

4.3 HARNESS FABRICATION

Two harnesses were fabricated for the MCC panels. Both used rectangular connectors and a three stage potting sequence in a low boot configuration. There was no ground strap or loop. Fabrication and cut length instructions are attached as Figure B-6.

Wire used for the harness was a nylon insulated ribbon cable with 28 Awg wire. The wire was stripped with a laser wire stripper and separated with a sharp knife. Contact fillers were installed as required.

4.4 SERIES STRINGING AND HARNESSING

The harness fabricated above was installed to the panel with lacing ties along the wire bundle. The connector was mounted to the panel by a twin pair of aluminum plates, mounted with hardware, and held in place with by clamping pressure across the width of the Tri-Hex.

Series wiring optic to optic was made with a 26 Awg jumper wire looped between the Tri-Hex grid and stress relieved. Terminations were soldered to the terminal feedthroughs using a silver filled solder and an alpha flux.

Figure B- 5. MCC PANELS - KITTING PLAN

Small Panel:

<u>String</u>	<u>Qty</u>	<u>Optic</u>	<u>Cell/%</u>
1	8	Ni	ASEC/19.81-20.1 Set 1
2	15	Ni/Cu/Ni	ASEC/19.81-20.1 Set 1
3	15	Ni/Cu/Ni	ASEC/20.11-20.7 Set 1
4	15	Ni/Cu/Ni	ASEC/20.11-20.7 Set 1
5	<u>15</u>	Ni/Cu/Ni	ASEC/20.11-20.7+ Set 1
	68		

Large Panel:

1	12	Ni	Varian
2	24	Ni	Varian
3	24	Ni	Spectrolab 17.51-18.6
4	24	Ni	ASEC/19.21-20.0 Set 1 & 2
5	24	Ni	ASEC/19.51-20.0 Set 1 & 2
6	24	Ni	ASEC/19.51-20.0 Set 1 & 2
7	24	Ni	ASEC/19.51-20.5 Set 1 & 2
8	<u>24</u>	Ni	ASEC/19.81-20.1 Set 1
	180		

16 Pin (Minimum) Connector-

<u>PIN#</u>	<u>COLOR</u>	(MIN) <u>LENGTH</u>
1	B	65"
2	R	65"
3	B	55"
4	R	55"
5	B	50"
6	R	50"
7	B	45"
8	R	45"
9	B	40"
10	R	40"
11	B	30"
12	R	30"
13	B	20"
14	R	20"
15	B	10"
16	R	10"

10 Pin (Minimum) Connector-

<u>PIN#</u>	<u>COLOR</u>	(MIN) <u>LENGTH</u>
1	B	30"
2	R	30"
3	B	25"
4	R	25"
5	B	20"
6	R	20"
7	B	15"
8	R	15"
9	B	10"
10	R	10"

Figure B-6. Harness Fabrication Instructions
for 15 x 21 and 15 x 56 Panels

Terminations were made to the harness bundle in accordance with the attached schematic Figure B-7. The schematic was developed from the best fit kitting plan to avoid electrical mismatch degradation. Terminations to the harness bundle were made using a western union splice soldered as above and sleeved with a shrink sleeve tubing of Kynar co-polymer series.

4.5 TESTING AND REWORK

The completed panel assembly was installed on the solar tracker and tested per procedures noted in the body of the report.

Optics identified with performance problems were removed and replaced with attrition quantities. Removal was difficult as the pop-pin is a one way device. The most effective removal technique was to drill out the pop-pin. A vacuum and shielding were used to protect the optics and chips were removed as they were generated. Replacement optics were installed and tested as above.

Thermistors were added to the panel to collect temperature information during test. Thermistors were bonded to the back of the primary mirror with conductive epoxy in an area where the S13GLO paint had been removed. The paint, however, had left a silicone contamination which made subsequent bonding with non-silicones nearly impossible. Abrasion and cleaning resulted in relatively weak bonds.



Schematic (66 Optic Panel)

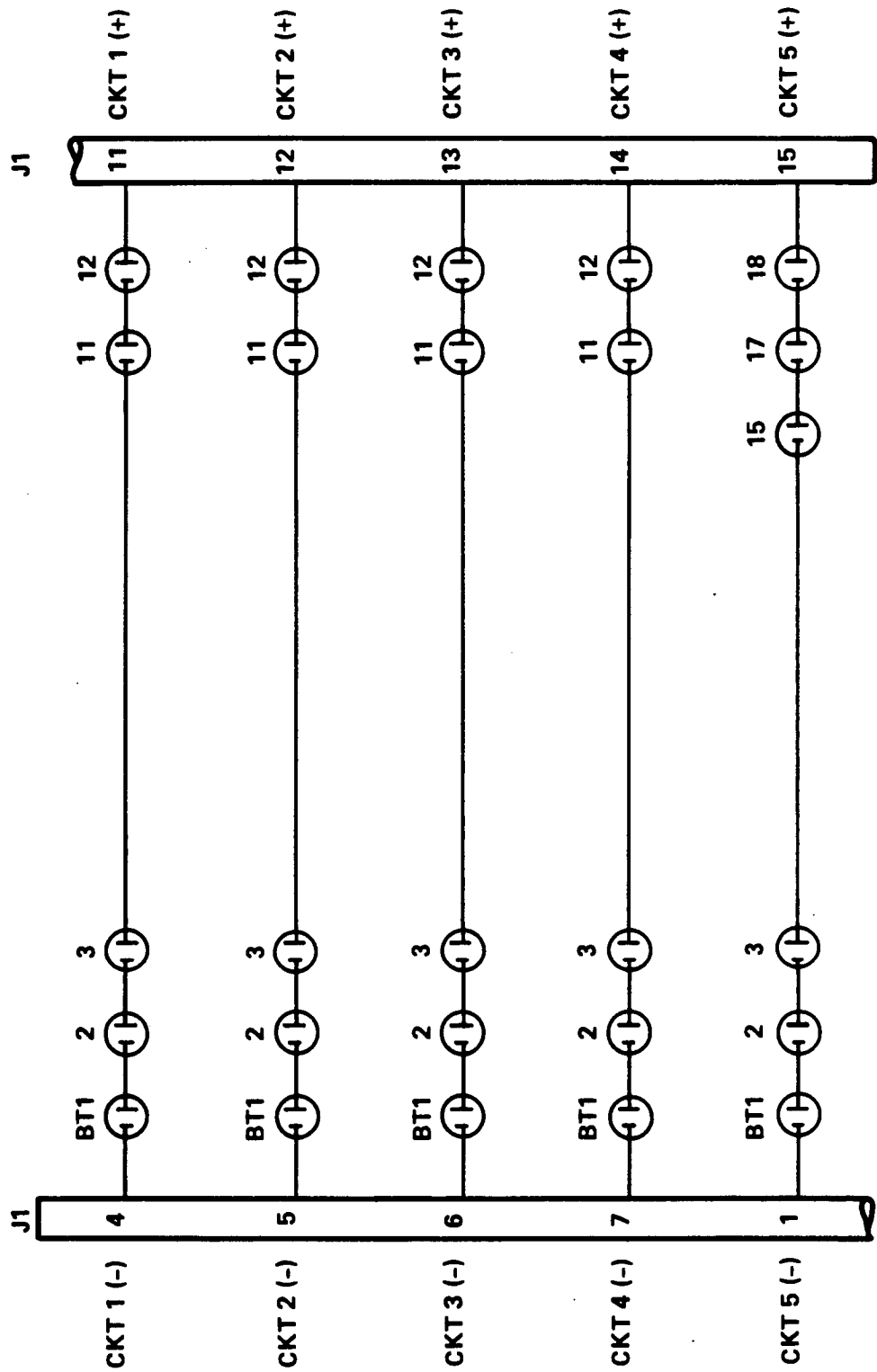


FIGURE B-7

APPENDIX C

STRUCTURE MANUFACTURING

BACKGROUND:

Previous NASA contracts and a TRW PMI Program demonstrated the feasibility of manufacturing a structurally sound tri-hex grid from a single tow graphite prepreg roving. It was believed that the low fiber volume/high resin content characteristics of panels which were previously fabricated could be improved by utilizing a trapped rubber molding (TRM) expansion process during cure (see Figure C-1). A major goal of the present NAS8-36159 contract was to develop this process, resulting in a higher fiber volume and lower resin content substrate. Development and co-curing of lightweight molded inserts, thin uniform wall thicknesses in the substrate and elimination of tool removal problems were also objectives of this contract.

TECHNICAL APPROACH:

The graphite prepreg roving materials chosen for evaluation were 6 K tow T-300/Fiberite 934 (350°F cure) and 6 K tow T-300/Fiberite 982 (250°F cure) systems. The effect of different cure temperatures on the TRM process needed to be established in order to select the best material from which to fabricate the tri-hex grid.

To establish expected material properties and determine the structural effect of crossing yarns, six graphite samples were fabricated using the TRM process. The expandable elastomer chosen was Dapocast 1-100 silicone casting compound (CTE 10.6×10^{-5} in/in/°F).

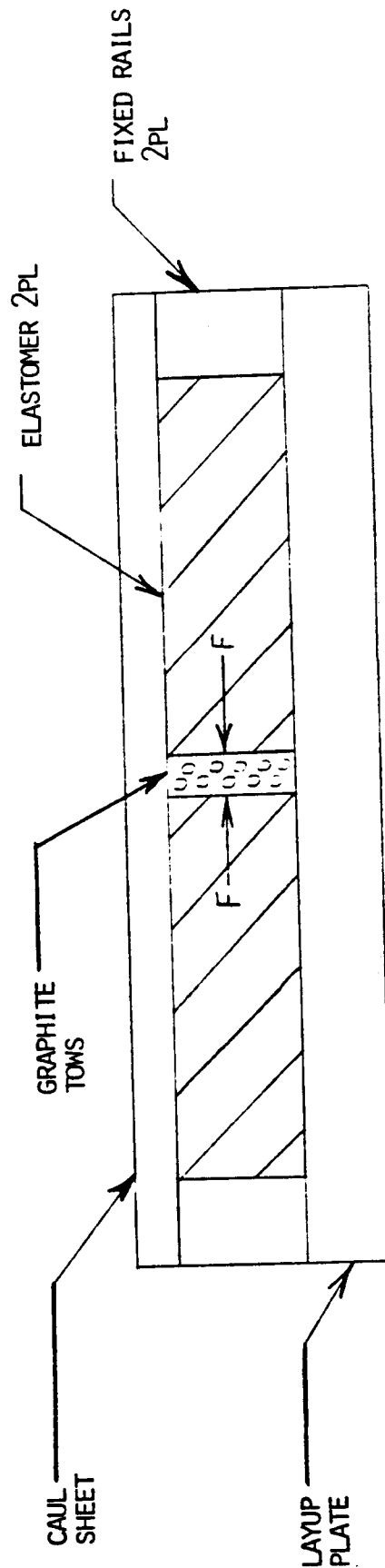
The rubber inserts were fabricated in the molds used to layup the straight and crossover samples by pouring the rubber with aluminum cores in place which replicated the graphite samples (see Figure C-2).

Three straight and three crossover samples were fabricated. The parts were first tested in bending and then specimens were cut from each part to determine specific gravity, resin content, void content and fiber volume. Findings are shown in Figure C-3. Failure of the straight strips occurred in a buckling mode due to the thin cross section. No structural degradation was seen in the cross strips at crossover points. The bending test set up is shown in Figure C-4.

MECHANICAL MANUFACTURING ENGINEERING DEPARTMENT

FIGURE C-1: TRAPPED RUBBER MOLDING CONCEPT

- BULK THERMAL DIFFERENTIAL EXPANSION.
- DAPOCAST 1-100 SILICONE ELASTOMER CASTING COMPOUND
(CTE 10.6×10^{-5} IN/IN/ $^{\circ}$ F VS. 1.3×10^{-5} IN/IN/ $^{\circ}$ F FOR ALUMINUM)



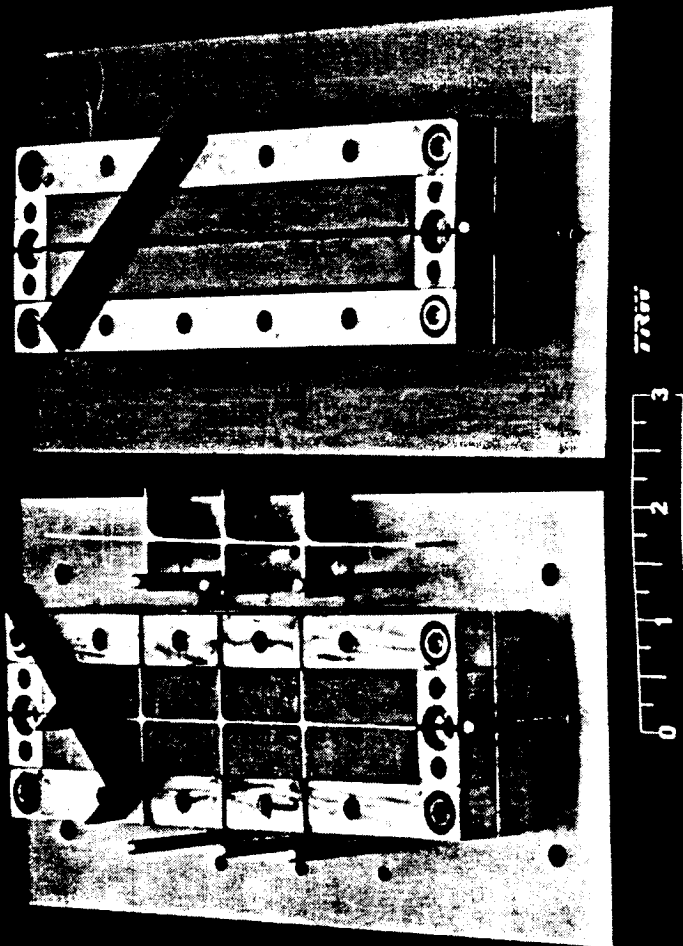


Figure C-2. Strip Samples and Tooling.

ORIGINAL PAGE IS
OF POOR QUALITY

FIGURE C-3: GRAPHITE TRI-HEX SAMPLE FINDINGS

S/N	TYPE	CURE TEMP (°F)	20 YARN THICKNESS (in)	SPECIFIC GRAVITY (gm/cc)	RESIN CONTENT (%)	VOID CONTENT (%)	FIBER VOLUME (%)	MAXIMUM BENDING LOAD (LB)
3A	CROSS	350	.020 - .023	1.5461	23.0	2.9*	67.9	42.50**
3B	STRAIGHT	350	.021 - .024	1.6367	23.5	0.0	70.1	19.75
4A	CROSS	350	.019 - .022	1.6367	22.5	0.0	72.1	20.85
4B	STRAIGHT	350	.023 - .027	1.6412	21.7	0.0	73.1	20.15
5A	CROSS	250	.019 - .029	1.5248	27.3	3.9*	66.7	29.35
5B	STRAIGHT	250	.027 - .030	1.5487	29.3	0.0	64.3	21.50

↑ NOTE THAT SAME NUMBER SAMPLES WERE CURED CONCURRENTLY.

* VOIDS WERE FOUND IN S/N 3A AND 5A SINCE SPECIMENS WERE CUT TO INCLUDE A CROSSOVER POINT. VOIDS WERE STILL LESS THAN THE ALLOWABLE VALUE OF 4%.

** THE HIGH MAXIMUM LOAD FOR S/N 3A WAS DUE TO A LIP WHICH EXISTED ON THE EDGE OF THE SAMPLE CAUSED BY THE INITIAL FABRICATION TECHNIQUE.

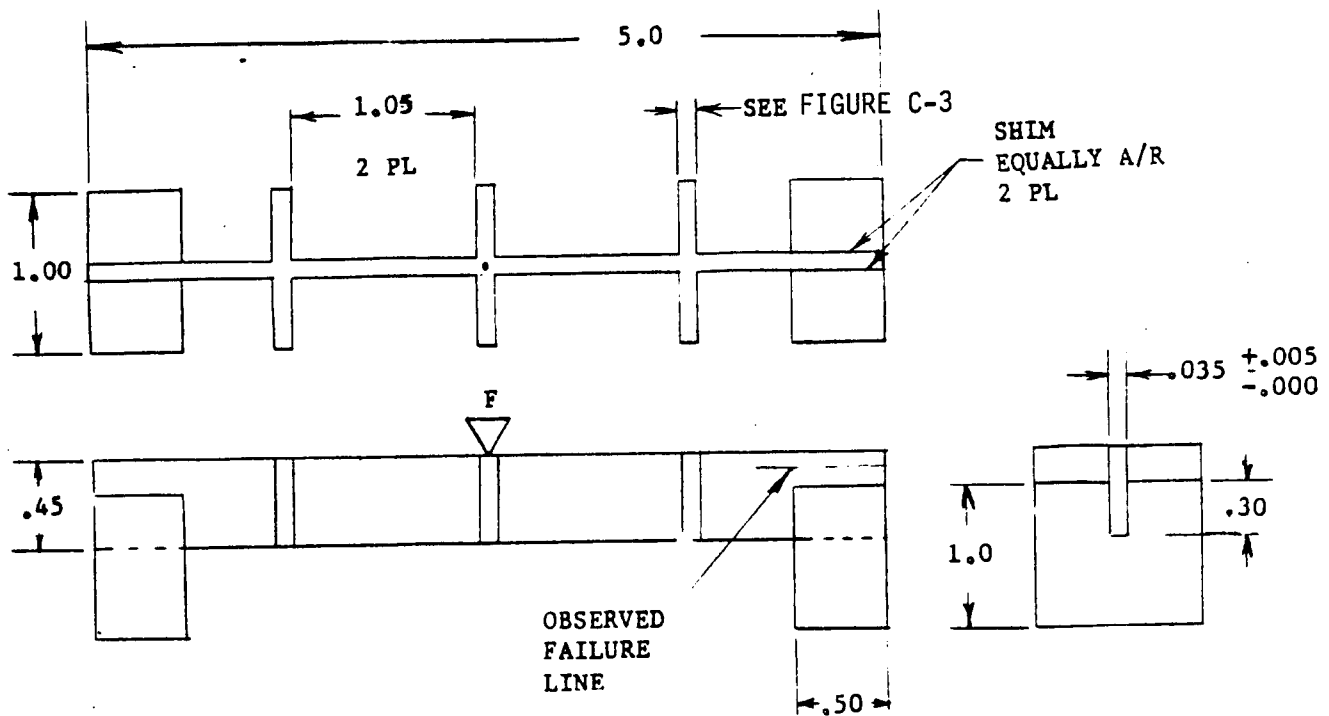


FIGURE C-4: CROSS STRIP SAMPLE IN TEST FIXTURE

TRIM AND PANEL LAYUP DEVELOPMENT:

Five mini-panels (5.0" x 6.0") were fabricated-two 350°F cure and three 250°F cure-to develop the optimum wrapping technique and tooling approach, verify the ability to co-cure inserts with the panel, and determine the degree of wall compaction which could be attained in a tri-hex structure (see Figure C-5). During fabrication of the mini-panels, the optimum debulking (compaction) schedule was developed and it was found that debulking after the third, sixth, eighth and ninth course resulted in a uniform structure. It was necessary to debulk around wrapping pins after each course. Debulking was performed using .24" thick x .5" wide stainless steel Starrett shim stock.

Two major tooling innovations were proven out on the mini-panels. The first was to fabricate a two piece rubber hex for expansion molding (see Figure C-6). Initially, all rubber pieces were installed on the layup plate and the tows were wrapped in between them. This was done since it was physically impossible to drop full size rubber pieces between the tows after wrapping without trapping some fibers underneath. A disadvantage of having all rubber pieces on the mold is you are essentially working blind since tows cannot be seen. This slows down the wrapping. The two piece rubber approach was based on the fact that two rubber pieces with the same volume as a single piece should perform the same thermally. This was proven to be true. The two piece hexes were fabricated by placing 1.500" diameter aluminum plugs in the mold before pouring the rubber (Figure C-7). The aluminum plugs were removed, the outer hex rubber was released and the central rubber core then poured in the same mold. The two rubber pieces were then separated and the outer hex cut through on one side for ease of installation in the layup.

The second major tooling breakthrough was the development of screw pins as wrapping pins (see Figure C-8). Initially, .125" diameter dowel pins, snug slip fit in the layup plate, were used as wrapping pins. The tri-hex grid tended to lock around the pins during cool down making part removal very difficult. By modifying 10-32 socket head cap screws into wrapping pins, we took advantage of the "screw jack" effect which could be used to remove pins from the backside of the layup plate, thus eliminating part removal problems.

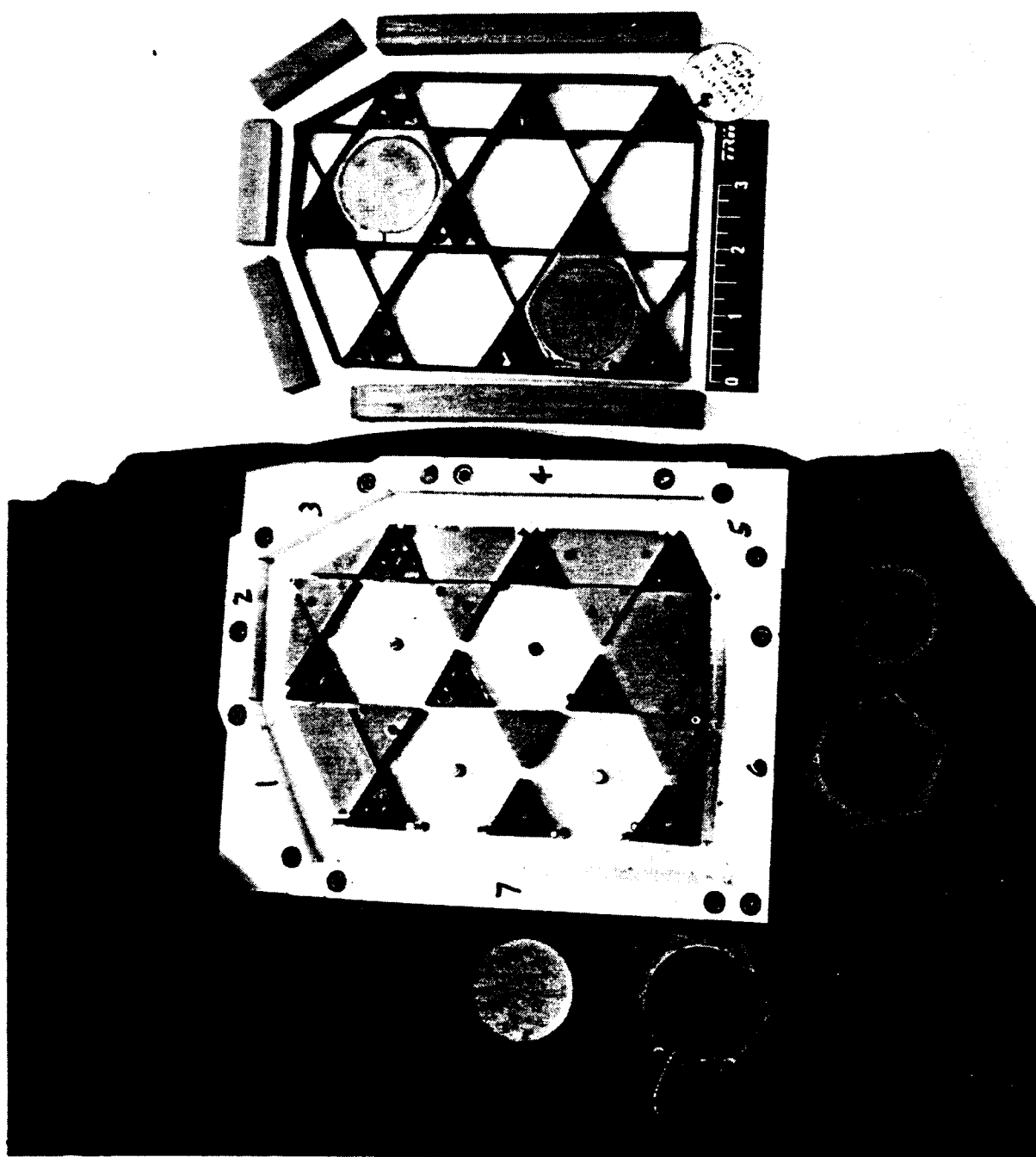


Figure C-5. Mini Panel with Tooling.

C6

ORIGINAL PAGE IS
OF POOR QUALITY

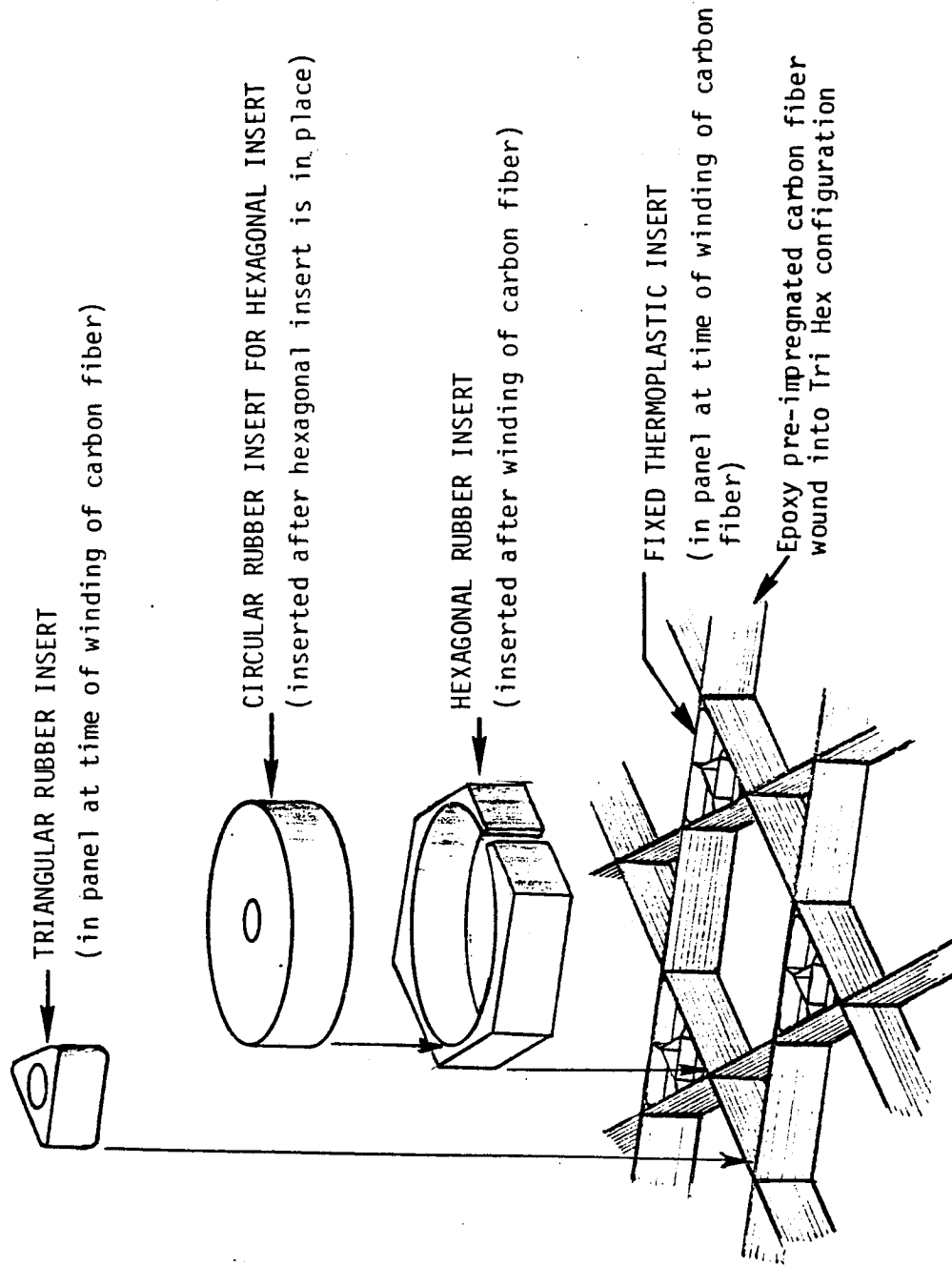


FIGURE C-6: INSERT TOOLING FOR TRI HEX GRID MAKES ASSEMBLY, WINDING OF FIBERS, AND DISASSEMBLY AFTER BAKEOUT EXTREMELY SIMPLE. SEMI-AUTOMATION OF PROCESS IS FEASIBLE.

ORIGINAL PAGE IS
OF POOR QUALITY

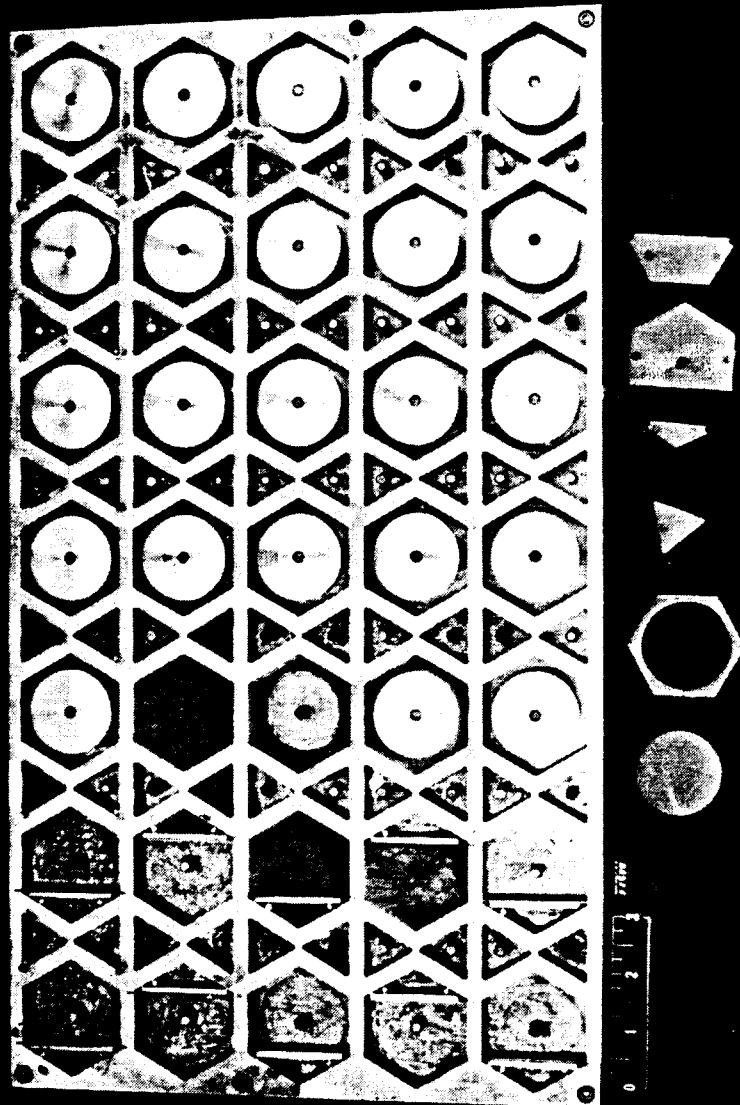


figure C-7. Rubber Insert Mold.

The first three mini-panels used machined epoxy glass triangular inserts as placeholders. Production type injection molded thermoplastic inserts for element mounting were co-cured with panels number four and five (see Figure C-9). Inserts were molded from 30% graphite fiber filled PPS (RYTON), PEEK and TORLON. It was found the PPS was easiest to mold, requiring very small gates. These gates had to be enlarged slightly for injection of PEEK material and enlarged to the maximum for TORLON. Inserts were tooled to the layup plate using .203" diameter teflon pins for location and 6-32 socket head cap screws for angular clocking and tie down.

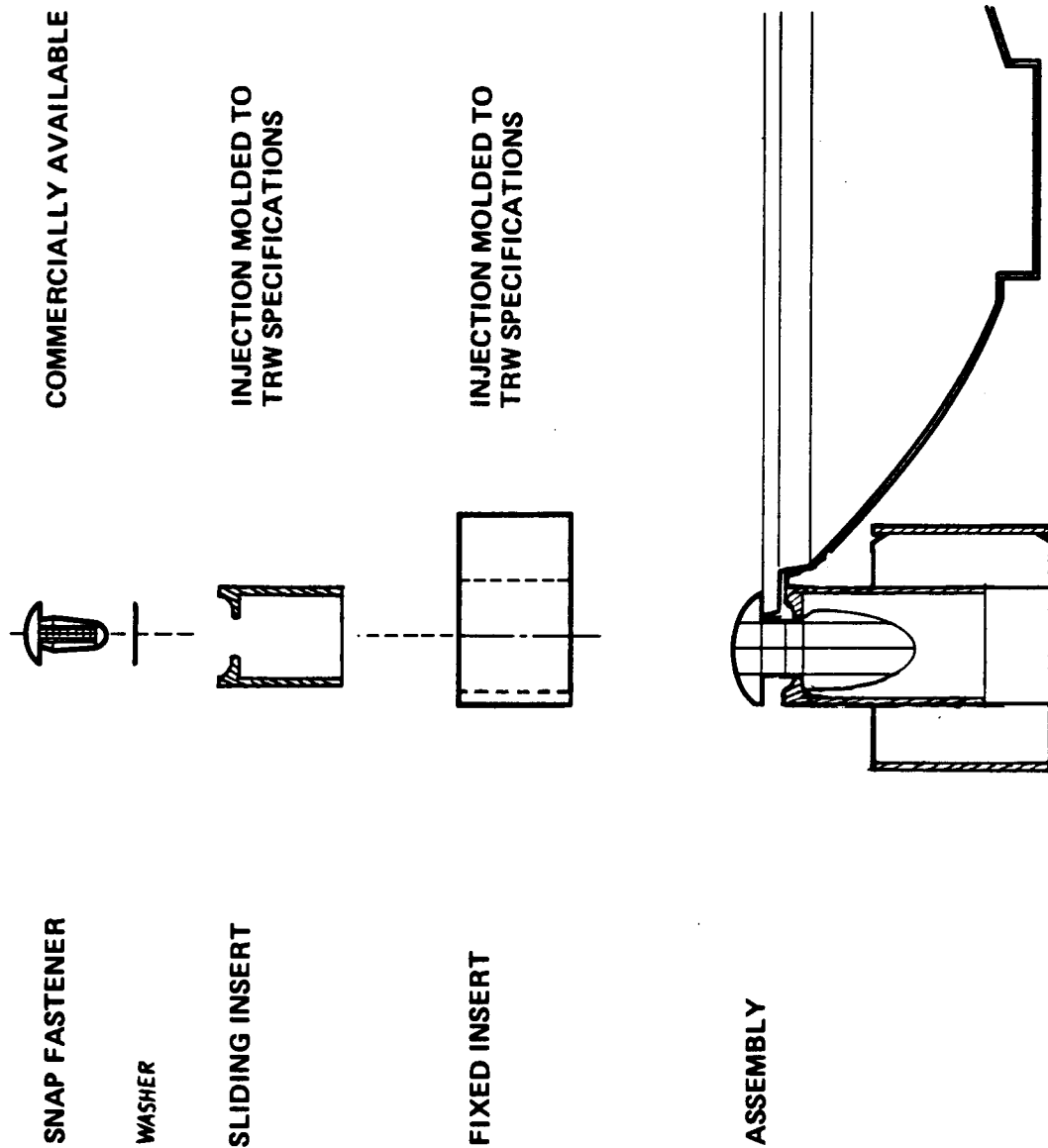
The method which evolved as the easiest way to fabricate the several hundred rubber pieces required for the 15" x 21" and 15" x 56" panels was to pour the rubber into an open mold overfilling slightly, and then clamping a caul plate with holes to it. This allowed excess rubber to extrude out and controlled thickness. De-airing of the initial Dapocast mix was found to be critical and allowing air to rise to the surface before covering with the caul plate helped cut down on voids. The thin cross section of the outer hex contributed to voids in some parts. This cross section should be increased slightly for any future fabrication by decreasing the diameter of the aluminum inner hex mold plug. It was found that post curing the Dapocast up to 400°F causes a color change from yellow to rust, but there is no degradation in properties unless continually used at this temperature. It also happened that one Dapocast mix resulted in "soft" rubber pieces. They had a Shore hardness of 30 A versus a normal value of 50 A. These soft pieces exhibited no detrimental difference in CTE when used for TRM.

The overall TRM Process Development Plan is shown in Figure C-10.

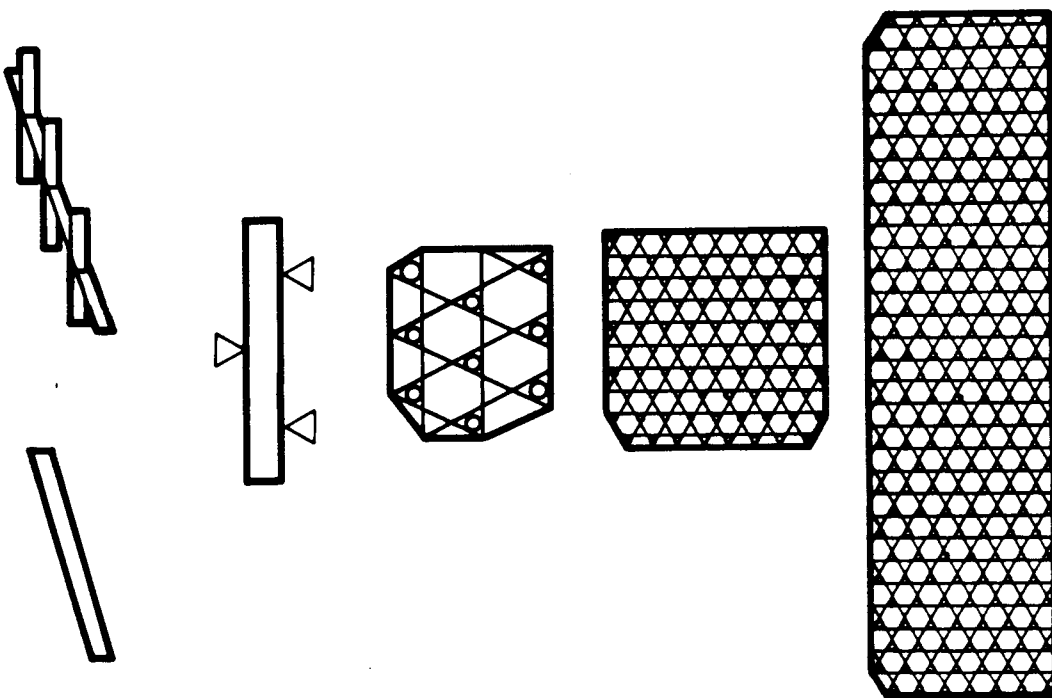
PANEL FABRICATION:

Based on the properties achieved in the strip samples and evaluation of the mini panels, it was decided to use the T-300/982 resin system for fabricating the 15" x 21" and 15" x 56" panels. Since this is a 250°F curing system, less internal stress due to thermal growth is built into the panel. The 15" x 21" layup tool and panel configuration is shown in

Baseline Insert Assembly Design



THG Process Manufacturing Development

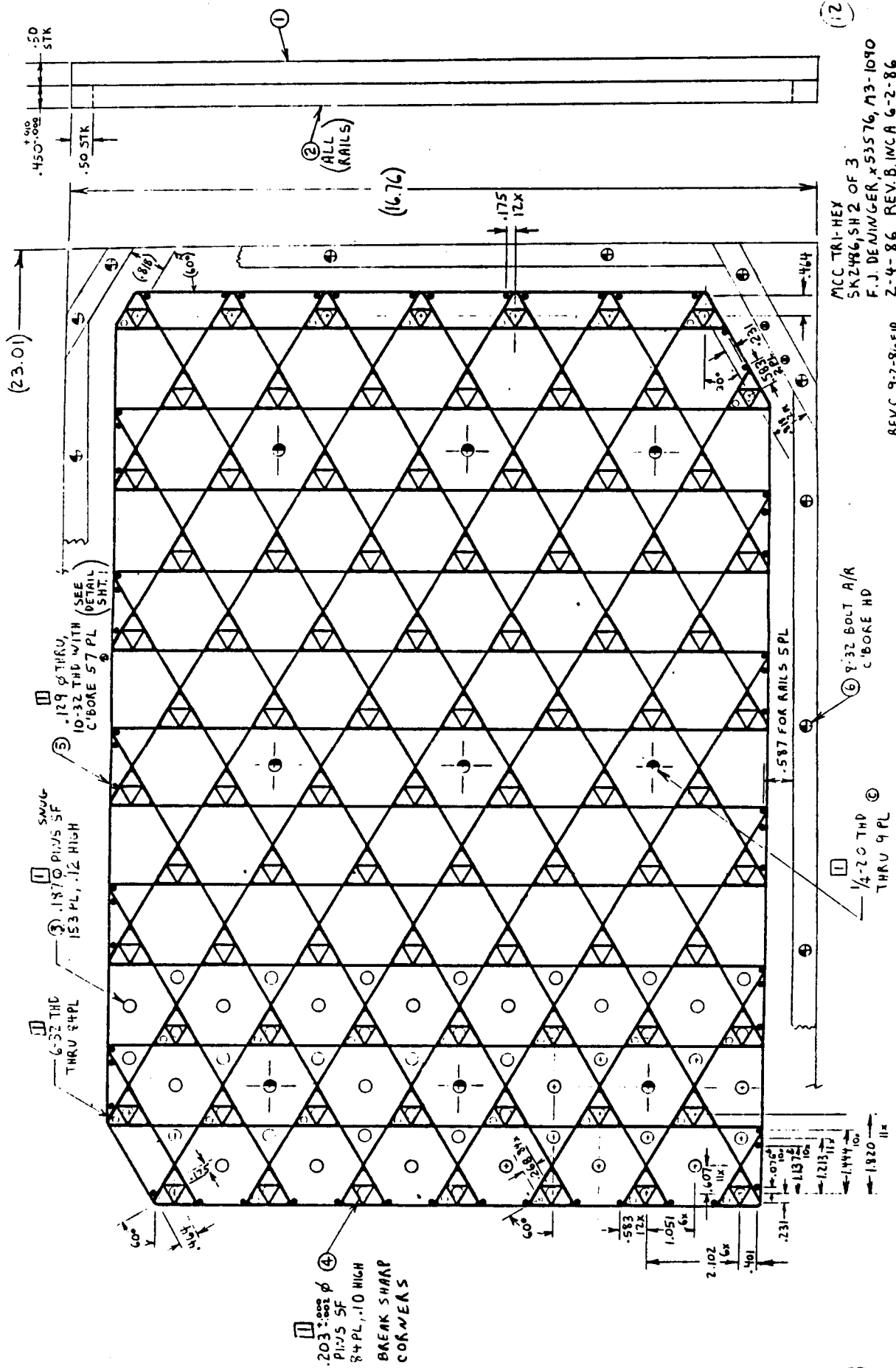


- DEFINE MATERIALS REQUIREMENTS
- MANUFACTURE SMALL TEST ARTICLES WITH VARIATIONS IN BASELINE PROCESS
- TEST AND EVALUATE TEST ARTICLES
- CHECK FOR STRUCTURE WEAKENING AT FIBER CROSSOVER
- MANUFACTURE SMALL TRI HEX GRID WITH INSERTS
- VERIFY GRID MEETS REQUIREMENTS
— SELECT BEST PROCESS PARAMETERS
- MANUFACTURE 18" x 18" GRID
- VERIFY ENGINEERING REQUIREMENTS,
INCLUDING FLATNESS
- MANUFACTURE 15" X 56" GRID

Figure C-11. The wrapping pattern is a six tow sequence (one course) repeated 9 times resulting in a total of 18 tows in each internal wall. The outer frame has a consistent pattern, but does not have the same number of tows at every location. To give a better appearance to the frame and further stiffen the structure, the frame was covered with T-300 6K tow unidirectional tape (MT3-103-3) around the periphery. This tape has a 350°F curing resin so it is not fully cured at the 260°F curing temperature, but it has reached the glassing temperature (T_g) and is securely bonded from the resin in the roving.

The graphite tows were drawn through a series of dies (.052", .043" and .033" diameters) utilizing the technique developed on a previous PMI program. This rounds out the flat fibers and makes it easier to uniformly wrap around inserts and pins. A 108 style bleeder cloth was placed on top of the layup and the caul sheet was clamped down with 1/4-20 socket head cap screws threaded into the layup plate. Rails and inserts were .450" high, but some rubber pieces were slightly higher so this extra clamping helped to eliminate loose tows. The panel was turned over so the bleeder side was down and resin would be soaked up during the three hour, 260°F, vacuum bag cure. The 15" x 21" panel was easily removed from the mold and met all requirements (see Figure C-12). The panel is shown in Figure C-13 with the 15" x 56" layup tool.

Since the tri-hex pattern repeats, the 15" x 21" layup tool was simply extended to accommodate the 15" x 56" panel. The layup procedure was the same as the 15" x 21", but the cure cycle was modified. In an effort to reduce thermal stresses in the part, it was cured for three hours at 200°F (beyond the T_g), wrapping pins were removed and the part was postcured for two hours at 260°F. When removed from the mold, the part was inspected and found to have a .240" bow. The walls of the grid tapered from .015"-.028" and this unbalanced condition was suspected as the cause of the bow. It was decided to build a second panel using a controlled compaction technique to guarantee an equal number of tows above and below the center line of the panel. The second panel was bowed .310" even though the walls were more uniform (.016"-.026"). This taper was



MCC TRI-MEX
SK2486, SH 2 OF 3
F. J. DENINGER, X53576, M3-1090
REV. C 9-2-86 FJD 2-4-86 REV. B, INCA 6-2-86

FIGURE C-11: TOOLING FOR THE SMALL THG PANEL WAS ALSO USED AS PART OF THE LARGE THG TOOLING.



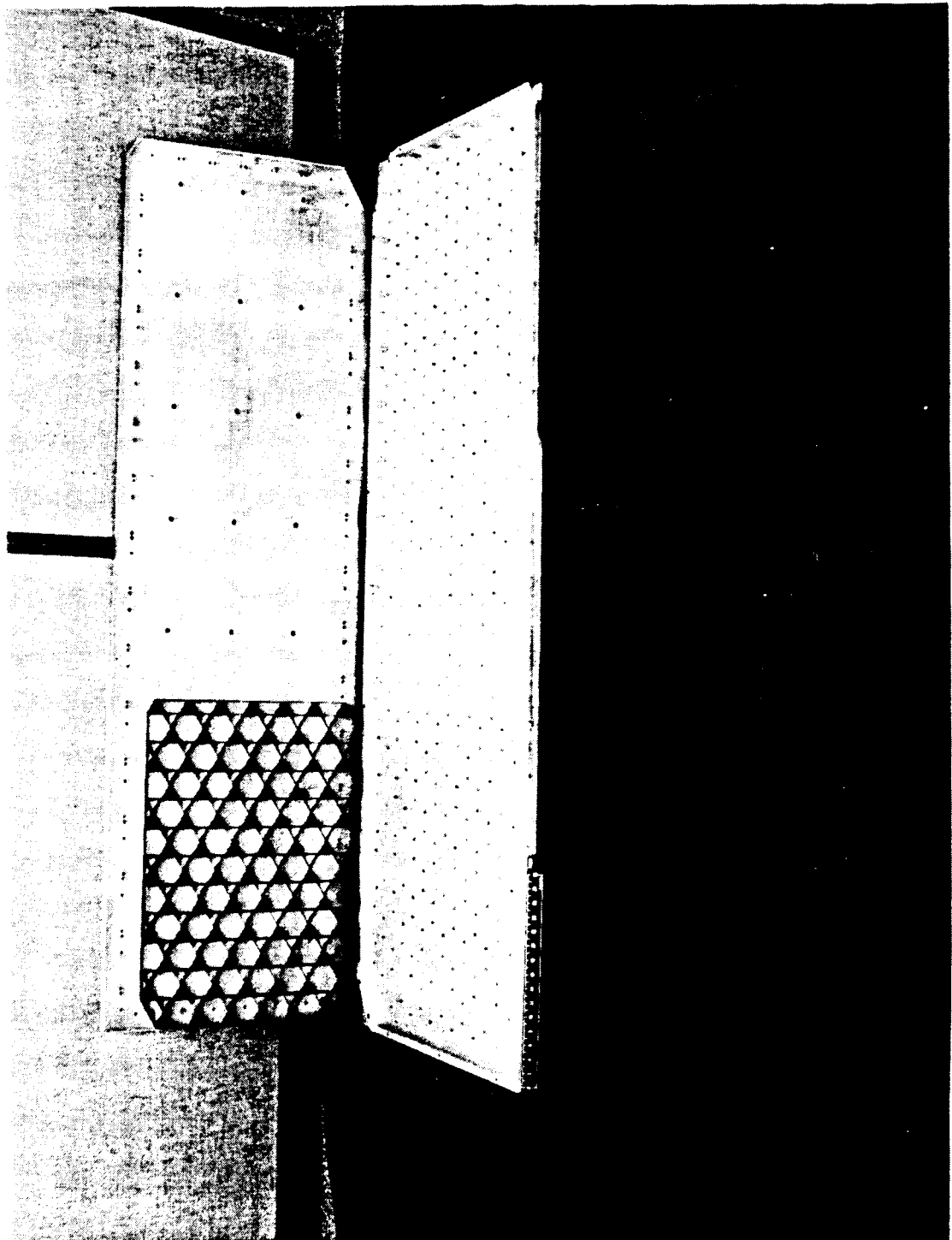
MECHANICAL MANUFACTURING ENGINEERING DEPARTMENT

FIGURE C-12: TRI-HEX GRID SPECIFICATIONS

PARAMETER	REQUIREMENT	GOAL	ACTUAL
FIBER VOLUME	40% MINIMUM	60% MINIMUM	64% MINIMUM
TENSION/COMPRESSION MODULUS (0°)	13 x 10 ⁶ PSI MINIMUM	20 x 10 ⁶ PSI MIN	15 x 10 ⁶ PSI MINIMUM (CALCULATED FROM SMALL BENDING SAMPLES)
WALL THICKNESS	.030" ± .010"	.020" ± .010"	.024" ± .002" (15" x 21") .021" ± .005" (15" x 56") .014" IN 10" (15" x 21") .007" IN 10" (15" x 56" after straightening) .066 G/CM ³ (15" x 21") .060 (15" x 56")
FLATNESS	.020" IN 10"	.005" IN 10"	
WEIGHT (LESS INSERTS)	N/A	.067 G/CM ³	1.5G (REDUCED 55%)
INSERT WEIGHT	REDUCE ALUMINUM WEIGHT OF 3.3G	.5G	
MATERIALS	SPACE COMPATIBLE	N/A	T-300 GRAPHITE/EPOXY PRE-PREG INJECTION MOLDED PEEK, RYTON AND TORLON 30% GRAPHITE FIBER FILLED.

"REQUIREMENTS" NEED TO BE MET FOR NAS8-36159 TEST ARTICLES.

"GOALS" REPRESENT A MORE EFFICIENT STRUCTURE. FUTURE PRODUCTION PANELS SHOULD MEET OR EXCEED THESE SPECIFICATIONS WHEREVER PRACTICAL.



ORIGINAL PAGE IS
OF POOR QUALITY

Figure C-13. 15" x 21" Panels with 15" x 56" Layup Tool

partially due to rubber triangle inserts allowing fibers to get underneath during wrapping. Longer pins to secure these inserts would eliminate this problem. The layup process is shown in Figures C-14, C-15, and C-16.

The decision was made to straighten both panels to gain data points even though panel #2 was planned for use as the deliverable article since it had a more uniform structure. They were heated to 310F for 16 hours while restrained in the direction opposite the bow as shown in Figure C-17. Panel #2 was placed back into the oven at 360° for 16 hours to further straighten it. The results are shown in Figure C-18. In summary, panel #1 was flat within .020" after one straightening and panel #2 was flat within .040" after two straightenings.

RESULTS/CONCLUSIONS:

- a. All tri-hex grid specifications for this contract have been met or surpassed (see Figure C-12).
- b. The TRM technique was extremely successful in increasing the fiber volume of the tri-hex grid structure.
- c. Injection molded thermoplastic inserts can be successfully co-cured with an epoxy based prepreg roving.
- d. A tri-hex grid can be easily removed from the mold when screw pins are used.
- e. Thermally induced residual stresses are built into the 15" x 56" structure as a result of aluminum layup tool expansion during cure, causing the panel to bow. A graphite layup plate and caul sheet is recommended for fabricating any tri-hex grid panel with a length or width dimension greater than 30".



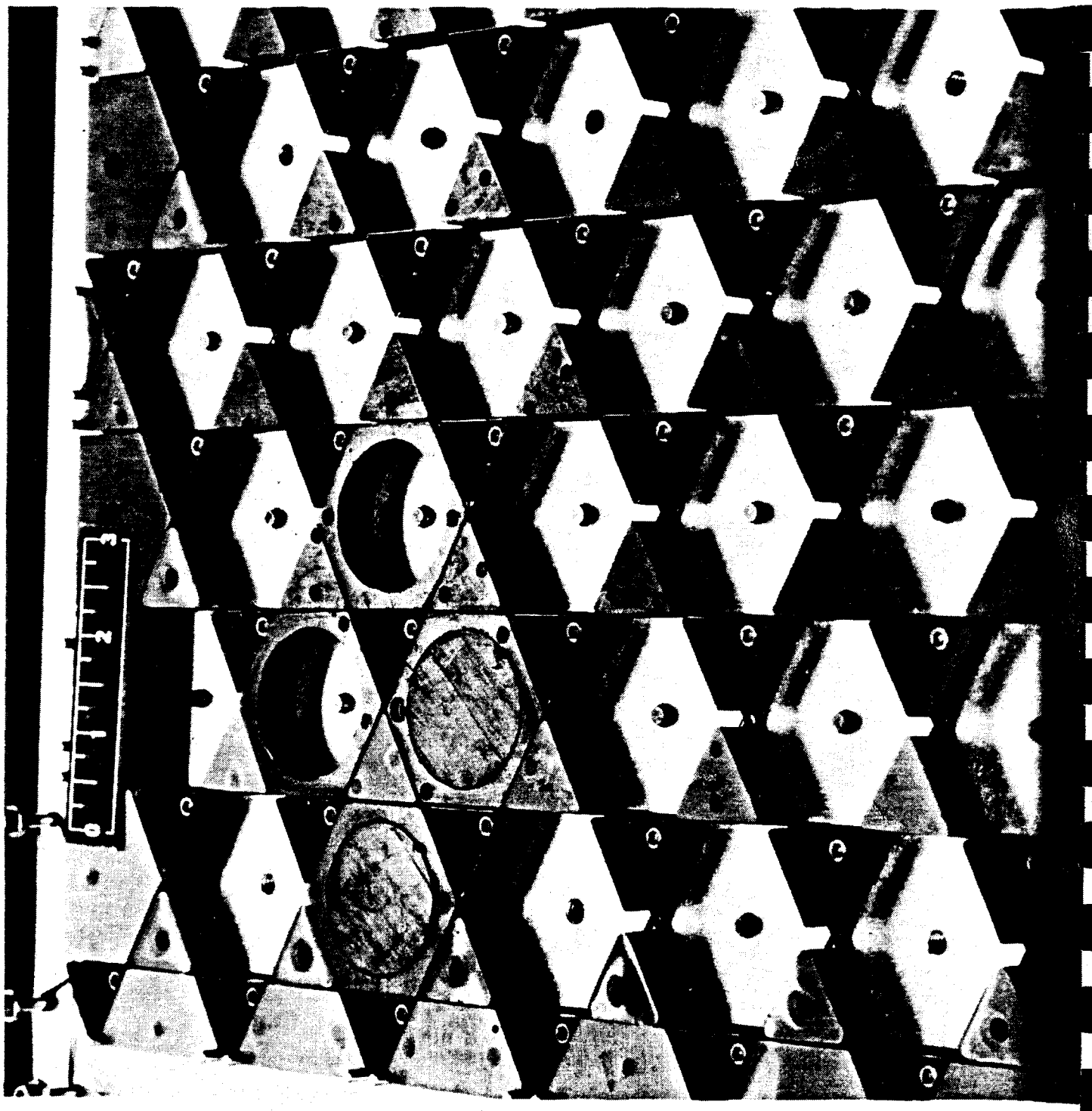
ORIGINAL PAGE IS
OF POOR QUALITY

Figure C-14. Drawing TOW Through Die.

ORIGINAL PAGE IS
OF POOR QUALITY.



Figure C-15. Layup Process.



ORIGINAL PAGE IS
OF POOR QUALITY

Figure C-16. Rubber Inserts Installed in Panel.

FIGURE C-17: STRAIGHTENING SETUP.

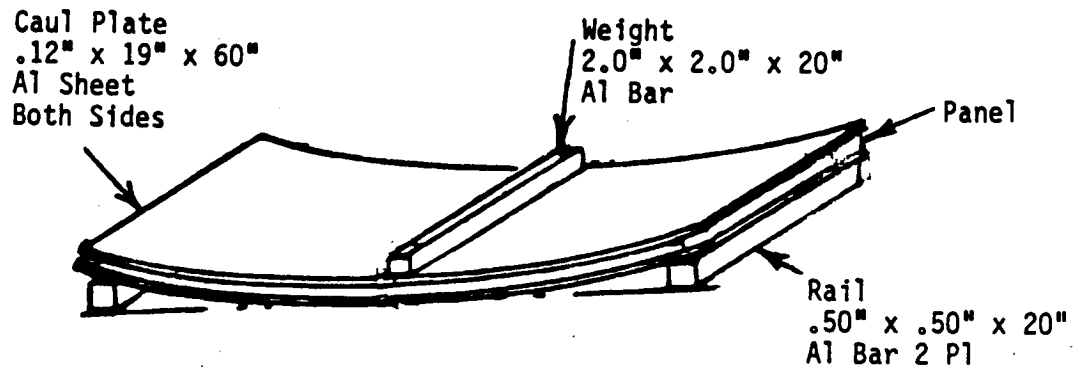
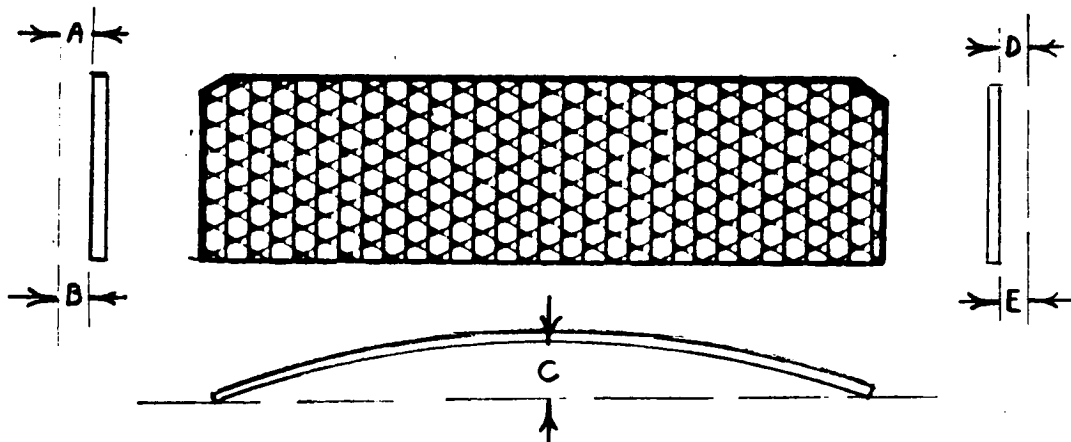


FIGURE C-18: 15" x 56" FLATNESS RESULTS.



PANEL #	DIMENSION	AFTER INITIAL CURE	AFTER FIRST STRAIGHTENING	AFTER SECOND STRAIGHTENING
1	A	.000	.000	N/A
	B	.000	.020	N/A
	C	.140	.010	N/A
	D	.050	.000	N/A
	E	.000	.010	N/A
2 (Deliverable Article)	A	.000	.000	.000
	B	.025	.000	.000
	C	.310	.080	.040
	D	.050	.010	.010
	E	.000	.000	.000